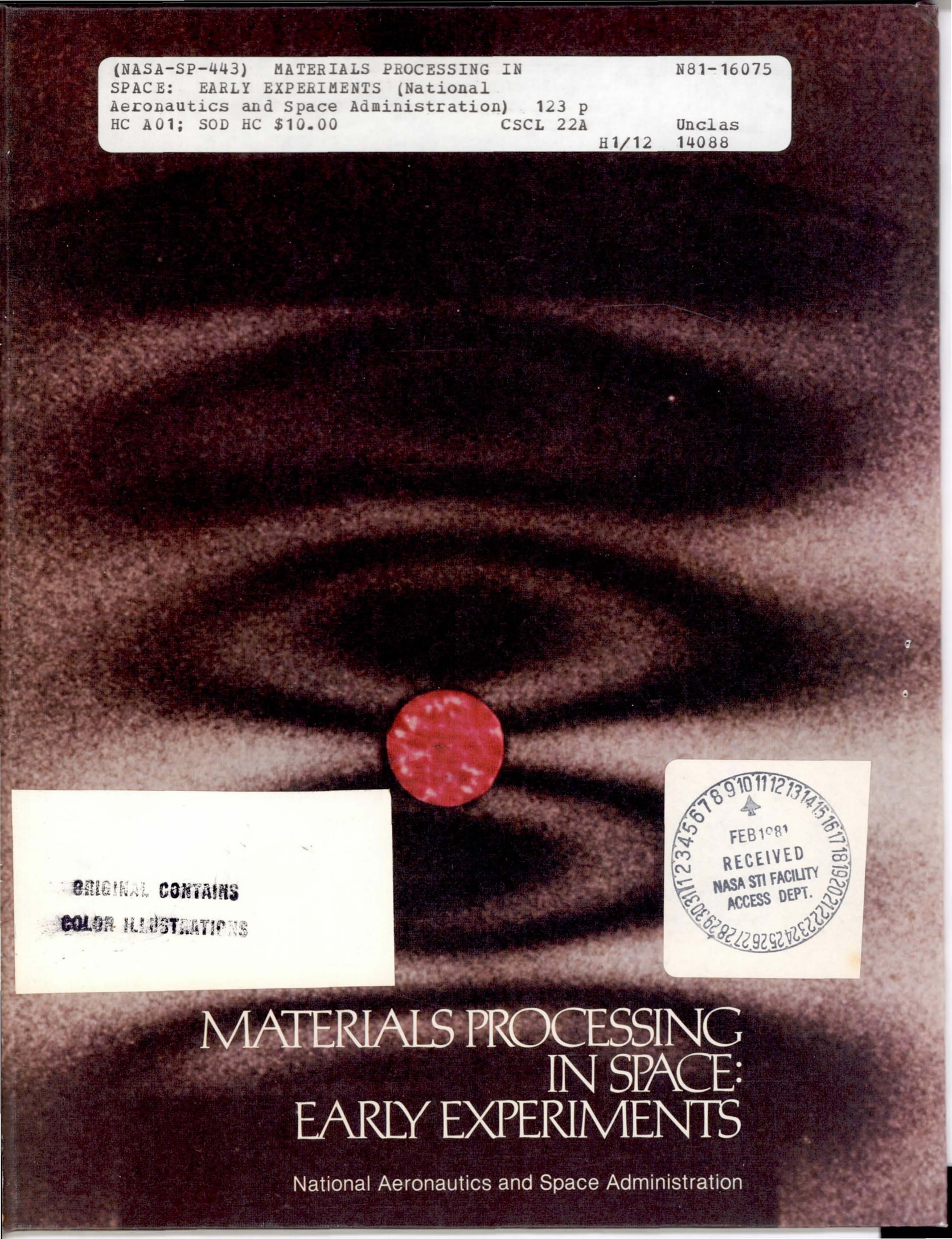

MATERIALS PROCESSING IN SPACE: EARLY EXPERIMENTS

National Aeronautics and Space Administration

MATERIALS PROCESSING IN SPACE: EARLY EXPERIMENTS

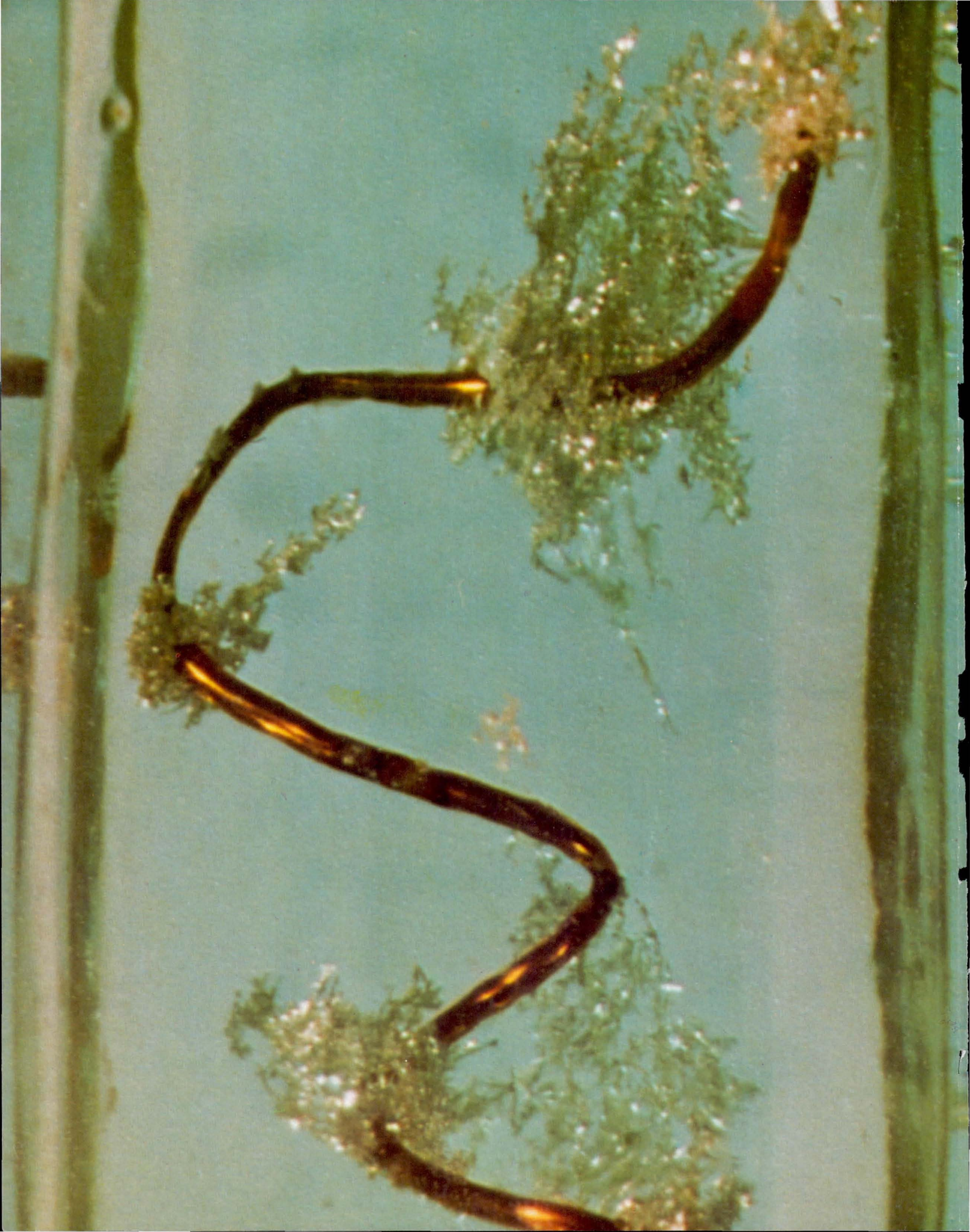

NASA SP–443

MATERIALS PROCESSING IN SPACE: EARLY EXPERIMENTS

Robert J. Naumann and *Harvey W. Herring*

Scientific and Technical Information Branch 1980
NATIONAL AERONAUTICS AND SPACE ADMINISTRATION
Washington, D.C.

Library of Congress Cataloging in Publication Data

Naumann, Robert J.
Materials processing in space.

(NASA SP ; 443)
Supt. of Docs. no.: NAS 1.21:443
1. Materials. 2. Manufacturing processes. 3. Skylab Programs. I. Herring, Harvey W., joint author. II. Title. III. Series: United States. National Aeronautics and Space Administration. NASA SP ; 443.
TA410.N28 670 80-607081

For sale by the Superintendent of Documents
U.S. Government Printing Office, Washington, D.C. 20402

FOREWORD

Although the interest in space processing of various materials began in the late 1950s and limited testing was done in drop towers and on some of the last Apollo flights, the Skylab experiments on solidification and crystal growth in space constitute the first extensive demonstration of materials processing in space, and the results substantially encourage the outlook for future applications in the field.

These experiments support the hypothesis that in the space environment, where one can escape the undesirable effects of gravity and utilize very high vacuum conditions, one will be able, when desirable, to study and better understand phenomena in materials processing that, in turn, will allow improvement of processes conducted on Earth. More important, however, it appears that one may be able to produce valuable materials in space that either cannot be produced on Earth at all or, if produced, are deficient in quality. The anticipated benefits to be derived from the absence of gravity were confirmed in some cases, perhaps even more decisively than might have been hoped for by materials scientists. In addition, many experiments produced some unanticipated and surprising results that will serve as a challenge to the scientific inquiries of future experimenters.

While the results reported herein do not support absolute conclusions as to what may be ahead in space processing, the evidence stimulates the anticipation of great advances in all those processes which are affected directly or indirectly by gravity. I visualize that one day there will be factories in space producing items for use on Earth. The Space Shuttle and Spacelab, now steadily approaching operational phases in the early 1980s, will offer the opportunity to make the next major advance in the emerging new field of processing materials in space.

William R. Lucas
Director, Marshall Space Flight Center
Huntsville, Alabama

PRECEDING PAGE BLANK NOT FILMED

INTRODUCTION

The environment of outer space offers unique opportunities for materials science and technology because of the condition of weightlessness and the unusual vacuum capability. The constraints inherent in studying and processing materials under Earthbound conditions can now be understood and hence diminished. In addition, access to space will enable us to extend the range and nature of process variables, enhancing our ability to control them. These new capabilities represent a fundamental increase in the sweep of our perspectives about materials which have been established after many thousands of years on Earth. Our challenge will be to understand and take advantage of the capabilities while simultaneously making access to space available for the performance of innovative materials processing studies and applications.

The history of materials technology is ancient and complex because it is synonymous with the history of civilization itself. The processing of materials is an art and science that dates back to prehistoric times. We are startled by the sophistication of swords made in medieval Damascus or the maturity of the 3000-year-old blast furnaces recently discovered in Africa. In fact, much of the practice of materials processing has been handed down from generation to generation; very little of the knowledge has survived the cultural transformations of shifting civilizations. Even today, much of the innovative technology in areas such as metallurgical solidification and processing of new glasses addresses an understanding of problems for which empirical solutions have long been known. Nevertheless, as we expand the limits of materials performance and generate new materials concepts for complex applications, such detailed knowledge is an essential prerequisite to progress. Consequently, the disaggregation of knowledge through historical and technological evolution, which has been so typical of the practice of materials preparation, can no longer be justified if our further technological growth is to proceed unhindered.

The environment of space offers unique opportunities for materials science while at the same time revealing our relatively immature understanding of processes. Such a lack of knowledge, in turn, limits our ability to take advantage of those opportunities. However, the challenge for us to address is the interdisciplinary nature of problems in materials processing so that we can form a proper scientific and technological base that will expand the limits of knowledge for others to build on. The global character of the environment of outer space is also encouraging international cooperation and helping us to transcend the cultural confinements that have traditionally limited the diffusion of new materials science and technology.

An understanding of the philosophy and status of materials science and technology is important for those who wish to take the initiative in exploring the advantages of the space environment for materials processing. The intrinsic objective of materials science and technology is to understand the relationships between the structure and the properties of materials. In this context, the term "structures" is used in a broad sense to include crystalline structure and defects, composition, and external morphology. The significance of the structure–sensitive properties depends intimately on the specific applications for which the material is to be used. For example, advances in solid state electronics stimulated by the communications and information industries after World War II have caused a dramatic maturing of materials science and deeper levels of understanding of the control of structure-property relationships in materials to meet increased performance demands. Important related advances in the characterization of the structure and composition of materials have also contributed to this increased sophistication. Unfortunately, our understanding of the

materials formation processes themselves has not kept pace with these advances. The complexity of processes used in the production of metals, chemicals, and crystals has made it necessary to understand them by modeling and simulating with simpler systems. Most major advances have come from the scaling up of production processes more by empirical engineering intuition than by fundamental contributions of science. The great cost of performing research on larger facilities precludes extensive work on them and thus further widens the gap between research and production. Many new high-technology industries spawned by new materials science are finding it difficult to sustain an adequate level of research activity and are rapidly reducing their edge in technology. All these pragmatic considerations serve as constraints to the involvement of materials and chemical scientists and technologists in basic studies of processing, whether on Earth or in space.

The history of new materials technology serves as an invaluable basis for understanding the nature and extent of involvement required for the innovation of new materials and processes. Much new technology has evolved from the general availability of new materials and processes which have been used in turn for novel and unplanned applications. The development of the solid state maser stimulated improvements in the growth of ruby crystals. The availability of these crystals to spectroscopists led to the discovery of the laser. Further improvements in lasing efficiency led to the development of neodymium-doped yttrium aluminum garnet (YAG) crystals. The availability of YAG crystals to magneticians was crucial to the discovery and development of magnetic bubble domain devices. Further uses of such oxide crystals as substrates for silicon epitaxial film deposition have resulted in a new class of low-noise semiconductor devices. Similar coupling of technology can be easily documented in new processing areas as well. The well-known Czochralski process of crystal growth by pulling from the melt, developed in the early 1950s for the growth of germanium crystals, was used to grow the first ruby crystals with sufficient structural perfection for use in the masers referred to previously. Until this development, sapphire and ruby crystals had been grown exclusively by the old Verneuil technique, which involved deposition from an oxyhydrogen flame under very high temperature gradient conditions. Such gradients lead to very high stresses and concomitant plastic deformation, which destroys the single crystalline nature of the boule. Subsequent to the use of the Czochralski process for ruby crystal growth, a whole new range of oxide single crystals has been prepared in new material systems that had not been known even to exist prior to this time. These new crystals have found a wide range of applications, including nonlinear optics, laser host materials, and substrates for magnetic bubble domain devices.

Another pervasive and undesirable feature of the Verneuil process is the uncontrolled nature of convection effects that occur in the molten pool because of the very high temperature gradients in this system. The nature of these convection phenomena has resisted understanding up to this point because of the complex and unknown effects of thermal and surface-tension-gradient convection. The weightless environment of space offers new capabilities by which such phenomena can be studied and possibly controlled to a measurable extent. These convection effects play a limiting role in establishing the compositional uniformity and low level of crystalline defects so essential to adequate performance of the materials for present and future applications.

It is interesting to consider the time rate of evolution of these innovations from conception to application. When old processes are used to prepare new materials, as described for Czochralski growth, the innovation time ranges from 15 to 20 years. The use of new processes to prepare old materials with improved properties, such as unidirectional solidification for single-crystal turbine blades or continuous casting for steel ingots, requires times from 20 to 25 years. The longer time for innovating new process technology is a result of both the complexity of the many variables required for process control and the lack of any knowledge base from which to evolve. It is in this context that the generation of new processing technology using the space environment must be judged.

John R. Carruthers
Director, Materials Processing in Space
National Aeronautics and Space Administration
Washington, D.C.

CONTENTS

Chapter 1. The Space Environment and the Promise of Space Processing 1

Chapter 2. Potential Applications of Space Processing 15

Chapter 3. The Evolution of Apparatus for Materials Processing in Space 33

Chapter 4. Processing Semiconductor Materials 49

Chapter 5. Metallurgical Processing 63

Chapter 6. The Behavior of Fluid in Low Gravity 75

Chapter 7. Post-Skylab Activities 89

Chapter 8. Future Programs 105

Acknowledgment 111

Index 112

On the cover—hologram showing a single-axis acoustic levitator levitating a clay particle.

Molten copper in a radiofrequency coil.

Chapter 1.

THE SPACE ENVIRONMENT AND THE PROMISE OF SPACE PROCESSING

In the conceptual years of space flight it was recognized that the orbital environment was in many ways different from that of Earth and that the design and construction of spacecraft to operate in this environment would be a formidable challenge. The primary environmental factors that had to be considered were the vacuum of space, energetic radiation from the Sun and other sources, and the near absence of apparent gravitational effects. Of these factors, the long exposure to a virtually zero-gravity environment is a truly unique situation that cannot be duplicated or even approximated for any length of time on Earth.

LOW GRAVITY

It is important to understand how the condition of weightlessness or apparent lack of gravity develops. Newton's law of gravitation tells us that any two objects have a gravitational attraction for each other that is proportional to their masses and inversely proportional to the square of the distance between their centers. A spacecraft orbiting at an altitude of 400 km is only 6 percent farther from the center of the Earth than it would be if it were on Earth's surface. From Newton's law, then, the gravitational attraction at that altitude is only 12 percent less than the surface value, and the spacecraft and all its contents are very much under the influence of Earth's gravity. The phenomenon of weightlessness occurs because the spacecraft and its contents are in a state of free fall.

An orbiting vehicle is continuously falling toward the center of the Earth in the same manner as an object dropped from a great height. The difference is that the orbiting vehicle is given an initial velocity such that its trajectory carries it beyond the surface of the Earth before the gravitational acceleration can pull it to the ground, as shown in figure 1.1. Since the spacecraft and every object in it are being accelerated at the same rate toward the center of the Earth, they fall at the same speed. Since the interior objects tend to remain motionless relative to one another and to the vehicle, they are said to be in a weightless or zero-gravity environment. As stated before, this description is misleading: The vehicle and all its contents are very much under the influence of gravity; they are only weightless relative to the reference frame moving with the vehicle. The physical basis for this argument is illustrated in figure 1.2. It is important to recognize that Einstein's principle of equivalence tells us that physical behavior inside a system in free fall is identical to that inside a system far removed from gravitating matter (fig. 1.3). Therefore the term zero gravity for a freely falling system is technically correct.

A zero-gravity environment is an ideal situation that, in practice, can never be completely realized in an orbiting spacecraft. There are a number of kinetic effects associated with an actual spacecraft that produce artificial gravitylike forces. Any unconstrained object in a spacecraft is actually in its own orbit around the Earth. Only if an object is located at the center of mass of the spacecraft will it have exactly the same orbit as the craft. If the spacecraft is held in an inertial orientation, that is, at constant orientation relative to the fixed stars, an object released motionless relative to the spacecraft at some distance from the center of mass along the flight path will have an orbit shape identical to that of the spacecraft but will always either lead or lag the position of the center of mass of the spacecraft. However, because of the inertial orientation of the craft, the object will

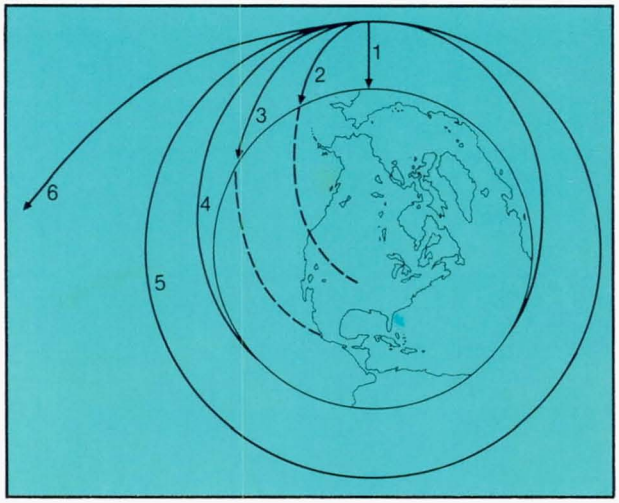

Figure 1.1. *Orbital paths of a falling body about Earth. To demonstrate that a spacecraft orbiting Earth is constantly falling, consider the various trajectories of an object dropped from a point above the sensible atmosphere. With no tangential velocity, the object falls straight down (trajectory 1). As the tangential speed is increased, the object still falls, but the initial speed carries it in a trajectory that is a segment of an ellipse, and the point of intersection with the Earth moves farther from the release point (trajectories 2 and 3). As the speed is increased further, eventually the object misses the Earth completely (trajectory 4). As the speed is further increased the trajectory becomes a circle, (trajectory 5), then a larger ellipse with the release point closest to the Earth. When the initial speed is 41 percent higher than circular orbit speed, the object follows a parabolic, or escape, trajectory and will never return (trajectory 6).*

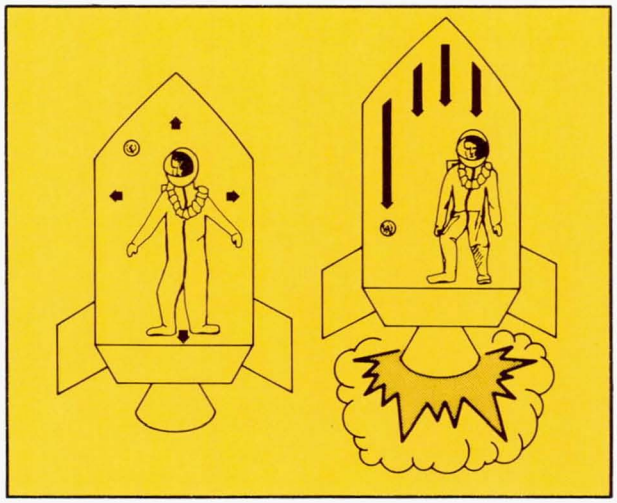

Figure 1.3. *Einstein's principle of equivalence between a gravity field and an accelerated system. Consider a man in a spaceship far enough removed from any gravitating mass to be truly in a zero-gravity field. A coin will float in the same way it did in the elevator (fig. 1.2) when the rope broke. If the man fires the rocket engine and accelerates at 1 gravity, the force is transmitted through the man to the coin, and the man feels the coin's weight. Now the coin will have whatever velocity the system had when the coin was released, but since the system is accelerating relative to the coin, the man sees the coin accelerate to the floor at the rate of 32 ft/s^2 (1 gravity). No experiment the man can perform can distinguish whether he is in a gravitational field or his system is being accelerated. Conversely, there is no physical difference between a state of free fall and the complete absence of a gravitational field.*

Figure 1.2. *The equivalence of free fall and weightlessness. A man in an elevator suspended by a rope is in a 1 gravity environment. If he drops a coin, it will accelerate to the floor at the rate of 32 ft/s^2. If the rope breaks, the entire system will accelerate at 32 ft/s^2. The coin behaves in exactly the same manner as before, but now the man sees it float in midair. Relative to the elevator, the coin is weightless.*

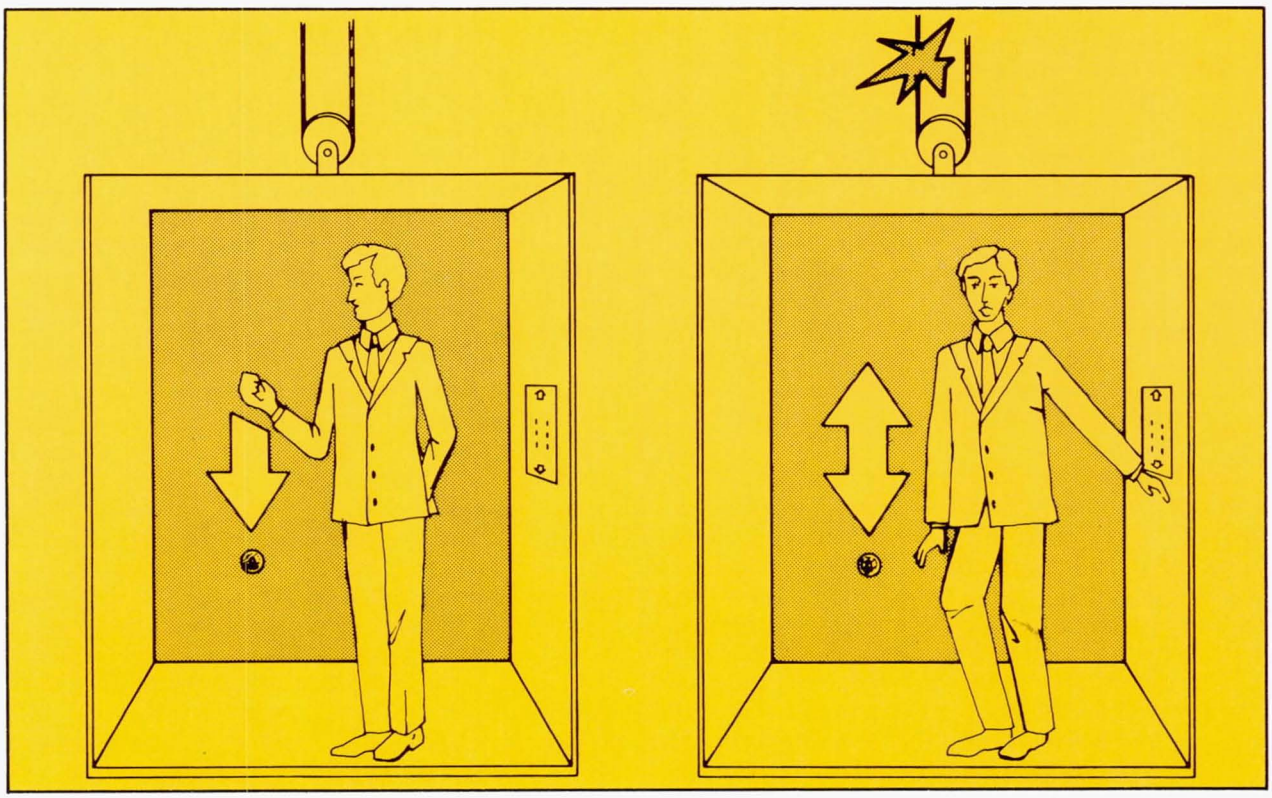

move in a circle around the center of mass during the course of an orbit, as may be seen in figure 1.4.

An object released motionless relative to the spacecraft at some distance from the center of mass along the radius vector from the center of the Earth will have an orbit slightly different from that of the spacecraft. Since the velocity required to maintain a circular orbit varies inversely with the square root of the distance from the center of the Earth, this object will have a slightly excess velocity which will put it into an elliptical orbit with a different period. This will cause the object to slowly drift away from its initial position as the spacecraft moves around the Earth (fig. 1.4). The accelerations required to continuously alter the trajectories of such interior objects to keep them in the same relative position are on the order of 10^{-7} g (1 ten-millionth of the Earth's gravity) for every meter of lateral displacement from the spacecraft center of mass.

Similar disturbances result in a spacecraft that maintains a fixed orientation relative to Earth. Now objects released motionless relative to the spacecraft, as discussed previously, will have additional velocities imparted because of the rotation of the spacecraft. These additional velocities will modify the orbit of the object, resulting in the motions relative to the spacecraft illustrated in figure 1.4. Again, the accelerations required to constrain an object in a fixed position relative to the spacecraft are approximately 10^{-7} g for each meter away from the center of mass.

The residual atmosphere even at orbital altitude exerts a slight drag force on the spacecraft and causes a small deceleration. A free object inside the spacecraft is not subject to this force and therefore has an apparent acceleration relative to the spacecraft. At an altitude of 400 km the force imparted to a spacecraft from this drag is approximately 0.001 Newton per square meter, which is only a hundred-millionth of the atmospheric pressure at the Earth's surface. For Skylab, this atmospheric drag resulted in deceleration on the order of 10^{-6} to 10^{-7} g.

These accelerations represent the quiescent background associated with near-Earth orbital flight. Normal operations within a spacecraft produce additional accelerations of a random nature (g-jitter), which are on the order of 10^{-4} to 10^{-6} g. For example, an astronaut nodding his head imparts an acceleration of this magnitude to the spacecraft.*

* A 10-kg mass oscillating with an amplitude of 10 cm at 1 Hz will impart an acceleration of 4×10^{-5} g to a 100-ton spacecraft.

Figure 1.4. Motion of objects inside a spacecraft. In an inertial orientation an object B released motionless relative to the spacecraft displaced along the flight path will have a similar orbit but will be slightly displaced in time. This will cause the object to execute a circle around the center of mass. However, object A, displaced along the radius vector, will have a higher orbit with a longer period. It will execute an expanding elliptical path about the center of mass until it eventually hits the wall of the spacecraft. In an Earth-fixed orientation object B has a slightly elliptical orbit because of the radial velocity component imparted by the spacecraft rotation, but the period remains the same. The object remains in nearly the same location relative to the spacecraft, executing a small motion above and below the flight path. Object A moves in a helical path, eventually encountering the spacecraft wall.

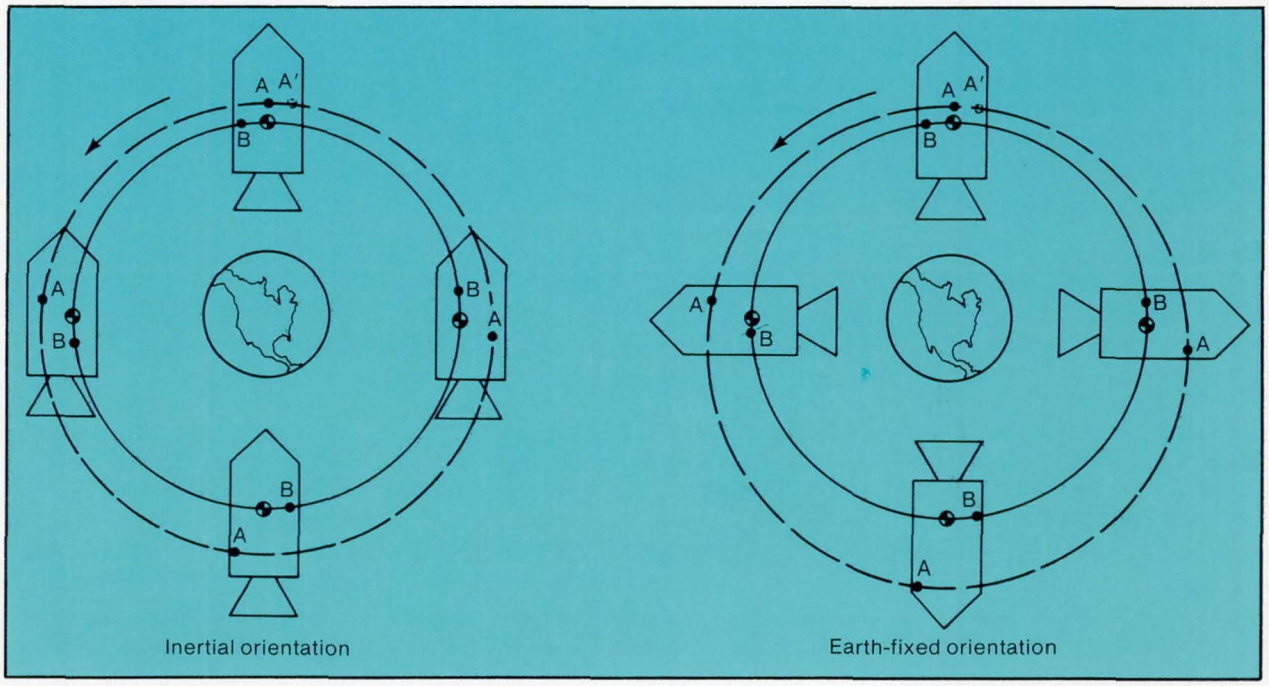

Accelerations resulting from astronauts' moving from one location to another within the cabin are on the order of 10^{-2} to 10^{-4} g when they start and stop, depending of course on the inertia of the spacecraft and how hard the astronauts push off and stop. All these extraneous accelerations must be considered in planning for space processing operations in space. For example, if an object is to be suspended in a furnace for containerless processing, there must be some force applied to it to counteract the residual accelerations and prevent impact with the furnace wall.

ATMOSPHERIC EFFECTS

The composition of the residual atmosphere at an altitude of 400 km is quite different from that of the sea level atmosphere. Instead of having 78 percent nitrogen and 21 percent oxygen with traces of argon, carbon dioxide, and so on, the residual atmosphere consists predominantly of atomic oxygen. Nitrogen and helium are the next most abundant species and constitute 5 to 20 percent of the residual atmosphere, depending on the amount of solar activity. The atmospheric density is less than one-billionth that of the sea level atmosphere. A consequence of this low density at orbital altitudes is that the residual atmosphere plays a negligible role in thermal transport, either by convection or conduction. The thermal control of a spacecraft must be accomplished totally by radiation balance. The equilibrium temperature of the spacecraft is that temperature at which the heat lost in the form of infrared radiation is equal to the heat absorbed from the Sun, the radiant energy absorbed from the Earth, and the heat generated within the spacecraft. By an appropriate choice of thermal control coatings it is not difficult to keep the temperature in the spacecraft interior in the range of comfort to human beings, that is, 25 ± 5° C.

The atmospheric pressure at 400 km altitude is approximately 10^{-7} torr.* Although this is not considered an ultrahigh vacuum, nonmetallic materials present on the exterior of a spacecraft can liberate significant quantities of vapor in such an environment. These outgassing products consist of adsorbed gas and water vapor, plasticizers, unreacted monomers, and fragments of the polymeric materials, usually methyl silicones, that are commonly used for paints, binders, and adhesives. These molecules typically diffuse from their origin to other regions of the spacecraft surface where they may redeposit and react under the influence of ultraviolet radiation from unfiltered sunlight to form films that can interfere with the optical and thermal control performance of a variety of components.

To remain in a circular orbit at 400 km, a spacecraft must travel at a speed of approximately 7.85 km/s. Since this is several times faster than the average speed of molecules in its vicinity, the spacecraft creates a bow wave and wake analogous to that of a boat moving in water. The wake region in the shadow of the spacecraft is essentially devoid of material. The pressure on the surface of the spacecraft facing the direction of motion is increased by this effect to a value of between 10^{-4} and 10^{-6} torr, depending on altitude. An observer looking forward in the direction of motion would see a highly collimated monoenergetic molecular beam composed mostly of atomic oxygen. The average velocity of the molecules impinging on the front surface of the spacecraft corresponds to the average velocity of molecules contained within a furnace operating at a temperature of 65 000 K.* This high-temperature, chemically active beam may offer some unique experimental opportunities for studying high-speed aerodynamics and molecular collision kinetics.

If the observer looks aft into the wake of the spacecraft, most atmospheric molecules will be moving away from him, as seen in figure 1.5. The only exceptions are occasional light atoms such as hydrogen or helium that have much higher than average velocity and can overtake the spacecraft. The flux of molecules incident on a surface oriented toward the wake direction is only 10^6 to 10^7 molecules/cm^2/s, which is equivalent to a pressure of only 10^{-14} to 10^{-15} torr. This is less than one-quadrillionth of the atmospheric pressure on Earth and is equal to or better than the vacuum obtained in the best ground-based facilities. The surface of a clean shield specially prepared to minimize outgassing can provide an ultrahigh vacuum facility. This space vacuum facility has an additional advantage in that it can accept high heat loads which the ground facilities cannot because of their cryogenic walls. In addition, the space vacuum facility has a virtually infinite pumping capability. Such a facility would be ideal for preparing ultraclean surfaces or for preparing ultrapure materials by high-temperature evaporation.

The potential for materials processing in space is only beginning to be explored. Undoubtedly, there are many possibilities not yet recognized. Most experiments thus far have been designed to examine the results of eliminating effects of gravity-driven convection and sedimentation and were constrained in many ways by the requirement that they had to be designed to take advantage of available flight

*A torr is the pressure required to support a column of mercury 1 mm in height. Sea level atmospheric pressure is 760 torr.

*However, the heat transfer from these "hot" molecules is negligible because of their relatively low density.

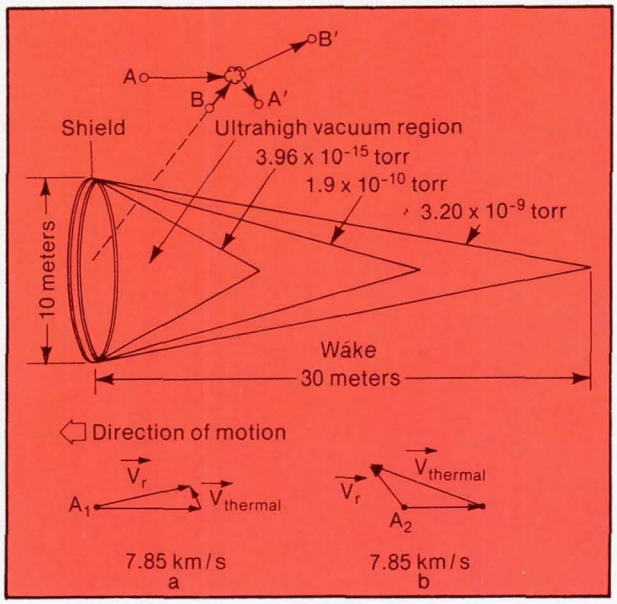

Figure 1.5. Concept of a space vacuum facility. A disc or shield moving at orbital speed (7.85 km/s) creates a region of extremely high vacuum in its wake. This can be understood by considering that, relative to the shield, all molecules have orbital speed added to random thermal velocities. For most heavier atmospheric molecules (O, N_2, O_2, etc.), the orbital speed is much higher than their thermal speed, so virtually all such molecules continue to move in the direction of the wake (a). Only the light molecules (H, He, H_2) occasionally have thermal speeds exceeding orbital speed and are able to enter the ultrahigh vacuum region (b). Outgoing molecules B from the high-vacuum region are scattered away by collisions with the high-speed residual atmospheric molecules A and cannot return. If mass B>> mass A, it is possible to scatter some A molecules into the high vacuum region.

opportunities. The exciting prospects of containerless melting and solidification and the use of the vacuum in the wake of a spacecraft are only beginning to be considered. The advantages of processing in space are described in detail in the following sections.

THE ABSENCE OF BUOYANCY-DRIVEN CONVECTION

In the history of materials science, significant advancements have been made when better means have become available to control process variables such as temperature, composition, and flows. The weightless environment of space offers a new dimension in process control, as demonstrated in the following paragraphs.

Convective flow is a result of virtually every Earth-based process involving fluids in which there are nonvertical thermal gradients, that is, temperature differences between two adjacent elements of fluid. Because almost all fluids expand when heated, even the slightest temperature difference causes the warmer element to become less dense (or more dense in the few cases such as water below 4° C where the fluid contracts when warmed). In a gravity field, the less dense fluid element weighs less and is therefore displaced by the heavier fluid. This results in a circulation or convective flow (fig. 1.6).

A second type of convection, referred to as unstable convection, results whenever a more dense fluid is above a less dense fluid. This happens often in the atmosphere since air is relatively transparent to solar radiation and therefore most heating takes place near the ground. Such an unstable situation can be maintained provided the buoyant forces driving the flow are small compared to the viscous forces opposing it so that an element that starts to rise has time to equilibrate with its surroundings. After a certain critical density gradient is reached, the element rises too fast to maintain this equilibrium, and spontaneous flow results, usually in the form of cells or vortex rolls that generally cause more mixing than the conventional convection discussed previously. This may be seen in figure 1.7.

Similar convective flows may be produced by compositional differences. The density of a liquid depends on the amount of dissolved material in it (for example, adding salt to water increases its density). Therefore, if there are concentration gradients in the liquid, that is, if regions exist with different amounts of dissolved material, the different densities will result in buoyancy forces that will drive a convective flow just as in the case of temperature gradients. An example of this can be seen in figure 1.8, which shows a

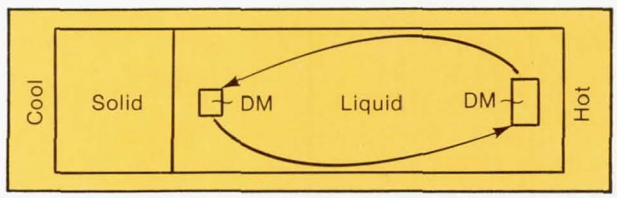

Figure 1.6. Natural convection in horizontal crystal growth. An element of mass near the cool end shrinks in volume, thereby increasing its density and causing it to sink as it is displaced by warmer, less dense fluid. At the same time a similar element of mass near the hot end expands, becomes less dense, and rises as it is displaced by cooler, more dense material. These combined effects cause a circulation that results in mixing the molten region, reducing the boundary layer at the solidification interface, and conducting heat through the liquid, which lowers the thermal gradient in the melt.

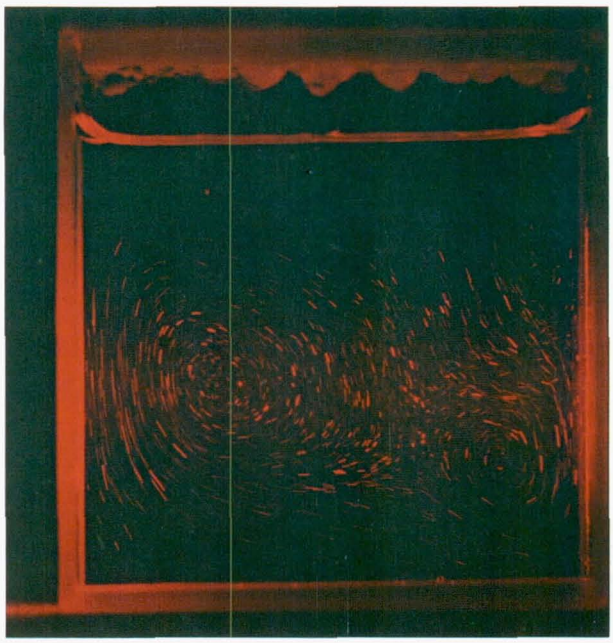

Figure 1.7. Unstable convection. A glass cuvette containing water and small latex spheres is heated at the bottom and illuminated from the side with a thin sheet of laser light. A time exposure reveals the traces of the small particles. Several convective swirls are formed as the warm water rising from the bottom is displaced by the cooler water from the top.

Figure 1.8. Schlieren photograph of a crystal growing from aqueous solution in Earth gravity. The convective plume is caused by the lower density of the growth solution after it has given up some of its solute to the crystal.

crystal being grown by the solution method. As the solute is incorporated into the growing crystal, the depleted solvent becomes lighter and rises in a plume above the crystal. The photograph was taken by the Schlieren technique, which highlights changes in the density of the liquid.

Convective flow is not necessarily undesirable. In many processes it is used to advantage to produce mixing or homogenization. However, it often complicates the process and makes it difficult (if not impossible) to predict accurately and control precisely the process parameters. The weightless environment can be exploited effectively to eliminate the driving force for convective flows that arise in molten metals, liquids, and gases because of density differences. Diffusion becomes the predominant mechanism for thermal and mass transport. Since diffusion processes can be accurately predicted mathematically, they are subject to much more precise measurement and control. For example, if the boundary values of temperature are known in a convectionless system, the thermal field is everywhere determined. Many processes do not require this precision of control, but in some it is crucial.

The virtual elimination of gravity-driven convection may have a number of important applications in controlling interface kinetics and dopant distribution in crystal growth, providing high thermal gradient to growth rate conditions for directional solidification, for studying the mechanisms responsible for macro- and microsegregation in castings, for preventing unwanted mixing in electrokinetic separation techniques, and for studying a variety of fluid dynamic effects that are often masked or overwhelmed by gravity-driven flows. A more detailed description of some of the applications is given in chapter 7.

The effects of convection can be minimized but not entirely eliminated in processes carried out on Earth by a number of strategems. In some systems it is possible to arrange things so that the hot region is above the cold region when it is desirable to avoid convective mixing. This is why directional solidification is carried out with the solidification interface below the melt. However, in some systems the segregation at the interface is such that a less dense composition is formed in the fluid above the interface. Figure 1.9 shows convective cells rising from such a system. Even without this complication, it is virtually impossible to avoid radial thermal gradients because of wall effects. Such gradients will produce an immediate flow, no matter how small they may be. The velocities of these flows, of course, are correspondingly less as the gradients are reduced.

A dimensionless parameter called the Grashof number, which is the ratio of buoyancy to viscous force, characterizes convective flow. The number is given by

$$Gr = \frac{g\ell^3}{\mu^2}\frac{\Delta\varrho}{\varrho} = \frac{g\ell^3\beta\Delta T}{\mu^2}$$

where β is the coefficient of expansion, g is the acceleration of gravity, ℓ is the characteristic dimension, ΔT is the temperature variation, and μ is the fluid kinematic viscosity. Two quite different systems will have the same scale convection flow if their Grashof numbers are the same. The actual flow velocity is given by $\sqrt{Gr}\mu/\ell$.

As an illustration, one might simulate a microgravity 10^{-6} g convective field by altering the other parameters in a 1-g field to give the same Grashof number. One could do this by making all the dimensions 100 times smaller, or by finding a fluid that is 1000 times more viscous, or by reducing the temperature variations by 10^6. Needless to say, this is not always practical; however, the application of strong magnetic fields to conductive melts effectively increases the viscosity and has been successful in reducing thermal convection in a number of processes.

It is important to recognize that simply setting g equal to a low value in the Grashof number does not really describe an orbital situation. The higher accelerations from internal motions do not represent a net impulse, since each acceleration is offset by an equal and opposite acceleration a short time later. Thruster firings represent net momentum changes, but they are of short duration and therefore do not drive sustained flows. Only the very low accelerations resulting from drag or from the kinetic reactions associated with the slightly different Keplerian orbits can produce sustained flows, and these tend to average to zero over the orbit. The behavior of fluids under these circumstances is not completely understood; it was the subject of investigation in some of the early flight experiments.

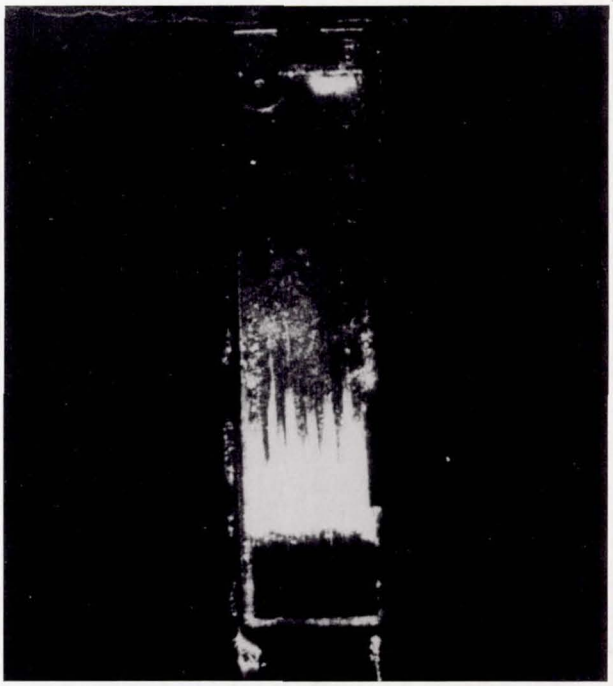

Figure 1.9. *Schlieren photograph of the convection cells caused by solutal convection. A transparent metal model material ($NH_4OH + H_2O$) is being directionally solidified by cooling the bottom of a cuvette. As the NH_4OH solidifies, H_2O is rejected at the interface (dark region at the bottom). Since H_2O is less dense than the NH_4OH solution, convective cells rise even though the thermal gradient would prevent thermally driven convection. These cells are easily seen by the Schlieren technique, which responds to changes in the index of refraction and diffracted light from the edges of the apparatus.*

THE ABSENCE OF SEDIMENTATION AND BUOYANCY

When a particle (such as a solid, a gas bubble, or a droplet of an immiscible liquid) is immersed in a fluid, it is subjected to a buoyancy force given by the product of the volume of the particle, the acceleration of gravity, and the difference in density between the particle and the suspending fluid. This force produces an acceleration that causes the particle to rise or settle, depending on the sign of the density difference term. This motion is opposed by the drag force, which for small velocities can be shown to be proportional to the linear dimension of the particle, the viscosity of the medium, and the velocity. For a sphere, the drag force is given by the Stokes formula,

$$F_D = 6\pi a\eta v$$

where a is the radius of the sphere, η is the viscosity, and v is the velocity.

The particle will quickly reach a velocity determined by equating the drag force to the buoyancy force, which for a sphere is given by

$$v = \frac{2a^2(\varrho - \varrho')g}{9\eta}$$

For aqueous solutions, $\eta \sim 10^{-2}$ g/cm/s, and the Stokes velocity is on the order of

$$v\ (\mathrm{cm/s}) \sim 10^4\, a^2\ (\mathrm{cm})$$

in Earth's gravity. For particles with sizes in the tens of micrometers, the Stokes velocity is $\sim 10^{-2}$ cm/s, and settling times are tens of minutes. For micrometer-sized particles, the settling times are tens of hours. As the particles

approach micrometer sizes, the gravitational potential energy approaches the thermal energy of the molecules in the liquid. This means that the random molecular collisions produce forces comparable to the buoyant forces, and the particles tend to be kept in suspension by these random velocities (Brownian motion). Thus in Earth's gravity it is possible to maintain a stable suspension of particles only if they are smaller than ~ 1 μm in size. In a low-gravity environment, it should be possible to maintain a suspension of much larger particles. This can be both an advantage and a disadvantage. For example, it should be possible to investigate processes involving suspensions, such as chemical fining of glasses, preparation of unique foams, floculation processes, Ostwald ripening, polymerization processes, and preparation of immiscible alloys. On the other hand, many of the convenient separations provided by buoyancy that we tend to take for granted on Earth, such as the removal of unwanted bubbles, will not occur in low gravity; attention must be given to alternative techniques for accomplishing these important separations.

The absence of sedimentation can be only poorly simulated on the ground. Gentle stirring can be used to maintain a suspension, provided the Stokes velocity is not too high. However, the flows involved often produce other unwanted effects, such as coagulation, that limit its usefulness. It is also possible to slowly rotate a container so that particles that tend to settle are carried by the viscous forces in the rotating fluid and the gravitational force vector effectively rotates around the particle, thereby averaging to zero. The limiting factor in this process is the centrifugal force, which causes denser particles to drift slowly to the perimeter and less dense particles to drift to the center.

ABSENCE OF HYDROSTATIC PRESSURE

Strictly speaking, it is the lack of hydrostatic pressure that accounts for the absence of buoyant forces, which results in the elimination of natural convection and sedimentation discussed previously. Another aspect of the lack of hydrostatic pressure is the elimination of the tendency for a liquid or solid to deform under its own weight. This means that liquids will take a shape that tends to minimize surface energy. Menisci formed from between gas–liquid–solid or liquid–liquid–solid interfaces will be determined solely by surface tension without hydrostatic distortion. This permits a more detailed investigation of a number of wetting and spreading phenomena, particularly effects such as a contact angle hysteresis and moving interfaces. Other studies that can be aided by the lack of hydrostatic pressure include critical point phase transitions, the shape and stability of liquid bridges or floating zones, and the coalescence of viscous droplets.

Normally the gravitation contribution plays a negligible role in molecular interactions. The one exception is near a phase transition critical point. As such a critical point is approached, the ensemble of molecules that are involved in thermal fluctuation is so large that the differences in gravitational potential over the ensemble become significant and the factors affecting the transition become dependent on gravity in a way that is not well understood. Furthermore, the times required to approach equilibrium are long, generally on the order of hours. Therefore, such experiments are logical candidates to be performed in a weightless environment.

The ability to form stable floating zones that are considerably larger in length and diameter than what is possible on Earth permits a detailed study of this important crystal growth method. Of particular interest is the problem of Marangoni convection, which is introduced by the fact that surface tension is dependent on temperature. Since a thermal gradient is required in the molten zone, a flow from the region of low surface tension to the region of high surface tension will result. The introduction of a surface contaminant such as an oxide layer or a liquid encapsulant will dramatically alter the surface tension and may be useful in controlling such flows. Floating zone growth and refining is an important technique used on Earth. It is limited to materials and size configurations for which the surface tension is large enough to contain the liquid under the force of the hydrostatic pressure. In space no such restriction exists. This has a major advantage in allowing the development of radically new configurations to tailor thermal profiles to produce sharp gradients and planar solidification interfaces essential to the prevention of constitutional supercooling and radial segregation in crystal growth. Also, the floating zone process in space will benefit by the improved control of concentration and temperature at the growth interface brought about by the absence of gravity-driven convection.

The absence of distortion from hydrostatic pressure may lead to other interesting applications. For example, it may be feasible to produce intricate castings without deformation in a weightless environment by use of a thin oxide skin. A thin skin would enable the casting to be processed with a very high thermal gradient which a thick mold would tend to level out. It may be desirable to machine objects such as high-temperature turbine blades before the blades are toughened by the final heat treatment. The blades could be coated with a thin layer of alumina to serve as a skin and taken to space for the final heat treatment. If substantial improvement from a complete melting and resolidification of either a dispersion oxide hardened blade or a directionally solidified eutectic blade can be realized, the added benefit may justify the space transportation cost.

The only way in which the effects of hydrostatic pressure on liquid surfaces may be effectively eliminated on Earth is to suspend material in a fluid of neutral density. This technique was developed by the Belgian scientist J. Plateau over 100 years ago and has been used recently to study the stability of floating zones (see chapter 6). The presence of the supporting fluid severely limits what can be accomplished, and the interfacial effects between the fluids produce extraneous forces that sometimes mask the effects to be investigated.

CONTAINERLESS PROCESSING

One of the most exciting prospects of processing materials in space is the ability to process uncontained liquids or melts. In the absence of other forces, the shape of a liquid in a weightless environment will assume a configuration that minimizes interfacial energy. For a completely uncontained liquid the equilibrium shape, or minimum-surface figure, is a sphere. In the condition of free fall the sphere remains essentially unaccelerated relative to the spacecraft. However, the small kinetic reactions originating in the slightly different trajectory of the freely floating sphere, the background jitter of the spacecraft, and the residual velocity imparted to the sphere upon release require an active position control if the sphere is to remain within the confines of the furnaces for any length of time.

This can be accomplished in a variety of ways. If a gaseous environment is permissible, acoustic drivers similar to loud speakers can exert an acoustic radiation pressure on the sphere. By setting up a standing wave by means of a reflector, a stable acoustic well will exist at one-quarter wavelength from the reflector, and the sphere will be retained in the center of this well provided the energies associated with the perturbing impulses do not exceed the energy of the well. Such an acoustic driver putting out 160 dB (1 W/cm^2) at 15 kHz can levitate a low-density solid sphere in Earth's gravity (fig. 1.10). However, liquid drops tend to deform and become unstable under such high-intensity sound fields (fig. 1.11). In low gravity substantially less acoustic power is required to maintain position control. The use of three orthogonal drivers can produce three-axis positioning and by appropriate phasing can also provide rotational control. These systems are discussed in more detail in chapter 3.

For systems requiring a vacuum environment, electromagnetic positioning can be used provided the sample has some conductance. A radio frequency field induces a current in the sample which in turn reacts to repel the inducing field. Figure 1.12 shows coil configurations that provide three-axis stability. Such devices can easily provide sufficient force to levitate a metallic sample at 1 g, as seen in figure 1.13. However, two difficulties arise. First, the power required to levitate the sample usually produces enough heat to melt it. Hence, it is not always possible to solidify the sample in a controlled manner. Second, there is a region along the axis of the coil where the B field is perpendicular to the surface of the sample. No force is produced at this

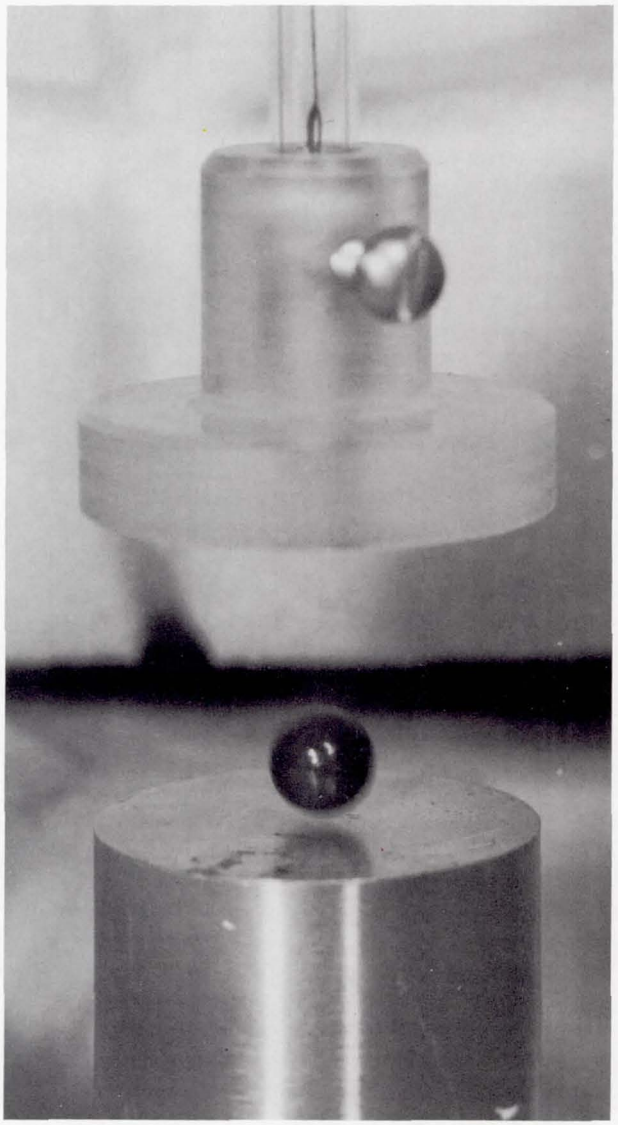

Figure 1.10. *Solid object levitated ultrasonically in 1-g field. The aluminum cylinder at the bottom is oscillating vertically at 15 kHz. The plastic reflector above is a reflector that sets up a standing wave pattern. The sphere is suspended by the high-pressure region just above the driver, and its center sits in the first low-pressure region or energy well at* $\lambda/4$ *above the driver.*

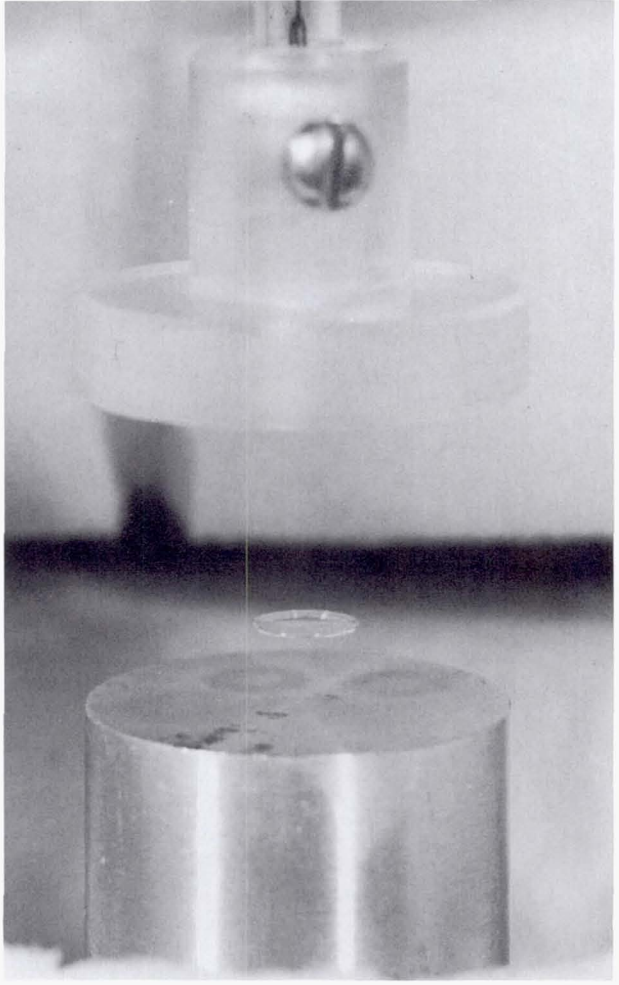

Figure 1.11. Glycerin drop levitated in the acoustic field shown in figure 1.10. Note the severe distortion caused by the combination of surface tension, hydrostatic pressure, and acoustic pressure. A less viscous material such as water disintegrates after the size reaches a few millimeters.

Figure 1.13. Molten sample of copper suspended in radiofrequency coil.

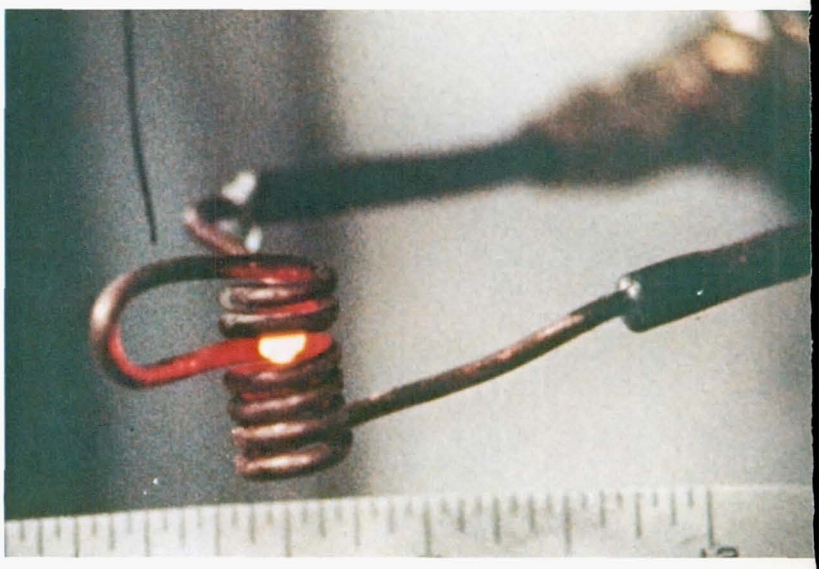

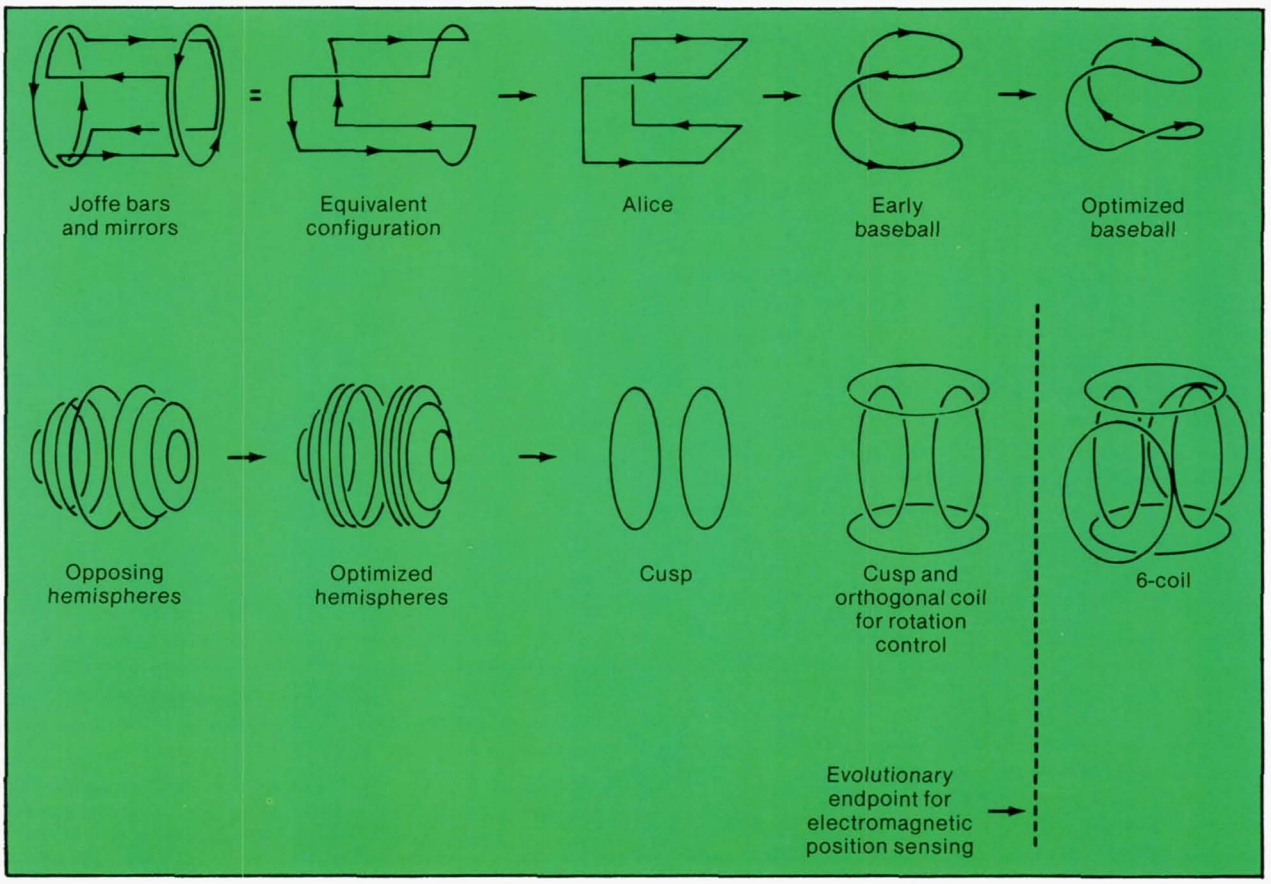

Figure 1.12. Coil configurations to provide basic three-axis positioning for a low-gravity electromagnetic containerless processing facility.

point, and when the sample melts in 1 g, hydrostatic pressure can overcome the surface tension and allow the sample to leak out.

Other mechanisms exist for position control, such as electrostatic repulsion and radiation pressure. If there were a requirement to avoid any force on the sample, a container could be literally flown around the sample by means of control jets.

One of the principal advantages of containerless processing is the elimination of wall effects such as contamination, nucleation, and induced strain. Since materials such as silicon and many of the oxide glass formers are highly reactive in the molten state (to the point of being universal solvents), considerable work has gone into minimizing container effects. These are discussed in more detail in chapter 7.

Silicon, for example, is grown by a semicontainerless process called the Czochralski method. A seed crystal is lowered into the free surface of a melt contained in a crucible. As it is slowly withdrawn, molten silicon adhering to it solidifies and a large cylindrical single crystal is pulled out of the melt (fig. 1.14). The melt will contain some crucible impurities

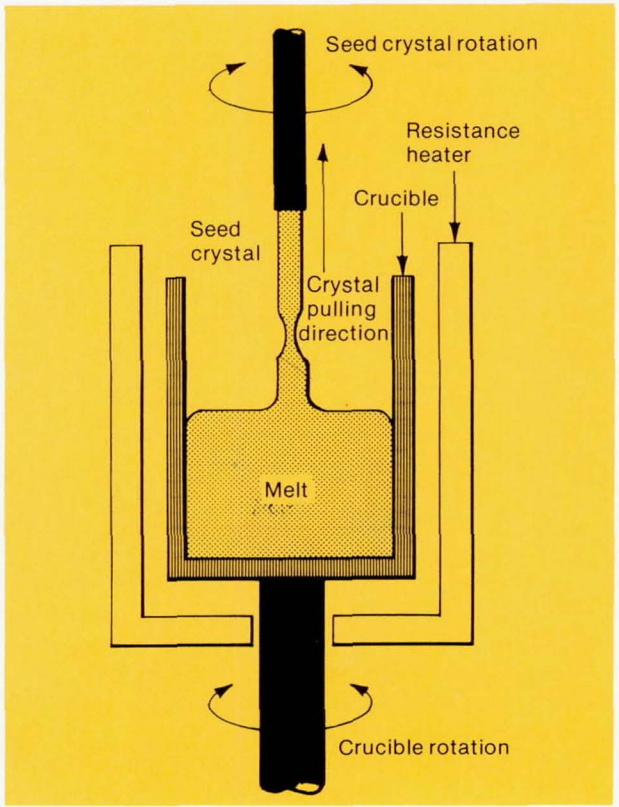

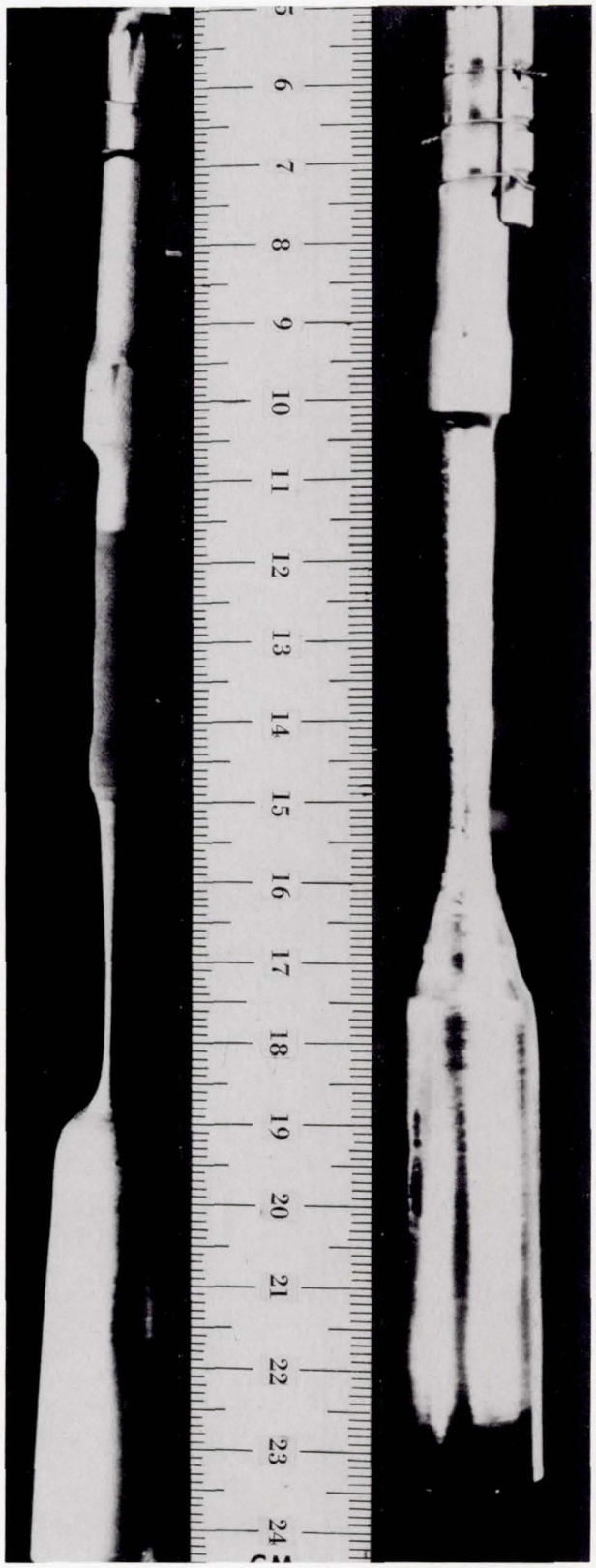

Figure 1.14. Crystal pulling by the Czochralski method. The technique of pulling from the melt first practiced by Czochralski in 1917 results in a crystal free of the physical constraints imposed by the crucible. Shown here are a schematic of Czochralski growth and photographs of crystals grown by this method. The necessity of having to maintain the melt in a crucible that often acts as a contamination source is one of the main disadvantages of this technique.

as well as whatever impurities were in the starting material. For applications that require very pure silicon, a semicontainerless process known as floating zone growth is used (fig. 1.15). A rod is suspended at both ends and a region in the middle is melted. The molten zone is supported by the surface tension of the liquid. By moving either the rod or the heater, the zone can be made to traverse the rod. Impurities generally have segregation coefficients less than unity, which means they are not incorporated into the growth region as readily as the pure substance. Instead of allowing them to accumulate at the interface until a steady state is reached, at which point they are incorporated into the material at their concentration in the melt, which is the technique for getting uniformly doped material (see chapter 4), convection is allowed to remove the impurities from the interface and they redistribute themselves in the melt. Thus the region behind the traveling zone is purified and the impurities are transmitted to the end of the rod. Repeated passes improve the purification process. The floating zone technique is an excellent method of preparing pure materials. Unfortunately, it does not remove all impurities, for example, those with segregation coefficients near unity, nor can it be used on Earth for systems with low surface tension.

Another technique for avoiding crucible contamination is skull melting. In this process the interior of the crucible is heated inductively while the wall of the crucible is cooled by pumping a coolant through coils surrounding it. In this way the crucible is protected by a skull of the starting material so that the molten reactive melt interacts only with its own solid. The primary disadvantage of this technique is the lack of control in the solidification process. Severe thermal gradients and an uncontrolled convective flow must necessarily be present at the solid–liquid interface. Control of nucleation and growth of the solidification in such a process is virtually nonexistent.

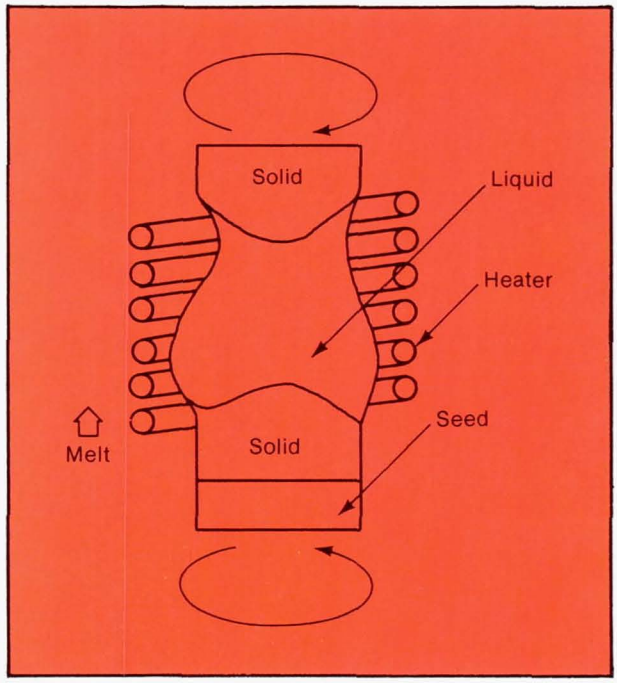

Figure 1.15. The floating zone growth method. This is a method of growing crystals of reactive materials in which the molten material is completely out of contact with solid containers. The crystal is first made in the form of a rod of suitably small size. Then radiofrequency heating is used to produce a thin liquid zone in the vertical rod. The zone is held in place by surface tension, and thus the height must be rather small (usually 1.3 centimeters or less). By seeding the initial melt with a single crystal, the floating zone method serves to grow single crystals. The method is especially useful for producing high-quality silicon. [After W. C. Dunlap, Jr., Introduction to Semiconductors. *Sketch from R. A. Laudise,* The Growth of Single Crystals, *(c) 1970. Reprinted by permission of Prentice-Hall, Inc., Englewood Cliffs, New Jersey.]*

ULTRAHIGH VACUUM PROCESSING

Ultrahigh vacuum processing can be accomplished in the shadow of a low outgassing shield designed to offer protection from the molecular beam resulting from motion through the residual atmosphere at orbital speed. Since any molecule evolving from the process is eventually lost to space, pumping capacity is virtually infinite. This is ideal for performing high-temperature purification of vapor deposition on ultraclean surfaces.

The ultrapurification of metals and certain semiconductors is an important problem both from the point of view of basic properties studies and the preparation of small quantities of ultrapure materials for specialized applications. At present most metals have not been purified to much better than parts per million, whereas electrically active impurities in semiconductors like silicon have been reduced to better than parts per trillion. Such impurities may very well mask the intrinsic properties of metals. For example, beryllium is unique among metals because of its lack of ductility. It is unknown whether this is a property peculiar to this particular metal or a result of impurities. Since beryllium has a very small ionic radius, the effect of impurity atoms on its properties can be quite large.

There are several purification techniques that require an ultrahigh vacuum during processes that involve high heat loads and large gas loads. These include vacuum melting, in which impurities that are more volatile than the sample are driven off; vacuum distillation, in which the sample material is separated from less volatile impurities; zone

refining, in which impurities are removed by rejection at the solidification interface; and electrotransport, in which a high current is passed through the sample, heating it to a near-molten state and removing impurities by electron collisions. The low-gravity environment allows the use of containerless techniques such as electromagnetic positioning to avoid container contamination in conjunction with space vacuum. This should result in orders of magnitude of improvement in the purity of metals.

The potential application for ultrahigh vacuum is the preparation of thin single crystal films by vapor deposition or by molecular beam epitaxy. Adsorbed gas atoms on the surface can be covered over by the deposited layer, forming impurities. They can also form nucleation sites, preventing the newly deposited atoms from migrating to their proper lattice sites. To prevent this requires an ultraclean environment as well as high substrate temperature to completely degas the surface. Also, reactive gases such as oxygen can readily combine with deposited atoms, forming unwanted oxides and upsetting the chemical stoichiometry.

Vacuum chambers on Earth can approach 10^{-12} to 10^{-13} torr. At these levels, the residual gas is negligible for most purposes. The length of time for the residual atoms to form a monomolecular layer on a surface is long compared to the process time. However, maintaining such systems is time consuming and costly, as is scaling up such facilities for production. Also, the pumping capacity for such chambers is limited unless large cryogenic panels are used. Such panels are not compatible with high heat loads. Therefore, it may be necessary or more economical to perform some of the previously described tasks in a space vacuum facility.

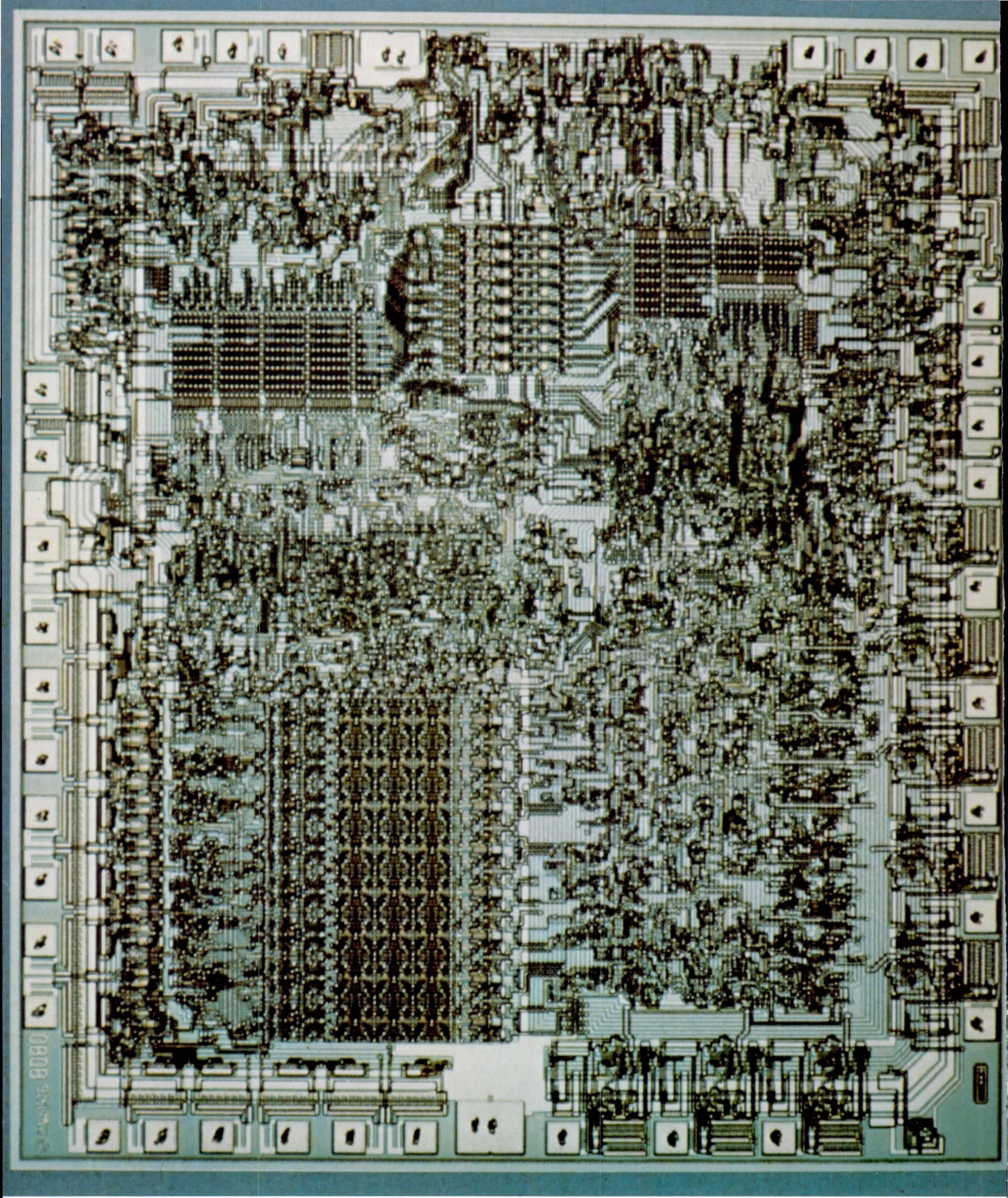

Chapter 2. POTENTIAL APPLICATIONS OF SPACE PROCESSING

Numerous applications that take advantage of low gravity come to mind. Some of these are in research, such as a study of the basic properties of materials or developing a better understanding of various processes and how they might be controlled. Others are in the actual production of unique materials, either in very limited quantities for research purposes to serve as paradigms for determining the limiting results of processes in which gravity effects are removed, or in larger quantities to fill certain high-technology needs that cannot be met by other means. Examples of these applications are given in the following paragraphs.

CRYSTAL GROWTH

The ability to grow high-quality crystals has revolutionized the electronics industry. Devices ranging from simple diodes to large computers on a single chip have been made possible by advances in the technology of growing single-crystal silicon (fig. 2.1).

Despite this highly advanced state of technology, there are still a number of problems in crystal growth that have not been solved. Although silicon can be highly purified as far as electrically active dopants are concerned, some contaminants such as oxygen are not easily removed by conventional floating zone refining. The effects of such impurities are a matter of debate. Preparation of ultrapure silicon by a containerless process in the ultrahigh vacuum of the wake of a specially designed orbiting vacuum facility might produce oxygen-free silicon for evaluation. If the improvements warrant it, the limited production of such ultrapure materials for highly specialized applications is feasible.

Another problem in the technology of silicon and other semiconductors is that of obtaining very uniform dopant distribution, particularly in the relatively high concentrations needed for certain applications such as infrared detectors. Various impurity atoms, called dopants, are intentionally added to produce the desired electrical properties in the crystal. Since only a few parts per billion of impurity can dramatically alter the electrical properties, a microscopically homogeneous distribution of dopant atoms is extremely important for applications in which it is necessary to have uniform electrical properties over a large area. Such applications include very large-scale integrated circuits such as microcomputers, imaging arrays, and image-processing arrays that combine the process computer into the same chip that contains the imaging array (fig. 2.2). It may be appreciated that the demand for better starting material increases with the complexity of the device.

For example, one method of producing highly homogeneously doped silicon is by neutron transmutation. Rods of silicon are placed in a nuclear reactor where the neutron flux produces nulcear reactions in some of the silicon atoms, changing them into phosphorus atoms, which serve as dopants to make an *n*-type material. (This process is discussed in more detail in chapter 4.) Since the reaction cross section is small, the transmutation reactions are distributed uniformly throughout the crystal. This is an extremely expensive process compared to the production of ordinary silicon, and although the demand for neutron-doped silicon represents only a small fraction of the market, there are cer-

Figure 2.1. *Photomicrograph of an 0.000185 in.^{2} Intel 8080A microprocessor chip. [Photograph courtesy of Intel Corporation.]*

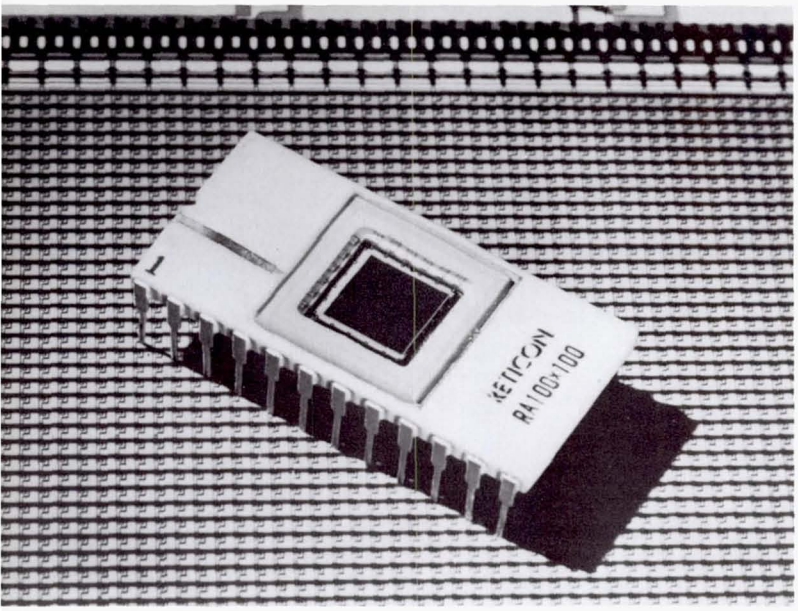

Figure 2.2. Reticon imaging array containing 10 000 discrete silicon photodiodes arranged with 60-μ center-to-center spacing. For many applications as many as 10^6–10^7 detector elements are required, each with identical electrical characteristics. [Photograph courtesy of Reticon Corporation.]

tain applications, such as the production of large rectifiers, for which industry is willing to pay the price. Unfortunately, the process is limited to phosphorus doping. This is not suitable for many applications such as infrared detectors where other dopants are required.

Another class of semiconductors in which a high degree of chemical homogeneity is essential is the class of alloy or solid solution semiconductors. In these materials the electrical characteristics are determined by the ratio of the components that make up the alloy. No dopants are necessary. Thus such materials are called intrinsic as opposed to, for example, doped silicon, which is an extrinsic material. Examples of alloy semiconductors are $Ge_{1-x}Si_x$, $Pb_{1-x}Sn_xTe$, and $Hg_{1-x}Cd_xTe$. Such materials are excellent infrared detectors. The band gap (the energy required to promote an electron to the conduction band) can be adjusted over a wide range by selecting an appropriate value of x. In this way the detector may be tuned to the particular wavelength desired. For example, setting $x = 0.2$ optimizes $Hg_{1-x}Cd_xTe$ to the 10.6 μm CO_2 laser wavelength. To produce a good focal plane detector, it is necessary to hold variations in x to ± 0.005 over the area to ensure uniform response. In addition, the carrier concentration in intrinsic materials can be kept low, and they are capable of extremely fast response. In fact, $Hg_{1-x}Cd_xTe$ has been termed the "ideal infrared detector material."

Unfortunately, it is extremely difficult to grow highly doped extrinsic semiconductors and alloy semiconductors and at the same time maintain a high degree of chemical uniformity. A great deal of effort has gone into trying to understand and control convective effects in such systems. Geometries designed to minimize convective effects are used, and in some cases high magnetic fields have been employed to effectively increase the viscosity of the melt. However, it is not always possible to maintain the degree of control desired for many applications. Unavoidable radial thermal gradients produce stirring of the melt at the growth interface, causing compositional variations. Thermal oscillations, believed to be caused by convective flow in the melt, produce growth rate fluctuations, resulting in alternating layers of excessive and deficient dopant levels called striations. The growth of such crystals in space should provide additional insight into the cause of growth oscillations and might result in greatly improved dopant or compositional homogeneity. The ability to produce such materials in bulk quantities would be a significant breakthrough in developing better starting materials for the fabrication of infrared detectors and other devices requiring similar uniformity.

Another crystal growth process that may benefit from the absence of gravity-driven convection is growth from the vapor. This can be accomplished either by condensation from a supersaturated vapor or by a chemical process in which a transport gas chemically reacts with the source material and is caused to react reversibly at the growth sites. In this reverse reaction, the desired atom is deposited on the growing crystal, and the transport atom or molecule is released to repeat the process. For materials with very low vapor pressures and/or high melting points, the latter process has an advantage because it does not require extreme temperatures.

The absence of gravity-driven convection should eliminate unwanted fluctuations in composition, temperature, and flow at the growing crystal. Since the growth rate is quite sensitive to these parameters, microfluctuations in the growth environment can introduce irregularities in the growing crystal. These structural or chemical defects degrade the electrical and optical performance of the crystal by acting as traps for charge carriers or as scattering or adsorption centers.

Hydrostatic pressure also puts a strain on solids, particularly when they are cooling just after solidification. Normally this is important only in large castings such as glass blanks for large telescope mirrors. However, there are certain crystals that are sufficiently delicate that they may suffer strain under their own weight at the growth temperature.

Mercuric iodide (HgI_2) is an example. This crystal is of interest as a portable nuclear radiation detector or gamma ray spectrometer. It does not have the energy resolution of the more sophisticated Ge: Li, Si: Li, or intrinsic Ge detectors that must be maintained and operated at cryogenic temperatures, but it promises to provide sufficient resolution at ambient temperature to be useful as a field unit for regulatory function, prospecting, bore hole analysis, and a host of other applications.

Unfortunately, the HgI_2 crystals produced on Earth have not attained the performance expected for the material (fig. 2.3). Also, performance varies considerably from crystal to crystal. The crystal has a layered structure with only weak bonding between the layers. It is believed that the high density produces sufficient strain field at the growth temperature to result in severe dislocation densities that degrade the performance. If space-produced HgI_2 crystals can approach the expected theoretical performance, this could become a significant contribution to nuclear monitoring technology.

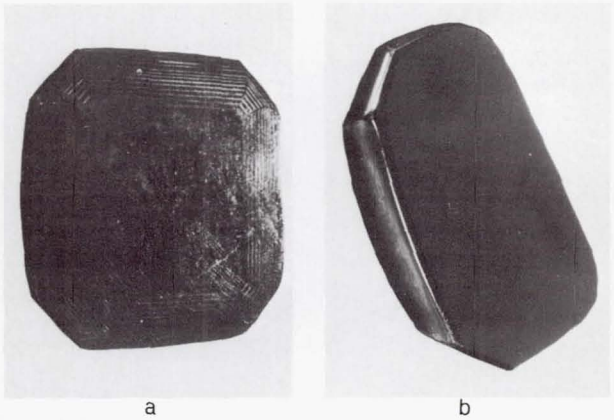

a b

Figure 2.3. Polished and etched mercuric iodide (HgI_2) crystals. The growth rings seen on crystal a are regions of higher etch pit density indicating dislocations. These were produced by the day-night temperature fluctuations in the laboratory. Crystal b was grown under better temperature control. It does have some banding, which could be detected under proper viewing conditions, but obviously much less than crystal a. This demonstrates the extreme sensitivity of crystal perfection to growth conditions. [Photograph courtesy of EG&G Energy Measurements Group.]

There may also be advantages to growing crystals from aqueous solution in space. As shown in figure 1.8, solutal convection is very much involved in such growth and in fact is an important mechanism for bringing fresh nutrient to the growing crystal. Under diffusion conditions prevalent in low gravity, the crystal would certainly grow more slowly, but it might also grow more perfectly. Crystals grown from solution often have microscopic inclusions that affect their optical and electrical properties. For example, triglycene sulfate (TGS) is an important infrared detector material, particularly in the far infrared. Theoretically it should have a detectivity (D^*) approaching that of $Hg_{1-x}Cd_xTe$ with the advantage of being able to operate at ambient temperature rather than at the low temperatures required by $Hg_{1-x}Cd_xTe$. Unfortunately, the actual performance of the material falls short of its theoretical performance by about a factor of 10. It is conjectured that this is caused by the presence of microscopic inclusions, but it is not known whether the inclusions are produced by convective effects. If an increase in performance could be obtained in a space-grown crystal, this would have a significant technological impact.

Another reason for growing crystals from aqueous solution in space is the fact that they are transparent and it is easy to study the growth process in great detail to see how the formation of certain defects relates to the growth environment. Since this environment can be controlled better in low gravity, this is an ideal place to study such effects. The knowledge can then be applied to optimize processes on Earth.

A novel crystal growth technique called electroepitaxy has been developed by H. C. Gatos of the Massachusetts Institute of Technology. Epitaxial layers of gallium arsenide (GaAs) are grown by passing an electric current through the melt. The current flow drives the As atoms to the solidification interface by a process known as electrotransport. The Peltier cooling at the solid–liquid interface removes the heat of solidification. This permits much better control over the growth process than is possible with the conventional slider technique and has produced superior GaAs epitaxial layers (fig. 2.4).

Next to silicon, GaAs is probably the most widely used semiconductor. It has many military and civilian applications in microwave equipment and in solid state lasers. Since most of the emphasis in device manufacture is on the precisely grown epitaxial layer containing the appropriate dopants, this research has immediate applications. However, there are still problems with the substrate material. Epitaxial layers tend to bury or mask defects in the substrate, thus allowing less than perfect substrate material to be used. However, defects in the substrate will often migrate to the surface and into the epilayer, causing the device to fail unpredictably. This phenomenon is especially prevalent in GaAs. Therefore, it would be of great advantage to be able to grow better substrate material.

The electroepitaxy growth process is too slow in its present form to be practical for GaAs substrate materials. However, it may be possible to use much larger currents in space, where much higher thermal gradients can be tolerated without convective disturbances.

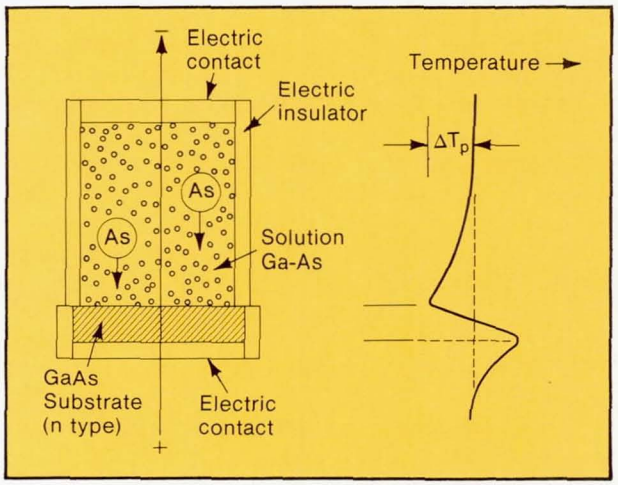

Figure 2.4. Electroepitaxy method for growth of gallium arsenide (GaAs). An electric current is passed through an isothermal melt. The current moves the As atoms in the solution of GaAs to the growth interface by a process known as electrotransport. Here growth is promoted by the Peltier cooling at the GaAs substrate. This process yields superior epitaxial layers compared to the conventional growth technique using graphite sliders.

METALS, ALLOYS, AND COMPOSITE MATERIALS

The ability to operate in the virtual absence of gravity has a number of interesting applications in the field of metallurgy, such as the study of the basic properties of pure metals, many of which are not known; the determination of phase diagrams of systems that are highly corrosive in the melt; studies of macro- and microsegregation during solidification of alloys; the determination of the role of gravity-driven convection in the microstructure of castings; the preparation of unique alloys or composites having components with large density differences; the study of nucleation and growth phenomena in the absence of wall effects; and the study of rapid solidification of highly undercooled melts. A brief summary of each of these topics is given in the following paragraphs.

The combination of containerless processing and the ultrahigh vacuum capabilities provided by an orbiting spacecraft offers unique opportunities in metal purification and the study of basic properties of ultrapure or highly corrosive systems.

There are virtually no data available on thermodynamic properties such as enthalpies, specific heats, heats of fusion, densities, viscosities, and surface tensions of liquid systems above 1000° C. These data are of interest in the design of high-temperature materials processes involving silicon, refractory oxides, sulfates, carbides, and nitrides. Containerless techniques not only avoid the corrosive reactions of the reactive melt with the crucible, they also avoid the temperature limitations normally imposed by the melting point of the crucible material. This extends the measurement range of such properties to extremely high temperatures. For example, it would be useful to know something about the thermodynamic properties of uranium oxide at, say, 5000° to 10 000° C to determine how to design a reactor core to resist a meltdown.

The measurement of such properties is not a simple matter, but there are various techniques for measuring heat capacities, enthalpies, and so on, involving "gulp" calorimeters and a variety of radiometric techniques. Surface tension and viscosity can be measured by perturbing a suspended droplet, causing it to oscillate. The natural frequency of oscillation is determined by the surface tension, and the damping of the oscillation is governed by the viscosity.

There are techniques for positioning two or more droplets and merging them without physical contact (fig. 2.5). These would be useful for studying phase relationships, solubility data, diffusion constants, and interfacial phenomena for multicomponent systems at high temperatures. One important application of such techniques is the study of slagging reactions that take place in magnetohydrodynamic (MHD) power systems. Such reactions occur because of trace quantities of alkali metals (sodium, potassium, and calcium) in the coal that is burned. The oxides of the metals form an

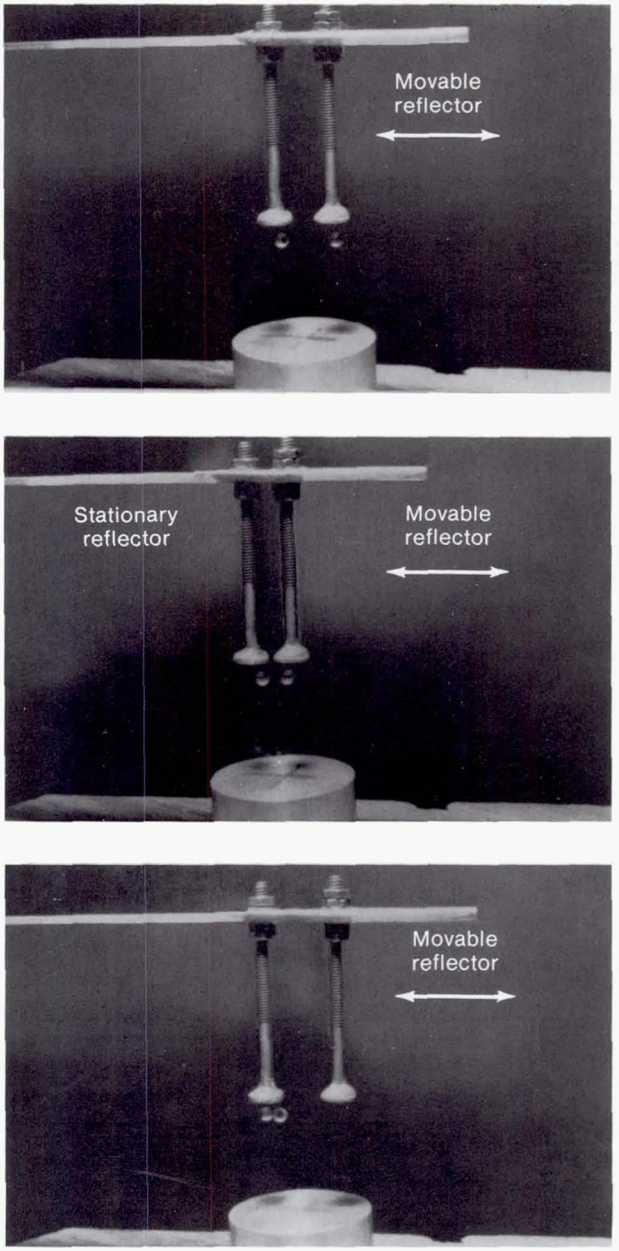

Figure 2.5. *Two spheres suspended in acoustic levitator. The interference between the reflected wave and the incident wave creates a stable pressure node at λ/4 below the reflector, as shown by the small sphere suspended by the acoustic pressure. The balls will remain suspended below the reflector regardless of where they are moved within the acoustic field produced by the driver at the bottom of the photograph. In space two molten droplets may be merged without physical contact simply by moving their reflectors together as shown in the sequence. This allows the measurement of reactions between highly reactive materials.*

insulating slag that coats the electrodes, preventing electricity from being produced by the process. Attempts have been made to render these slags conductive by intentionally seeding the combustion with iron. Unfortunately, the iron-alkali metal oxides that are formed react with virtually everything at high temperature, making it very difficult to study the basic properties of the system.

The solidification of metallic alloy systems is a very complex process. Even though the constituents may be thoroughly mixed in the melt, as they begin to solidify segregation occurs because of the difference in solubility between the solid and liquid phases. This results in the enrichment of one of the constituents near the interface, changing the composition and the density and giving rise to solutal convection. Of course, thermal gradients are involved in any solidification process, so there is also the possibility of thermal convection. The change in composition often results in a lowering of the solidification temperature of the melt ahead of the interface, producing constitutional supercooling and causing interfacial breakdown and dendritic growth unless large thermal gradients are involved to prevent it. As treelike dendrites (fig. 2.6) grow into the melt, flows associated with the solidification process cause dendrite arms to melt or break off and carry the dendrite particles to other parts of the melt where they nucleate new grains. Only recently have these processes begun to be understood well enough to enable to control them to produce the desired microstructures.

There is still much to be learned about the solidification process. For example, what is the relative importance of gravity-driven flows produced by thermal and solutal convection as opposed to nongravity-driven flows produced by volume changes during solidification and other effects in the dendrite multiplication process? What is the importance of this process relative to constitutional supercooling in producing the fine-grained, equiaxed structure usually found in the center of castings? These types of questions can be systematically studied by comparing experiments performed in space at low gravity with those performed in 1 g or higher in centrifuges (fig. 2.7).

Another type of solidification process that can benefit from low gravity is high-gradient directional solidification. This technique is particularly useful for producing lamellar or rodlike structures in eutectic alloys (see chapter 5 for a more detailed discussion). This unique microstructure produces highly anisotropic properties in metals, resulting in exceptionally high strengths along a particular direction, which is very useful for applications such as turbine blades. Such microstructures are also being investigated for unusual electrical properties, magnetic properties, and optical properties.

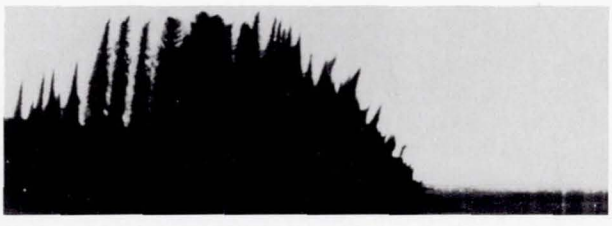

Figure 2.6. Dendrites growing into the melt in a transparent metal model system consisting of $NH_3OH + H_2O$.

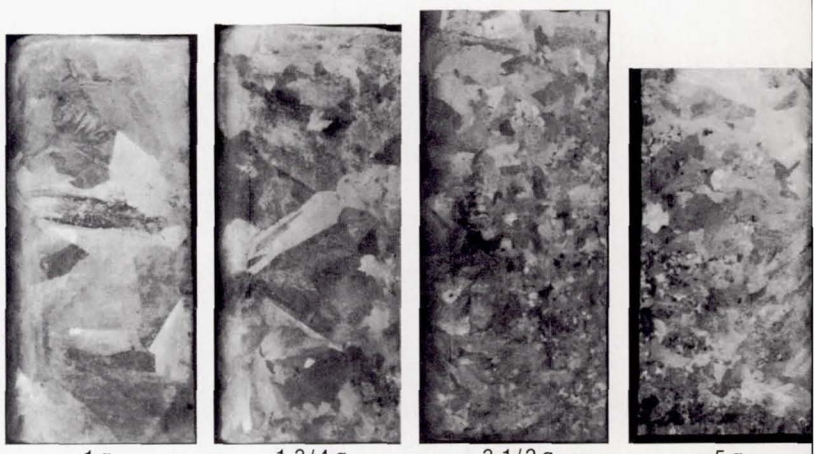

Figure 2.7. The influence of gravity on the microstructure of a casting. These ingots, consisting of Sn-15 w% Pb, were cast in a special centrifuge furnace. Note that the grains get much larger as gravity increases, indicating that gravity plays a role in dendritic multiplication and transport.

The microstructure produced by these processes is determined by the thermal gradient G and the growth rate R. Convective stirring in 1-g processes increases the heat transport in the melt, making it more difficult to maintain a high gradient. Also, convectively driven growth rate fluctuations make it difficult to operate at very low growth rates in Earth gravity. Substantially higher G/R ratios should be obtainable in space, extending the range of materials that can be investigated and that can produce unique microstructures. This capability is also necessary for growing crystals such as the solid solution systems from the melt, as discussed in chapter 4. It may also prove interesting to directionally solidify materials with off-eutectic compositions or complex, multicomponent eutectics that are affected more by convective mixing at the interface than are the simple binary eutectic systems.

The absence of distortion from hydrostatic pressure may lead to some interesting applications. For example, it may be feasible to produce intricate castings in a weightless environment by use of a thin oxide skin without deformation. Such a thin skin would enable the casting to be processed with a very high thermal gradient which a thick mold would tend to level out. It may be desirable to machine objects such as high-temperature turbine blades before the blades are toughened by the final heat treatment. The blades could be coated with a thin layer of alumina to serve as a skin and taken to space for the final heat treatment. If substantial improvement from a complete melting and resolidification of either a dispersion oxide-hardened blade or a directionally solidified eutectic blade can be realized, the added benefit may justify the space transportation cost (fig. 2.8).

Perhaps the most exciting application of space for the study of solidification is the ability to solidify with or without physical contact with the melt. This avoids container-

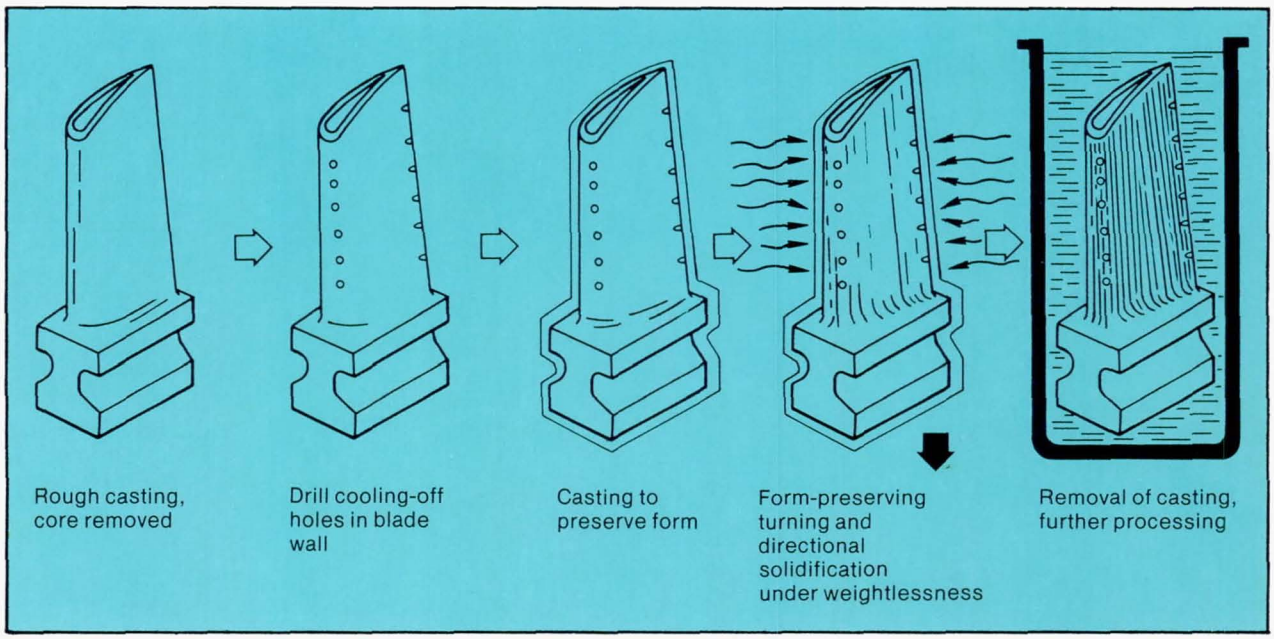

Figure 2.8. *Application of skin technology to heat treatment of a turbine blade. The thin oxide skin applied on Earth after the blade is finally shaped is sufficient to preserve the form during melting in space. This thin skin allows directional solidification under extremely high gradients that would be diffused by conventional mold techniques.*

induced nucleation and allows the material to be cooled below its normal solidification point by a substantial amount. Homogeneous nucleation can be studied in greater detail than was hitherto possible. New phenomena occur when solidification takes place at such high undercooling. The solidification will most likely be initiated at only a few points, and perhaps only one. The solidification front will proceed very rapidly, perhaps in a diffusionless mode. The released heat of solidification causes a rapid increase in temperature that may be seen as a bright flash and may remelt some of the sample. It may be possible to hypercool some samples, that is, undercool them sufficiently so that the sudden release of the latent heat does not cause any melting. Figure 2.9 shows samples that were undercooled in the drop tube at Marshall Space Flight Center.

Needless to say, some unique microstructure will result from this type of solidification. The solidification can occur so rapidly that the atoms do not have time to rearrange themselves in their minimum energy configuration. This could result in an amorphous or glassy structure even for metals. Some metal glasses are now formed by splat cooling and have very unique properties, such as extreme resistance to corrosion, great strength, and resistance to fracture, and extreme magnetic "softness." By extreme undercooling, such structures can be prepared in bulk form rather than in thin sheets or wires. The factor that determines whether a glassy structure forms is the time-temperature-transition (T-T-T) diagram (fig. 2.10).

It may also be possible to form metastable phases in peritectic systems such as Nb_3Ge and Nb_3Sn. These have the A-15 structure that is found in superconductors with the highest known transition temperatures (fig. 2.11). These structures are not obtained by normal solidification, but must be achieved by rapid solidification. For this reason such materials are only produced in thin sheets or wires, which are not suitable for neutron diffraction studies to determine lattice constants and structure. A detailed understanding of how superconductor performance relates to microstructure could open the way to better strategies for its reproducible enhancement and control.

The elimination of buoyancy forces in the weightless environment allows particles, gas bubbles, or immiscible fluids to remain in suspension indefinitely. This has a number of implications ranging from the possibility of creating new alloys and composites to fundamental studies of interfacial phenomena, bubble dissolution, and colloidal systems.

A number of composite materials have unique properties in a dispersed phase. The fibers are usually supported externally while the matrix material is solidified. For some applications it is desirable to form a composite with short, randomly oriented fibers throughout the matrix material. At present, this can only be accomplished by powder metallurgy techniques in which the fibers are mixed with a fine metallic powder and hot pressed to near the theoretical density. If the composite were melted in Earth's gravity, the fiber materials would settle to the bottom or rise to the top, depending on the relative density difference. It is not known how the strength and other properties of the composite prepared by the hot pressing techniques compare with those of composites prepared from the melt in a low-gravity environment.

Another class of technologically important composites is that containing microscopic oxide particles, such as oxide dispersion-hardened materials that retain their strength at high temperatures. These composites are important for applications such as high-temperature turbine blades. In another example, it is known that the incorporation of alumina (aluminum oxide) into silver or copper halide matrix greatly enhances the ionic conductivity without allowing electron transport. Such a solid state electrolyte could have important applications in improving battery

Figure 2.9. Comparison of the microstructure of niobium (Nb) droplets solidified containerlessly. Left—a single grain supercooled about 500 K. Below—multigrain sample that was not supercooled and shows evidence of a shrinkage cavity. (Magnification 20x)

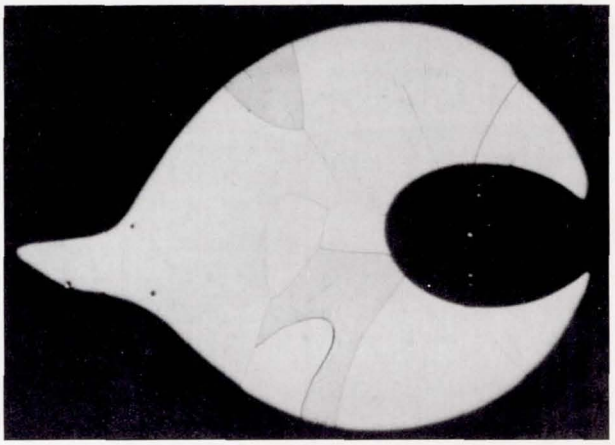

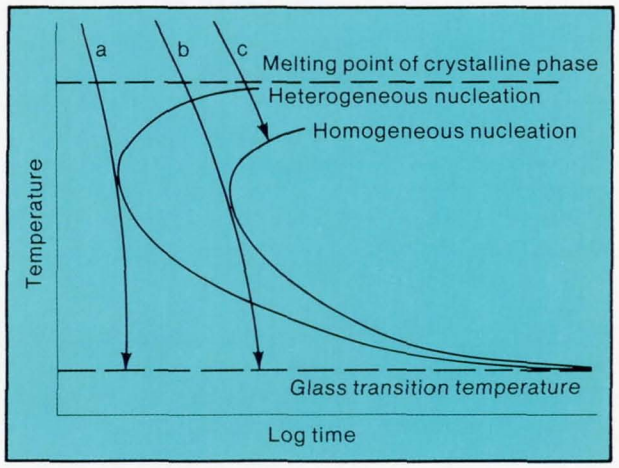

Figure 2.10. Schematic of time-temperature-transition (T-T-T) diagram for a glass-forming system. The C-shaped curve represents the time required to crystalize a given volume fraction at the indicated temperature. The nose of the curve results from the competition between the driving force for crystallization, which increases with decreasing temperature, and the atomic mobility, which decreases with decreasing temperature. If the cooling is sufficiently rapid (a), a glass is formed. By using a containerless process to eliminate heterogeneous nucleation, the glass-forming range is increased (b). Much greater undercooling is possible (c), producing unique microstructures and allowing homogeneous nucleation to be studied unambiguously.

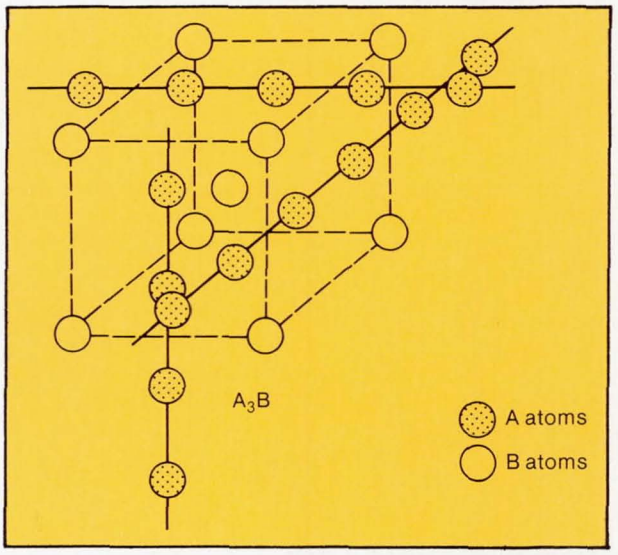

Figure 2.11. Atomic arrangement of A-15 compounds, which are the best superconductors known today. These compounds have the composition of A_3B, and the A atoms are long chains with two atoms on each face of a body-centered-cubic B lattice.

technology. In general, the particle sizes of interest are so small that they tend to stay suspended by Brownian motion even in 1 g. However, convective stirring during heating and solidification can cause agglomeration of the fine dispersoids, which can lead to sedimentation. It may also be of interest to prepare special samples with larger particles to elucidate certain mechanisms or size dependence in the phenomena of superionic conduction.

Another type of composite that may have interesting properties is uniform closed-cell metal foam. These foams could be formed by adding a "blowing agent," which would decompose into a gas just above the melting point, to a metal powder. For example, graphite and a metal oxide, which will form carbon monoxide at high temperatures, could be added. The bubbles should nucleate more or less uniformly throughout the mixture, producing a closed-cell metallic foam with a remarkable strength-to-weight ratio. Control of the bubble size and number should be possible by controlling the amount of gas produced and the production rate, which could be accomplished by varying the amount of reactants and the temperature.

The formation of in situ composites from immiscible systems may be possible. There are some 500 alloy systems that have a miscibility gap, that is, a region in the phase diagram in which the two molten materials will not mix, just as oil and water fail to mix. Alloys of such systems cannot be formed by conventional solidification because the melt must be cooled through this miscibility region in order to solidify. Since the two liquids have different densities they immediately come out of solution in normal gravity. In principle, these should remain in suspension in low gravity and form a finely dispersed composite. If such composites can be formed in space, this offers a rich area in which to look for new systems that might have some interesting mechanical and electrical properties, such as high transition temperature superconductors that can be easily drawn into wire, unique bearing material, improved electrical contact materials, and alloys with high strength-to-weight ratios.

GLASS AND CERAMICS

One of the most important applications of containerless processing is the ability to make unique glasses that cannot be made by conventional techniques. A glass differs from a crystalline solid in that a glass lacks the long-range order of a crystalline lattice (fig. 2.12). Also lacking are abrupt changes in lattice structure at the grain boundaries where crystal lattices of different orientations grow together. These differences are responsible for the useful and unique properties of glasses, for example, optical clarity, resistance to grain boundary corrosion, the lack of a definite melting temperature, and superior strength and mechanical properties. For many applications a glass is a good substitute for a single crystal and is generally much cheaper to produce.

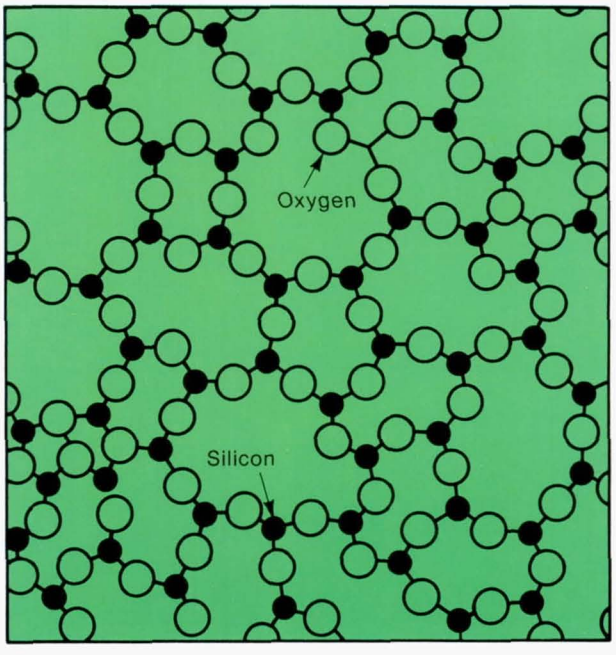

Figure 2.12. The atomic structure of a silicate glass. According to generally accepted models, glass is a random array of polyhedral molecules linked together at their corners. In a silicate glass, the molecules are tetrahedrons in which a silicon atom is surrounded by four oxygen atoms. These are linked together in a random fashion as represented two-dimensionally to the left. In a crystalline substance, all the angles between the Si-O bonds are the same, and a regular structure results.

Virtually any solid substance could have its atoms rearranged into an irregular lattice to form an amorphous solid or glass. The tendency of a material to solidify into either a glass or a crystalline material depends on the relative difference in the energy of an ordered versus a disordered structure and the ease with which atoms can move about in the substance. Most good glass-producing compounds have a small energy difference between ordered and disordered structure and are fairly viscous in the melt. They can easily be solidified into the glassy state in which the viscosity continues to increase with decreasing temperature until the atoms become so sluggish that they never find the slightly lower energy configuration of the crystalline lattice. On the other hand, most metals have large disordering energies and low viscosities. Therefore, their atoms will rapidly fall into an ordered array or crystalline lattice when cooled. A glassy state can be obtained only by chilling the substance so

rapidly that the atoms become frozen in place before they can arrange themselves in the lowest energy configuration. In some metallic systems glasses can be formed by a process called splat cooling in which molten material is squirted against a cryogenic surface. Cooling rates in excess of 10^{6}° C per second can be obtained in thin films by this process.

A material can be cooled to well below its normal solidification temperature provided it is denied nucleation sites in the form of crystallites or impurity particles. If a material can be undercooled to achieve a sufficiently low viscosity before it solidifies, a glass will result. In many potential glass systems, the container wall provides nucleation sites and the material devitrifies (crystallizes) during solidification. Containerless processing can extend the ability to form glasses to a much wider range of materials than is currently possible.

This technology may result in a wider range of choices for the optical designer in terms of properties such as index of refraction, transmissivity, dispersion or Abbe number, and so on. Such an increase in the availability of design choices brought about by the recent development of rare earth glasses vastly simplified lens design and reduced the number of optical elements required to make a high-quality lens. The result has been the excellent camera lenses now available at moderate prices that vastly outperform the best systems that were available 10 or 20 years ago.

Another important application may be improvements in laser host glasses. In a laser, the lasing action is provided by dopant atoms such as neodymium or chromium imbedded in a host material such as ruby, yttrium aluminum garnet (YAG), or a variety of glasses. It has been found that by increasing the content of calcia (CaO) in a neodymium-doped glass, the cross section for stimulated emission of the lasing line could be enhanced, resulting in a higher lasing efficiency. Unfortunately, this increase also results in an increased tendency for the glass to devitrify. Containerless processing may extend the range of glass compositions that could be used as laser hosts, resulting in significant advances in the technology.

The elimination of trace impurities such as submicrometer-sized droplets of platinum or other crucible material in glasses that are dissolved by the melt becomes extremely important in high-energy laser applications. Such dispersions may not be detrimental in some of the more pedestrian applications, but when terawatts are being passed through an optical component, localized absorption at such sites could have catastrophic results. Also, the ability to make high-purity glasses from inexpensive starting materials could have a significant impact on the use of optical fibers for communication. For example, it may be cheaper in some cases to use a borosilicate glass that has been containerlessly melted and drawn rather than one made by the current process, which involves chemical vapor deposition of pure silica.

The lack of buoyancy in low gravity has a drawback in that new ways will have to be sought to eliminate or remove bubbles. Of course, this is a problem in the production of glasses on Earth, since glasses tend to be viscous and large energies are required to remove all the bubbles by heating. Chemical fining agents are often added to promote bubble dissolution. Sometimes it is difficult to determine the effectiveness of such fining agents because of the competing process of bubble rise. It may be of interest to study fining techniques in space, where individual bubbles can be studied directly over relatively long periods of time.

The absence of buoyancy in containerless processes carried out in a weightless environment provides the opportunity to study problems such as bubble centering mechanisms in a droplet. For surfaces that are separated by only a few molecular layers, such as soap bubbles, surface tension acts to center the bubble and would provide a surface of uniform thickness were it not for gravitational distortion. What is not so obvious is whether the much weaker, long-range molecular forces would tend to provide a similar centering in droplets with thicker surfaces, such as hollow glass spheres, or whether other mechanisms such as oscillation or differential cooling rates can be made to provide bubble centering (fig. 2.13).

The production of hollow glass spheres that have a high degree of concentricity has become of considerable interest to the Department of Energy for use as fuel containment shells for inertially confined fusion (ICF) experiments (fig. 2.14). A mixture of deuterium (D) and tritium (T) gas is diffused through such a glass shell at high pressure. The shell is then imploded by simultaneously converging high-powered laser or electron beams on it, which compresses and heats the D-T mixture to the several hundred million degrees required for thermonuclear fusion. The energy released can be trapped and used for power production.

Although there are many technical problems to be overcome before this technique can become a practical source of

Figure 2.13. *Demonstration of a bubble centering mechanism during a KC-135 flight using a water droplet containing an air bubble. Oscillations were introduced mechanically by Taylor Wang of the Jet Propulsion Laboratory (in background, out of focus). The flows in the spherical liquid shell apparently cause the bubble to become centered.*

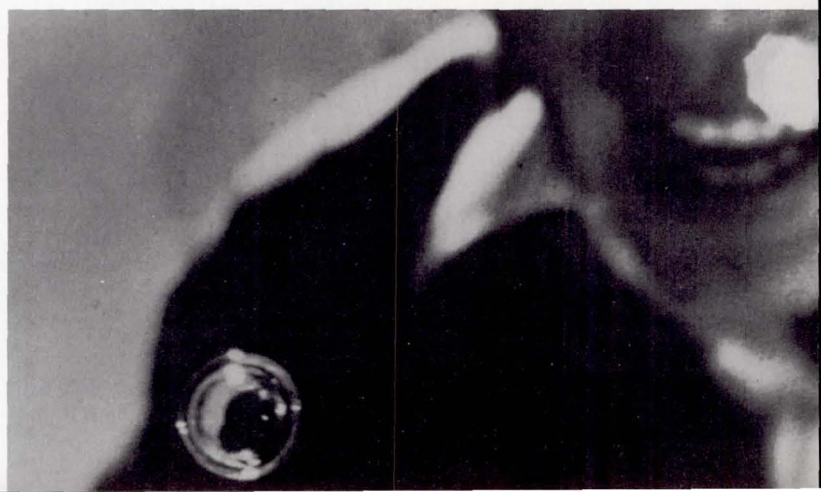

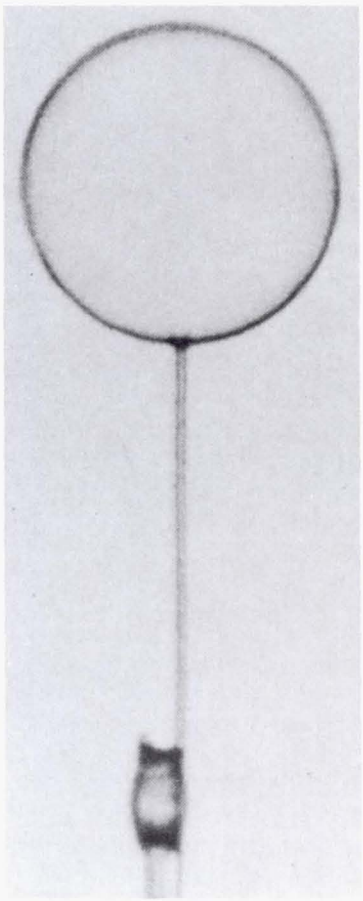

Figure 2.14. Laser fusion target mounted on a sting ready to be installed in the test chamber. The target consists of a glass shell, 100 μm in diameter, filled with a mixture of deuterium and tritium gas at approximately 100 atmospheres. Intense laser beams converging on the target cause several thousand fold compression, reaching the threshold of heating required for ignition of the thermonuclear fusion reaction. The tremendous energy release may be captured and used as a power source.

Figure 2.15. Schematic of one of the many configurations of fuel container targets being tested for use in the inertial confinement fusion program. The heart of most such designs is a highly concentric spherical glass shell containing the high-pressure fuel. The multilayer coatings to increase the coupling between the laser beam and the target are deposited on the basic glass shell after the gaseous fuel has been diffused through the glass walls.

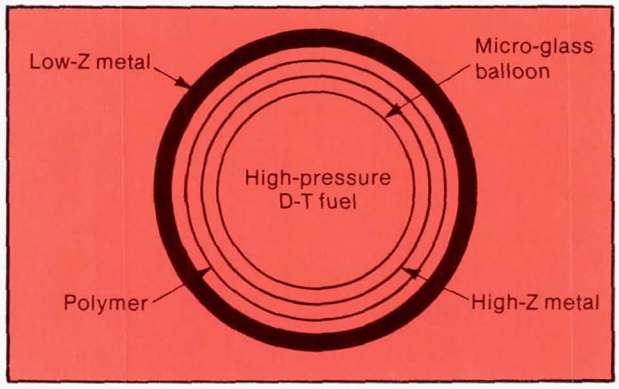

energy, inertially confined fusion is one of the more promising long-term solutions to the energy problem. No long-lived radioactive isotopes are produced by the fusion process, so the nuclear waste storage problem is eliminated. Also, there is sufficient deuterium in the oceans that can be readily extracted to supply the world's energy needs for literally millions of years.

One important detail in the process is the design and fabrication of the fuel containment target. The simplest and most widely used configuration has been spherical glass shells containing either gaseous D-T or a frozen shell of D-T (fig. 2.15). A variety of coatings or ablative pushers have been added to improve the coupling between the beam and the shell. The energy available with current lasers restricts the size of the confinement shell to a few hundred micrometers in diameter. Eventually, shells up to several millimeters in diameter will be required to produce useful power levels. Large-scale generation of power will require the manufacture of tens of thousands of such confinement shells per day at less than 6 cents per shell.

It can be appreciated that a high degree of concentricity and surface smoothness is required to enable the sphere to be uniformly compressed by a factor of 1000 without severely distorting or jetting before the fusion temperature is attained. Several methods are now available for manufacturing confinement shells that are satisfactory for today's research requirements. These involve containerless techniques using tube furnaces in which the shells are blown and solidified. Since the shells are partially suspended by aerodynamic forces and are not in free fall, buoyancy forces still act on the bubble. Yet a high degree of concentricity is achieved for spheres up to several hundred micrometers in diameter with wall thicknesses of tens of micrometers, indicating that some form of centering forces are acting. The details of the process are not well understood.

So far it has not been possible to produce satisfactory confinement shells with the diameter that will eventually be needed as more powerful lasers become available. Whether the processes can be improved or whether there is fundamental limitation imposed by the buoyant forces is not yet known. Experimentation in a weightless environment should be able to assist in such studies and could provide an alternate method of producing such spheres if it turns out that buoyant forces do indeed limit the terrestrial processes.

Other possible applications of the low gravity environment involve high-temperature heat treatment of glasses of complex shapes without deformation due to sagging. Since ion exchange rates are accelerated at high temperatures, chemical tempering of such complex glass forms could be accomplished readily without deformation. This absence of hydrostatic deformation will also allow crystallization of shaped vitreous materials to be evoked rapidly in a high-temperature, low-viscosity regime, producing a glass ceramic without shape distortion.

FLUID AND CHEMICAL PROCESSES

The complexities in many processes involving fluids and chemical reactions due to thermal and solutal convection often make it difficult to sort out the relative importance of various effects and in addition confuse the measurement process. This is especially true in the measurement of diffusion coefficients, solubility rates, thermal conductivities of fluids, and other parameters affected by convective transport. In many cases some of the more subtle nongravity-driven flows resulting from volume change, capillarity, Soret diffusion, thermoacoustic effects, and so on, are overwhelmed, masked, or suppressed by the more dominant gravity-driven flows in Earth processes. Sometimes it is important to recognize and account for these flows in order to be able to control various processes. In many cases it is advantageous to perform idealized experiments that are simple enough to compare with a tractable model. Consider how difficult it would have been to discover Newton's laws of motion had it not been possible to experiment with systems in which drag forces could be made negligible compared to inertial forces. Once the nongravity effects are properly accounted for, the models can be extended reliably to include the gravity effects present in Earth processes, just as drag can be incorporated into Newton's laws of motion once the basic principles are understood.

One example of this is the study of the interaction of flow fields, temperature fields, and convective effects in continuous flow electrophoresis. In this process a sublaminar flow of an electrolyte buffer solution is established in a thin rectangular channel. A sample stream is introduced into the buffer stream and is acted on by an electric field applied in the transverse direction. This separates the components in the sample stream according to their electrophoretic mobility. Control of this process is difficult at best. Wall effects distort the sample stream. Slight differences between the sample and the buffer produce sedimentation effects. Joule heating from the passage of the electric current causes a temperature rise in the fluid. Heat extraction through the walls minimizes the temperature rise but produces both horizontal and vertical thermal gradients that tend to produce convective flows. These in turn transport heat and affect the temperature distribution in the buffer. The flowing buffer tends to stabilize against overturning flows, but additional distortions to the sample stream result. The temperature change in the buffer also results in viscosity changes that further distort the sample stream. Finally, the passage of current through the buffer and the selective effects of the membranes separating the electrode chambers from the flow chamber can produce changes in ionic concentration across the chamber that result in both solutal and thermal convection because of the resulting uneven heat generation within the buffer solution.

This description gives some idea of the complexities that can arise in what might at first glance appear to be a simple process. Clearly a number of the effects that distort the sample stream are gravity dependent, while others are not. Low-gravity experiments may be the only way to sort out the effects to assess their relative importance. Once these are understood, it may be possible to optimize the Earth-based design to live with gravity-driven flows, establish the limitations of what can be done with Earth-based electrophoresis, and design space electrophoretic devices to take maximum advantage of the low-gravity environment to improve the performance and expand the limits of the separation process.

The control and understanding of dendritic growth processes is important because these processes are responsible for the origins of chemical inhomogeneities and other defects in castings, ingots, and welds. More subtle effects include crystallographic texturing of solidified materials, nonequilibrium phases, reduced corrosion resistance, and less-than-optimum mechanical strength and toughness. A theory has been developed for dendritic growth as a function of undercooling. For large undercooling the growth rate is sufficiently rapid to be unaffected by convective effects. However, at small undercooling, convective flows dominate the process, causing the shape and growth rate to become quite dependent on orientation (fig. 2.16). This

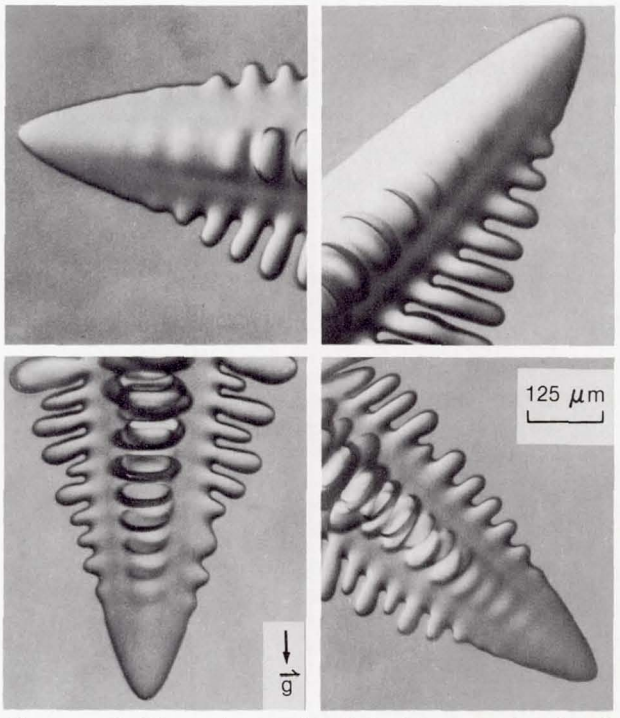

Figure 2.16. Photomicrographs of dendrites showing the effect of orientation with respect to the gravity vector. This is evidence that dendrite growth is affected by gravity-driven flows under certain conditions.

complication makes it difficult to test the basic theory at small values of undercooling. Experiments carried out in low-gravity to avoid this complicating effect could provide a critical test of the theory of dendritic growth.

Another important process that might be performed in the absence of convective flows is the growth of very delicate organic crystals. There are a number of biologically important substances, such as various proteins, for which it is desirable to know the detailed molecular structure. X-ray crystallography of proteins, which requires a crystal only 0.5 mm in each dimension, provides much information regarding the atoms comprising the protein and their relative configurations about each other; however, it does not detect hydrogen atoms. Neutron crystallography, on the other hand, does provide information about the position of hydrogen atoms but demands a much larger crystal (1 cm in each dimension). Protein crystals for X-ray crystallography are routinely and successfully grown using available ground-based technology, but growing the large crystals needed for neutron crystallography is a much more difficult problem. Microgravity might assist in this process by eliminating the deformation produced when the growing crystal must lie against the wall of a vessel and by eliminating concentration-driven convective flow in the protein solution.

The absence of buoyant forces allows fluid systems with widely differing densities to remain in suspension more or less indefinitely. This is useful for the investigation of the nucleation, growth, and coalescence of bubbles, flocculants, colloids, and hydrosols, and their behavior in thermal gradients and acoustic fields. Apart from fundamental interest, such studies have important applications in many industrial processes.

For example, Ostwald ripening is a process in which larger particles in a suspension tend to grow at the expense of smaller particles in order to minimize the total interfacial energy of the system. Although this process has been studied, the kinetics are not well understood, primarily because of the difficulty of maintaining a suspension without stirring, which affects the transport in a complicated manner. Since Ostwald ripening is important in many precipitation processes, including precipitation and dispersion hardening of superalloys used to fabricate high-temperature gas turbine blades, there is an impetus to understand it in more detail. A low-gravity experiment can keep such particles in suspension long enough to study the change in size distribution as a function of time and concentration, which can provide the experimental data required to evaluate the kinetics.

The formation of flocs is an important industrial process for the removal of impurities in large systems. Unfortunately, little is known about the formation of a floc. At present there are two competing theories: the bridging theory (adsorption of single polymer on more than one colloidal particle) and the network theory (polymer molecules associate in solution to form a network that traps the colloids as it settles). The ability to observe the growth of flocs without sedimentation might allow experimenters to discern which mechanism is dominant. In addition, the effects of agitation on the growth of large flocs can be studied under controlled shear conditions in the absence of sedimentation.

To understand many foaming processes it is important to know the surface charge on bubbles in an electrolyte in order to understand the ionic adsorption as a function of pH and interface curvature. These data would be useful in understanding the kinematics of froth and flotation techniques. This is a difficult measurement to make because of the rapid rise of bubbles caused by buoyancy. In a low-gravity environment, bubbles can be kept in suspension more or less indefinitely. The application of an electric field to the electrolyte causes the bubble to move by electrophoresis. A measure of the electrophoretic mobility can be directly related to the surface charge (zeta potential) of the bubble.

Liquid membrane technology may be important in low-gravity. Although this concept has been known for some time, liquid membranes have never been widely used in industrial separation processes. In low-gravity it may be possible to encapsulate fine dispersions of two immiscible liquids with a third mutually immiscible liquid to form a liquid membrane. The very large surface area afforded by such a configuration and the ability to keep such systems in suspension for long periods of time may allow certain purification or extraction processes that are difficult to effect by other means.

The rheology of a fluid system is sometimes affected by sedimentation. For example, to model the flow of blood in the circulatory system, it is necessary to know the viscosity of blood as a function of shear rate. Because of the interaction between the red cells, blood is a highly non-Newtonian fluid with a viscosity that increases dramatically at low shear rates. Attempts to measure viscosity at very low shear rates are thwarted by the fact that the red cells come out of suspension during the time required for the measurement.

Precipitation processes of ferric hydrous oxides and other inorganic materials have been studied extensively since they appear in various natural minerals as well as in pigments, catalysts, coatings, and flocculants. Furthermore, corrosion of iron and steel products consists of one or more iron (hydr)oxides. Despite numerous investigations, little is known about the mechanism of precipitation of these materials. Ample evidence is available to show that the solid phase formed in solutions of ferric salts varies considerably in chemical and structural composition, particle size, morphology, color, magnetic and surface properties, and other characteristics. Very slight changes in the environment can have a very large effect on the type of precipitate produced. Thus it is desirable to study the formation and growth of the inorganic precipitates in the quiescent conditions of low gravity where the fluid environment can be held relatively

constant and can be precisely determined. The lack of sedimentation allows the growth of the precipitates up to tens of micrometers, which is required to investigate some of the properties.

Another example of a physical chemical process that requires weightlessness for investigation is the interaction between a second-phase particle or a bubble and an advancing solidification front. There is a repelling force called the disjoining pressure that tends to push the second-phase particle ahead of the solidification front. On the other hand, there is also a drag force that opposes this motion. Therefore, it would appear that slow-moving solidification fronts tend to exclude foreign particles or bubbles, but fast-moving fronts tend to incorporate them (fig. 2.17). The question is, what is the critical speed and how does it relate to particle size, shape, and composition? Lifshitz developed a theoretical treatment for the disjoining pressure. However, calculation is difficult because it requires detailed knowledge of the optical constants of the material over the entire spectrum, which generally is not well enough known. Since the forces involved are on the order of 10^{-5} g, such measurements can be made only in a weightless environment.

It was found quite by accident a number of years ago that a polyvinyl latex grown by polymerization of a monomer in the presence of a surfactant and water yielded a vast number of microscopic spherical particles that were nearly identical in size (fig. 2.18). The size distribution was so narrow that the particles became widely used as calibration standards for electron microscopy. In a short time these monodispersed particles found a remarkable number of uses, ranging from seriological tests for a number of diseases to measuring pore sizes in biological and other membranes. The current market for products based on monodispersed latex spheres is approximately $30 million per year.

During growth, the latex spheres are kept in suspension by Brownian motion until they reach about 2 μm, at which point they tend to sediment or cream. They can be kept in suspension by gentle stirring, but extreme care must be taken to prevent flocculation or the initiation of a new batch of particles. For this reason, monodispersed spheres are not commercially available in sizes larger than 2 μm.

Figure 2.17. *Interaction between a solidification front and second-phase particles. Glass beads ranging in size from 20 to 80 μm are dispersed in molten durene. The durene is being directionally solidified from bottom to top at the rate of 4.0 μm/s. Particles A, C, and D have been engulfed by the solidification front after being pushed a short distance. Particle B is still being pushed. Such experiments are useful in understanding the solidification of composite materials.*

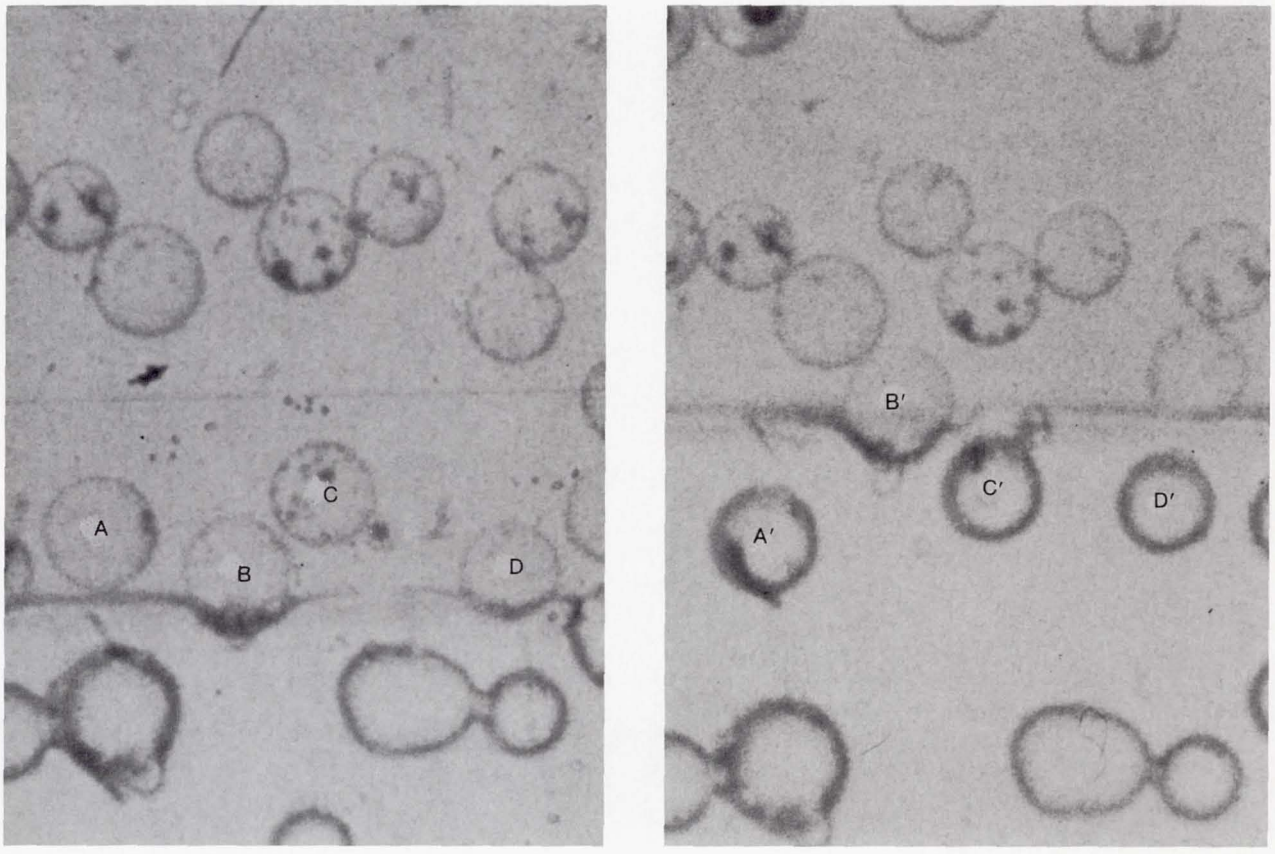

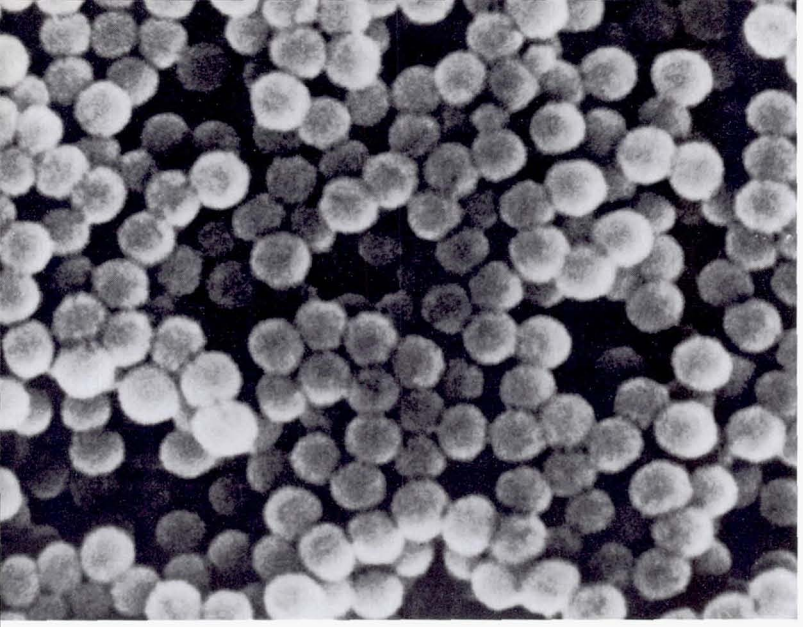

Figure 2.18. Scanning electron micrograph of monodisperse latex spheres. Notice the uniformity of the particles; each particle is 0.4 μm in diameter. (Magnification 20 000x)

It may be possible to produce larger monodispersed latex spheres by keeping them suspended in a weightless environment. There is a requirement for larger particles to calibrate blood cell counters and to investigate transmission through membranes with larger pore sizes. Considering that the small sized particles sell for $35 per 10 ml solution containing 5 percent latex, this amounts to about $70 000 per kilogram of monomer. The production of such particles in space could very well prove commercially feasible.

Strictly speaking, it is the lack of hydrostatic pressure that accounts for the absence of buoyant forces, which results in the elimination of natural convection and sedimentation discussed previously. Another aspect of the lack of hydrostatic pressure is the elimination of the tendency for a liquid or solid to deform under its own weight. This means that liquids will take a shape that tends to minimize surface energy. Menisci formed from between gas–liquid–solid, or liquid–liquid–solid interfaces will be determined solely by surface tension without hydrostatic distortion. This permits a more detailed investigation of a number of wetting and spreading phenomena, particularly such effects as contact angle hysteresis and moving interfaces. Other studies that can be aided by the lack of hydrostatic pressure include critical point phase transitions, the shape and stability of liquid bridges or floating zones, and the coalescence of viscous droplets. Again, the objective is to perform an idealized experiment that is simple enough to compare with a tractable model. Examples are given in the following paragraphs.

Normally the gravitational contribution plays a negligible role in molecular interactions. The one exception is near a phase transition critical point. As such a critical point is approached, the ensemble of molecules that are involved in thermal fluctuation is so large that the difference in gravitational potential over the ensemble becomes significant and the factors affecting the transition become dependent on gravity in a way that is not well understood. Furthermore, the times required to approach equilibrium are long—generally on the order of hours. Therefore, such experiments are logical candidates to be performed in a weightless environment.

There are two difficulties imposed by the gravitational field in measuring the properties of a fluid near the critical point: (1) All such measurements average over a finite distance. Since the slope of the critical isotherm approaches zero at the critical point, the small change in pressure over the averaging distance due to gravitational potential can have rather large effects in the volume of the fluid. (2) As the vapor nears the critical point and begins to condense, the large density difference between the liquid and vapor causes rapid separation of the two phases. Both difficulties should be alleviated by low-gravity experimentation.

The distortion of fluid shapes because of hydrostatic pressure interferes with the accurate measurement of surface-related phenomena such as contact angle, contact angle hysteresis, and the effect of moving interfaces on contact angle. One potentially interesting problem along these lines is the study of the liquid interface formed between three spheres, and the capillary instabilities and irreversibilities encountered in filling and removing the liquid. This would be a model of a theoretical problem considered by Haines in 1930 in which he attempted to describe phenomena encountered in many technologically important applications such as water in soils, extraction of oil from porous media, the wetting and drying of textiles, and so on.

PROCESSING OF BIOLOGICAL MATERIALS

Another important technology that could benefit from the elimination of buoyancy-driven convection is the separation and purification of biological materials such as cells, cell components, cell surface antigens, proteins, and hormones. Advances in fundamental knowledge are often stimulated by improvements in the ability to subdivide a complex system into individual components for study. For example, our understanding of the immune system was recently enhanced by the recognition that there were two distinct classes of lymphocytes, each with a specific function. The B-lymphocyte has the primary role of producing antibodies and is responsible for humoral immune responses. The T-lymphocyte, which is produced in the thymus, has a more complex role. It serves as a "killer cell" by interacting directly with a foreign cell or tumor cell and killing it. It also acts as a "helper cell" by somehow stimulating B-lymphocytes or other components of the immune system. Recent evidence suggests that there may be as many as five subclasses of T-lymphocytes, although we do not yet have the capability to produce a good enough separation to study the functions of the subclasses. The ability to understand and control the immune system is extremely important in

preventing the rejection of transplants and treating disorders in the immune system. In fact, one of the major puzzles in the problem of cancer is why the immune system apparently loses the ability to recognize and kill malignant cells.

There are a host of other important separation problems that could have important applications in biomedical sciences, for example, isolation of beta pancreatic cells to determine how their production of insulin is regulated and possibly the production of human insulin; purification of whole islets of Langerhans for transplants as a cure for juvenile onset diabetes; isolation and purification of hemopoietic stem cells for treatment of certain types of leukemia; isolation of cells from organs that produce various hormones and enzymes such as urokinase, erythropoietin, and human growth factor; separation of bull sperm for selective breeding; high-resolution separation of various proteins such as subclasses of immunoglobins and cell surface antigens on an analytical scale to determine molecular structure and function; and purification of proteins such as synthetically produced polypeptide hormones on a preparatory scale for research and as pharmaceutical products.

A variety of separation techniques have been developed over the years to attack these problems: density gradient centrifugation, various types of chromatographies such as affinity chromatography and high-pressure liquid phase chromatography, fluorescence-activated cell sorting, various types of electrophoresis such as gel electrophoresis and continuous flow electrophoresis, isoelectric focusing, and liquid phase partitioning (sometimes referred to as counter-current distribution). Each of the available techniques has its own problems that limit the range of application. In many cases a multiplicity of techniques is required to solve a specific problem.

A number of these techniques, particularly electrophoresis and isoelectric focusing, are limited by convection and sedimentation. Thus they are logical candidates for space experimentation to determine the extent to which gravity effects limit the process, how the process may be optimized, and the possible improvement that could be achieved by performing the process in space.

Electrophoresis is based on the net charge obtained on the particles to be separated when introduced into a buffer solution (fig. 2.19). Ions in the buffer solution combine with certain molecules on the surface of the particle to be separated, resulting in a net charge on the particle surrounded by a sheath of opposite charge in the buffer solution. An applied electric field causes an ionic current to flow in the buffer solution and interacts with the charged double layer surrounding the particle to produce a force. The particle moves with a velocity such that the electric force is balanced by the viscous drag in the buffer. This velocity for a given applied field is called the mobility of the particle. Since the charge produced on the particle by the buffer depends on the surface molecules, particles with different surfaces (such as different cell types) should exhibit differences in mobility and should therefore be separable by this process.

The other electrokinetic technique, isoelectric focusing, takes advantage of the fact that the mobility of the particle varies as a function of the pH of the buffer (fig. 2.20). In fact, there is a value of pH, called the isoelectric point (pI), at which the mobility of a particle reverses sign. A special buffer that establishes a pH gradient when subjected to an electric-field is used. Particles to be separated are driven to their isoelectric points, where they are continually focused or constrained by the pH gradient.

The electrokinetic separation processes are easily upset by any convective flow. Electrophoresis is usually carried out using a porous medium such as paper or a gel that allows molecules to migrate but suppresses any convective flow. This procedure is presently one of the most powerful tools available for the analytical separation of proteins where only nanogram to microgram quantities are required. However, it has not been successfully scaled up to separate proteins on a preparative scale where milligrams to kilograms are required. Also, gel electrophoresis is not applicable to cells because of the small pore size of the stabilizing medium.

The continuous flow technique is the most promising for using any of the electrokinetic separation methods for preparative scale applications. The sample and the buffer are introduced into a separation chamber, as shown in figure 2.21. A transverse field is applied, causing the sample components to spread according to their mobility, and the separated sample plus buffer is collected by a series of sample tubes at the bottom of the chamber.

Such devices have been used for a number of years, but the gravity-driven convection imposes several limitations on their performance. The current flow in the buffer produces heat that must be dissipated through the walls. Therefore, the flow chamber must be made very thin, generally less than 1 mm, to minimize the temperature rise and to prevent unstable convection caused by temperature inversions. Even so, there must exist nonvertical temperature gradients due to the heat transfer to the wall. To prevent convective circulation from this effect, it is necessary to limit the applied field to reduce the heating and employ sufficient flow velocity to maintain a unidirectional flow. This limits the degree of separation that can be obtained. Also, the restriction of the thickness of the chamber limits the size of the sample stream and intensifies the distortions due to the wall effects. By operating with a much thicker chamber in a weightless environment, it should be possible to increase both the resolution and throughput of continuous flow electrokinetic separation.

The other technique that could be dramatically improved in a low-gravity environment is liquid phase partitioning or counter-current distribution (fig. 2.22). Cells to be separated are shaken with an immiscible two-phase aqueous polymer mixture, usually dextran and polyethylene glycol

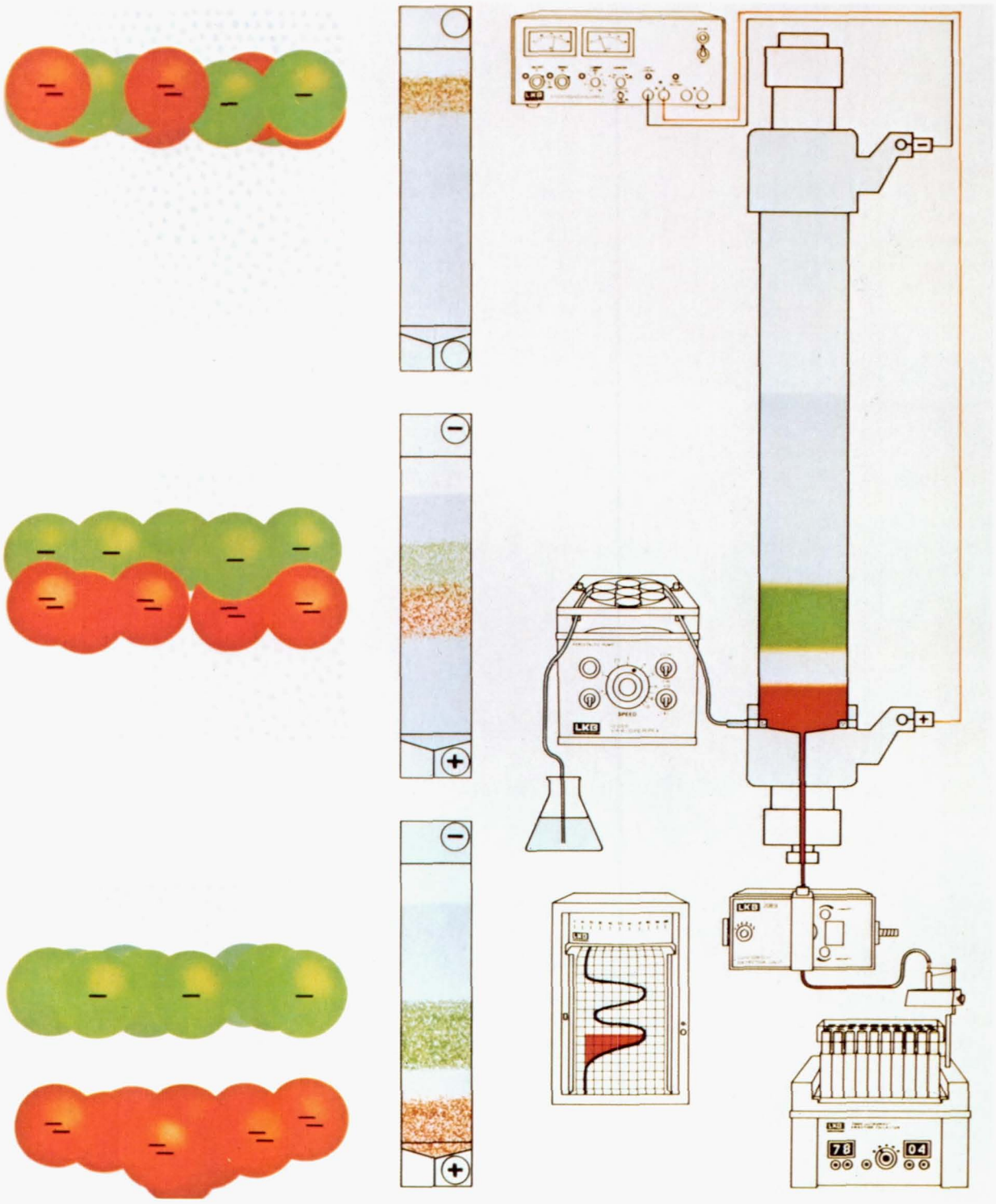

Figure 2.19. *Conventional electrophoresis. In conventional electrophoresis the sample components are separated based on their differences in net charge, size, and shape. The separation takes place at a constant pH and ionic strength. Polyacrylamide gel, cellulose, or granulated gels are used as stabilizing media. The sample is applied as a narrow zone on top of the stabilizing gel and when the electric field is applied, the sample components migrate into the gel. Separation in the stabilizing media takes place because of the different mobilities of the sample components. The separated zones migrate one after the other out of the gel into the funnel-shaped elution chamber, where they are then flushed out by a continuous stream of elution buffer. [Photograph courtesy of LKB Instruments, Sweden.]*

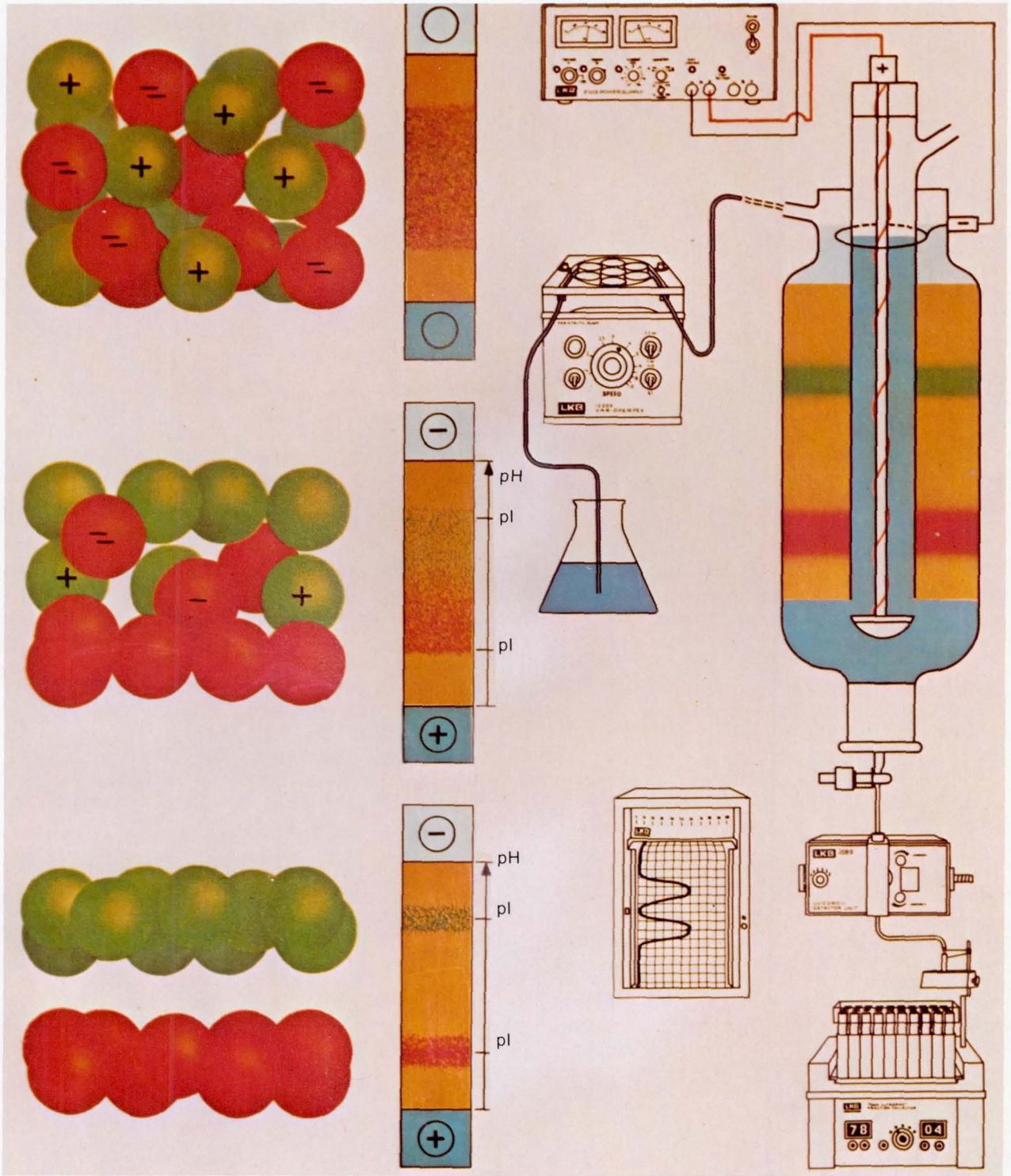

Figure 2.20. *Isoelectric focusing. In isoelectric focusing the sample components are separated in a pH gradient according to differences in isoelectric point (pI). Ampholine carrier ampholytes are used to create the pH gradient and when an electric field is applied, the pH gradient is rapidly formed. The sample is applied either as a zone or throughout the whole column. Charged sample components migrate toward the electrode of opposite charge. The net charge is continuously reduced during migration in the pH gradient. At a pH value equal to the pI of the sample, the net charge is zero and migration stops. The sample components are focused at their respective pI values, forming concentrated and narrow zones. [Photograph courtesy of LKB Instruments, Sweden.]*

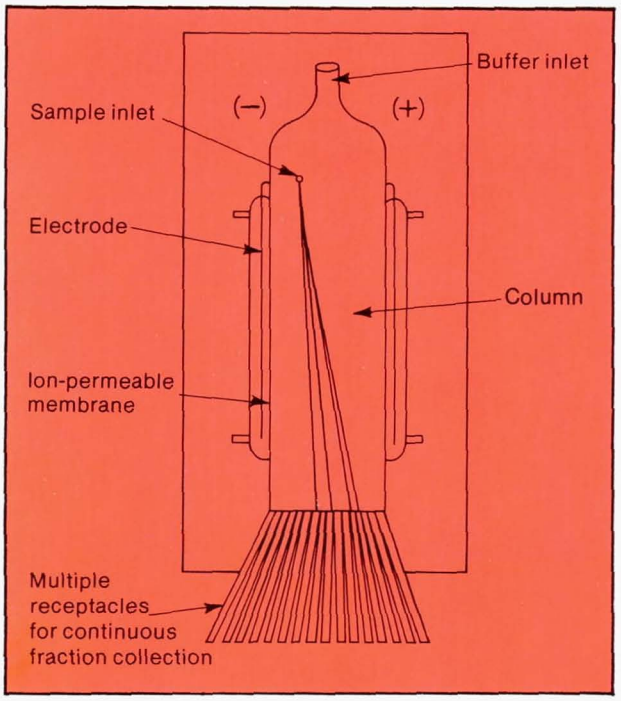

Figure 2.21. Continuous flow electrophoresis. A continuous flow of buffer solution from top to bottom is maintained through this apparatus. The sample is injected continuously, and the individual constituents are deflected by the horizontally applied electric field. Each constituent is deflected differently according to its superficial electric charge, and the separated sample plus buffer is collected by a series of sample tubes at the bottom of the chamber. Sedimentation is minimized by operation in a vertical orientation and by rapid buffer flow through the cell. Convective disturbance due to joule heating of the buffer is minimized by making the separation between cell walls as small as possible and by active cooling through the walls. However, if the separation is reduced below 1 to 2 mm, resolution is degraded by wall effects.

(PEG). Depending on the surface properties of the cells, they have a preference for one phase over the other. As the solution settles, the denser phase settles to the bottom of the container, leaving the lighter phase on top, just like the separation of oil and water. The cells that are partitioned into the less dense phase collect at the interface, while the cells that are partitioned into the more dense phase settle to the bottom.

The partitioning coefficient can be controlled by several techniques. Adding a small amount of certain salts to the polymer solutions provides a means of separating according to the surface charge, which is largely a property of the glycoprotein molecules imbedded in the cell membrane. An even more exciting possibility is the use of affinity ligands. The ligands can be attached to the molecules of the PEG phase by a simple esterification reaction. Examples of reactions between the affinity ligand and the large cell are antibody to antigen, hormone to receptor, and enzyme to substrate. In this way specific cell types can be separated from a mixture of other cells.

The primary limitation of this process is the tendency for cells to sedimentate through the interface between the two phases during the separation process. This should be avoided in a low-gravity environment.

Figure 2.22. Liquid phase-partitioning of cells. Cells to be separated are shaken with an aqueous solution of two immiscible polymers, usually dextran and polyethylene glycol (PEG). Most cells (B) partition at the interface. Cells to be separated have molecules of PEG bound to ligands that have a special affinity for specific receptor sites on the cell surface. These cells (A) tend to stay in suspension in the PEG phase (a), along with some B cells that also partition statistically into the PEG. As the system comes to equilibrium (b), the cells tend to sedimentate and clump at the interface, which may cause difficulty in the physical separation. In low gravity (c) this sedimentation is avoided and the surface area at the interface is vastly increased. Several methods of agglomerating the droplets have been suggested and await testing.

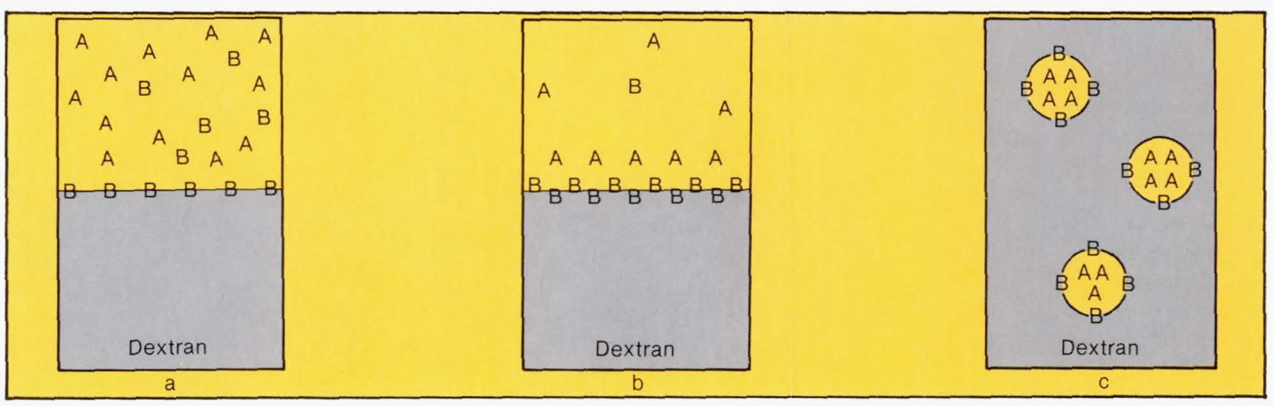

Chapter 3.

THE EVOLUTION OF APPARATUS FOR MATERIALS PROCESSING IN SPACE

THE INCEPTION OF SPACE PROCESSING

Interest in materials processing in space began to evolve in the late 1950s from several different disciplines. The behavior of fluids in spacecraft was the object of a number of research efforts to design propellant management systems and other fluid systems required by emerging space technology. The development of spacecraft thermal control systems that utilize change of phase of materials for heat storage prompted questions concerning solidification phenomena in zero gravity. The possibility of the erection and repair of large structures in space by brazing and welding raised issues concerning the flow of liquid metals dominated by capillary forces.

In considering the likely behavior of liquids and solidification processes in the low-gravity environment of an orbital spacecraft, it was recognized that this environment might be useful for a variety of unique processes. This prompted a number of experiments utilizing drop towers, research aircraft flying parabolic trajectories, and small "carry-on experiments" on the last several Apollo flights. This chapter reviews the evolution of apparatus leading to the development of the facilities for the melting and solidification experiments flown on Skylab.

EARTH-BASED EXPERIMENTAL ACTIVITIES

Drop Tower Experiments

A convenient facility for stimulating a low-gravity environment on Earth, albeit briefly, is the drop tower represented schematically in figure 3.1. An experiment package is placed in a canister as shown, and the canister is given sufficient downward thrust by small rocket motors to overcome the decelerating forces of air resistance and guide rail friction. The experiment package is then in a state of free fall within the canister. The drop tower depicted in the figure is located at the Marshall Space Flight Center and, with a drop height of 90 meters, is capable of providing a low-gravity environment for approximately 4 seconds.

Drop tower tests proved to be of considerable value in the verification of experimental concepts and the development of apparatus flown on Skylab. One example involved the dispersion and solidification, in a drop tower experiment, of the two normally immiscible elements gallium (Ga) and bismuth (Bi). Because solidification occurred in a low-gravity environment, the more dense material did not fall to the bottom of the container, and the product of the experiment was a solid mixture of finely dispersed particles of the two elements, as may be seen in figure 3.2. It was found that the degree of dispersion produced a unique temperature dependence of the electrical resistivity of the solid quite unlike the pure materials (fig. 3.3). These results suggested that immiscible materials processed in space could form an entirely new class of electronic materials and led to the development of Skylab experiments of a similar nature.

Figure 3.1. Low-gravity drop tower. Drop towers are used extensively to simulate the low gravity of space. An experiment package is dropped from a height, and it experiences a condition of low gravity during the period of free fall. The drop tower depicted here is located at George C. Marshall Space Flight Center and is capable of accommodating a relatively large experiment package. The drop height of 90 meters provides approximately 4 seconds of low gravity. A surprising amount of data can be gathered during this period.

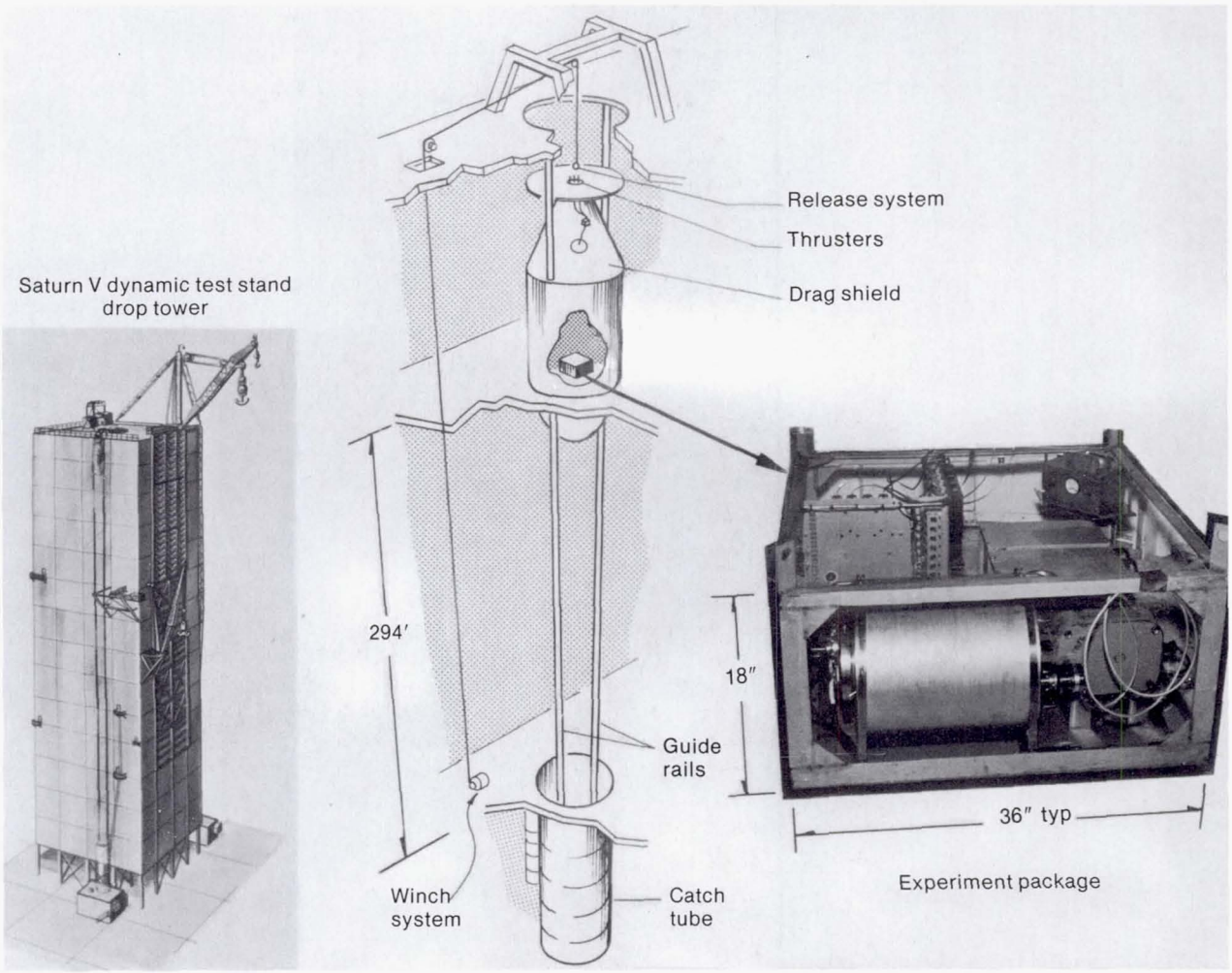

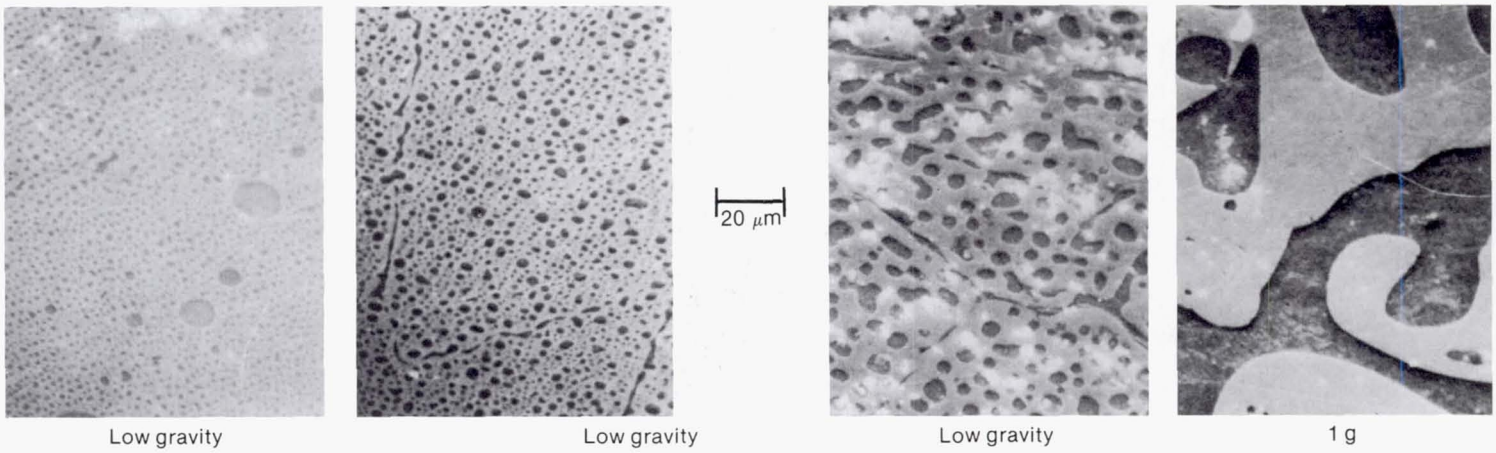

Figure 3.2. Microstructure obtained by rapidly cooling and solidifying samples of gallium (Ga) and bismuth (Bi) during free fall. The darker regions are Ga-rich particles with diameters in the range of 1 to 5 μ dispersed in a Bi-rich matrix (light grey region). The dispersions obtained for the samples where microstructures are shown in low-gravity environments are associated with different solidification times in low gravity with typical cooling rates of 5 x 10^3 K/S. A ground control sample was processed under otherwise identical conditions, except that the sample was not dropped. Note the coarse and highly separated structure of the alloy solidified at 1 g. The drop tower experiments on Ga-Bi have shown the major impositions of gravity in controlling the phase separation rates and consequently the microstructure of immiscible or monotectic alloys.

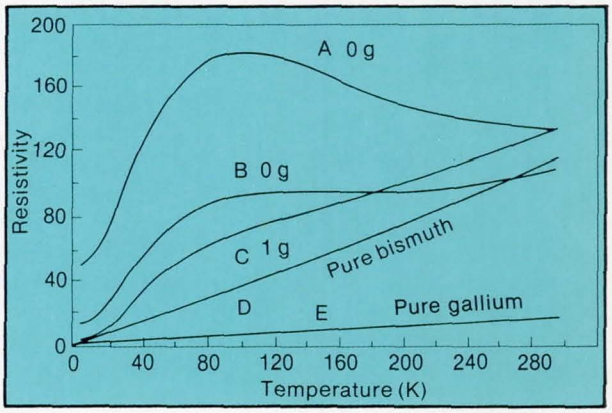

Figure 3.3. Electrical resistivity of the immiscible alloy Ga-Bi processed in the drop tower. Curves A and B represent samples processed in zero gravity, with different microstructures obtained by varying the cooling rate. Curve C corresponds to the 1-g control sample, and curves D and E are the resistivities of the pure elements.

Experiments on Research Aircraft

The use of aircraft flying parabolic (Keplerian) trajectories provided an order of magnitude increase over drop tower tests in the time that low-gravity conditions could be sustained for experimentation. An airplane flying the trajectory indicated in figure 3.4 provided 10 to 20 seconds in which the objects within were freely falling. The minimum gravity level obtainable by this method was approximately 10^{-2} g and unsteady—not a suitable environment for precise experiments. Nevertheless, the extended time permitted researchers to verify the functioning of several Skylab experiments as they were being developed (fig. 3.5).

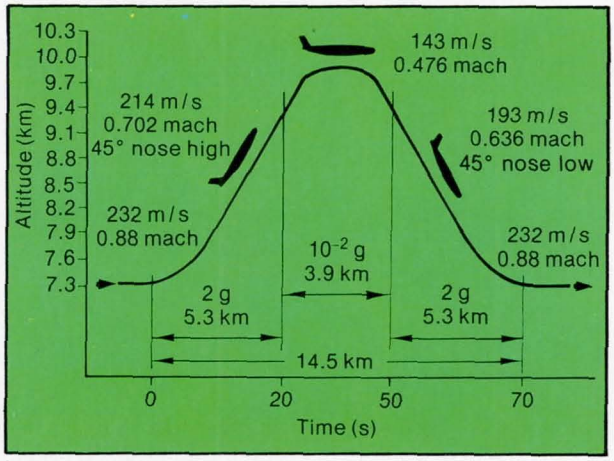

Figure 3.4. Low gravity in aircraft flight. This figure shows the Keplerian trajectory, a series of aircraft maneuvers designed to produce low gravity conditions for experimentation. The reduced gravity environment exists for less than 30 seconds and is useful for crew training and experiment hardware development and verification tests.

Figure 3.5. Low gravity inside a research aircraft. This photograph was taken during the reduced gravity phase of a Keplerian trajectory maneuver. The experiment package is a precursor to one of the Skylab experiments.

PRELIMINARY EXPERIMENTS IN SPACE

The Apollo Experiments

During the trans-Earth coast period of the Apollo 14 mission, a set of experiments was performed which verified that, in low gravity, mixtures of materials of different specific gravities remain stable in the liquid state and during freezing; that is, the materials do not unmix because of sedimentation as they do on Earth. This set of experiments, referred to as the composite casting demonstration, is pertinent to this discussion because it was conducted in the first space processing furnace, a precursor to some of the Skylab apparatus.

The composite casting furnace, shown in figure 3.6, employed an electrical resistance element and a thermostat to provide a uniform temperature of 140° C within a cylindrical cavity. The mixtures to be processed were enclosed in sealed cartridges, shown in figure 3.7. The use of cartridges to contain materials samples provided a simple standard interface between the experiment and the furnace. The cartridges were heated in the furnace cavity and then, while still in the cavity but with the furnace switched off, cooled by putting a cold mass in contact with one end. In certain cases the rate and direction of heat flow during cooling were deliberately influenced by the placement of appropriately shaped pieces of metal within the cartridges. These appear as light regions in the figure. This early development of thermally designed cartridges set the stage for the design of furnaces and cartridges for Skylab experiments.

The composite casting demonstration showed that multiphase composites with components of different densities could be solidified from the melt without phase separation in a low-gravity environment. This was demonstrated in two groups of experiments. In the first group, fibers, particles, or gases were mixed into a molten matrix of indium and bismuth and solidified. The space-processed samples did not exhibit the separation of the dispersed phase from sedimentation or buoyancy effects as did the control samples; however, the dispersions were not completely uniform. The other group consisted of experiments with two- and three-phase immiscible mixtures of sodium acetate, paraffin, and either fibers, particles, or gases. Reasonably stable dispersions of the immiscibles were achieved in the space-processed samples which could not be duplicated on Earth (fig. 3.8).

Fluid experiments were conducted on Apollo 14 and Apollo 17 to ascertain the effects of weightlessness on heat flow and convection for selected configurations. These experiments provided data on surface-tension-driven flow independent of gravity and on convection caused by spacecraft and astronaut movements. The apparatus is shown in figure 3.9. Very vivid Benard cells were observed in a 2-mm layer of Krytox 143A2, a perfluoro alkylpolyether, which was heated from the surface opposite the free surface (fig. 3.10). This demonstrates that convective flows are not completely eliminated in a space experiment and that careful design of the experiment is necessary to control the fluid motion. In this case the convection is driven by surface tension. Since surface tension decreases with temperature, the system would have a lower energy if the warmer fluid below displaced the cooler fluid at the surface, resulting in an instability that causes overturning flow after a certain critical thermal gradient is reached. This is similar to the unstable convection caused by a more dense fluid overlaying a less dense fluid in a gravitational field, as discussed in chapter 1, except that in this case the driving force is not dependent on gravity.

The amount of convective heat flow resulting from residual vehicle accelerations was measured in CO_2 using a radial cell configuration with a stub heat at the center, and in liquid H_2O and sugar solution using cylindrical tubes heated at one end. Temperatures were measured by observing the color change of liquid crystals fixed to the test cells. On Apollo 14 the temperature distribution in the cells indicated 10 to 30 percent more heat transport than could be accounted for by conduction. The experiment was repeated on Apollo 17, substituting argon (Ar) for CO_2 in the radial

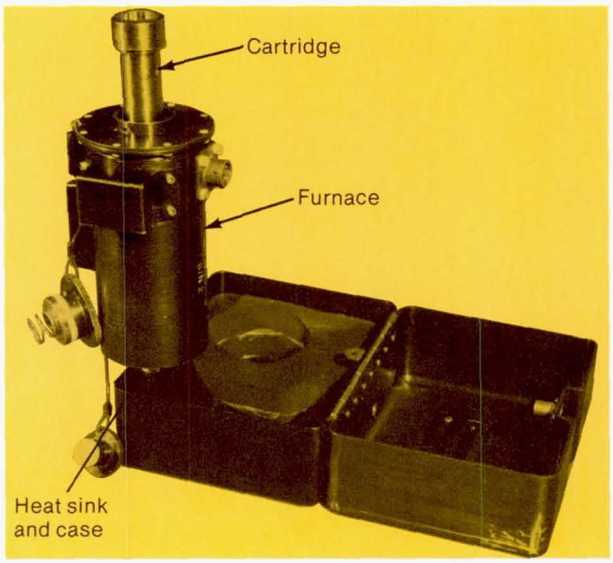

Figure 3.6. Apollo 14 composite casting apparatus. The sample cartridge was inserted in the furnace cavity. Following the experiment operations, which included heating and manual shaking if required, the furnace was removed from the operational position shown and placed in the heat sink well of the case for passive cooling.

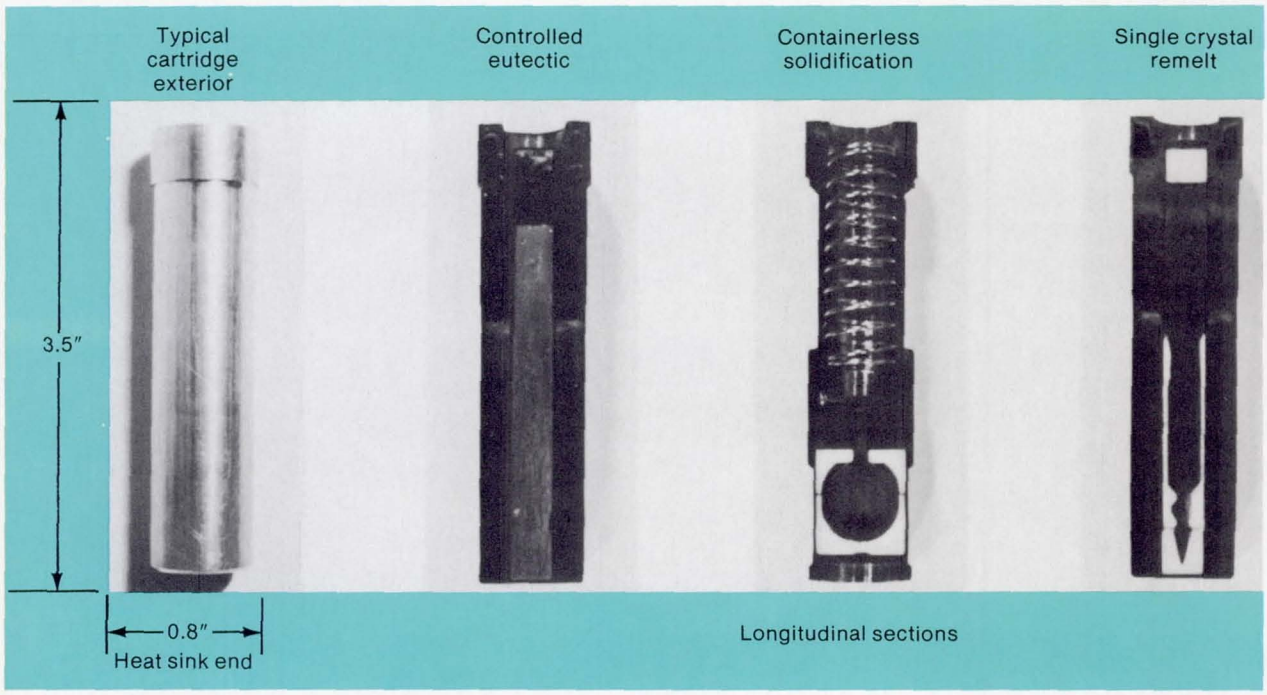

Figure 3.7. Cartridge designs for the Apollo 14 casting furnace.

Figure 3.8. Apollo 14 immiscible materials processing (sodium acetate-paraffin). The radiograms show that the sodium acetate and paraffin were completely segregated in the control sample and almost completely dispersed in the flight sample. In the flight sample, the paraffin was primarily dispersed in the sodium acetate except at the top center of the sample where three large drops of paraffin coalesced and enclosed some sodium acetate spheres. Duplex dispersions, consisting of a thin shell of paraffin surrounding a sphere of sodium acetate, were seen at various locations in the flight sample, as shown in the magnification.

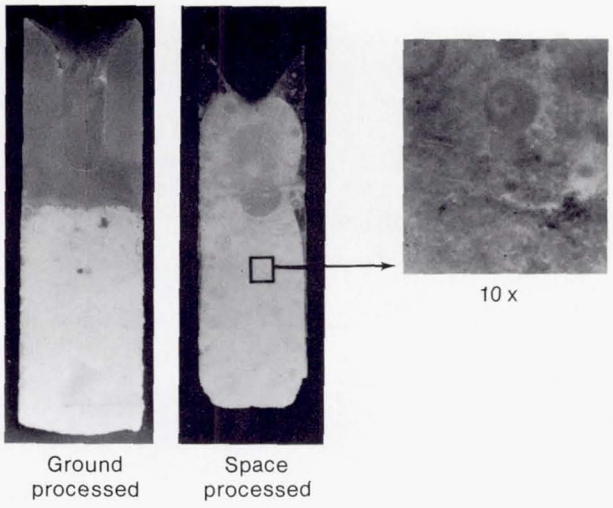

cell and Krytox oil for the H_2O and sugar solutions. Tracer particles were added to the Krytox oil to study fluid motions. No significant heat flow in addition to that predicted from pure conduction or significant movement of the marker particles were observed. Apparently the difference was due to different levels of crew activity on Apollo 14.

The third type of demonstration experiment conducted on Apollo spacecraft was an attempt to perform an electrophoretic separation in a free column. Convective flow resulting from Joule heating severely distorts the separation on Earth unless a gel or other supporting technique is used to suppress the convective flow. The use of a supporting medium restricts the types of separation that can be performed. For example, cells generally cannot pass through the gel.

The Apollo 14 experiment consisted of three electrophoretic columns containing a borate buffer. The samples consisted of (1) a mixture of red and blue dyes, (2) human hemoglobin, and (3) deoxyribonucleic acid (DNA) extracted from salmon sperm. The object of the experiment was to observe the shape and distortions of the sample band as it moved under the influence of the applied field. No attempt was made to collect the samples. The data were recorded photographically; unfortunately, poor lighting and camera positioning impaired the quality of the photographs. It was possible to determine that the red and blue dyes were transported along the tube, but the shape of the sample band was severely distorted by the electro-osmotic flow along the column walls.

Figure 3.9. Apollo 14 heat flow and convection experiment apparatus.

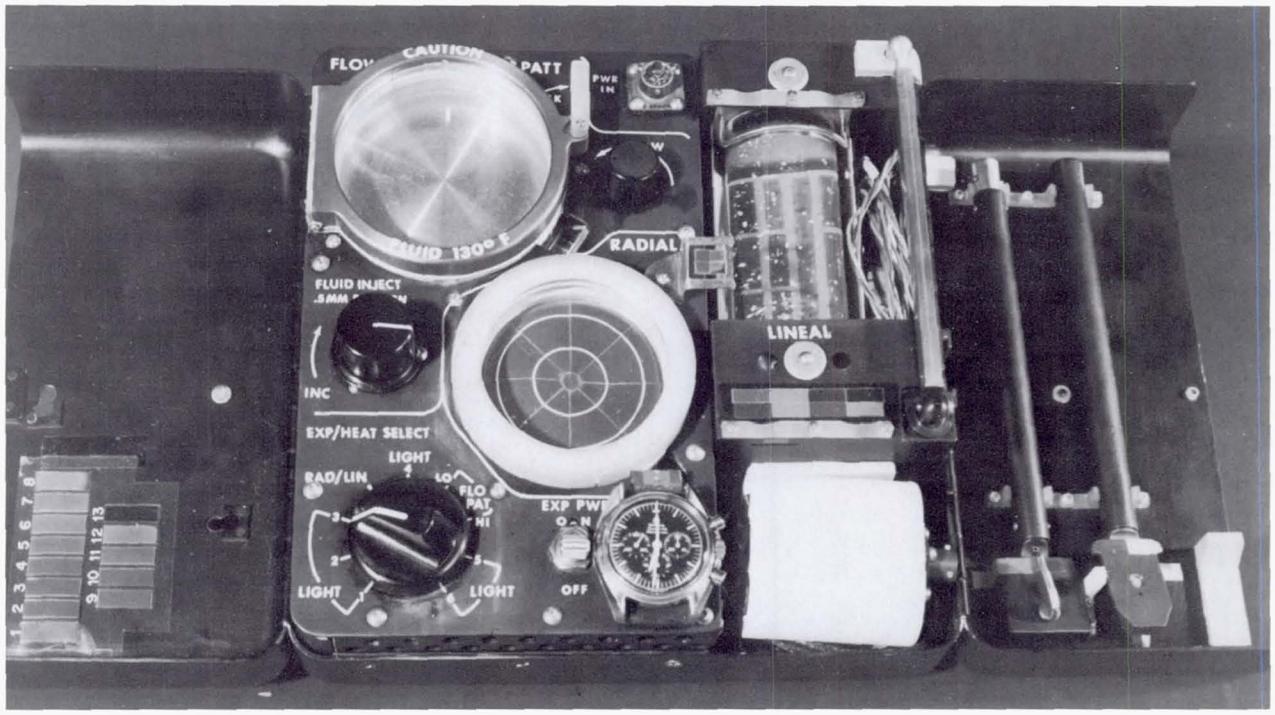

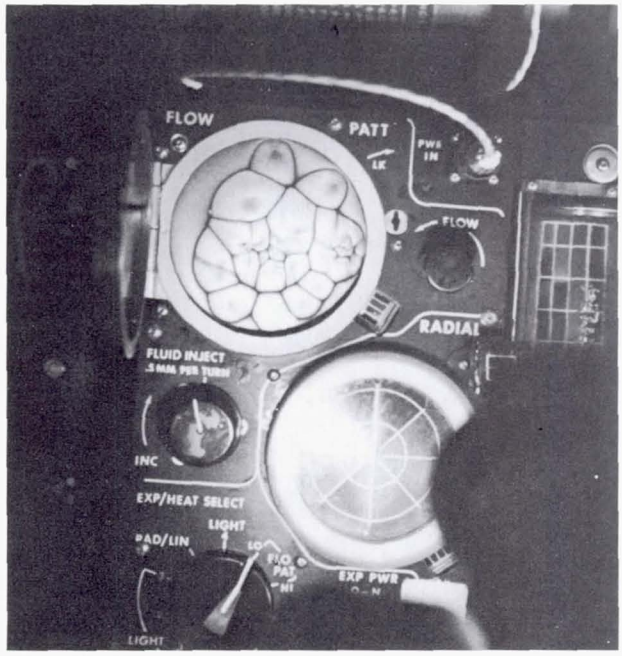

Figure 3.10. Apollo 14 heat flow and convection experiment. The chamber in the center contains Krytox oil and is heated from the bottom. Surface-tension-driven convection produces convection patterns similar to Bernard cells even in the absence of gravity. The lower right-hand cell contains liquid crystal material that changes color when temperatures reach certain values. This was used to study heat flow in the absence of gravity-driven convection.

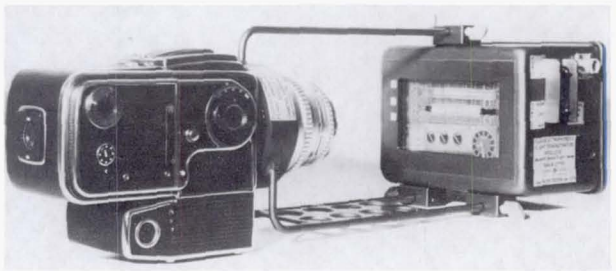

Figure 3.11. Apollo 16 electrophoresis demonstration apparatus.

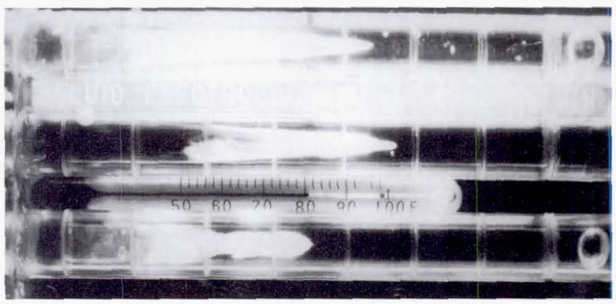

Figure 3.12. Electro-osmotic flow distortion in the Apollo 16 electrophoresis experiment. The bullet-shaped flows result from distortions by electro-osmotic flow—another form of nongravity-dependent flow that must be considered in the design of low-gravity experiments.

An improved version of this experiment was flown on Apollo 16 (fig. 3.11). In this experiment the sample consisted of a mixture of two sizes of monodispersed polystyrene latex particles, 0.2 and 0.8 μm in diameter, respectively. The data were recorded photographically. A slight separation between the two sizes of particles was barely discernible in spite of the severe distortion of the sample by electro-osmotic flow (fig. 3.12). This flow results from the fact that the walls of the tube absorb ions that attract a layer of oppositely charged ions in the buffer. In an electric field the layer of charge in the fluid moves, causing the buffer flow to move along the walls. This flow, combined with the return flow in the center of the tube, produces the bullet-shaped distortion. It was found later that the flow could be eliminated by a suitable coating on the walls that effectively has a zero zeta potential. Again, this serves to illustrate the care that must be taken to eliminate extraneous flows in designing low-gravity experiments to take advantage of the lack of buoyance-driven convection.

Sounding Rocket Experiment

To develop and test apparatus and experiment concepts at a time when manned space flight opportunities were not available, sounding rockets were used. In these suborbital vehicles, low-gravity conditions exist during the unpowered coast phase after launch and before reentry into the atmosphere. The amount of time during which accelerations remain below about 10^{-4} g is usually 4 to 7 minutes.

The first sounding rocket experiment was flown in 1971 using the furnace shown in figure 3.13 and 3.14. It had a resistance-heated cavity that accepted the same cartridges as the Apollo 14 furnace. Additional features of this furnace were an automatic sequencer triggered by the launch acceleration and a water quench capability that was necessary because the specimen had to be melted and resolidified within the short low-gravity time available. The water reservoir is the hemispherical dome on the top of the furnace.

During the flight the specimen was only partially melted and was not fully resolidified prior to reentry. The results were nonetheless interesting in that the experiment reconfirmed the stability of gas bubbles in a melt in low gravity. It also revealed that the heat transfer from the melt to the cartridge wall can be different in space from what it is on Earth. In the low-gravity environment of space, the liquid material tends to "free float" inside the cartridge, and hence the thermal contact between the melt and the cooled cartridge wall is poor. This effect, incidentally, was also observed in Skylab experiments, where it was not detrimental because the experiment times were quite long (hours rather than minutes).

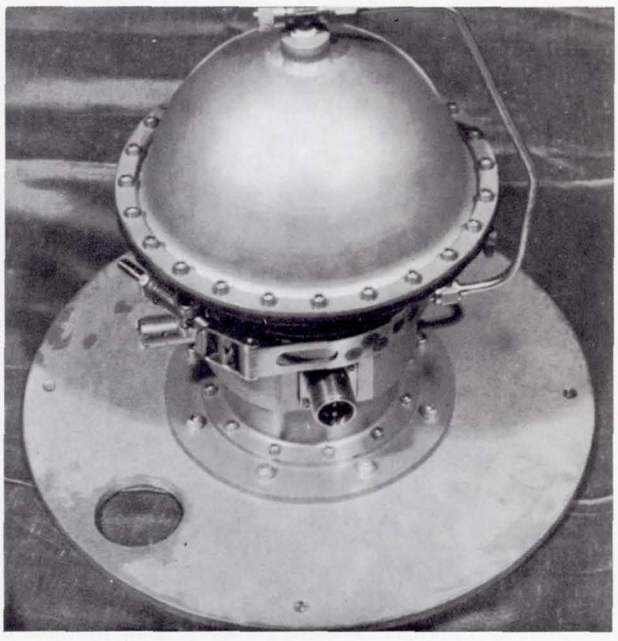

Figure 3.13. *Furnace for early sounding rocket flight.*

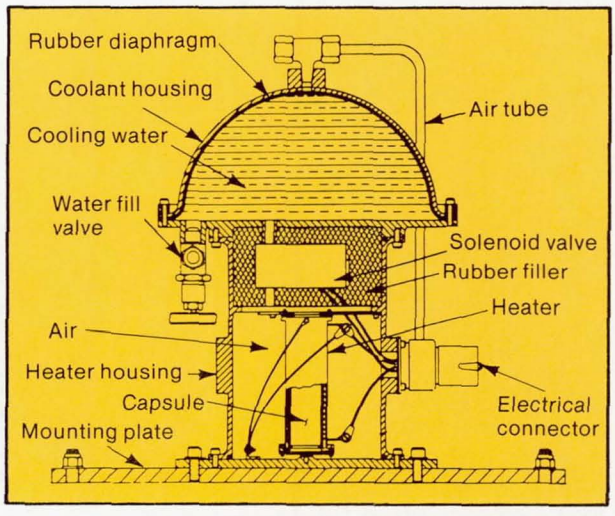

Figure 3.14. *Schematic of the furnace shown in figure 3.13. This furnace was mounted in the payload bay of an Aerobee 200 sounding rocket during a 1971 flight. The design is rather crude by present standards. The rocket was spin stabilized during the coast phase, and since there was at that time no means to uncouple the furnace, it was necessary to locate only a single cartridge along the axis of rotation to minimize acceleration due to centrifugal force.*

SKYLAB EXPERIMENTAL FACILITIES

The first materials processing experiments approved for Skylab were the welding and brazing demonstrations originally motivated by the desire to fabricate and repair large structures in space. These experiments had been under development since 1964 and were accepted for flight in 1966. As interest in processing experiments in a weightless environment grew, facilities were expanded to accommodate five additional experiments, which were accepted in 1969. The Multipurpose Electric Furnace and ten additional experiments were proposed in 1971 and accepted for flight in 1972.

For the purpose of classification and description, it is appropriate to distinguish between two types of melting and resolidification apparatus: the type in which materials are held in a container or crucible and the type in which processing is accomplished while the materials are uncontained. Clearly, the energy sources, heat transfer mechanisms, and apparatus configurations will be different, as will the possibilities for manipulating the molten materials.

Apparatus for Contained Materials Processing

In the experimental apparatus described thus far, samples to be melted are contained in cartridges or crucibles. The cartridges are convenient to handle and provide a simple interface between furnace and experiment. Heat transfer between the sample and the controller is usually more efficient, making it easier to provide steep gradients and rapid quench rates. Crucibles also provide control of the shape of the sample and can eliminate free surfaces if Marangoni convection causes unwanted flows.

The Multipurpose Electric Furnace was designed for processing samples contained in cartridges. The basic design was patterned after earlier flight versions but had more sophisticated control and higher temperature capabilities. The essential features of the Multipurpose Electric Furnace are shown in figure 3.15, and a photograph in figure 3.16. Three equally spaced experiment cavities were heated at one end by electrical resistance elements, and the heat was extracted at the opposite end through a chill plate. Because the furnace was thermally shielded and internally evacuated, the primary thermal links between the heated zone and the cold plate were the cartridges inserted in the three cavities. The cartridges, which had a standard external configuration, were used to contain the experiment material and, by careful thermal design, to control the temperature profile to which the material was exposed throughout the experiment. The furnace was provided with controls to set any desired maximum temperature in the heated zone up to 1050° C, to vary the soak time, and to reduce the temperature of the heated zone at one of several predetermined constant rates. The performance curves are shown in figure 3.17.

The use of the furnace and the methods described previously imposed limitations on the experiments that could be performed and on the materials that could be proc-

Figure 3.15. *The Skylab M518 Multipurpose Electric Furnace. This cut-away schematic identifies the major engineering features and illustrates the ideal heat flow pattern from the heated region through the cartridge to the heat extractor plate.*

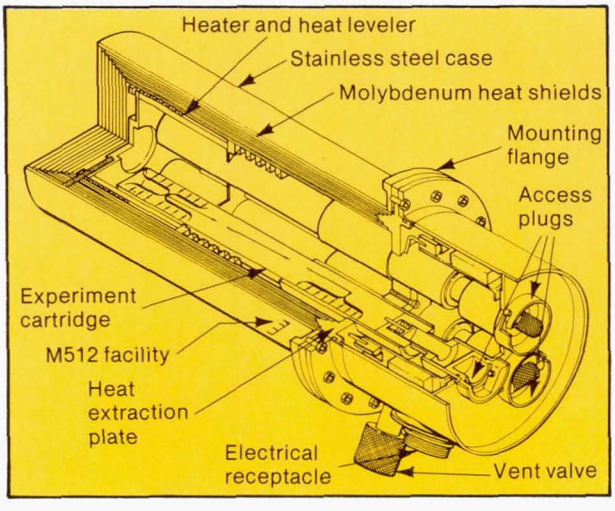

Figure 3.16. *Major components of the Skylab M518 Multipurpose Electric Furnace system. The control package automatically governed the various operating parameters of the furnace. Experiment material samples were contained in sealed ampoules which in turn were encased in stainless steel cartridges.*

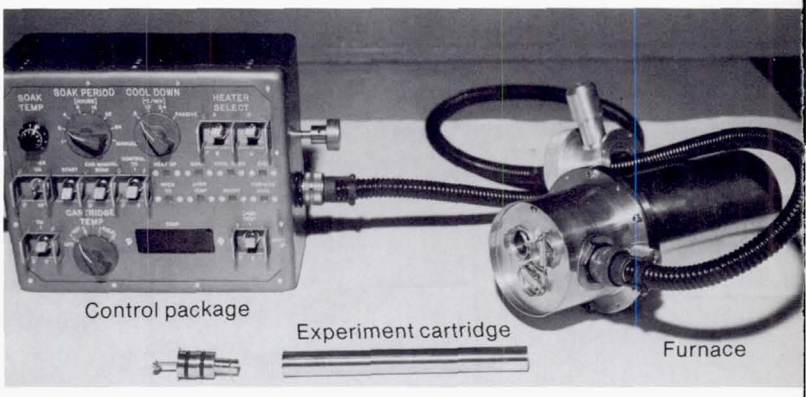

Figure 3.18. Thermal profiles in the M518 Multipurpose Electric Furnace. A sample placed in the heat leveler region (first 4 cm) is cooled isothermally. A sample in the gradient region may be directionally solidified, but note that both the growth rate and gradient change with time.

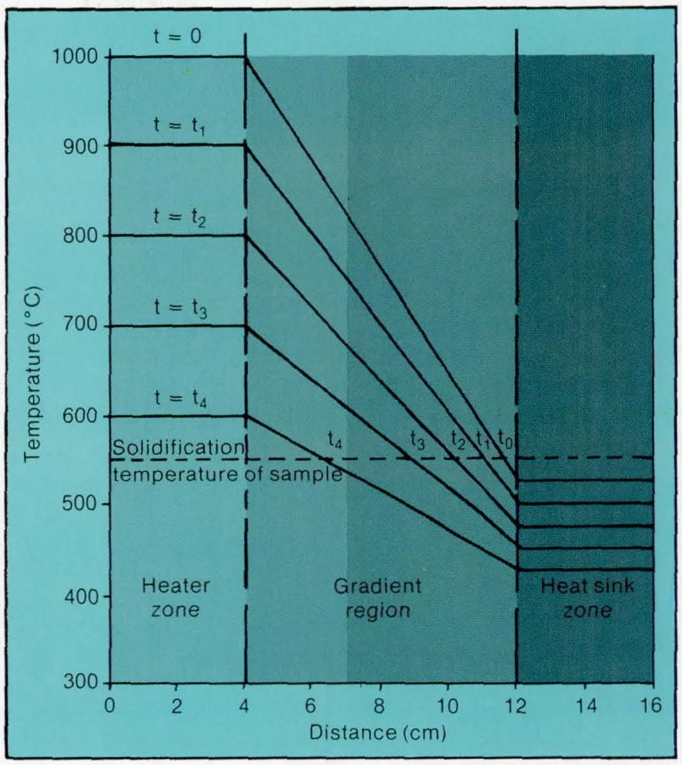

essed. Because the material was contained, it was not possible to process highly corrosive materials, materials with very high melting points, materials for which no contamination from the container wall could be tolerated, or materials for which other effects brought about by contact with the wall (e.g., nucleation) had to be avoided. Another shortcoming lay in the fact that the furnace could only be controlled from one end. The profiles in the gradient region are shown in figure 3.18. For uniform cooling, a sample being directionally solidified is subjected to an accelerating growth rate and decreasing thermal gradient—not an optimum condition for maintaining a stable growth interface.

To overcome some of the disadvantages of containment, a hybrid system can be devised wherein a quasi-free sample is held within a cartridge; the molten liquid is held in place by a nonmelting support such as a rod or a wire. This means was used in several experiments. In one, for example, an indium antimonide crystal was grown without wall confinement but attached to an indium antimonide monocrystalline rod through which the heat was extracted as the sample solidified (fig. 3.19).

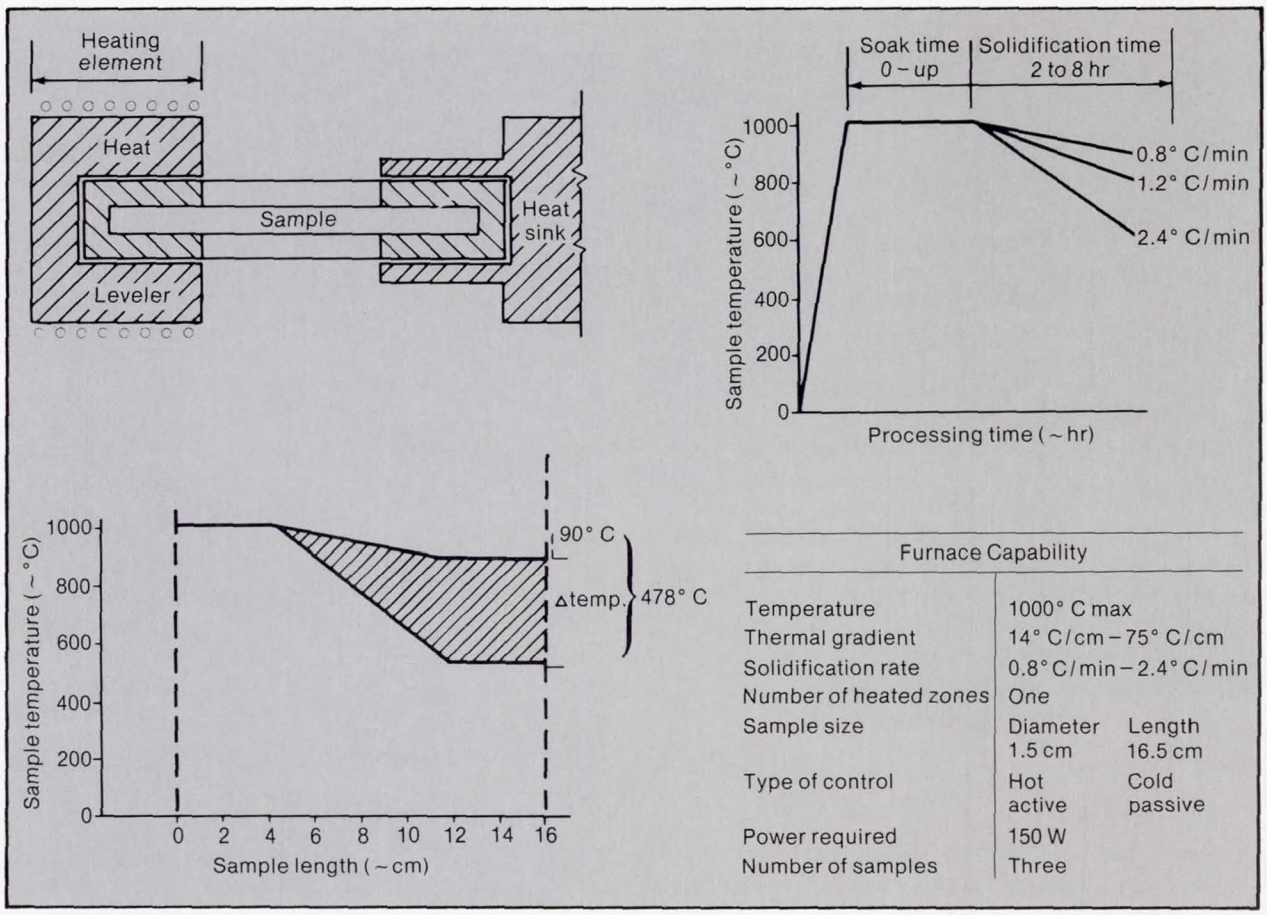

Figure 3.17. Performance capability of the M518 Multipurpose Electric Furnace developed for Skylab.

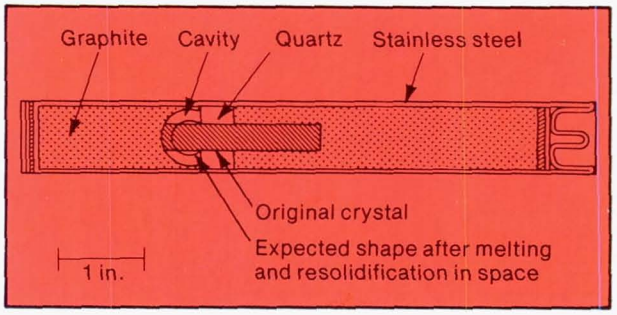

Figure 3.19. Cartridge design for semicontainerless processing. The experiment was designed so that only the portion of the original crystal extending into the cavity would be melted. It was anticipated that, in the absence of gravity, surface tension would draw the molten portion into a spherical globule in contact only with the unmelted portion of the crystal.

Apparatus for Brazing in Space

The one nonelectric heat source flown was used for the Skylab tube brazing equipment, of which a detailed discussion is presented in chapter 5. The energy to melt the braze alloy was supplied by the reaction of chemicals. The general configuration of the experiment is shown in figures 3.20 and 3.21. The cavity temperatures and thermal profiles proved to be reproducible to within a few percent. The energy of the chemical exotherm is on the order of 650 calories/gram. In the configuration shown, the specimen reached a temperature of 1050 ± 40° C within 90 seconds of ignition. There is no apparent reason why chemical energy sources of this type should not be used in the future to melt suitably contained materials, providing a long soak time is not required.

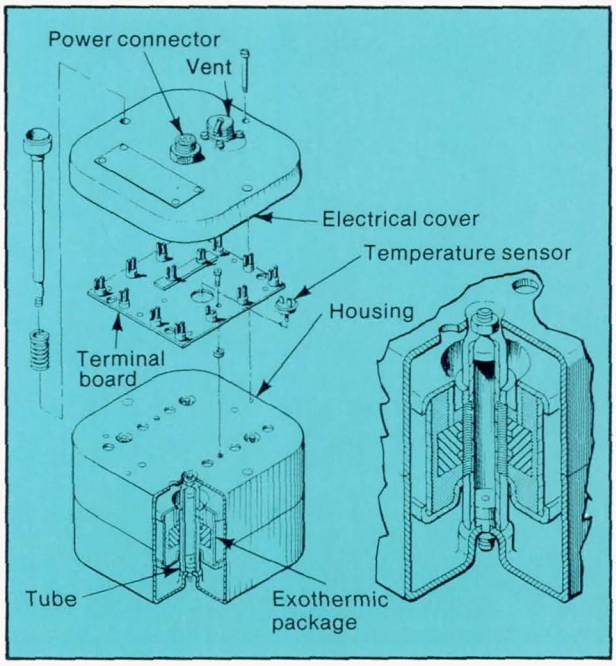

Figure 3.20. Exothermic brazing experiment.

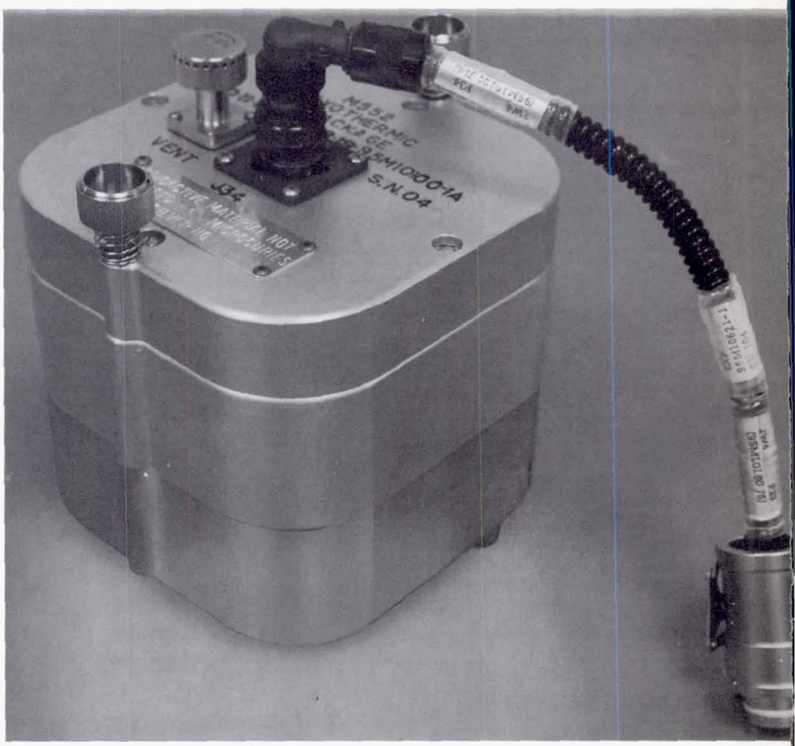

Figure 3.21. Exothermal brazing experiment package assembled and ready for mounting in the M512 Material Processing System.

Apparatus for Containerless Processing

Three factors influence the design of apparatus for processing uncontained materials in space: (1) positioning the freely floating materials in relation to the processing apparatus, (2) heating and cooling the materials, and (3) manipulating the materials, if necessary.

As explained in the preceding chapter, freely floating masses tend to drift relative to the spacecraft because of the effects of orbital mechanics and the slight residual accelerations of the spacecraft and hence of the apparatus housed within it. Under these circumstances the forces required to hold a material specimen in position in the processing apparatus are only on the order of 10^{-4} to 10^{-6} of the terrestrial specimen weight. Several options exist. The simplest is to hold the specimen mechanically; for example, on a sting from which the specimen may or may not be released upon melting. If the specimen is released upon melting but is small and freezes rapidly, no constraint may be needed after melting because the specimen drifts slowly into contact with elements of the apparatus. Larger or slow-to-freeze specimens must be levitated (or held in position) by electromagnetic or acoustic forces.

With the specimen exposed, many means are available for supplying the energy necessary to melt it. The specimen may, of course, be held within a heated cavity, but other possibilities include electron beam impingement, imaging an intense source such as an arc lamp on the specimen, induction heating, or use of a solar furnace.

The first freely floating containerless solidification experiment was performed on Skylab. The samples for the sphere-forming experiment were held on the wheel depicted in figure 3.22, each sample on a ceramic pedestal. To process successive specimens, the wheel was indexed. The specimens were melted by an electron beam directed normally to the plane of the wheel, as shown by the arrow in the figure. Upon melting, each specimen separated from the wheel and was free to "float" within the evacuated process chamber. The specimen size had been chosen such that solidification would occur within 10 to 20 seconds; that is, before the specimen could drift into contact with the chamber wall. A few specimens were made to stay attached to their stings; one of these is seen on the upper part of the wheel. The specimen marked "target" was made of tungsten and was used for alignment and focusing of the electron beam gun before the initiation of the experiment sequence.

The constraint on specimen size in the sphere-forming experiment could have been avoided and better control of the heating and cooling could have been provided if a levitation system had been incorporated into the apparatus. In fact, an electromagnetic levitator was under development but was not used on Skylab. The coil design was proven effective in drop tower tests. However, there was insufficient time to work out all the systems problems and qualify the apparatus to meet the Skylab launch schedule.

Another technique for providing position control of a containerless specimen is by means of acoustic radiation pressure. A standing acoustic wave is set up by source and a reflector, as shown in figure 3.23. Diffraction effects from the edges of the source and reflector provide radial restoring forces. Even though these forces are weaker, they are sufficient to confine the object in the acoustic field.

The concept can be carried to three dimensions, as shown in figure 3.24. In this configuration rotational control can be achieved by varying the phase relationship between the acoustic drivers. Feedback control can be used to provide a more precise sample position control.

These devices were under development during the time experiments were being readied for Skylab. Although successful demonstrations had been carried out in drop tower tests and experimental aircraft flights, neither the acoustic nor the electromagnetic positioning was sufficiently developed to commit to flight on Skylab.

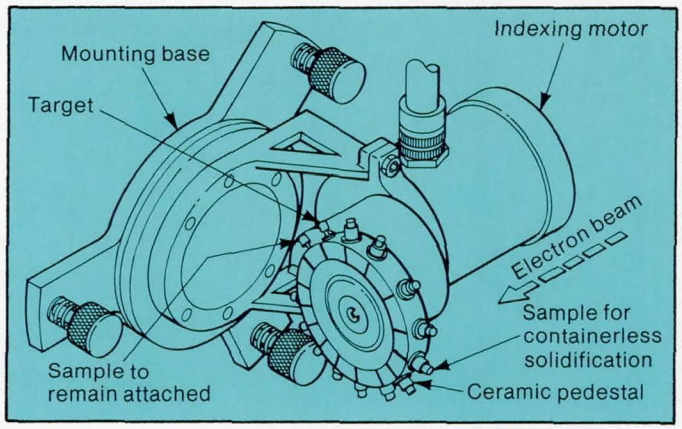

Figure 3.22. *Apparatus for the Skylab M553 sphere-forming experiment. The basic apparatus used to perform the containerless melting and solidification experiment is shown. Fourteen material samples and a tungsten target for initial electron beam alignment were mounted on a wheel that could be rotated to successively position each sample in the path of the beam for melting. Three samples were attached to the wheel so they could remain during solidification. The other 11 samples were attached by devices that allowed the molten metal to be released and to solidify while floating freely in a chamber.*

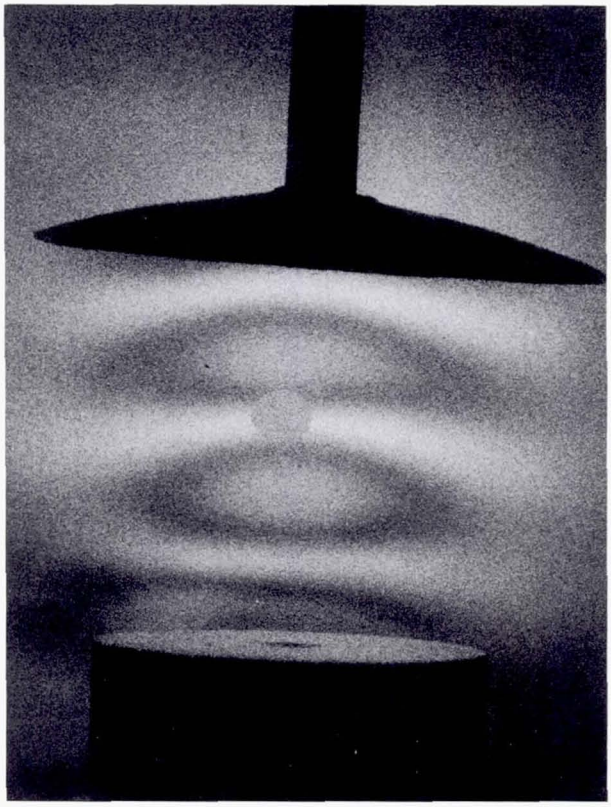

Figure 3.23. Hologram showing the sound pressure field in a single-axis acoustic levitator levitating a 3-mm clay particle. The small sphere is levitated by the sound pressure at a null in the acoustic field. In 1 gravity it is supported by the high-pressure region (dark area) below.

Figure 3.24. Triaxial acoustic levitator. The three acoustic drivers produce a three-dimensional standing wave pattern in the plexiglass chamber. An energy well in the cell is at the null point. The acoustic pressure away from this null point is sufficient to levitate and position a light object such as a ping pong ball.

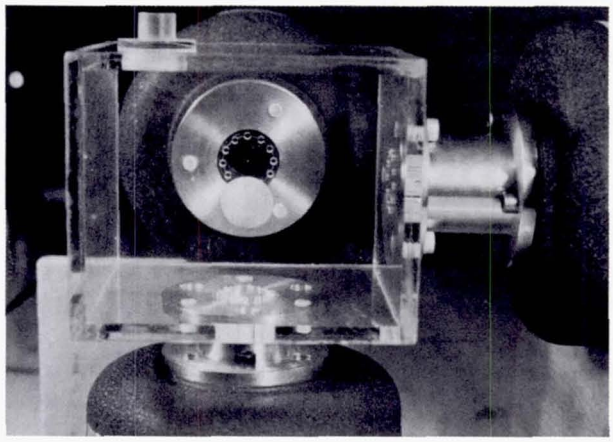

The Skylab Materials Processing System

All Skylab space processing experiments involving the melting and resolidification of materials were performed in the Materials Processing Facility, shown in figure 3.25. The facility was mounted on a honeycomb panel that served as a conductor of heat to the spacecraft structure and, in turn, was attached to the Multiple Docking Adapter structure of the Skylab vehicle by shock mounts. The facility provided modular capability for performing experiments and consisted of the following main parts:

- Work chamber
- Control panel
- Electron beam gun and batteries
- Stowage boxes for experiment modules and ancillary equipment

The work chamber incorporated a single mount to accommodate each experiment module in turn. The mount, which was directly attached to the honeycomb panel, served as a heat sink with a predetermined and calibrated thermal impedance. Near the mount and inside the chamber was an electrical connector through which power and command signals were provided to all the experiment modules except the Multipurpose Electric Furnace, which was a late addition and used only the heat sink / mount and the vacuum capability of the chamber. The furnace control system is described later in this chapter.

The work chamber could be vented to space and thus provide an evacuated environment for the experiments when desired. Windows, illumination, and a system of mirrors within the work chamber permitted viewing of the experiments in progress and photography using a fixed camera. The mirrors permitted the viewing of events not directly in the line of sight, and they shielded the viewing ports from metal vapor generated during experiments in which the electron beam gun was used. Gauges on the control panel (fig. 3.26) allowed the experimenter to monitor chamber pressure, certain temperatures, and the current and voltage of the electron beam. In addition, switches and potentiometers served to initiate and control the individual experiments.

The metals-melting and sphere-forming experiments used the electron beam gun to melt specimens. This very compact gun had an output of 2 kW (100 mA at 20 kV). The high-voltage power supply was contained in a canister pressurized with an insulating gas, perfluoropropane (C_3F_8). The filament and focusing devices were exposed to the vacuum of the work chamber. The gun, powered by

Figure 3.25. The Skylab M512 Materials Processing Facility. This facility was located in the multiple docking adapter section of Skylab and could be vented to space through the 4-inch vacuum line shown at left. The work chamber featured electrical connections and a universal mount designed to accommodate the individual apparatus for each melting and solidification experiment interchangeably.

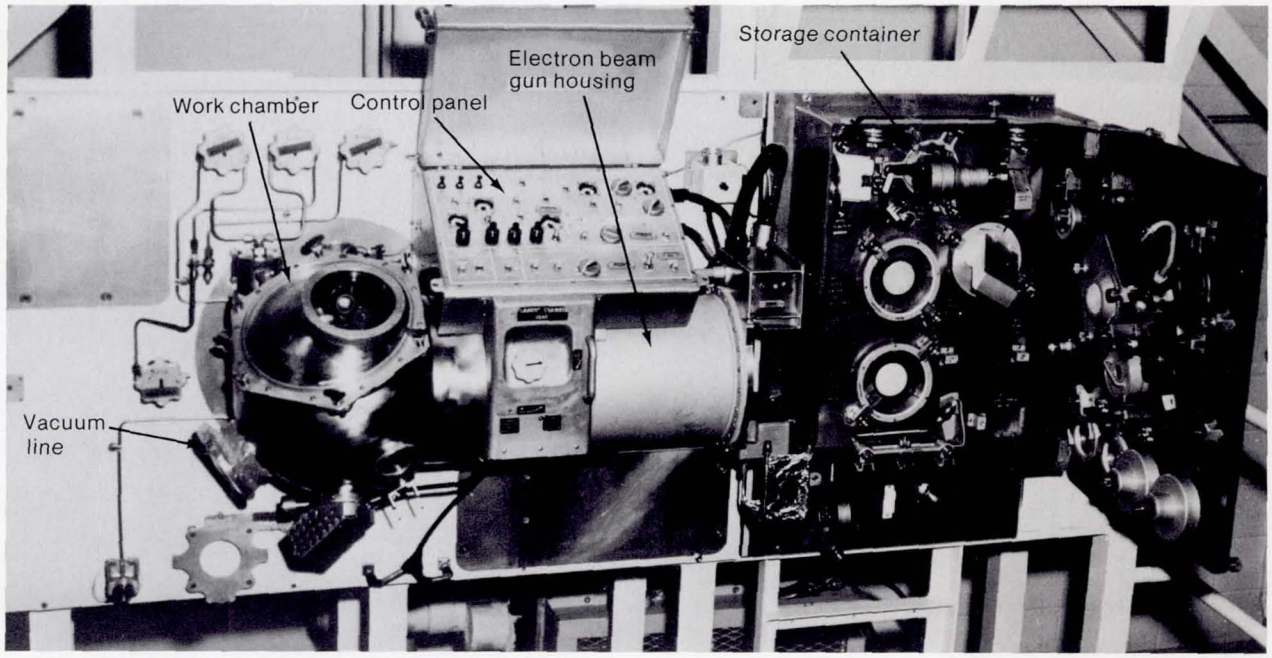

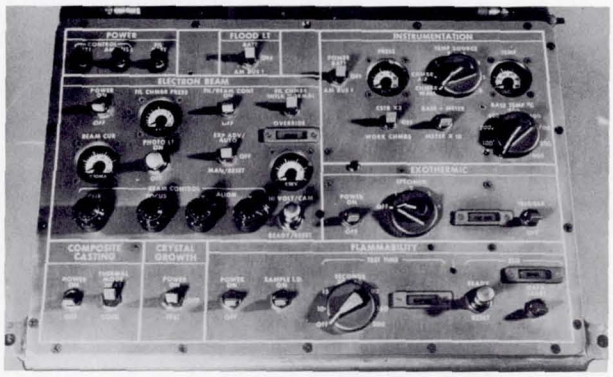

Figure 3.26. The M512 Materials Processing Facility control panel. The controls were grouped into sections associated with particular experiment operations. The instrumentation section contained one pressure gauge (PRESS) to monitor pressure in the work chamber. A second gauge (FIL CHAMBER PRESS) in the electron beam section measured vacuum conditions. The electron beam controls were used in both the metals-melting and sphere-forming experiments described in chapter 5.

batteries, was independent of spacecraft power; the exothermic brazing experiment derived its igniter power from these same batteries. All other experiments operated on spacecraft power.

Most of the experiment modules and their accessories were stored in the stowage container shown in figure 3.27. To perform an experiment the appropriate module with its accessories was mounted in the chamber. Three experiment modules in their installed configurations are shown in figure 3.28. The metals melting experiment employed rotating discs driven by a motor. The electron beam was focused on a tungsten target incorporated in each disc; the disc was then rotated at constant speed to make a weld bead and was finally stopped to melt a puddle. Three discs of different materials were provided for this experiment, and they were processed successively (see chapter 5). Specimens for the sphere-forming experiment were carried on two wheels that were successively mounted on an indexing motor. Each wheel carried a tungsten focusing target and 14 specimens. After each specimen was melted by the electron beam, a new specimen was indexed into position. The exothermic brazing experiment container held four exotherm packages. After the chamber was evacuated, the exotherm packages were fired one at a time at approximately 2-hour intervals. The long intervals were necessary to allow for cooling between operations.

The Multipurpose Electric Furnace system (described previously and shown in fig. 3.16) consisted of the furnace,

Figure 3.27. The M512 Materials Processing Facility accessories stowage container.

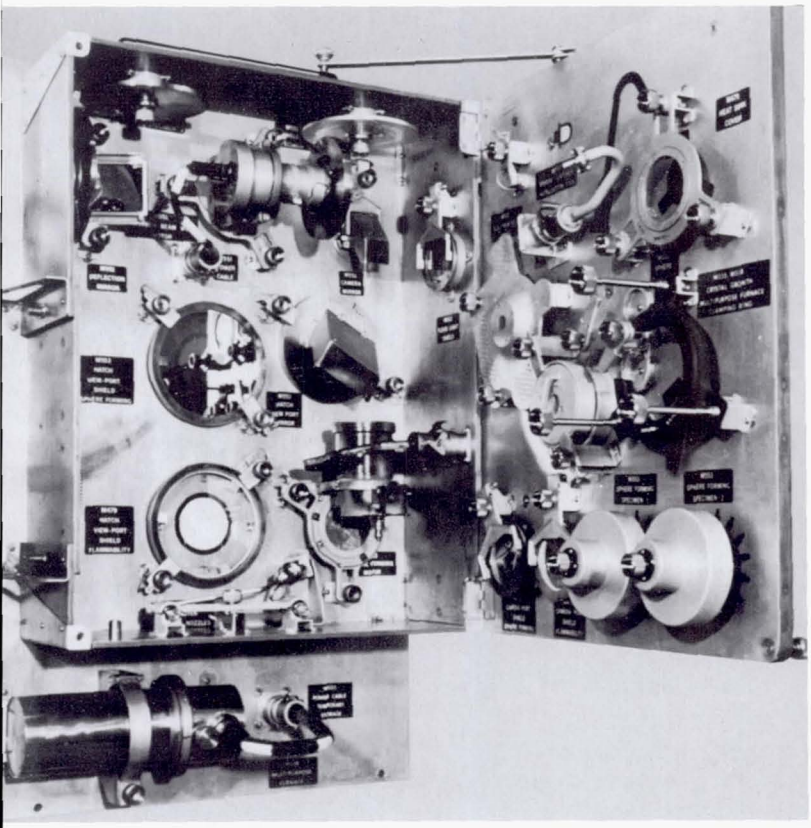

a control package, and interconnecting cabling. To perform the 11 Skylab experiments that used this system, the furnace was installed in the work chamber, as shown in figure 3.29, the control package was mounted on a special adapter, and interconnections were made from the controls to the furnace, to the Skylab power receptacle, and to the Skylab telemetry system. After the insertion of each set of three cartridges for an experiment, the work chamber was evacuated and the experiment was initiated after setting the appropriate peak temperature, soak time, and cooling rate. Lights indicated which particular period of the total cycle had been reached. Thermocouples at the "hot" and "cold" ends of the cartridges provided information that was telemetered to the ground for real-time evaluation of the progress of the experiments.

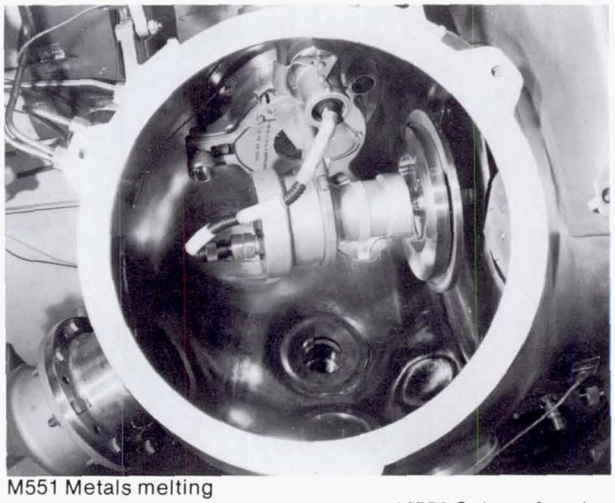

M551 Metals melting

M552 Exothermic heating

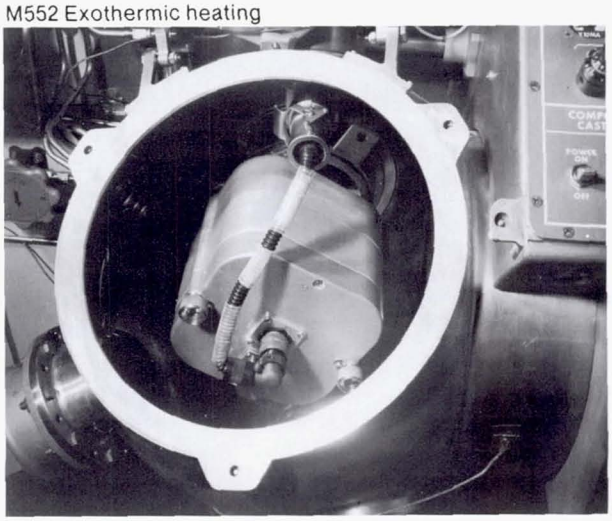

M553 Sphere forming

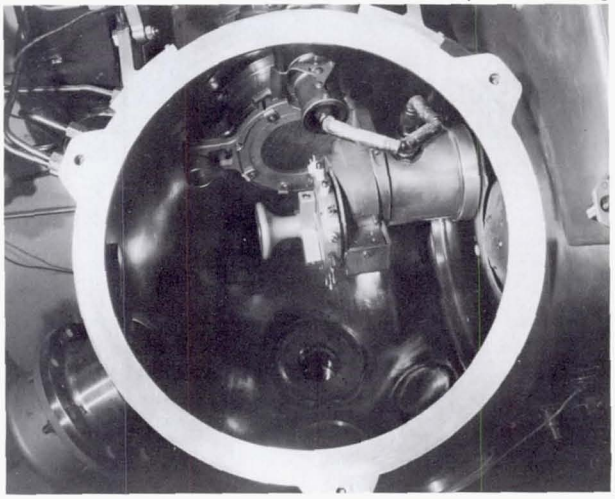

Figure 3.28. *Experimental apparatus installed in work chamber. The operational hardware configurations of three materials processing experiments developed in conjunction with the Materials Processing Facility are shown. For each experiment, various equipment items from the stowage container were assembled, and the experiment modules were mounted in the work chamber as shown. All three experiments used the same mounting provisions and electrical connections inside the chamber (see chapter 5).*

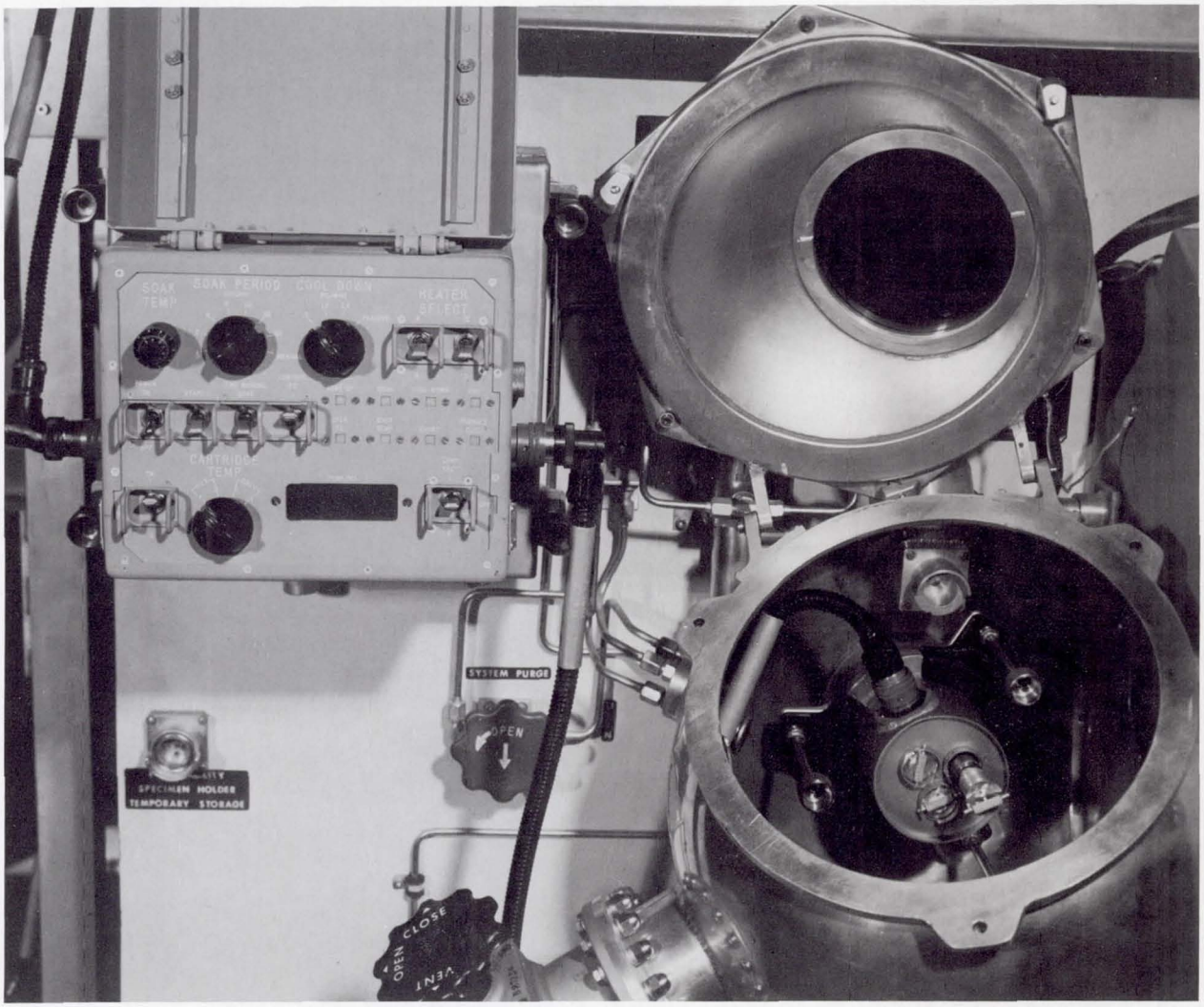

Figure 3.29. The M518 Multipurpose Electric Furnace system installed in the M512 Materials Processing Facility.

Miscellaneous Design Considerations

In designing a space processing system it was necessary to consider a number of requirements other than those dictated by the experiments themselves. These included data acquisition, ground support equipment, crew training, and safety. The principal means of gathering data from the experiments was postflight examination of the specimens produced in space. Processing data were available from records on gauge readings written and spoken by the astronauts and from film taken of the electron beam welding and sphere-forming experiments. The Multipurpose Electric Furnace was connected to the Skylab data system; temperatures as a function of time were telemetered to the Mission Control Center during the experiments conducted in the furnace.

A space processing facility duplicating the actual flight unit was constructed and made available for crew training at the Johnson Space Center. The experiment operating procedures were revised several times in light of the experience gained during crew training.

In the design of any flight equipment, crew safety is, of course, of paramount importance. Many features were incorporated into the Skylab space processing system to ensure safety. A line led from the processing chamber through the wall of the spacecraft to the vacuum of space. Two valves were installed in this line so that, in the event of the failure of one valve or a break in the line, the danger of venting the whole craft to space was minimized. Other concerns were associated with the electron beam gun, since X-rays are generated by an electron beam impinging on metal. To shield personnel, leaded glass had to be used in the chamber veiwing ports. In other regions the chamber wall provided enough protection. Precautions were also taken to prevent the electron beam from cutting through the chamber wall in case of operator error. A heavy tungsten target plate was incorporated in the area of the wall that could be affected. No experimental equipment can be made inherently completely safe; therefore, other concerns were addressed by having very specific instructions and sequences called out in the operating procedures.

Chapter 4. PROCESSING SEMICONDUCTOR MATERIALS

Five experiments involving the processing of semiconductor materials were performed during the Skylab mission. These experiments were of extreme interest, partly because of the key role played by semiconductors in our technology and partly because gravity exerts a significant influence on processes by which the materials are produced. The primary purpose of these experiments was to examine the influence of gravity-driven flows on the solidification process, with particular emphasis on the distribution of the dopant atoms that give the semiconductor material its desired electrical properties.

SEMICONDUCTORS AND THEIR UNIQUE ELECTRONIC PROPERTIES

Our highly technological society depends on many materials, each with unique properties. In electronic applications, the extent to which a material conducts electricity is of primary interest. The ability to conduct electricity depends on two factors: how many electrons are available and the extent to which they can move unimpeded through the material. Most electrons in a solid are tied up in the bonding of atoms to atoms or molecules to molecules and are not available for electronic conduction. The distinguishing feature of metals is that they have ample "free" electrons available for electrical conduction; conductivity depends only on the mobility of the electrons under the influence of an applied driving force or voltage. Generally the conductivity increases at lower temperatures because there are fewer collisions between the free conduction electrons and the vibrating lattice.

Semiconductors, on the other hand, have virtually no conductivity at very low temperatures because almost all the electrons are either bound to the atomic nuclei or occupied in the bonding of atoms to atoms. One of the features that makes these materials so useful is that some of the electrons are loosely bound and can be readily promoted to conduction electrons by absorption of photons or by thermal agitation. This property is useful in making devices such as detectors and thermistors.

Perhaps the most useful feature of semiconductors is the fact that the conductivity can be dramatically altered by the addition of trace impurities called dopants. For example, the addition of 1 part per million of arsenic to silicon increased the conductivity by a factor of 10 000. Not only is it possible to tailor the conductivity within wide limits, but it is also possible to choose the sign of the charge carriers by the type of dopant material added. For example, the addition of boron to silicon requires fewer electrons from the silicon to form chemical bonds, and free electrons are left to respond to electric fields. Such a material is called *n* type because electrons, which have negative charge, carry the current. On the other hand, doping with phosphorous requires more electrons from the silicon than are available to provide chemical bonding. The "holes" that are left also respond to an electric field and cause conduction, just like free electrons, except that they behave as if they have positive charge. Such a material is called *p* type material because the holes that carry the current have a positive charge (see fig. 4.1).

The fact that semiconductors can be made in both *n* and *p* types is the basis for the entire solid state electronics industry. A junction between *n* and *p* regions transmits current in only one direction, resulting in a diode or rectifier. Photons absorbed near the junction produce electron-hole

Space-grown crystal.

Figure 4.1. The effects of dopants in silicon. An ordinary Si atom (a) has 14 protons in the nucleus, which are electrically balanced by 14 electrons arranged in shells containing 2, 8, and 4 electrons, respectively. The outer shell can contain 8 electrons. In a pure Si lattice this is fulfilled by each Si atom sharing an electron with its neighbors (b). The electrons are tightly bound and are not free to conduct electricity. The addition of a phosphorous atom (c) which has 5 electrons in its outer shell, provides a free electron for conduction, yielding an n-type material. The addition of a boron atom (d), which has only 3 electrons in the outer shell, leaves a "hole" which can act as a positive carrier, yielding a p-type material.

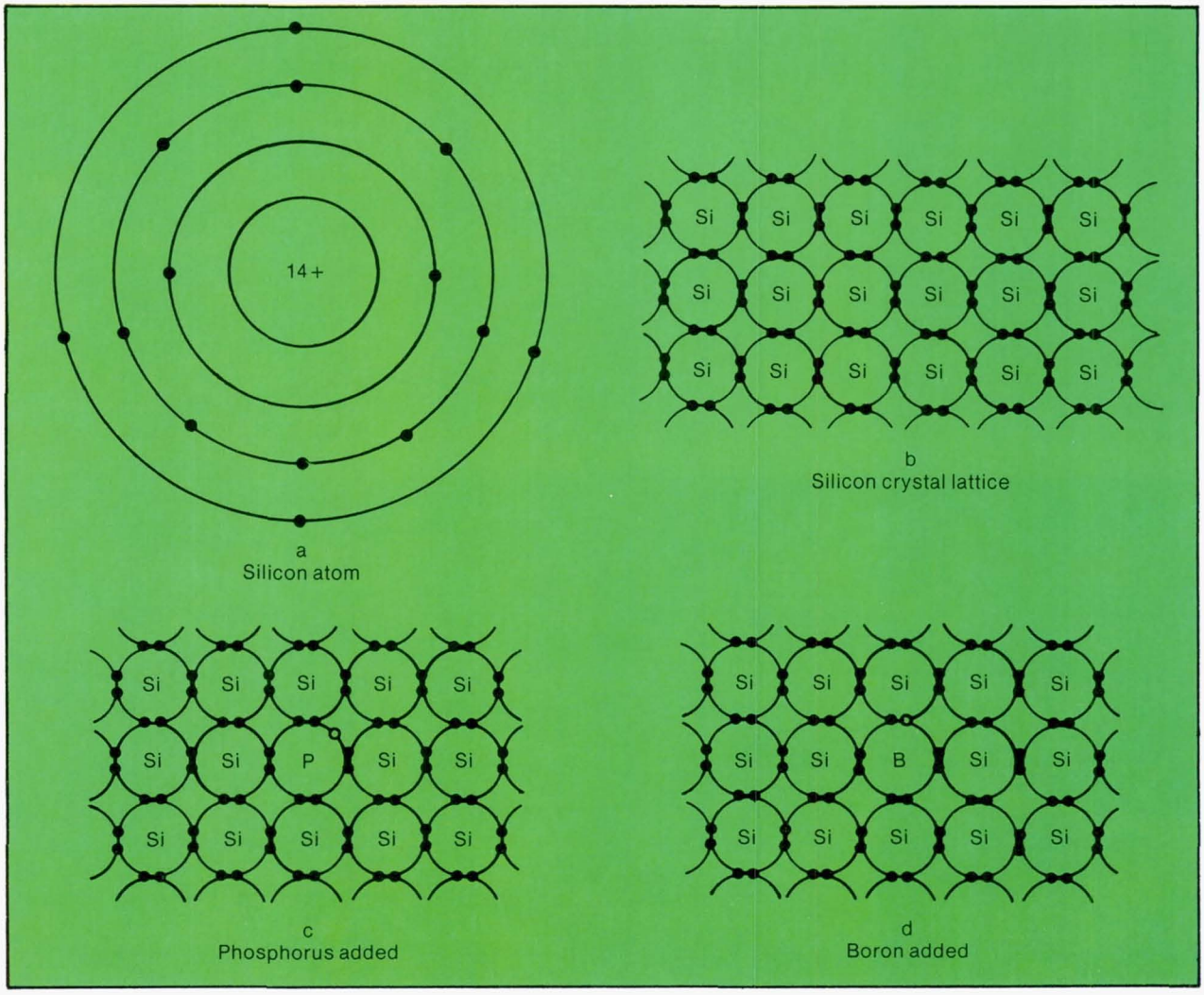

pairs that can be collected, forming a current that is proportional to the light intensity. This is the basis for photodetectors as well as solar cells. The process can be reversed; current can be run through the device, generating light at the junction. This is the principle of the light-emitting diode (LED) now used so widely for electronic displays. The addition of a second junction to form either an *n-p-n* or a *p-n-p* sequence produces a transistor. The center region, called the base, blocks current flow in either direction. However, a small control current flowing from the base to one end can cause a much larger current to flow from end to end.

The development of the present solid state technology has been made possible by the ability to grow nearly perfect crystals of ultrapure semiconductor material. The purity is required to prevent unwanted atoms from masking the effect of the added dopants. The degree of purity required can be appreciated by considering that most substances, for example, metals, can only be purified to parts per million. Since there are approximately 10^{23} atoms per cm^3 of solid, this implies 10^{17} impurity atoms per cm^3. Dopant levels in semiconductors run as low as 10^{11} atoms per cm^3. This implies impurity levels less than parts per trillion.

Not only is purity essential, but the extreme sensitivity of the electrical properties to the dopant concentration requires a great deal of control of the distribution of the dopant atoms within the crystal to ensure uniform electrical properties.

It is also necessary to use material that has a high degree of structural perfection. Structural perfection implies complete natural ordering of the atoms or molecules that make up the solid. Most semiconductor materials of current importance are crystalline substances, that is, their atoms are arranged internally in some definite periodic pattern. Deviations from this pattern are known as crystalline or structural defects. They may be relatively minor, such as an occasional atom missing or out of place (a vacancy, or point defect), more extensive in the form of an entire row of extra or missing atoms (a dislocation, or line defect), or massive regions of internal disorder (an intercrystalline boundary, or surface defect). These are illustrated in figure 4.2. All defects have the undesirable effect of interfering with the internal flow of conduction electrons. In fact, intercrystalline boundaries are such effective barriers to conduction that they are generally intolerable in electronic devices. Thus most semiconductors must be single crystals in order to be useful.

In device manufacture, it is customary to simultaneously produce a large number of circuits on a single chip of material, usually silicon. Imperfections or the lack of chemical homogeneity reduces the yield of the number of useful devices. For most applications, the yield that is presently available is acceptable to the point that it is not economical to spend more dollars on better starting material. Only for highly specialized applications such as large focal plane arrays or other large complex devices is the current technology inadequate. For these applications the goal is to obtain a uniformly doped, defect-free crystal that will yield the maximum performance inherent in the device and the material.

The Skylab experiments were designed to explore the potential for minimizing impurities and structural defects and for controlling the distribution of dopant atoms by processing in a low-gravity environment.

Figure 4.2. Defects in crystals.

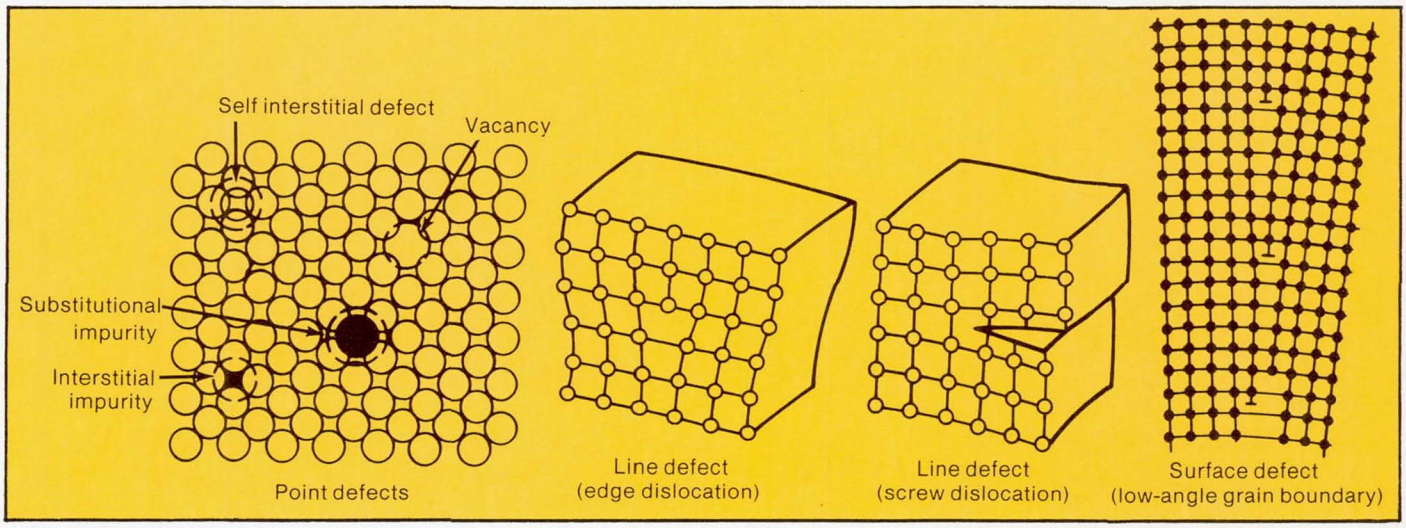

TECHNIQUES OF CRYSTAL GROWTH

Single crystals of semiconductor materials are produced on Earth by effecting controlled solidification from a saturated solution, a saturated vapor, or directly from molten material. One Skylab semiconductor experiment was designed to achieve solidification from the vapor and four experiments were designed to achieve solidification from the melt.

In the simplest vapor growth system, crystal growth occurs by physical vapor deposition. Polycrystalline material is located at one end of a closed container, or ampoule, and a small "seed" crystal may or may not be placed at the other end. The ampoule is placed in a furnace such that the end containing the source of polycrystalline material is at a temperature sufficiently high that some of the material vaporizes. This vapor fills the ampoule, and at the cooler end it condenses and returns to the solid state. The seed serves as a locus of condensation and provides the appropriate structural model for preferential crystal growth. If experimental conditions are appropriate, the crystal structure

of the seed will be perpetuated during condensation and a large single crystal will be produced. If no seed crystal is used, the material condenses directly on the container wall. Nuclei are usually formed at microscopic surface imperfections on the wall, with the result that a seedless process usually produces a multitude of small crystals.

Crystals can also be grown by chemical vapor deposition, as was the case in the Skylab experiment. The difference is that the vapor is formed by chemical reaction of the source material with a transport agent at the hot end of the ampoule, and solid material is deposited when the reverse reaction occurs at the cold end (fig. 4.3). Again, if experimental conditions are appropriate, one or more single crystals are produced. These techniques for growth from the vapor phase are referred to as closed vapor transport, meaning that the growth ampoule is completely closed during growth. Single crystals may also be grown from the vapor phase by allowing an appropriate mixture of gases to flow through a condensation region. The depleted gas may then be exhausted or replenished and recycled. Such systems are referred to as open or flow-through systems.

In crystal growth from a melt, it is necessary that solidification occur in a controlled unidirectional manner. In the simplest cases, the material is contained in a cylindrical crucible that is slowly withdrawn from the open bottom of a vertical tube furnace into a cooler environment, causing solidification to proceed gradually from the lower end upward. This is referred to as the Bridgeman or Stockbarger technique (fig. 4.4). If withdrawal is accomplished slowly and uniformly, and the initial growth is monocrystalline, the remaining material may grow as a single crystal. The probability of obtaining a large crystal is enhanced if a previously obtained small crystal (a seed crystal) is used to initiate solidification, that is, if the seed is placed in the bottom of the crucible and not allowed to melt. Other techniques are used, including crucibles with conical bottoms to encourage initial solidification at a single point.

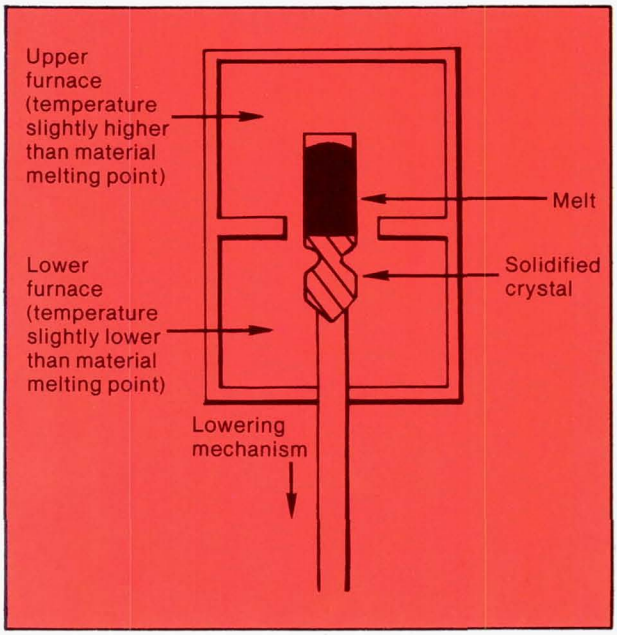

Figure 4.4. Bridgeman or Stockbarger technique of crystal growth. The Bridgeman-Stockbarger technique essentially produces crystal nucleation on a single solid-liquid interface by carrying on the crystallization in a temperature gradient. The material to be crystallized is usually contained in a cylindrical crucible that is lowered through a temperature gradient. This causes an isotherm normal to the axis of the crucible to move through the crucible slowly enough that the melt interface follows it. Usually the whole crucible is initially molten and the first nucleation is several crystallites. If the tip of the crucible is conical, only one nucleus is suitably oriented and dominates the growing interface.

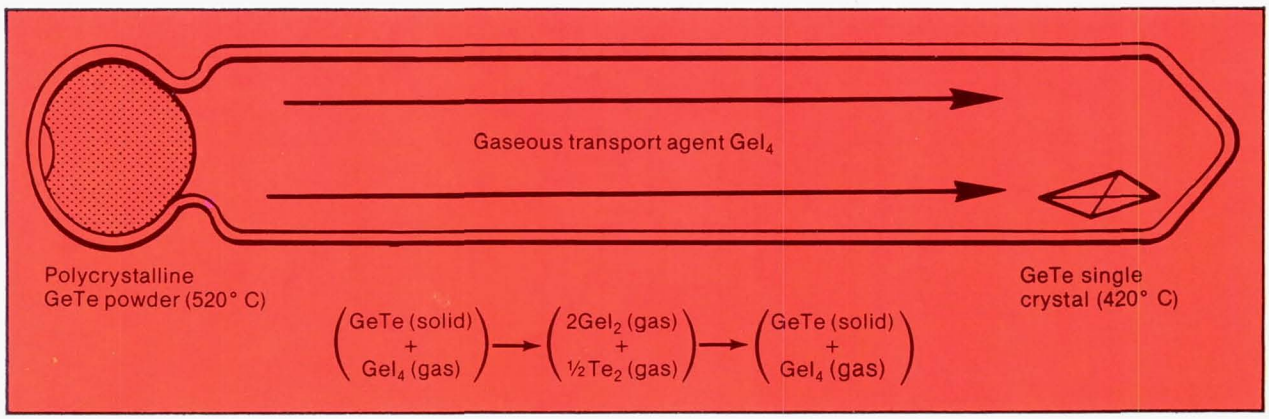

Figure 4.3. Crystal growth by chemical vapor transport. This shows the growth of germanium telluride (GeTe) using iodine as a transport agent. Iodine, in the form of GeI_4, picks up additional Ge at the source (hot end) and becomes 2 GeI_2. This is converted back to GeI_4 at the crystal interface, with the extra Ge atom being incorporated into the lattice. The Te has a high enough vapor pressure to be transported by ordinary sublimation.

The constraints involved in developing the Skylab program did not allow the development of a furnace with a precise translation control of the sample within the heated cavity (or of translating the heated cavity relative to the sample, which produces the same effect). Instead, as discussed in chapter 3, it was necessary to employ a gradient freeze technique in which the overall temperature of the furnace is reduced while the upper portion is maintained at a higher temperature than the lower portion. This essentially accomplishes the same purpose, but since there is control only at the hot end, uniform growth rates and gradients could not be maintained.

MELT GROWTH EXPERIMENTS

A total of four melt growth experiments were attempted on Skylab. As discussed previously, the gradient freeze technique does not provide high thermal gradients and uniform controlled growth rates. Also, the maximum temperature capability of the furnace (~ 1000° C) restricted the materials that could be used in the experiments. For this reason, most of the investigators chose materials such as InSb and Ge which, although they have some importance in device applications, serve primarily as models for other, more important systems.

It is important to understand some of the processes that go on in solidification that affect the distribution of dopants or alloying components. A typical phase diagram for a binary or pseudobinary system in which the constituents are completely miscible in both liquid and solid phases is shown in figure 4.5. As a melt of some composition is lowered to the liquidus temperature, a solid begins to form, but of considerably different composition from the melt. Solute B tends to be rejected by the solidifying solid and pushed ahead of the solidification front. The freezing solid contains substantially less impurity than the original melt. In fact, this is the principle of the important process of zone refining used to purify a multitude of elemental as well as organic materials. The ratio of the concentration of B in the solid to the concentration of B in the liquid at the interface for a given temperature is called the distribution coefficient or segregation coefficient, K_0.

In a directional solidification of a melt, the composition is initially X_1, or the distribution coefficient times the original melt composition. For systems in which the addition of a solute depresses the melting temperature (the case considered here) the distribution coefficient is less than unity, which means that the dopant level is initially lower in the solid than in the original melt. As solidification progresses, the rejected solute increases the concentration in the melt. In a convectionless situation, a diffusion layer builds up rapidly, increasing the solute concentration in the vicinity of the interface. Eventually the concentration reaches X_2 so that the concentration in the solid is X_0. At this point a steady state is reached in which the solute becomes incorporated into the crystal at the same rate it enters the diffusion region. The more rapid the growth, the less time the solute has to diffuse away from the diffusion layer, resulting in a sharper diffusion layer and a more rapid achievement of steady state growth, as may be seen in figure 4.6. Once steady state growth is reached, the composition will remain uniform until the diffusion layer encounters the end of the growth ampoule. This entrapment will rapidly increase the concentration above X_2 and will result in a high concentration of solute in the crystal near the end.

In a highly convective or stirred melt, the diffusion layer is essentially spread throughout the melt, causing a continually changing composition in the melt as solidification progresses. This results in the dopant profile shown in figure 4.7. The two profiles in the figure represent extremes. A partially mixed melt would produce something intermediate to these extreme cases.

The uniform distribution of dopants obtained by the diffusion-controlled process is obviously desirable for applications in which it is important to produce a large number of wafers with uniform dopant distribution. Since it is difficult to approach diffusion-controlled conditions in 1 g,

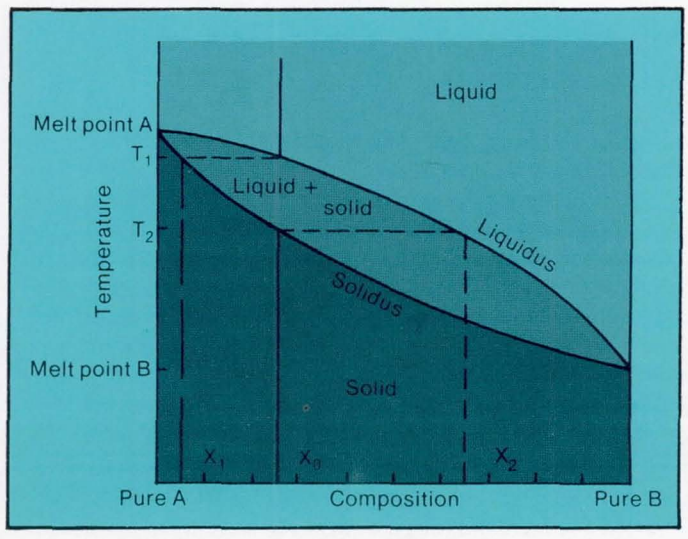

Figure 4.5. A typical phase diagram for a solid solution binary or pseudobinary compound $A_{1-x}B_x$. Let X_0 be the starting composition in one melt. As the temperature is lowered to T_1, the material that solidifies has composition X_1. In the absence of convective mixing, it is possible to build up a steady state diffusion layer with composition X_2 at the interface such that composition X_0 is solidified.

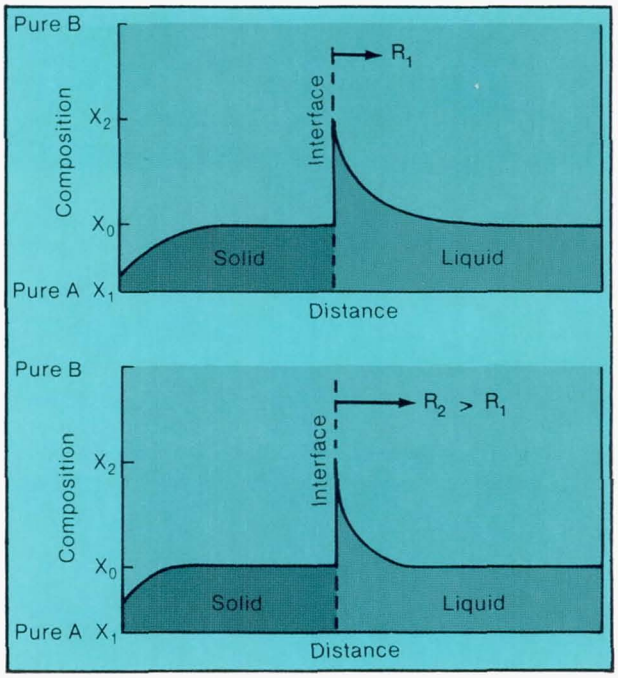

Figure 4.6. Composition profiles at steady state for different growth velocities (R, growth rate). At steady state the component A is incorporated into the solid at the same rate it enters the diffusion region. A slower growth velocity allows more time for the rejected material at the interface to diffuse away, producing a broader diffusion region. Also, a longer time is required to reach the steady state composition.

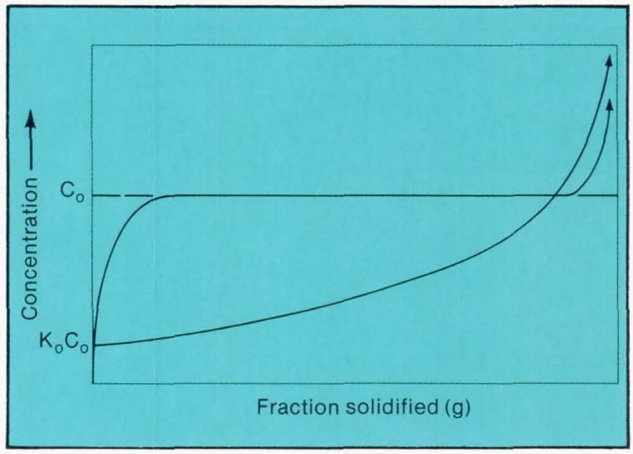

Figure 4.7. Concentration of dopants after normal freezing versus fraction solidified for complete convective mixing in the melt (top) and diffusion-controlled growth with no convective mixing (bottom).

several alternatives are used. One is to restrict the region of melt to a short zone and let this zone move through the material to be processed. Since the zone is short, the rejected solute, even when mixed with the molten material in the zone, will eventually increase the concentration until steady state growth is reached. However, for various practical reasons, the length of the zone must be longer than the diffusion region and steady state growth cannot be achieved in as short a distance. In the other technique, known as zone leveling, a charge of the dopant is placed just ahead of the seed crystal. The concentration of this dopant is chosen to be C_0 / K_0 where K_0 is the distribution coefficient and C_0 is the desired dopant level in the solid. If K_0 is small and the desired C_0 is low, the change in concentration in the traveling zone is negligible, and reasonably uniform dopant distribution can be obtained. This technique is not satisfactory, however, when large concentrations of dopants or alloying agents are required.

Experiment M562, Steady State Growth and Segregation Under Zero Gravity of Indium Antimonide

The potential advantages of crystal growth in a low-gravity environment were most dramatically demonstrated by the M562 experiment conducted by A. F. Witt and H. C. Gatos to study dopant segregation in the absence of gravity-driven convection. As stated previously, it is highly desirable to prepare uniformly doped semiconductors so that the electrical properties are the same throughout the material. Several factors tend to prevent this from happening in Earth processes.

The first problem, discussed previously, arises from convective stirring that continually changes the dopant concentration ahead of the solidification front. One of the objectives of the experiment was to determine whether the diffusion-controlled dopant distribution could be maintained in the melt, giving the theoretical dopant profile shown in figure 4.7.

The second impediment to obtaining uniform dopant concentrations comes from growth rate oscillations. It is well known that in most solidification processes the growth interface does not progress uniformly but, instead, progresses in a series of jerks or jumps. Sometimes the interface may even melt back or recede before it jumps forward again. Thermocouples imbedded in the melt have recorded temperature fluctuations that correlate with the observed growth rate fluctuations. The exact details of the process that produce these temperature fluctuations are not completely understood but are generally attributed to convective effects. If the growth rate is suddenly increased, the

concentration of dopant atoms ahead of the interface is increased because of the additional pile-up, and the rate of dopant incorporation is increased. Therefore, the growth rate fluctuations result in dopant striations throughout the crystal.

Witt and Gatos prepared InSb crystals by conventional Czochralski growth. Three types of crystals were processed under identical conditions: an undoped crystal, a tellurium (Te)-doped crystal (10^{18} Te atoms per cm^3), and a tin (Sn)-doped crystal at a high doping concentration (10^{20} Sn atoms per cm^3).

One group of crystals was processed during Skylab III by slowly melting the crystal back over a portion of its length, soaking it for 60 minutes to achieve thermal equilibrium, and then directionally solidifying it by means of a controlled power reduction. The experiment was repeated during Skylab IV with the addition of mechanical shock and an interruption in the cooling to provide time reference marks on the growing crystal and to examine the growth transient.

After retrieval, the crystals were sectioned and etched to reveal the dopant striations. Figure 4.8 shows a striking difference between the portion that was melted and recrystallized in space compared to the Earth-grown portion. The pronounced striations indicating compositional inhomogeneities in the Earth-grown region reflect irregular variations in growth conditions caused by rotation effects and uncontrolled gravity-induced thermal convection in the melt. No microscopic compositional fluctuations are present in the portion of the crystal that was grown in space, demonstrating that the growth rate fluctuations are in fact gravity-related and can be eliminated by processing in a low-gravity environment.

The dopant distribution was measured quantitatively by means of Hall effect measurements and ion microprobe scanning. It can be seen in figure 4.9 that the dopant distribution closely resembles the theoretical behavior for a diffusion-controlled solidification (shown in fig. 4.7). The initial transient required for the concentration at the solidification interface to reach the steady state value was completed in less than 1 cm. The dopant distribution was extremely uniform throughout the remainder of the crystal. The results of the ground control samples are also shown. Even though these were processed in a vertically stabilizing thermal gradient, continual changes in dopant concentration were observed, indicating that convective stirring took place because of unavoidable lateral thermal gradients.

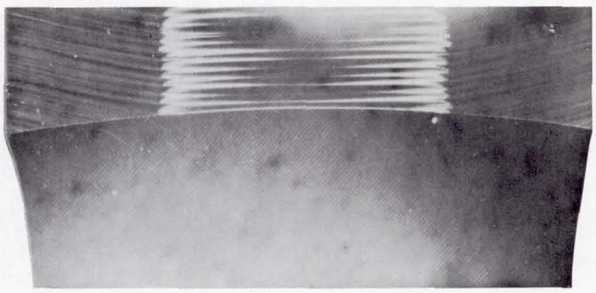

Figure 4.8. Etched longitudinal section of Te-doped InSb crystal grown on Skylab. In this photomicrograph, chemical etching reveals a striking difference in dopant segregation between the upper portion of the crystal (grown on Earth) and the lower portion (melted and regrown in space). This sort of microscopic inhomogeneity results from convective stirring of the solidification front in crystal growth on Earth and has an adverse effect on the performance of electronic devices made from semiconductor materials.

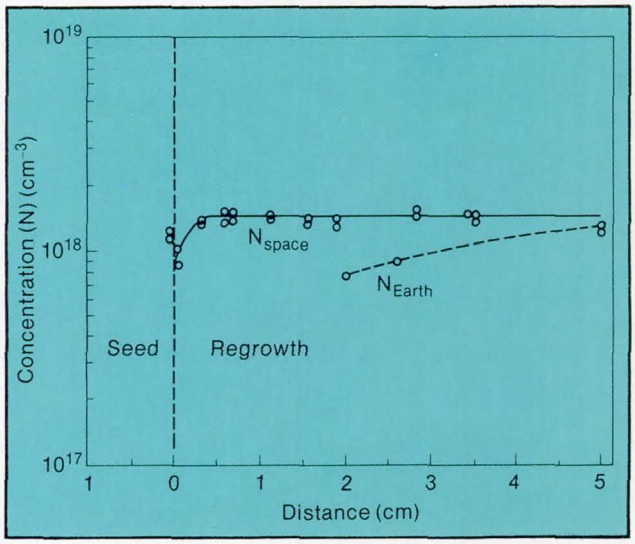

Figure 4.9. A comparison of dopant concentration profiles for crystals grown in space and on Earth. The dopant concentration curve (N_{space}) indicates a transient in the initial portion of the regrowth region, as predicted theoretically. The transient ends at a distance of approximately 0.5 cm from the regrowth interface, and from that point dopant concentration remains constant. The dopant concentration (N_{Earth}) for a crystal regrown on Earth under otherwise identical conditions never becomes constant, reflecting continuous convective disruption of the solidification process.

An unexpected bonus came from the steady state growth experiment. For reasons that are not completely clear, the Te-doped samples did not maintain close contact with the crucible wall during the solidification process but instead assumed a fluted configuration, with narrow ridges forming the only wall contact (fig. 4.10). This left the majority of the crystal with a free surface. Since there are large thermal gradients in the solidification process, the variations in surface tension along a free liquid surface would be expected to produce a surface-tension-driven flow (Marangoni convection). There has been concern that such flows would prevent floating zone processes carried out in space from achieving the desired homogeneity in dopant distribution. There was no evidence of such flows in this experiment, possibly because of a thin oxide film on the free surface that may have prevented such disturbing flows. Although this is by no means conclusive, it does indicate that such flows may be controllable.

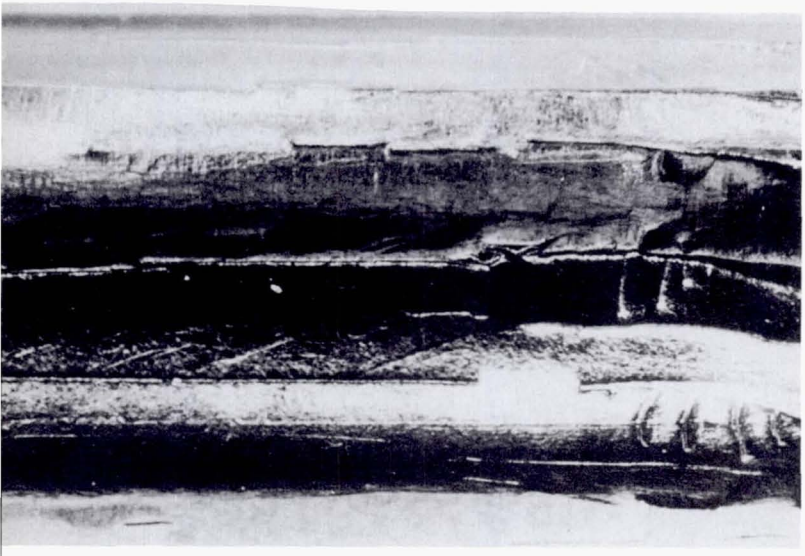

Figure 4.10. *Exterior surface of Te-doped InSb crystal grown on Skylab. The surface of this crystal was characterized by the presence of irregularly spaced ridges parallel to the direction of growth. The ridges were in contact with the wall of the quartz ampoule in which the crystal was grown. The regions between the ridges exhibited the characteristics of growth from unconfined melts. This phenomenon had not been observed previously in solidification from contained melts.*

Experiment M560, Seeded, Containerless Solidification of Indium Antimonide

Another experiment involving InSb was conducted by H. U. Walter of the University of Alabama, Huntsville. An attempt was made to grow a crystal in a quasi-containerless technique by melting back a conventionally grown cylindrical crystal in a cavity and using adhesion and surface tension to keep the melt in contact with the original rod, which served as the seed. The configuration is illustrated in figure 3.15. Several crystals were grown in this manner, ranging from heavily doped Se (10^{19} atoms per cm^3) to undoped compositions. The intent of the experiment was to examine the growth configuration, evaluate whether there was an increase in perfection obtained by eliminating container-induced strain, and examine the homogeneity of the dopant distribution in the growth process.

Since the melt was an approximately spherical drop, it was expected that the crystal would solidify into a spherical shape also, which is the reason the growth cavity was made with a hemispherical end cap. Figure 4.11 shows that this did not happen. Instead, a teardrop shape developed. This shape is determined by the meniscus angle (the angle between the solid–vapor interface and the liquid–vapor interface at the solid–liquid–vapor interface) and the volume change associated with solidification (fig. 4.12). The peculiar tip was produced when the crystal, being longer than anticipated, grew into the crucible wall.

Of particular interest is the faceted appearance of the crystal. The facets appear as well-developed growth facets consistent with the crystalline symmetry of the material and are essentially optically flat (fig. 4.13). This illustrates rather dramatically that in low-gravity the shapes of solidifying solids are dominated by forces intrinsic to the solidification process itself. X-ray topographic analysis (fig. 4.14) shows no evidence of grain boundary defects on the facets, indicating a high degree of crystalline perfection.

Etch pit studies showed significantly fewer defects in the remelted crystal than in the original material, with the dislocation densities decreasing with distance from the original solid–liquid interface. There were some dopant striations, however, which is puzzling in light of the results obtained by Witt and Gatos. Whether these are inherent in the growth process or result from thermal or acceleration events during the solidification process is not clear, and, unfortunately, there was insufficient instrumentation to determine this. The Principal Investigator has suggested a theory based on kinetic supercooling of the melt during the transient growth region to explain the growth rate fluctuation that caused the striations. A more extensive stability analysis is required to confirm this explanation.

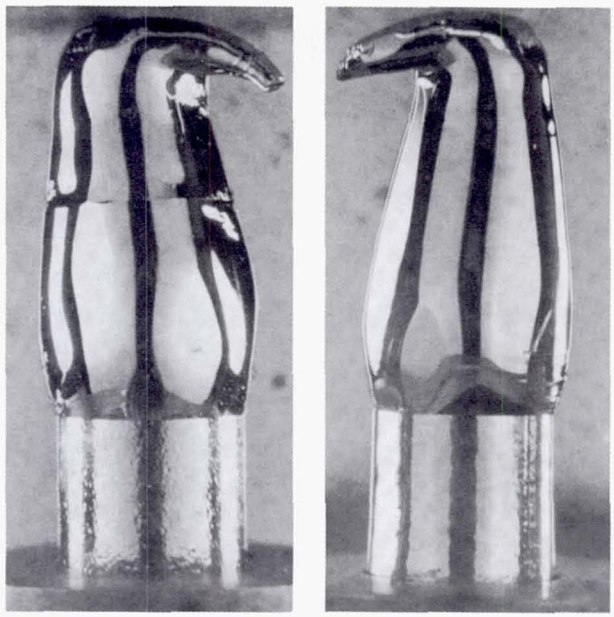

Figure 4.11. *InSb crystals grown uncontained on consecutive Skylab flights. An overall view of two representative samples processed on the second (left) and third (right) Skylab flights reveals extremely smooth and reflective surfaces. All samples grown during the second flight exhibited the annular groove. The most plausible explanation is that a spacecraft maneuver, 52 minutes after cooldown was initiated, produced an acceleration sufficient to cause a growth disturbance.*

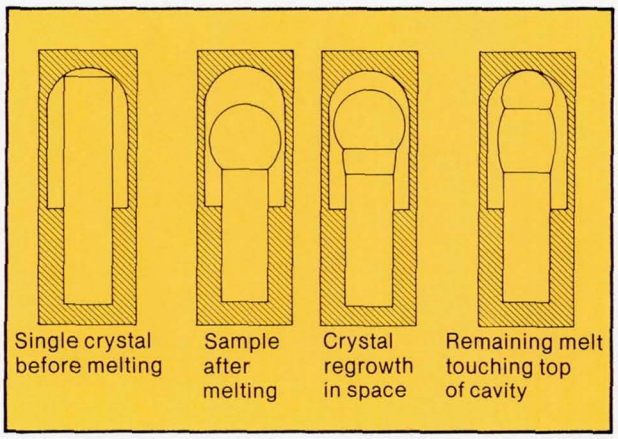

Figure 4.12. Containerless growth of InSb crystal on Skylab.

Figure 4.13. *Facets on InSb crystal grown uncontained on Skylab. Facets grown on these crystals were typically flat to within a few hundred Angstrom units (1 Angstrom unit = 10^{-10} m) as may be seen by this phase contrast image. The colored lines indicate steps that appear on the curved portion of the crystal.*

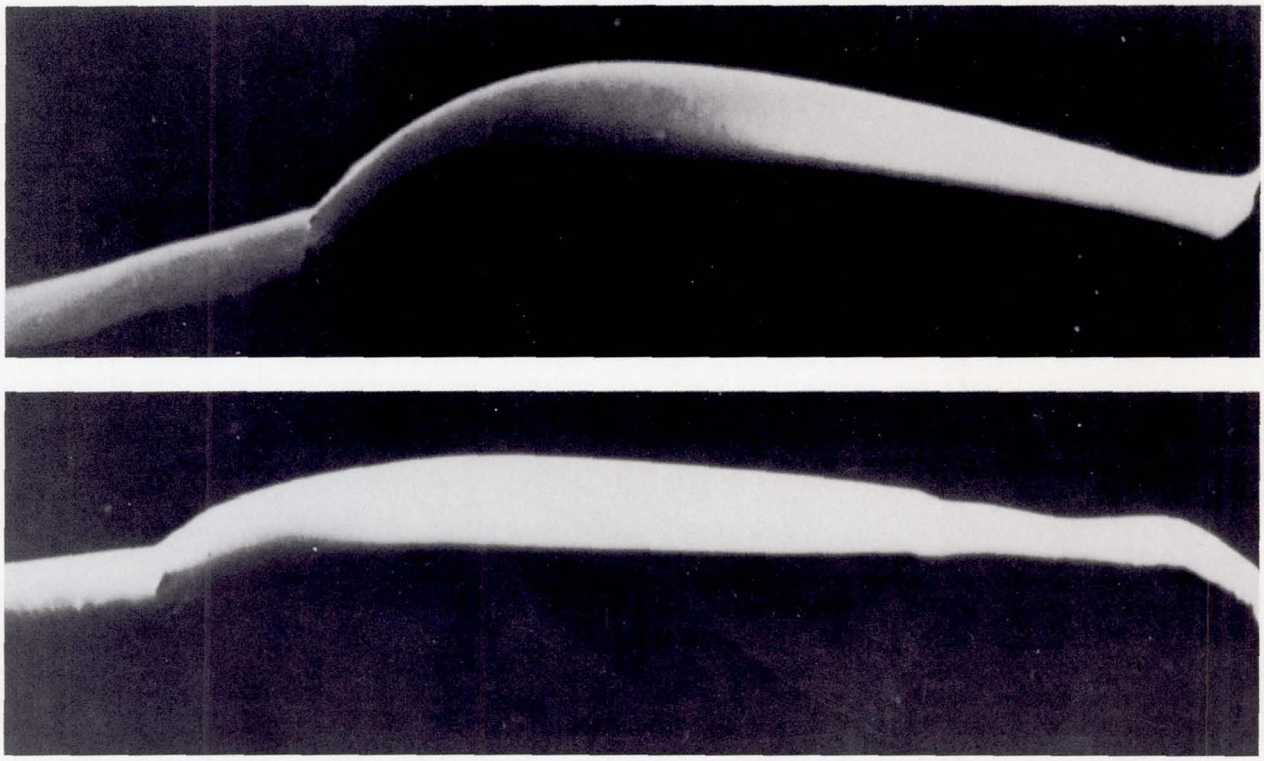

Figure 4.14. *Reflection topographs of crystals grown uncontained on Skylab show no grain or lattice misorientation. Geometrical irregularities of the crystal surface show up on the topograph as well; shadows are cast by small oxide specks that can be seen on some of the pictures. Aside from this, the space-grown portion exhibits flawless single crystals. Only at the very end of the space-grown samples do irregularities appear. However, this is to be expected since this portion was grown under increasing radial thermal gradients and the material was then in contact with the mold.*

Experiment M559, Influence of Gravity-Free Solidification on Microsegregation

Conducted by J. T. Yue and F. W. Voltmer of Texas Instruments, Inc., experiment M559 was designed to investigate the distribution of dopants in germanium solidified in a low-gravity environment. Three types of crystals were prepared by conventional Czochralski growth containing the following dopants: Ga (8×10^{16} atoms per cm^3), B (2×10^{15} atoms per cm^3), and Sb (4×10^{14} atoms per cm^3). The crystals were melted back and allowed to resolidify directionally. The flight samples were compared with identical sets melted and resolidified on the ground in both horizontal and vertical position. The vertical samples were processed in a thermally stable configuration.

Some contamination was apparently acquired from the graphite crucible which doped the samples in an unwanted manner, making it difficult to interpret the dopant distribution in the lightly doped samples that contained B and Sb. Good data were obtained from the more heavily doped Ga sample.

The dopant segregation was measured using a spreading resistance probe. Figure 4.15 shows the radial distribution of dopants in the space-processed sample compared with the ground control samples. As may be seen, the space processed samples show much less radial segregation, as evidenced by the long, flat portion of the curve. A marked increase in dopant distribution is seen near the surfaces of the space-processed and the ground control samples. The space-processed sample necked down in diameter and had a free surface in the regrowth region. Surface tension flow might have produced this distribution. The ground control samples had no such free surfaces, but may have been influenced by conventional convection driven by radial thermal gradients.

The spreading resistance measurements used for measuring the dopant distribution had a resolution of 5 μm, thus allowing dopant concentration fluctuations to be measured on a microscopic scale. It can be seen from figure 4.15 that the amplitude of such fluctuations is considerably reduced in the space-grown crystal. The degree of microsegregation (mean square value of these fluctuations over a 100-μm interval) was 0.4 percent for the space-grown crystal compared with 1.6 percent and 2.2 percent, respectively, for the ground control samples.

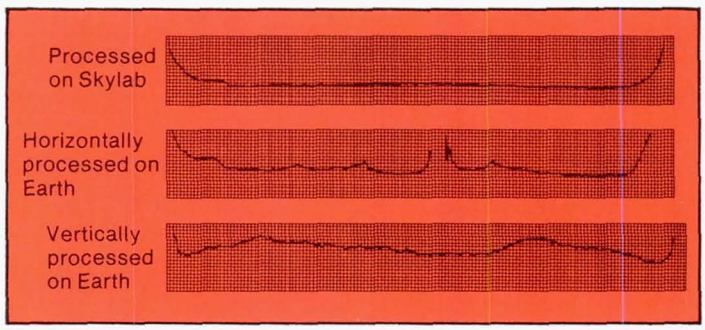

Figure 4.15. Resistivity profiles showing microsegregation in germanium. These graphs illustrate the most significant result of the experiment: influence of gravity-free solidification on microsegregation in germanium. A comparison of the resistivity profiles of three gallium-doped germanium crystals is shown. All three curves were made with the two-probe spreading resistance methods at 5- μm steps. The radial profiles were measured at 0.5 cm away from the original solid–liquid interface. Each unit on the horizontal axis is 100 μm. Microsegregation was reduced by five times and macrosegregation was reduced by six times for the Skylab processed crystal. Fluctuations in resistivity are inversely proportional to fluctuations in solute compositional variations.

The dopant distribution in the axial direction is somewhat confusing. The crystal did not grow long enough to reach steady state growth. The initial transient of dopant concentration appeared to be sharper in the ground control samples than in the flight sample, exactly the opposite of what would be expected. The reason for this difference is not understood.

Experiment M563, Directional Solidification of InSb-GaSb Alloys

The directional solidification experiment, developed by W. R. Wilcox of the University of Southern California, addresses an important class of materials, that is, the controlled bandgap solid solution semiconductors such as Hg_{1-x} Cd_x Te and Pb_{1-x} Sn_x Te that are important infrared detectors. The system chosen is In_{1-x} Ga_x Sb, which does not have the technical importance of the previously mentioned materials, but is simpler to work with because it does not have the high vapor pressure associated with Hg or the sensitivity to mechanical strain of the PbSnTe system. It does serve as a useful model of these systems in many respects.

The difficulties of growing ternary solid solutions from the melt are many. To a first approximation the systems behave as pseudobinary systems in which InSb and GaSb behave as two separate components that can coexist in a crystalline lattice in any mixture. The phase diagram is similar to that discussed at the beginning of the chapter (fig. 4.5). As the temperature is lowered for a given composition to the solidus line, the first material to solidify has a considerably different composition from the starting material. If convective stirring can be prevented, the diffusion layer will gradually become richer in the other component

until a steady state is reached, at which point the composition of the growing crystal is the same as the melt, as was demonstrated in the steady state growth experiment.

Another problem arises in dealing with moderate concentrations of the solute. The material in front of the growth interface is enriched by the lower melting point material, so the solidification temperature is reduced. However, a short distance away, that is, the length of the diffusion layer, lies the much higher melting point material (fig. 4.16). In other words, the solidification front is at the solidus temperature. For controlled planar solidification it is necessary for the temperature everywhere in the melt to be above that of the local liquidus. Unless the thermal gradient is steep enough to meet the condition, a phenomenon known as constitutional supercooling will result in which the plane interface breaks down and dendritic growth takes place, destroying the single crystal growth process.

Since the diffusion layer becomes smaller at more rapid growth rates, the required gradient increases directly as the growth rate increases. Conversely, a lower growth rate reduces the requirement for high gradients but adds two additional problems. First, much longer times and growth distances are required to reach steady state. Second, the growth oscillations discussed are required to reach steady state. Second, the growth oscillations discussed previously may exceed the critical growth rate and cause interfacial breakdown. For these reasons, melt growth of materials such as HgCdTe have not been feasible in 1 g.

Wilcox chose 0.1, 0.3, and 0.5 as values of X for the composition of the samples. Based on the knowledge of the phase diagram and the predicted performance of the furnace, he hoped to have one composition within the stable growth region, one in the unstable growth region, and one on the borderline between stable and unstable. As discussed previously, the gradient freeze furnace used on Skylab did not lend itself to well-controlled growth rates and gradients, and all the samples exhibited unstable growth. Clearly, a much better furnace with controlled directional solidification is required to do this experiment properly.

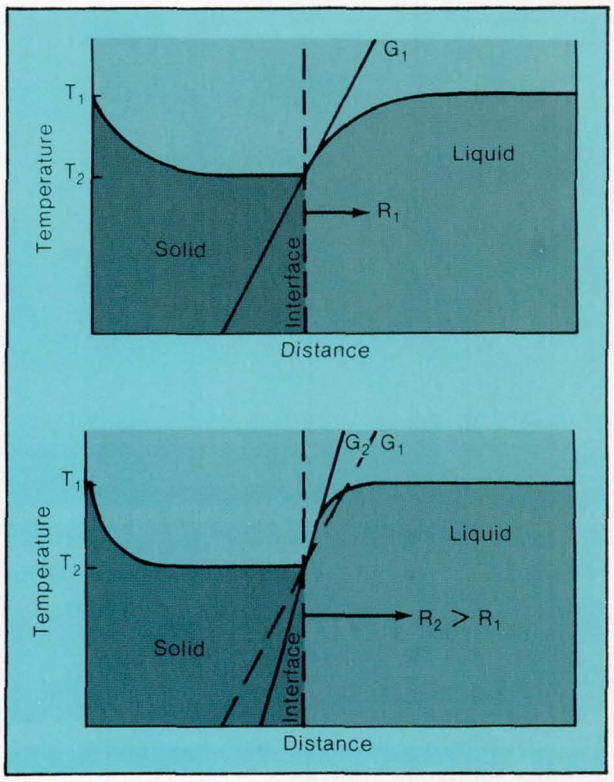

Figure 4.16. *Solidus and liquidus temperatures for the system in figure 4.6. (G, gradient; R, growth rate). To prevent constitutional supercooling and interfacial breakdown, it is necessary to keep the temperature above the liquidus curve. This requires a temperature gradient that becomes steeper as the growth rate increases. If gradient G_1 is applied to growth rate R_2 (bottom curve) the material in the orange region will be below its liquidus temperature and will solidify, causing interfacial breakdown.*

VAPOR GROWTH EXPERIMENTS

Experiment M556, Crystal Growth by Vapor Transport

This experiment, conducted by Heribert Wiedemeier of the Rensselaer Polytechnic Institute, used iodine as a chemical vapor transport agent to grow GeSe and GeTe. The primary purpose was to examine the transport process in the absence of gravity-driven convection and to determine if the diffusion-controlled conditions had any effect on crystal morphology and perfection. The choice of the materials was dictated by the furnace capability, and although these particular materials are of limited interest for device applications, they serve as useful models for systems with more technological importance.

The chemical reactions that govern the transport of GeSe are GeSe (solid) + GeI_4 (gas) $\longleftrightarrow$ 2 GeI_2 (gas) + 1/2 Se_2 (gas). A similar reaction takes place with the GeTe system. As seen in figure 4.3, the iodine transports the Ge while the Se or Te is transported by sublimation. For extremely low pressures of the transport agent (GeI_4), the transport of material from the hot zone to the cold zone is controlled by the chemical reaction rate of the transport agent with the source material. In effect this means that the rate of crystal growth is limited by the number of transport agent molecules available for reaction with the source material. As the pressure is increased from this initially low value, the transport rate increases proportionately until a critical pressure or concentration of transport agent is reached at which sufficient gas molecules exist in the ampoule so that flow is im-

peded by intermolecular collisions. There is then an intermediate range in which a further increase in pressure results in a reduction in the mass transport rate since the frequency of collisions will be increased. In this range of transport agent pressures, the mass transport rate is considered to be diffusion controlled, even though there may be a significant amount of convection, and the rate is proportional to the change in pressure of the transporting gas between the hot and cold end divided by the total pressure. Further increases in pressure can result in a steep increase in the mass transport rate. The reason for this is that massive convection becomes operative. This is the situation for Earth-based experimentation. In the absence of gravity, it was anticipated that convection would not occur, resulting in only two pressure ranges of significance, namely, that where transport is reaction rate dependent and that where the rate of transport is entirely diffusion controlled. The type of mass transport is important since it significantly affects the growth habits (external shapes) and perfection of the semiconductor crystals produced.

Every crystal has a natural structure or ordering of the atoms or molecules. The structure of GeSe is simple cubic; that is, the entire solid can be generated by translating in three-dimensional space a cube with atoms located at the four corners. The structure of a crystal, if it is grown under ideal conditions, will dictate its overall bulk shape and surface characteristics. For a cubic structure, we would expect the as-grown crystals to be shaped either as cubes or rectangular prisms. On Earth these shapes are not observed because growth by vapor deposition is dominated to varying degrees by convective transport. For the GeSe system, the best Earth-grown crystals are produced at pressures slightly less than that corresponding to the onset of massive convection. These crystals are very thin platelets with an irregularly shaped periphery, typically with edge dimensions on the order of 4 mm. Since growth is not seeded, crystals usually begin growing on the walls of the cylindrical ampoule and therefore exhibit a general curvature. At higher transport pressures, single crystals are not obtained due to massive convective transport. The deposited material is dendritic in nature; that is, growth occurs to produce many thin, needle-like shapes.

Three vapor transport crystal growth ampoules were processed simultaneously in the Multipurpose Electric Furnace on each of two Skylab flights. The primary objective was to learn what effect the absence of convection in a low-gravity environment would have on the size, habit, morphology, and perfection of the resultant crystals. In each set of three ampoules the concentration or pressure of GeI_4 was varied in such a way that if the growth experiments had been conducted on Earth, the convective contribution to mass transport would have been extensive, moderate, and slight. Four of the ampoules contained polycrystalline GeSe as the source material, and two contained GeTe. The first experiments were conducted in a temperature gradient of 520°–420° C between the source and the seed. Sufficient time elapsed between the two flights on which these experiments were performed to permit a preliminary analysis of initial results. The surprising observation was that mass transport rates were much greater than predicted. To confirm that these rates were not anomalous, the second set of three ampoules was processed in a lower temperature gradient of 412°–346° C. These also yielded higher than expected growth rates.

A comparison of crystals grown on Earth and in space revealed distinct morphological differences. Typical GeTe crystals from the ampoules designed for moderate convective contribution to mass transport on Earth are compared in figure 4.17. The crystals grown on Skylab have more compact growth habits, their edges are better defined, and their facets are smoother—all evidence of a higher degree of crystalline perfection. External differences between crystals grown in space and on Earth were expected to be less pronounced for the case on which the GeI_4 pressure was kept low (slight convective contribution to mass transport on Earth). However, the crystals grown on Earth exhibited steps and ledges on their facets, whereas the Skylab-grown crystals were uniformly smooth.

The most pronounced difference in growth morphology was expected for GeSe crystals processed at high transport

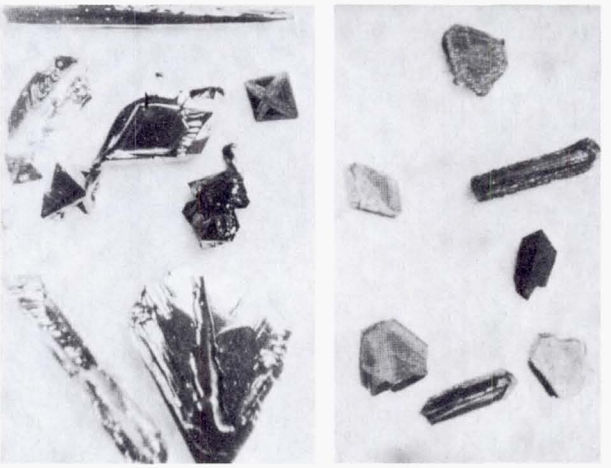

Earth grown Skylab grown

Figure 4.17. *A comparison of GeTe crystals grown on Earth and in space. Representative crystals grown by vapor deposition on Earth are needles and platelets with distorted surfaces and hollow growth habits. The Skylab-grown crystals have considerably more compact habits, and their facets exhibit a greater degree of smoothness and crystalline perfection. The dull appearance of the crystals grown in space results from condensation of the transport agent during the long cooling period dictated by the Skylab apparatus. In a dedicated process, this would be prevented by removing the ampoule from the furnace and quenching the vapor source.*

gas pressure, because the convective contribution to mass transport would be extensive on Earth and negligible in space. The effect of convective turbulence was very apparent in the crystals grown on Earth, yielding only dendrites with a distinct curvature. The Skylab crystals are much superior. In the absence of convective interference, individual well-developed single crystal platelets were obtained.

One of the Skylab crystals shown in figure 4.18 is 18 mm long, approximately six times larger than expected, and is about the size and shape most desirable for electronic device production. Evidently this large crystal grew freely suspended without touching the ampoule. It happened to be oriented in the proper direction to grow toward the source of the vapor, and it kept this favorable orientation because it was weightless and therefore did not shift its position as it grew. The two sides of this crystal are shown at higher magnification in figure 4.19. The surfaces are actually much smoother than they appear in the figure because of contamination by transport agent deposited on the surfaces when the ampoule was cooled.

A variety of techniques were employed to compare the structural perfection of crystals grown on Earth and in space. One involved thermal etching of their surfaces. This is accomplished by heating the crystals in a vacuum until a very small amount of surface material vaporizes. Vaporization or etching occurs preferentially at points of intersection of dislocations with surfaces and forms pits that are visible under a microscope. Typical regions of thermally etched crystals are compared in figure 4.20. The greater perfection of the Skylab crystal is obvious; it contains fewer pits (defects) per unit of area.

An interesting and unexpected result mentioned earlier was observed relative to the extent of mass transport.

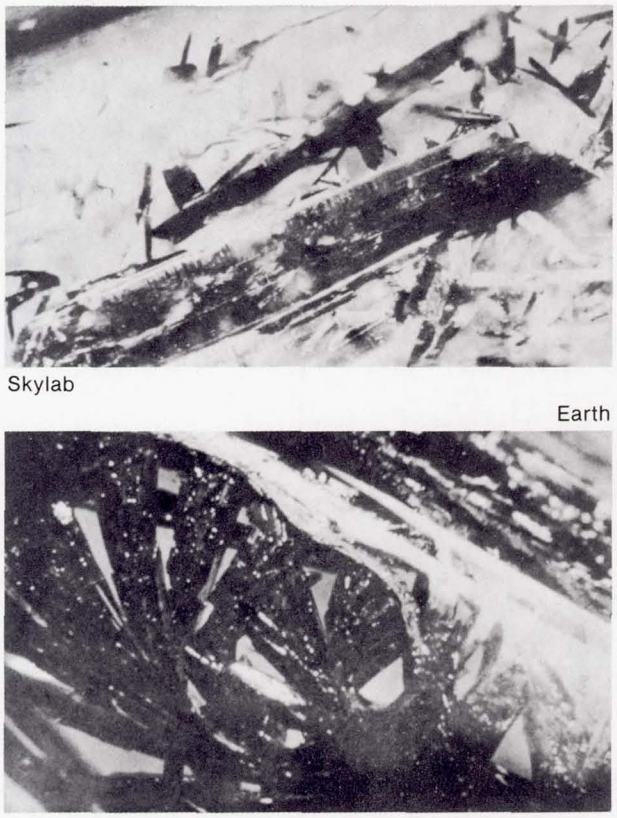

Figure 4.18. *Deposition regions in GeSe ampoules processed at high transport gas pressure on Earth and in space. The most pronounced difference in growth morphology was predicted and observed for the GeSe system when the transport gas pressure was high enough to cause an extensive convective contribution to mass transport on Earth. The condensation region of the ampoule processed on Earth contains curved dendrites representative of the effect of convective turbulence on crystal habit. In the absence of convective interference on Skylab, individual well-developed crystal platelets were obtained.*

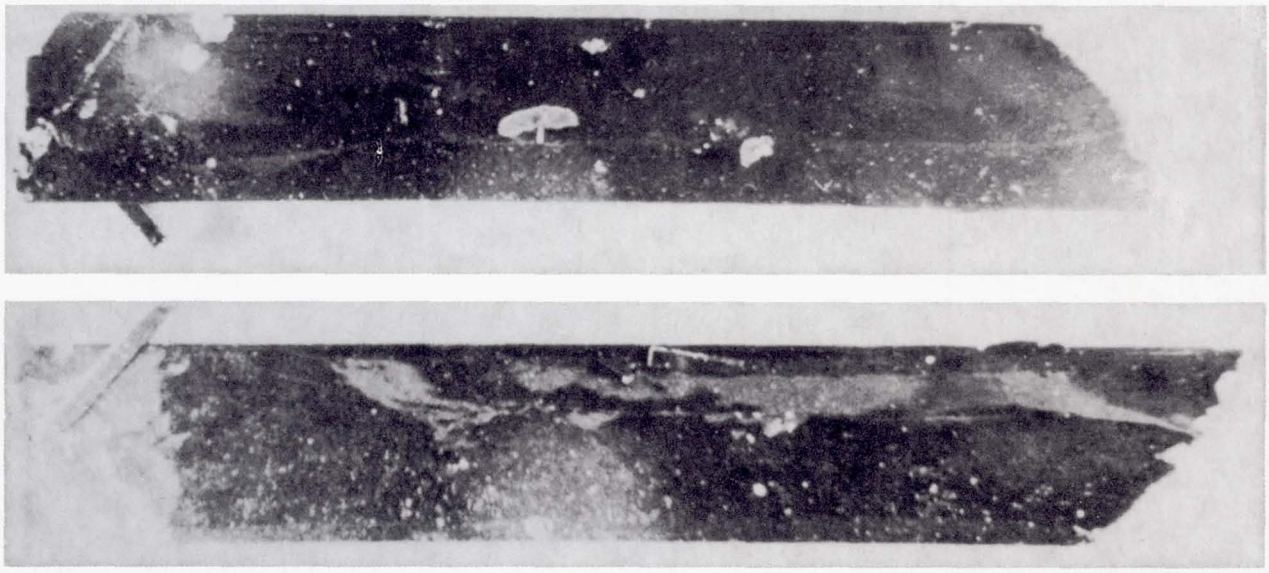

Figure 4.19. *Front and back surfaces of largest GeSe single crystal grown in space.*

Experiments on Earth in which the transport rate is thought to be primarily diffusion controlled produce crystals with a characteristic appearance. This same appearance was typical of crystals grown on Skylab at higher transport gas pressures. However, the crystals grew several times faster in space than was expected by extrapolating the laboratory experiments to higher pressures along the diffusion branch (fig. 4.21). Several explanations are possible. Either an unsuspected transport mechanism is operating in low-gravity in addition to diffusion, or the transport in the space experiments was purely diffusive and some convective process is acting in 1 g to retard the diffusive transport. These results stimulated some intensive work in the laboratory to try to straighten out the various transport processes. This is discussed in chapters 7 and 8.

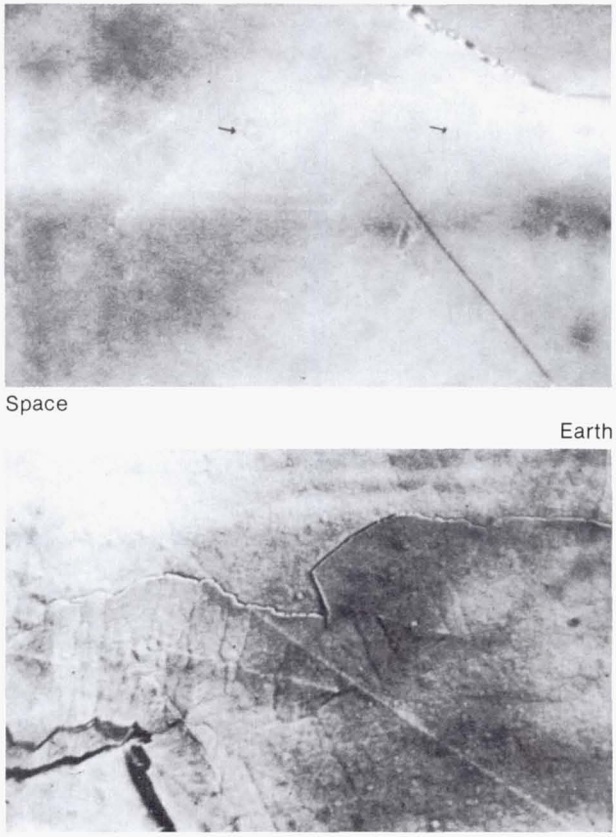

Figure 4.20. Cleaved GeSe crystals after etching. Optical photomicrographs of cleaved, thermally etched surfaces of crystals grown on Earth and on Skylab are shown for comparison. The higher degree of structural perfection of the Skylab crystal is evident in that its surface was less affected by etching. Two etch pits are marked by arrows. The crystal grown on Earth is completely covered with pits.

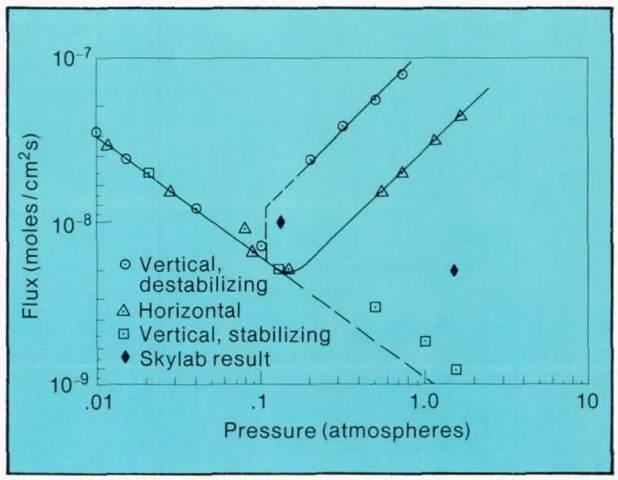

Figure 4.21. Observed transport rates for GeSe + GeI_4 system for 524° C source temperature and 422° C seed temperature. The transport rates for pressures below approximately 0.1 atmosphere are insensitive to the orientation of the ampoule and are considered to be on the diffusion branch. At a critical value of pressure unstable convection results in the vertical unstable configuration. Natural convection overcomes the diffusion-controlled flow near 0.15 atmosphere, and the vertical stable configuration resembles the extrapolated diffusion branch. The slope of the experimentally determined diffusion branch is approximately equal to −3/5, which is the expected slope obtained from theoretical considerations. The remarkable finding is the fact that the fluxes observed on Skylab were significantly higher than the values obtained from extrapolating the diffusion branch.

Chapter 5. METALLURGICAL PROCESSING

In the processing of a useful metal product, there is almost always at least one processing operation involving melting and solidification: to extract the pure metal from its ore, to mix metals to form an alloy, to cast the metal into a specific shape, or to join pieces of metal by welding. While the metal is liquid and while it is solidifying on Earth, it is subject to the same gravitational influence discussed previously for semiconductor materials. A fundamental difference between semiconductors and metals, however, is that the latter rarely find application in the form of single crystals. Furthermore, the effects of gravity in most metallurgical processing are generally beneficial or innocuous. The metallurgical processing experiments on Skylab were chosen primarily to elucidate the unknown effects of a low-gravity environment on certain processes, to determine to what extent nongravitationally driven flows operate in the processes, and to explore the possibilities of containerless solidification.

Segregation can occur in molten metal systems on Earth, with more dense phases settling and less dense ones rising. In most alloys of current practical significance, however, this does not present an unmanageable problem. In fact, the segregation phenomenon is used for the removal of unwanted gases and impurities from a melt. Alloys in which constituents would segregate because of widely divergent densities are made without melting by sintering mixtures of powders under pressure.

Thermal convection also occurs in molten metals on Earth because warmer, less dense material nearest a heat source tends to rise because of buoyant forces, whereas the cooler, more dense material tends to sink. The resultant circulation can be sufficient to overcome sedimentation, causing dense particles to be distributed more or less uniformly throughout the melt. It can also cause newly solidified dendritic crystals, protruding from a solidification front into the liquid, to be broken off and circulated. This mixing and stirring of the melt is usually beneficial in that it provides the uniform distribution of constituents and random orientation of crystals (grains, in metallurgical terminology), both of which are desirable characteristics in most practical applications of metals.

WELDING AND BRAZING EXPERIMENTS

The Skylab mission presented the opportunity to explore some unknown aspects of metallurgical processing in a low-gravity environment. It has already been mentioned that welding and brazing experiments were planned in anticipation of a future need for proven joining techniques in the construction and repair of structures and machinery in space. These experiments were not only desirable from an engineering standpoint, but also for the fundamental scientific knowledge they were likely to provide. For example, it was not known if surface tension and other forces acting to keep a molten puddle of metal intact would be sufficient to keep it from being blown away in space by the force of an impinging electron beam used as a heat source. In the brazing experiment, the extent to which molten metals would flow under the influence of capillary forces unimpeded by gravity was of primary interest. Both experiments provided an opportunity for fundamental studies of solidification mechanics in a weightless environment.

Experiment M551, Metals Melting

This experiment was developed by E. C. McKannan and R. M. Poorman of the Marshall Space Flight Center. The objectives were (1) to study the behavior of molten metal in low gravity with particular attention to the stability of the molten puddle and its interface with the solidified melt, (2) to characterize metals solidification in low gravity with regard to grain size, orientation, and subgrain patterns as might be affected by the difference in convection during solidification, and (3) to determine the feasibility of joining and casting metals in space.

The experiment was performed in the Skylab Materials Processing Facility, using the electron beam gun as a source of heat for melting. Disc-shaped specimens of varying thickness were mounted on the motorized mechanism shown in figure 5.1. It provided rotation of the discs with respect to the fixed electron beam. Electron beam welding on Earth is performed in a chamber evacuated to an extremely low pressure. In the Skylab experiment, the necessary vacuum was obtained by venting the interior of the work chamber to space.

Discs were fabricated from three metals: stainless steel containing chromium and nickel (type 304), a high-strength aluminum alloy (2219-T87), and pure (99.5 percent) tantalum. Each disc was placed in the work chamber, the work chamber was vented overboard, and the welding was performed. The sharply focused electron beam was impinged on the thinnest portion of the disc as slow rotation began (2.6 revolutions per minute). During the first 45 degrees of rotation, the specimens were sufficiently thin so that the beam penetrated through the metal. The disc thickness then increased gradually during the next 90 degrees of rotation to the extent that the electron beam penetrated fully, but did not cut through. After an additional 90 degrees of full penetration, the disc thickness gradually occurred in 45 degrees of rotation. At this point, the beam was terminated, the disc was rotated an additional 22 degrees, and the beam was reinitiated and defocused for times from 15 to 45 seconds to permit a large molten metal pool to form and solidify. After the experiment, a typical disc appeared, as shown in figure 5.2.

There was no significant difference in the external appearance of welds made with identical apparatus in space and on Earth. The experiment proved that surface tension in the absence of gravity is sufficient to hold a molten weld puddle in place, and thus demonstrated that welding operations in space are feasible using techniques identical to those employed on Earth.

Typical welds from the three specimen types produced in space and on Earth are compared in figures 5.3, 5.4, and 5.5. In each case, the comparison is made on the basis of polished and chemically etched cross sections photographed through a microscope at two different magnifications to reveal the size, shape, and orientation of grains.

Typical sections of partial penetration welds made in 2219-T87 aluminum are shown in figure 5.3. The weld nugget solidified on Earth is composed of large columnar grains oriented perpendicular to the interface between the weld puddle and the unmelted base metal. This grain structure is typically observed in welds and castings produced on Earth. In contrast, grains in the weld nugget produced on Skylab are considerably less elongated. Another obvious difference between the Skylab and Earth-based welds is the width of the heat-affected zones in the base metal adjacent to the nugget. The heat-affected region in the Skylab specimen is much more extensive.

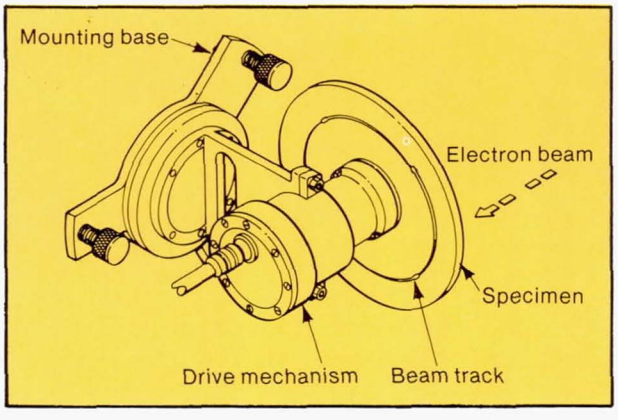

Figure 5.1. *Apparatus for the metals melting and welding experiment.*

Figure 5.2. *Metals melting and welding specimen after processing on Skylab. The stainless steel specimen shows the path traversed by the electron beam. The thickness varied to permit complete and partial penetration of the beam. The specimen was cut through from the 9 to 11 o'clock positions. At the 12 o'clock position, a molten puddle was formed to allow detailed studies of metal resolidification to be made.*

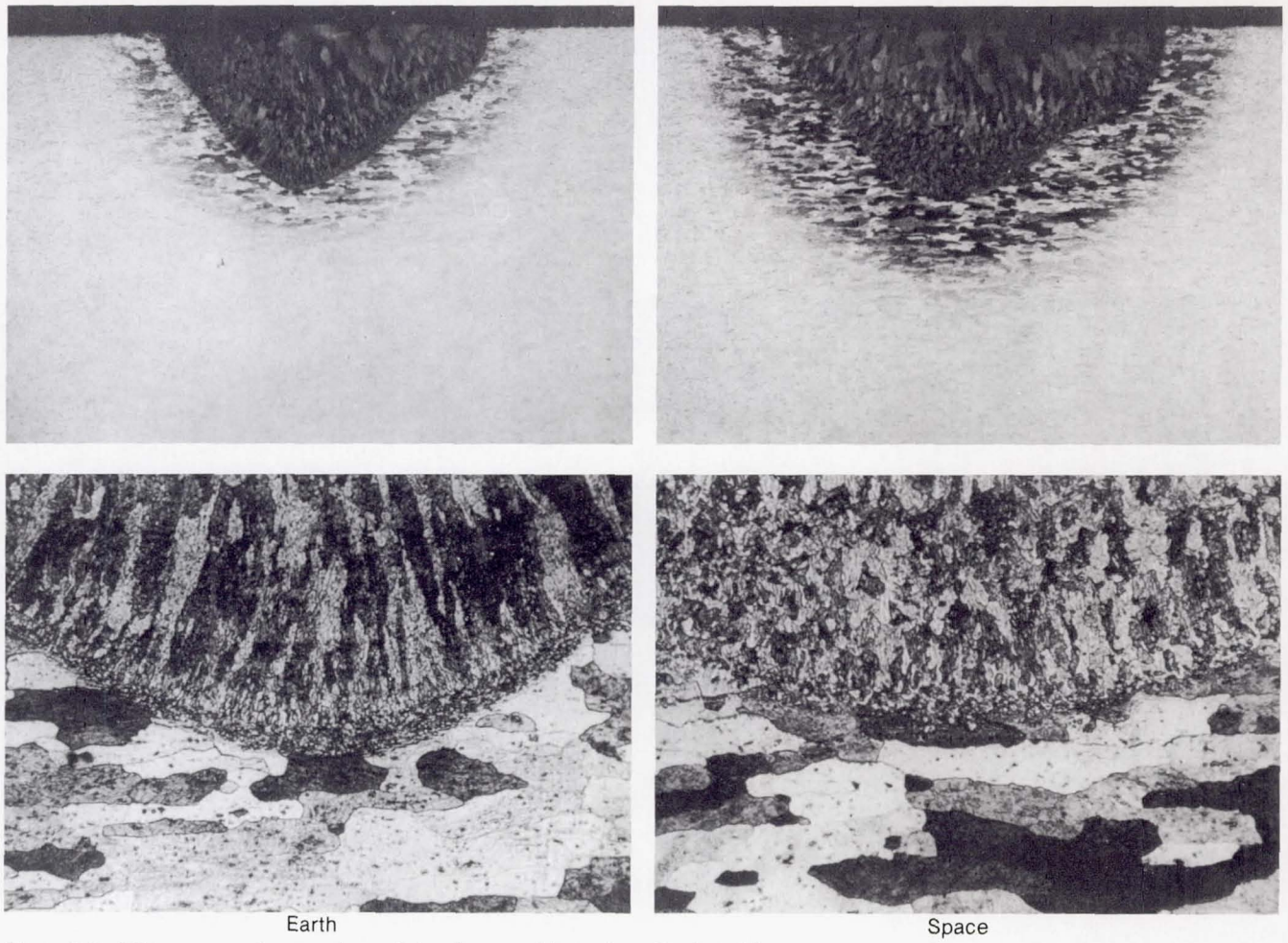

Earth Space

Figure 5.3. Microstructural comparison of aluminum welds made on Earth and in space.

Figure 5.4. Microstructural comparison of stainless steel welds made on Earth and in space.

Earth Space

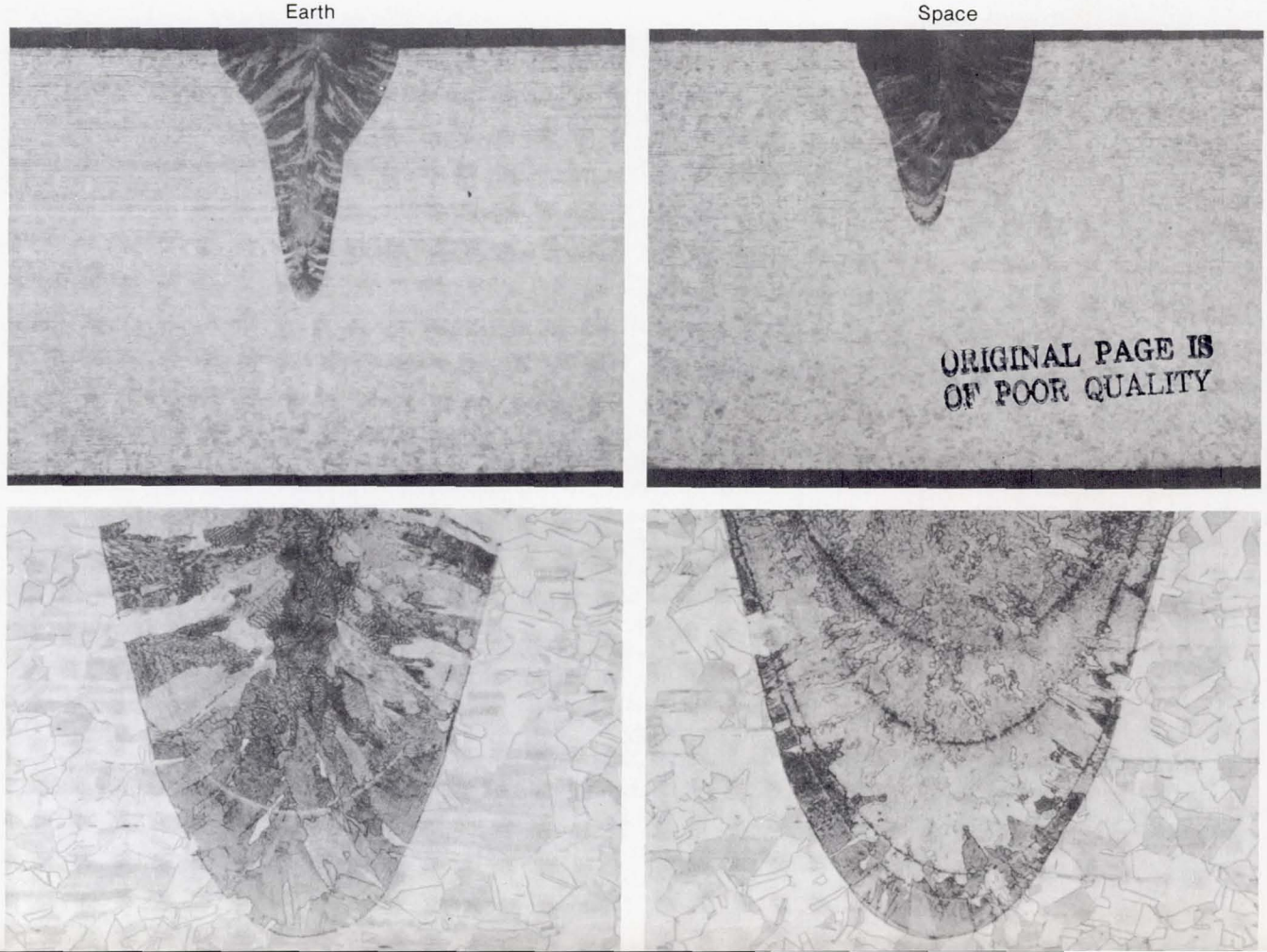

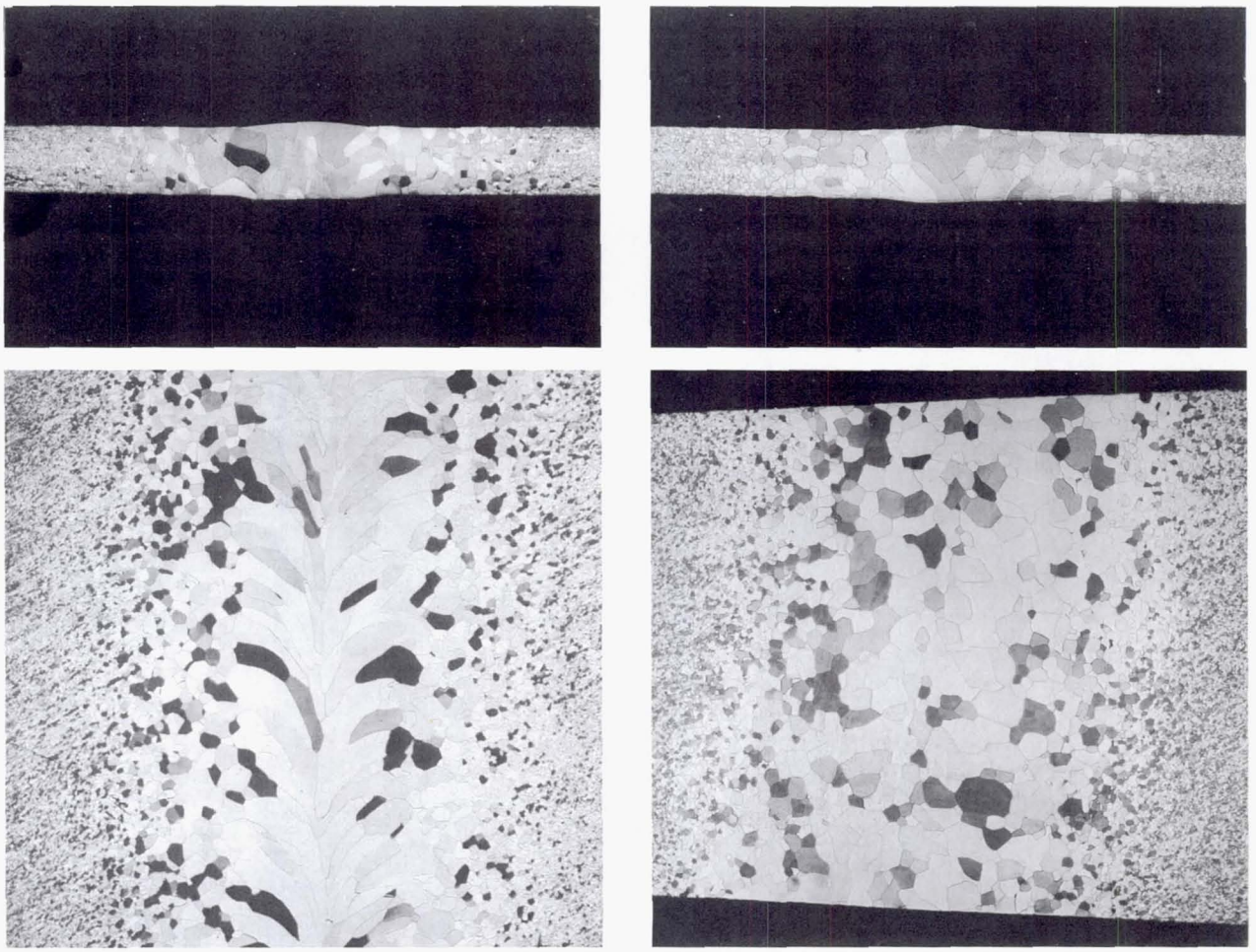

Figure 5.5. *Microstructural comparison of tantalum welds made on Earth and in space.*

The partial penetration regions of 304 stainless steel discs are typified by the photomicrographs of figure 5.4. The molten zones are narrower and the interfaces sharper than in the aluminum welds discussed previously because of the lower thermal conductivity of steel. The different nugget shapes result from a slight difference in electron beam power profile and focus. As with the case for aluminum, large elongated grains perpendicular to the interface between the weld puddle and the unmelted base metal are observed in the nugget of the weld produced on Earth compared to finer grains in the nugget of the Skylab weld which solidified in low gravity. The bands obvious in photographs of both specimens at the higher magnification have not been satisfactorily explained. They may be the result of some subtle, undetected instability of the electron beam.

Sections of full penetration welds in tantalum discs are shown in figure 5.5. Since this metal was commercially pure, with no secondary elements except a trace amount of columbium, there were no complex precipitates during solidification, and large distinct grains were formed. The most interesting observation from the specimen welded on Earth is that residual vortices left behind after the electron beam passed were frozen into the grain structures. This typically occurs because the high melting point and thermal conductivity of tantalum result in rapid cooling of the molten region. Although the thermal characteristics were identical and the weld parameters were similar on Skylab, the residual vortices were erased in the grain structure of the specimen welded in space.

The experiment demonstrated the feasibility of electron beam welding, cutting, and melting in the low-gravity environment of space. The only significant difference noted between the Earth-based and the low-gravity results was the formation of the finer, more equiaxed grains in the low-gravity sample. This is completely contrary to what one would expect since the strong convective flows associated with the 1-g sample should be effective in forming the equiaxed zone through dendrite remelting and transport. A satisfactory explanation for this result has not been found.

Experiment M552, Exothermic Brazing

The objectives of the brazing experiment were to evaluate the feasibility of brazing as a tube-joining method for the assembly and repair of hardware in space, and to investigate the mobility, mixing, and capillary behavior of molten braze alloy in low gravity. The experiment was conducted by J. R. Williams of the Marshall Space Flight Center.

A brazed joint involves filling a carefully controlled gap between surfaces of two metals to be joined with a different molten metal called the braze alloy, and then cooling the joint so the braze alloy solidifies and serves as a cement. The melting point of the braze alloy is always considerably less than that of either metal to be joined (the base metals), and, unlike welding, the base metals are not melted. The bond between the braze alloy and a base metal is formed by superficial alloying due to diffusion across the interface between the two, reacting to form intermetallic compounds, liquid metal penetration of base metal grain boundaries, or any combination of these effects. Filling the gap between the base metals is accomplished by capillary action and is influenced by the surface tension of the molten braze alloy, the width and uniformity of the gap, the tendency of the braze alloy to wet the surfaces of the base metals, and the extent to which gravitational forces oppose capillary flow.

The heat source for melting braze alloys on Skylab was an exothermic chemical reaction of the thermite variety. A thermite reaction involves the reduction of a metal oxide by a metal with greater affinity for oxygen, with the accompanying liberation of a considerable amount of heat. This chemical heat source is particularly suited for space applications because a compact package can be prepared that accurately delivers a prescribed amount of energy. The package can be sized to produce no more heat than required and can be insulated so that no exposed surfaces reach high temperatures. The reactants are stable. The reaction proceeds in the absence of oxygen and thus can be used in space. The products are substantially solid, and therefore there is no appreciable formation of gas to act as a potential contaminant. On Skylab, activation energy necessary to initiate the reaction was provided by an igniter fired by a brief pulse of electric current.

The braze specimen consisted of a tube, a sleeve designed to slip over the tube to provide a specific clearance or gap, tapered spacer inserts designed to wedge between the tube and sleeve to fix the clearance uniformly around the tube, and braze alloy rings that snapped into grooves near each end of the sleeve. The specimen was then surrounded by thermite mixture and insulation to form an experiment assembly, as shown in figure 5.6. Four such assemblies were prepared for brazing on Skylab: two with pure nickel tubes and sleeves, and two made from stainless steel. The braze alloy was composed of 72 percent silver, 28 percent copper, and 0.2 percent lithium by weight.

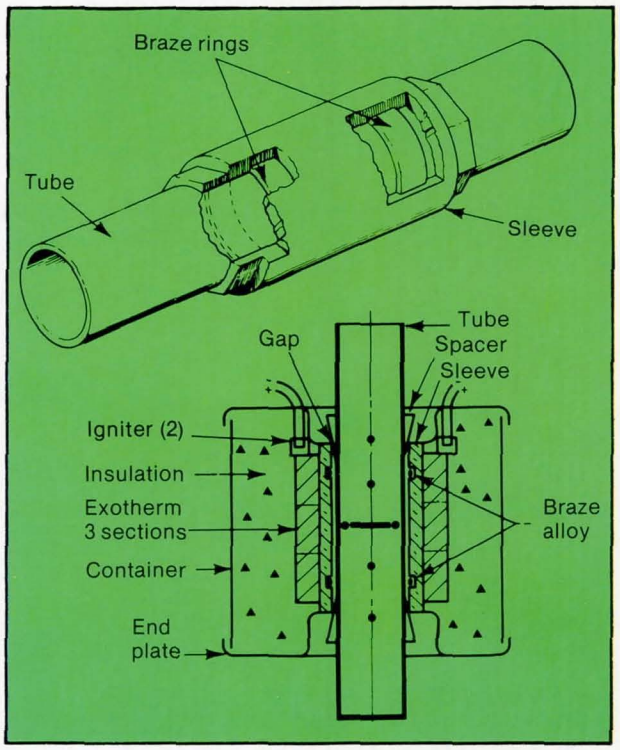

Figure 5.6. Schematic representation of the Skylab M552 exothermic brazing apparatus.

The Skylab brazing experiment verified that brazing is feasible in space, as may be seen in figure 5.7. Because there is no gravitational force in space to act in opposition, gaps in braze joints were filled much more readily by capillary flow of the molten braze alloy. In one of the Skylab specimens, a joint with a gap of 0.5 mm was successively brazed, and it is assumed that greater gaps could be tolerated. On Earth, gaps 10 times smaller must be maintained to ensure a completely brazed joint. Gap tolerances for fabrication in space could be relaxed considerably, and many joints that would have to be welded on Earth could be made by brazing in space.

Some unexpected results unrelated to braze quality were recorded in the form of different interactions between liquid and solid metals in space and on Earth. Under identical conditions of exposure in the two environments, the braze alloy apparently dissolved nickel much more rapidly in space than on Earth. Similarly, copper from the braze alloy penetrated solid stainless steel more extensively in space. This unanticipated behavior has not been explained. A full appreciation of its significance must await the opportunity for additional experimentation on liquid–solid metal interactions in space.

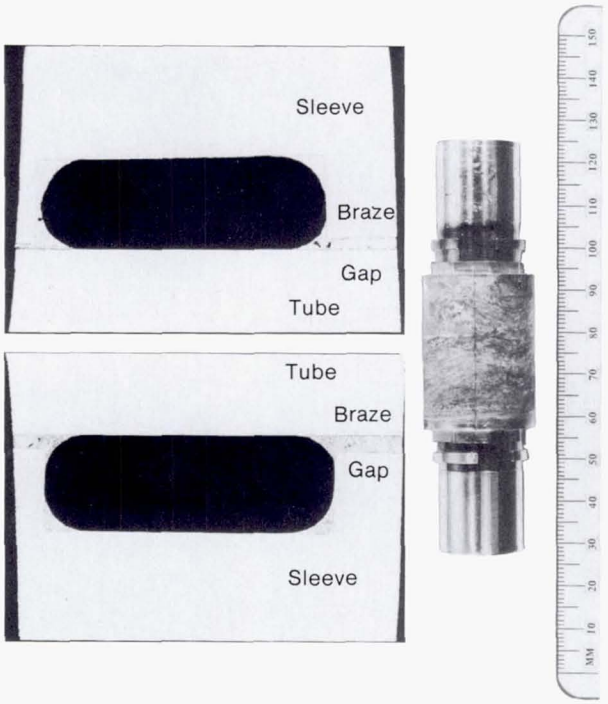

Figure 5.7. Braze joints produced on Skylab. Brazed specimens exhibit complete filling of the braze gap. The large black areas in the photomicrographs are void areas in the ring grooves in which the braze material was initially placed. The fillet formation produced on Skylab is significantly different from that produced on Earth.

COMPOSITES

One rather obvious use of the low-gravity environment for metallurgical applications is the preparation of composites containing materials with different densities from the melted base metal. In 1 g, the dispersed material, which generally has a different density from the host material, either settles or rises when the host material is melted. There are means of overcoming this by using long externally supported fibers or by hot pressing powders. However, these techniques are not completely satisfactory.

For some applications it is important to have randomly oriented fibers. Also, many of the desirable strengthening fibers, such as single crystal whiskers are available only in very short lengths. The powder particles are necessarily small and have a high ratio of surface area to volume. Their surfaces are invariably covered with an oxide film which, although thin, translates into an appreciable oxygen content in a solid produced from the particles. Theoretical density is impractical to achieve in a powder metallurgy product, and the resulting voids and vacancy concentrations can be detrimental.

In addition, there are potential electrical and mechanical applications of alloys formed from fine dispersions of immiscible alloys. These can only be prepared in bulk form on Earth by the previously mentioned powder techniques, with the same problems from voids and oxide layers described previously.

Experiment M557, Immiscible Alloy Compositions

One potential technique for preparing fine in situ dispersions that is only possible in space is the solidification of an immiscible system. Many metallic systems exhibit a miscibility gap in their phase diagram, which means that certain compositions cannot be solidified directly from the melt, as discussed previously, because as the temperature is lowered in the immiscible region, the two liquids separate like oil and water, and quickly unmix because of the density differences of the two fluids. At low-gravity it should be possible to maintain a fine suspension of the immiscible materials during solidification, as was shown by Yates on Apollo 16 and by Lacy and Otto using the drop tower (see chapter 3).

The Skylab experiment was the responsibility of J. L. Reger of the TRW Systems Group. The objective was to compare the microstructures and electrical properties of samples of immiscible metal mixtures melted and solidified on Earth and in space. Specimens were enclosed in cartridges and processed in the Multipurpose Electric Furnace in the same way as on experiments discussed previously except that three different specimens were contained in ampoules within a single cartridge. These were positioned so that two were in the isothermal portion of the furnace and one was in the gradient region.

One isothermal ampoule contained an alloy consisting of 76.85 weight percent gold and 23.15 percent germanium, selected because it exhibits almost complete solid state immiscibility. The other ampoule contained a mixture of 45.05 percent lead, 45.06 percent zinc, and 9.89 percent antimony and is characterized by immiscibility below a certain temperature in the liquid state. Above this "consulate" temperature the liquids are miscible, and a single-phase homogeneous solution is formed. The gradient ampoule was filled with an alloy of 70.20 weight percent lead, 14.80 percent tin, and 15.00 percent indium. This alloy was selected to determine if the tin phase could be

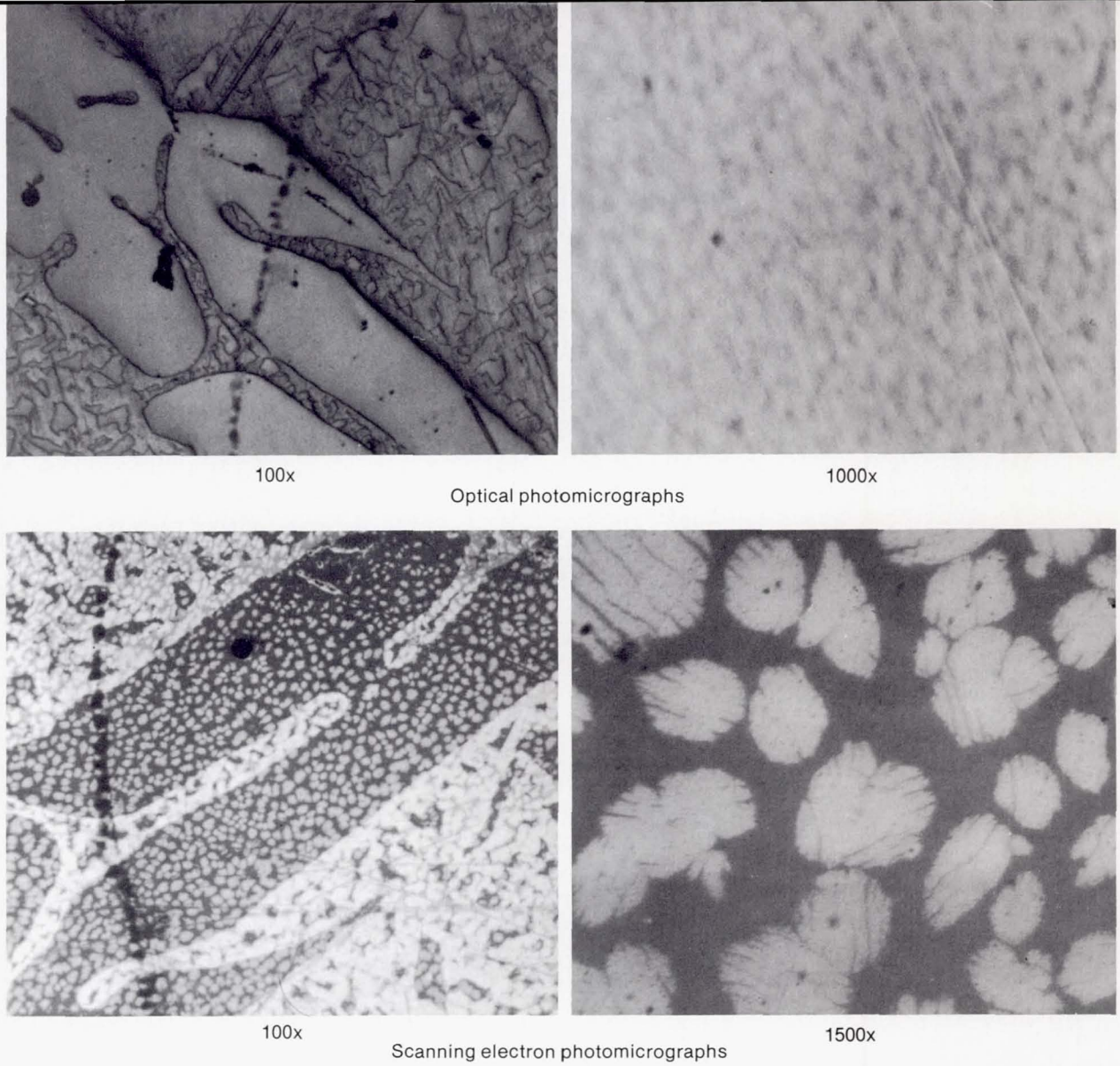

Figure 5.8. Microstructural examination of Skylab's gold-germanium specimens show the fine dispersion of germanium in the gold matrix.

preferentially oriented by directional solidification. The ampoules in the isothermal portion of the furnace were melted at a temperature above the consolute temperature of the lead-zinc-antimony alloy and allowed to soak for a sufficient time to allow complete mixing of the elements by diffusion. The gradient ampoule was fixtured so that the cold end would not melt. This afforded the opportunity to compare, in one specimen, material solidified in space and on Earth.

The experiments showed some interesting microstructural modifications when the alloys were solidified in a low-gravity environment. In general, specimens solidified in low gravity showed a more homogeneous structure (fig. 5.8) but did not have the fine uniformly dispersed structure obtained for gallium-bismuth in the drop tower experiments. There was a slight apparent increase in magnetic coercive strength found in the lead-tin-indium alloy directionally solidified in low gravity. A secondary superconducting transition was observed (fig. 5.9) in the lead-zinc-antimony sample solidified in space which may result from the fine dispersion of lead in the zinc-antimony matrix. The gold-germanium samples processed in space exhibited superconductivity of 1.5 K, whereas the ground control samples did not. This indicates the presence of a different phase that formed in the flight samples.

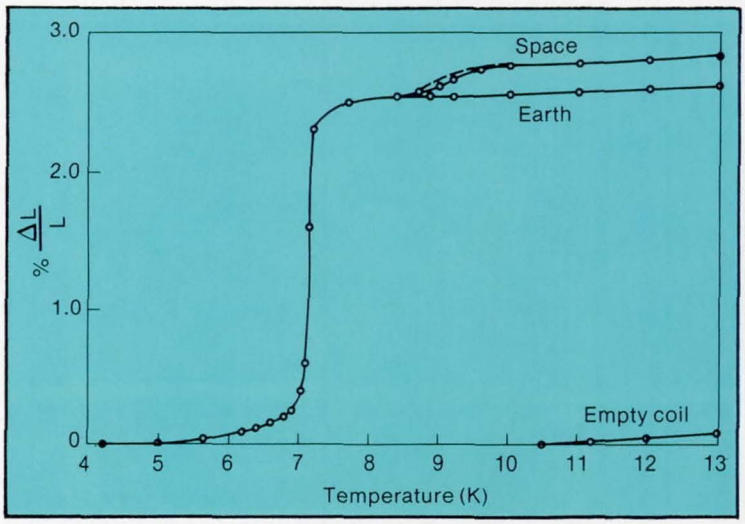

Figure 5.9. Superconducting transition behavior of lead-zinc-antimony specimens processed on Earth and in space.

Experiment M561, Silicon Carbide Whisker Reinforced Silver Composite Material

This experiment, developed by a team from the Japanese National Research Institute for Metals led by T. Kawada, was directed toward preparing a high-density, uniform dispersion of silicon carbide whiskers in a silver matrix from the melt. The starting material was prepared in the conventional manner, using powder techniques with 2 to 10 volume percent silicon carbide whiskers. The powder grains averaged 0.5 μm in diameter, and the whiskers were 0.1 μm in diameter and 10 μm in length.

After the mixture was compacted and sintered at 900° C in a hydrogen atmosphere, it was hot pressed. The samples were then soaked above the melting point of silver for 5 hours. Recognizing the fact that there was no mechanism such as Stokes bubble rise to remove the remaining voids in low gravity, a spring-loaded plunger was contained in the ampoule to compress the mixture of 60 kg/cm^2, which was considerably above the calculated 19 kg/cm^2 required to crush the voids between the particles and the whiskers.

Both the flight and ground control samples exhibited a densification during melting, but some voids were found in all the samples. The distribution of the whiskers was fairly uniform in the flight samples, whereas they tended to cluster near the top of the sample in the ground control tests. Figure 5.10 is a photomicrograph of sections of the flight and ground control samples. A corresponding uniformity in microhardness was found in the flight sample, whereas the ground control samples equaled the hardness of the flight samples near the top where the whiskers tended to congregate. Elsewhere the hardness was significantly diminished. It was also found in bend load tests that the low-gravity samples did not exhibit brittle fracture, as did the ground control samples, but instead showed large ductility. This is attributed to the more uniform distribution of whiskers.

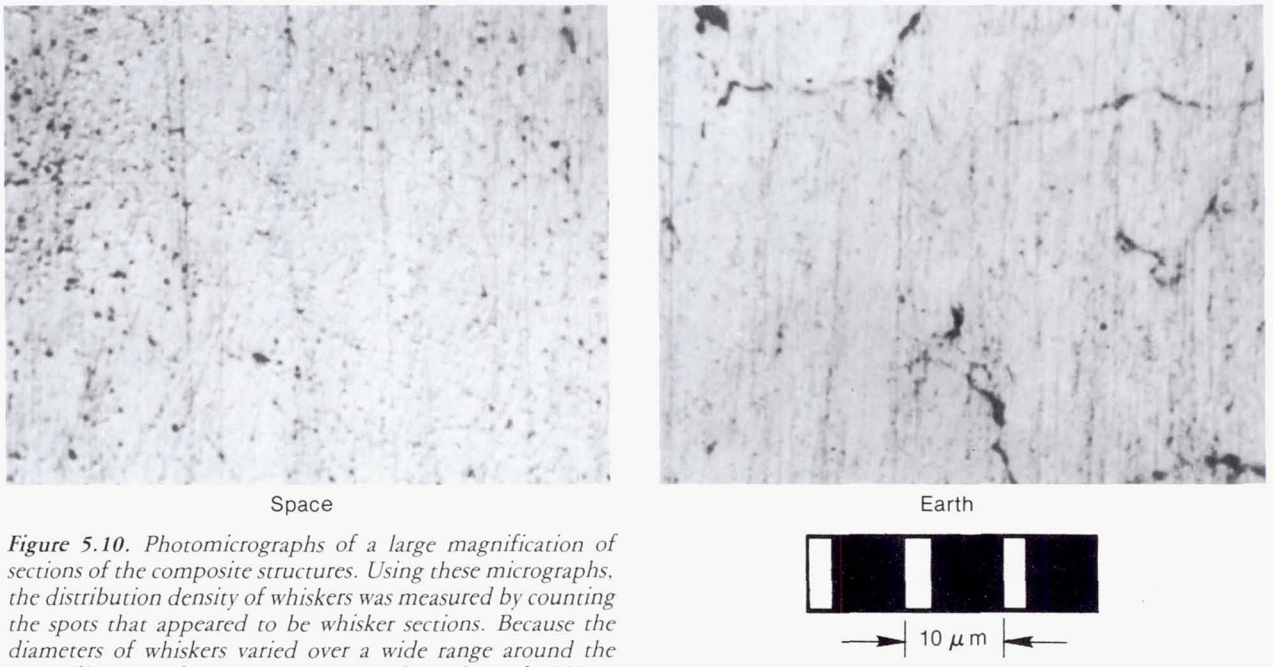

Figure 5.10. Photomicrographs of a large magnification of sections of the composite structures. Using these micrographs, the distribution density of whiskers was measured by counting the spots that appeared to be whisker sections. Because the diameters of whiskers varied over a wide range around the mean diameter of 0.1 μm, the counted numbers of whiskers depended on the resolving power in the microscope and on photographic conditions.

DIRECTIONAL SOLIDIFICATION OF EUTECTICS

Eutectics can be directionally solidified to form in situ composite structures that contain rods on one phase in a matrix of another or to form alternating plates or lamella of the two phases. The directionality of their structures produces anisotropic properties that can be used to advantage in a variety of applications, such as improved high-strength, high-temperature materials for use in gas turbine blades, or materials with unique optical, electronic, magnetic, or

superconductive properties. It has become increasingly clear that significant effort must be made in process control to obtain the high-quality, low-defect, continuous microstructure required for the intended applications.

To understand the formation and properties of eutectic alloys, it is instructive to examine the phase diagram for a typical eutectic, in this case aluminum-copper (Al-Cu). The diagram shown in figure 5.11 identifies the phases that will coexist in equilibrium as a function of both temperature and composition. The phases to be considered are:

Liquid—a molten solution of Al and Cu having the basic composition of the alloy at temperatures above the curve abc. At lower temperatures prior to complete freezing, liquid composition is described by curve abc.

α—a solid solution of copper in aluminum whose composition is given by curve cde.

θ—a solid solution based on the intermetallic compound $CuAl_2$ or, stated differently, $CuAl_2$ which may be slightly nonstoichiometric. Its composition is represented by curve fga.

The alloy of interest relative to one space processing experiment contains 66.8 percent Al. Upon cooling from the liquid state, this alloy solidifies at 548° C to produce a solid composed of a mixture of the phase α and θ. This alloy is unique because it freezes at a single temperature rather than over a temperature range, and because the freezing temperature is the lowest of all alloys in the system. For these reasons, the 66.8 percent Al alloy is known as a eutectic. Eutectics are not unique to binary alloy systems. Another Skylab experiment described later was concerned with the two-compound eutectic, sodium chloride (NaCl), with sodium fluoride (NaF), that forms in the ternary (three-component) system, Na-Cl-F.

As such a eutectic mixture is cooled to the solidification temperature, the α and θ phases simultaneously begin to

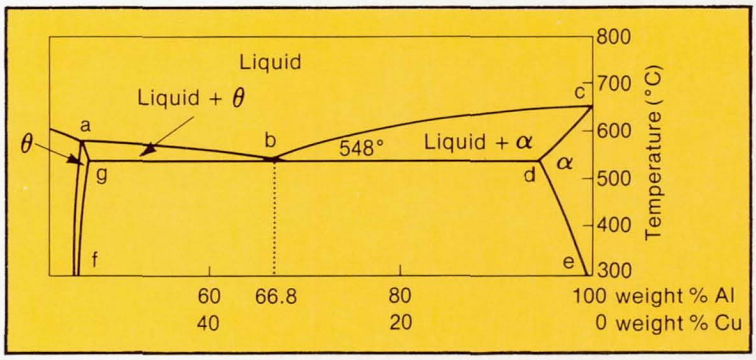

Figure 5.11. Partial phase diagram for the aluminum-copper alloy system.

solidify. If the solidification is controlled and unidirectional, the α phase will reject the θ phase and vice versa, with the result that the two phases will grow in separate regions along the direction of heat flow. If the eutectic point is such that the two phases are present in nearly equal amounts, as in the case for Al-Cu, alternating plates or lamellae of the two compositions form oriented along the direction of solidification. If the eutectic point is such that one phase is a small fraction of the total volume, it may solidify as isolated rods, plates, or spheres imbedded in a matrix of the predominant phase. Since the molecules must find their appropriate growth region by diffusion, the spacing between the alternating structures varies as the inverse square root of the growth rate.

Since the solidification of a eutectic is primarily a diffusion-controlled process, it should not be directly influenced by gravity. However, the orderly growth is often disrupted. The rods or lamellae are flawed by misalignments or discontinuities. The primary purpose of the two experiments involving directionally solidified eutectics was to investigate the influence of gravity driven convection on this process.

Experiment M566, Aluminum-Copper Eutectic

This experiment, developed by Earl Hasemeyer of the Marshall Space Flight Center, investigated the effect of gravity on the directional solidification of eutectics to determine if improvements in rod or lamellae continuity and structure could be obtained by reducing convective flow. The choice of Al-Cu was dictated by furnace capability and by the fact that this system has been extensively studied and is a well-known model system for eutectic solidification.

The samples were prepared by directional solidification on the ground, sheathed in graphite, and sealed in standard stainless steel cartridges. They were melted back in space and directionally solidified by lowering the temperature while maintaining a thermal gradient.

An inspection of the specimens after processing revealed that the diameter of each specimen solidified in space was reduced in the regrowth region, giving the specimen an hourglass shape. This effect was not observed in specimens processed on Earth under identical conditions. The reduced diameter was caused by the failure of the alloy to wet its graphite container. In the absence of gravity, surface tension was the predominant force in shaping the liquid mass, and the liquid withdrew from the container walls in a natural attempt to minimize its surface energy. This opens the possibility for surface tension driven convection which could have affected the solidification.

A comparison of the flight and ground control samples shows little if any differences in the microstructure (fig. 5.12), indicating that gravity-driven convection plays no significant role in the generation of faults and terminations of the lamellae, Unfortunately, there is no way of obtaining a time correlation between the observed faults and acceleration events on the Skylab to determine if the faults corresponded to gravity spikes or other events that could produce flow.

It should be mentioned that nearly perfect Al-Cu lamellae have been produced on Earth by the use of very precisely controlled growth conditions.

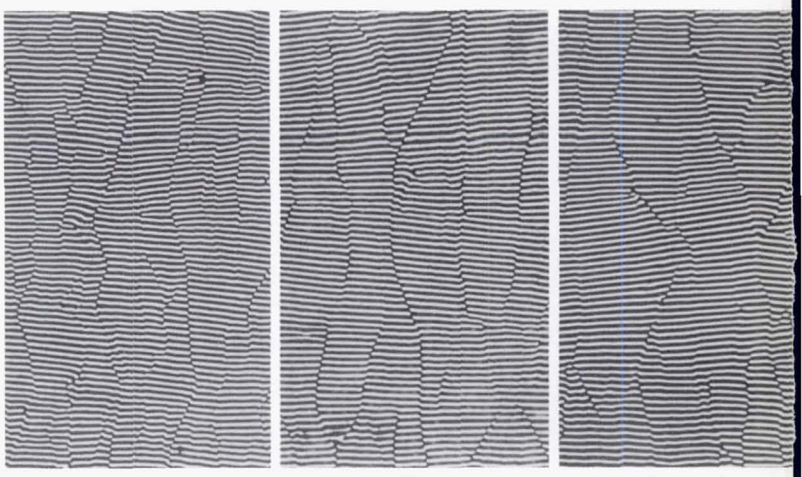

Figure 5.12. *Cross section of specimens of directionally solidified aluminum-copper eutectic showing internal faults.*

Experiment M554, Metal and Halide Eutectics

The second Skylab experiment dealing with directional solidification of a eutectic was developed by Alfred Yue of UCLA. In this experiment a eutectic salt composition was chosen that contained 79 percent NaCl and 21 percent NaF. With this composition NaF rods form in a NaCl matrix. The single crystal NaF has excellent transmission in the infrared, which provides a convenient means of evaluating the rod perfection. In addition, it was thought that such a material might have applications as an infrared waveguide if the fibers could be made continuous.

Cartridges of the same configuration as those for the Al-Cu eutectic experiment were used, and melting and freezing in space were accomplished in the same multipurpose furnace. Specimens were melted and then solidified in a temperature gradient on Skylab and under similar conditions on Earth.

A representative longitudinal section from a NaCl-NaF eutectic grown vertically is shown in figure 5.13. The NaF fibers are aligned parallel to the direction of growth but are discontinuous. In figure 5.14, a similar section cut from a specimen processed on Skylab is shown. This photograph was taken at a lower magnification to provide a more expansive field of view, and it appears that the NaF fibers are not only aligned but are also fairly continuous. A more convincing demonstration of the improved continuity of the space-grown fiber is a comparison of the optical properties (figs. 5.15 and 5.16).

It has been subsequently shown that continuous rods of NaF in a NaCl matrix could be grown on Earth by careful control of the growth process.

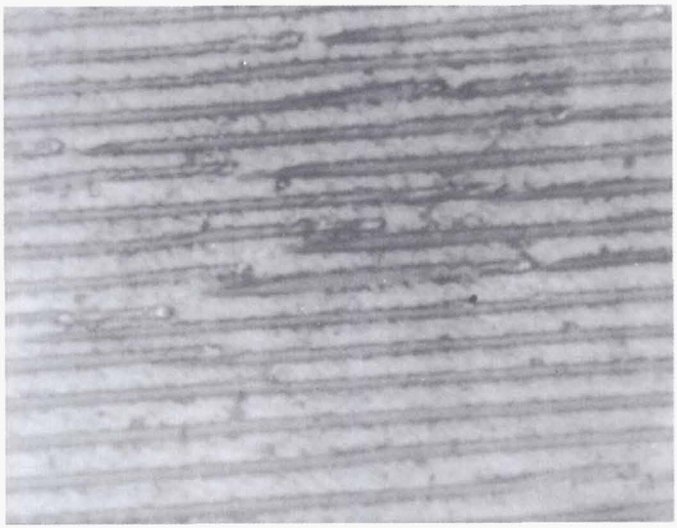

Figure 5.13. *Longitudinal section of specimen of NaCl-NaF eutectic directionally solidified on Earth showing discontinuous NaF fibers.*

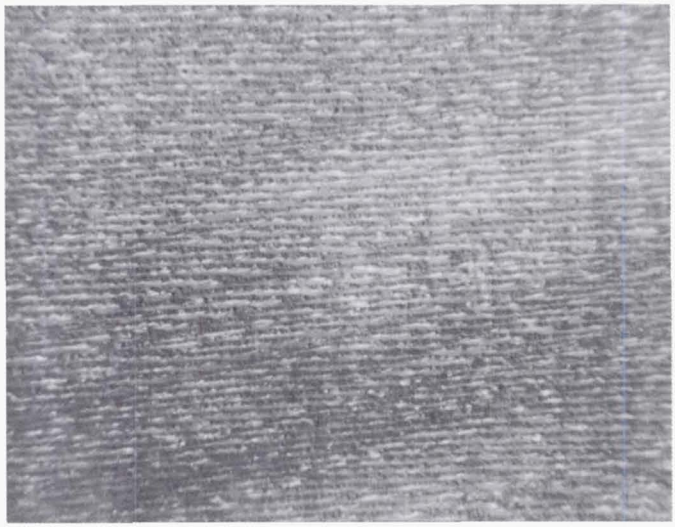

Figure 5.14. *Longitudinal section of specimen of NaCl-NaF eutectic directionally solidified in space showing continuous NaF fibers.*

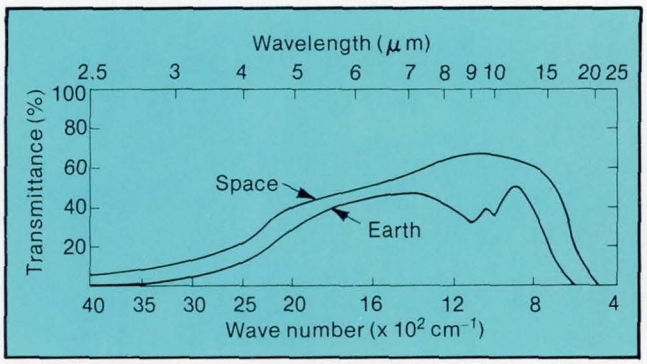

Figure 5.15. Infrared transmission curves for NaCl-NaF directionally solidified eutectic specimens.

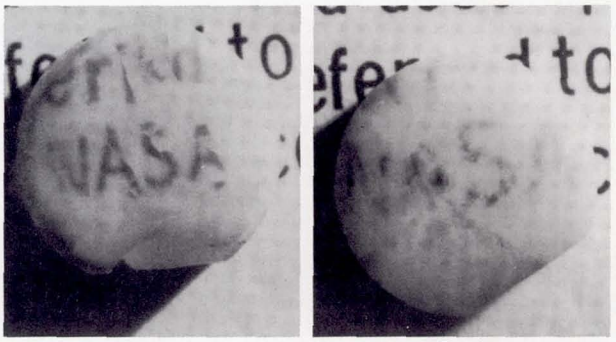

Figure 5.16. Comparative optical transparency of directionally solidified NaCl-NaF eutectic specimens.

CONTAINERLESS MELTING AND SOLIDIFICATION

One of the most unique opportunities afforded by space processing is the possibility of containerless melting and solidification. Although metallurgists have been conducting levitation melting and solidification experiments for many years using electromagnetic field forces for suspension, these experiments have produced very small globules of metal, only a few millimeters in diameter, which were solidified without the contaminating effects of a crucible or container. A great deal of energy must be expended to levitate even small masses of metal, and this limitation has essentially rendered levitation melting impractical for purposes other than research. Furthermore, the violent stirring produced and unwanted heating by the induced currents associated with the levitation process limit the ability to solidify materials in a containerless mode. These effects may also limit the amount of undercooling that can be achieved. The much smaller force required for positioning in space allows almost completely independent control of heating and virtually eliminates premature nucleation. This allows solidification to take place under the quiescent conditions required for undercooling and other phenomena to be investigated. The first step in this direction was taken with a containerless solidification on Skylab.

Experiment M553, Sphere Forming

As discussed in chapter 2, neither the acoustic nor the electromagnetic position system was far enough along in development to be considered for use on Skylab. An attempt was made to perform containerless solidification by melting drops on a pedestal, detaching them and letting them solidify while floating freely in a chamber. The float times were limited, and there was no control to prevent the particles from touching a wall before solidification occurred.

The containerless melting and solidification experiment was conducted by D. J. Larson of the Grumman Aerospace Corporation and E. A. Hasemeyer of the Marshall Space Flight Center. Its objective was to determine the effects of a low-gravity environment on the solidification of metals in the absence of a mold or container. Using the low gravity of space, castings of pure metals and alloys could be produced without the contamination that results from interactions with molds and containers. It was anticipated that supercooling (cooling below the normal freezing point without solidification) could occur because the freely floating molten metal would not be in contact with the container walls that provide many of the nucleation sites for the initiation of solidification. As a result, extremely fine-grained microstructures and uniformity of alloy constituent distribution could be attained.

The apparatus employed for the containerless solidification experiment was described in chapter 3. Two wheel assemblies were prepared with samples of pure nickel, nickel alloyed with 1 weight percent silver, nickel with 12 weight percent tin, and nickel with 30 weight percent copper. Specimens were approximately 6 mm in diameter after solidification. Nickel and nickel alloys were selected for the experiment because solidification theory for the face-centered cubic crystal structure exhibited by these materials is the most advanced.

None of the samples appears to have solidified completely before contact with a wall, as was evident by flat sur-

faces found on the samples. Also, there was no method for determining when solidification occurred or for estimating the degree of undercooling attained.

Typical in the Skylab-processed specimens were the three distinct regions of solidification shown in figure 5.17. One region, shown at the bottom of the figure, resulted from heterogeneous or localized nucleation at the pedestal base or at unmelted solid adjacent to the base, and solidification progressed upward. A second region appeared as a spherical cap at the top of the figure and resulted from homogeneous or general nucleation on the liquid surface. From this cap, solidification progressed laterally on the surface and radially inward. The third region was the last to solidify. This is the central portion of the sphere, where the surface is pocked with shrinkage porosity caused by the volume contraction associated with the relatively rapid transformation from liquid to solid of the major portion of metal in the sample.

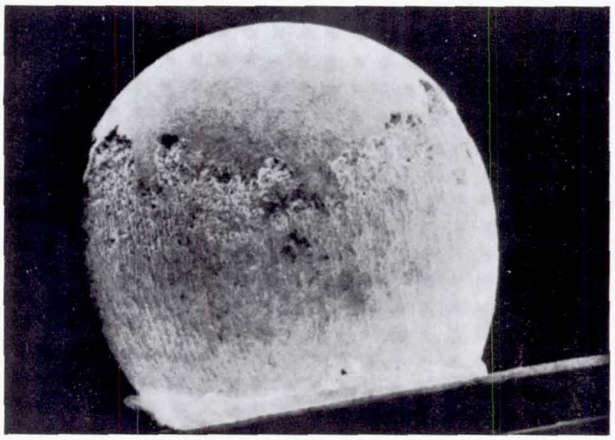

Figure 5.17. *Nickel-30% copper sample after melting and resolidification on Skylab.*

Chapter 6

THE BEHAVIOR OF FLUID IN LOW GRAVITY

Several experiments and a number of demonstrations were performed during the Skylab missions to elucidate the behavior of fluids in space. The purpose of these experiments was to confirm hypotheses on how systems would behave in a low-gravity environment, to determine to what extent residual accelerations and non-gravity-driven convection affected processes, and to provide graphic demonstrations of fluid behavior in space for classroom use and to stimulate new ideas for low-gravity research.

Two of the experiments, Zero-Gravity Flammability and Radioactive Tracer Diffusion, were selected prior to flight and influenced the design of the apparatus on Skylab. The other experiments were conceived during the Skylab mission as it became evident that the crew had time to perform additional experiments. The additional experiments were performed mostly with equipment found on board, although in some instances special apparatus was carried up by the replacement crew.

Experiment M479, Zero-Gravity Flammability

Of great concern in the design of a spacecraft is the flammability of the materials used in its construction. Extensive testing of the flammability of these materials had been done on the ground, but it was recognized that combustion processes would be quite different in a low-gravity environment where there is no convective flow to bring oxidants to the flame or to remove combustion products. This experiment, developed by J. H. Kimzey of the Johnson Space Center, was primarily devoted to verifying the adequacy of the procedures used to test the materials and to confirm theoretical expectations of flame behavior in a diffusion-controlled environment.

Although the experiment was not motivated by materials processing, the physics of this process is very similar to that of some of the materials experiments. Also, it is conceivable that combustion research in low gravity might be of value to study the role of other flow effects such as Marangoni or surface-driven convection in the combustion process. Such knowledge is required to develop accurate models of combustion which can be used to guide the development of more efficient combustion systems or to find more effective ways to control or prevent fires.

Thirty-seven experiments were conducted using six different materials. The primary objective was to note the extent of surface flame propagation and flashover to adjacent materials. All tests were performed in the work chamber of the Materials Processing Facility described in chapter 3. The atmosphere was 65 percent O_2 and 35 percent N_2 at 5 psia, just as in Skylab.

In a low-gravity environment, flames are completely different in appearance from those on Earth, as one might expect. Instead of the teardrop shape formed by the rapidly rising combustion products, a flame in low gravity is corona-like, surrounding the fuel, as depicted in figure 6.1. Since diffusion is the only process bringing in oxygen and removing exhaust products, burning rates are considerably slower, except for the case of thin, highly flammable material in which the flame spreads rapidly over the surface. Nonmelting materials, such as paper, tend to be self-extinguishing. Porous materials, such as polyurethane foam, are thoroughly impregnated with oxygen and tend to burn vigorously, as may be seen in figure 6.2. An interesting smoke pattern was noted when the fire burned itself out (fig. 6.3).

Figure 6.1. A comparison of fuel burning on Earth (1 g) and in zero gravity shows the impact of convection on a fire. On Earth, the hot gaseous products of combustion rise from the flame zone by the process of convection, allowing colder air to enter and mix with the fuel, creating a steady state condition. Without convection, a flame has a somewhat spherical corona that isolates the fuel from the surrounding atmosphere. As the oxygen is depleted, the flame quickly recedes and darkens. The condition depicted here is transitory.

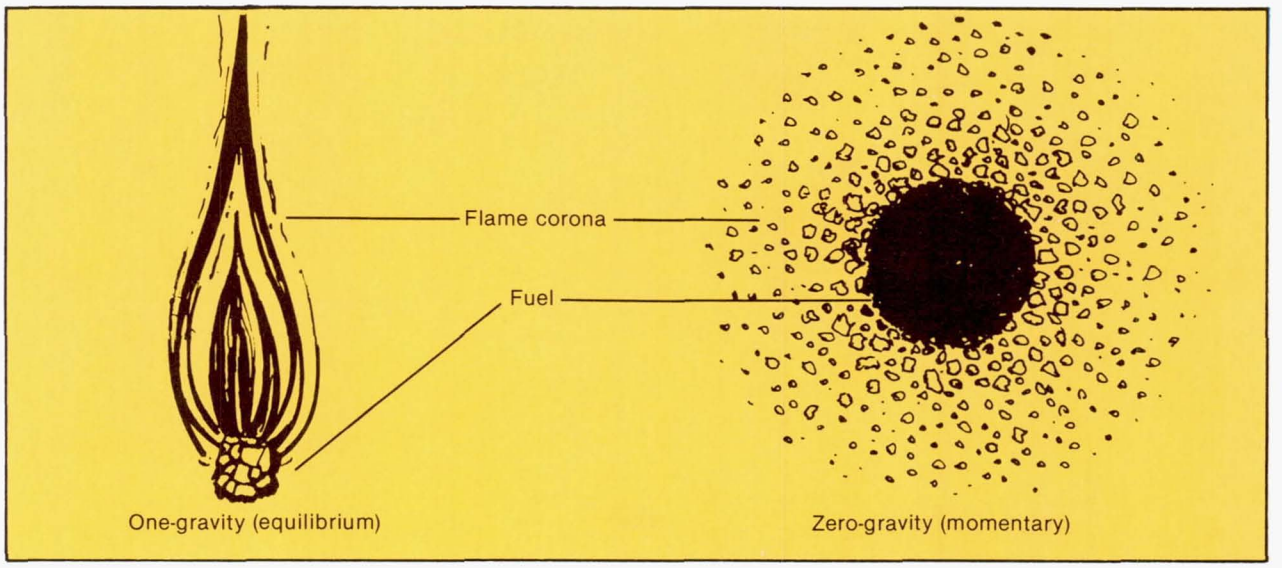

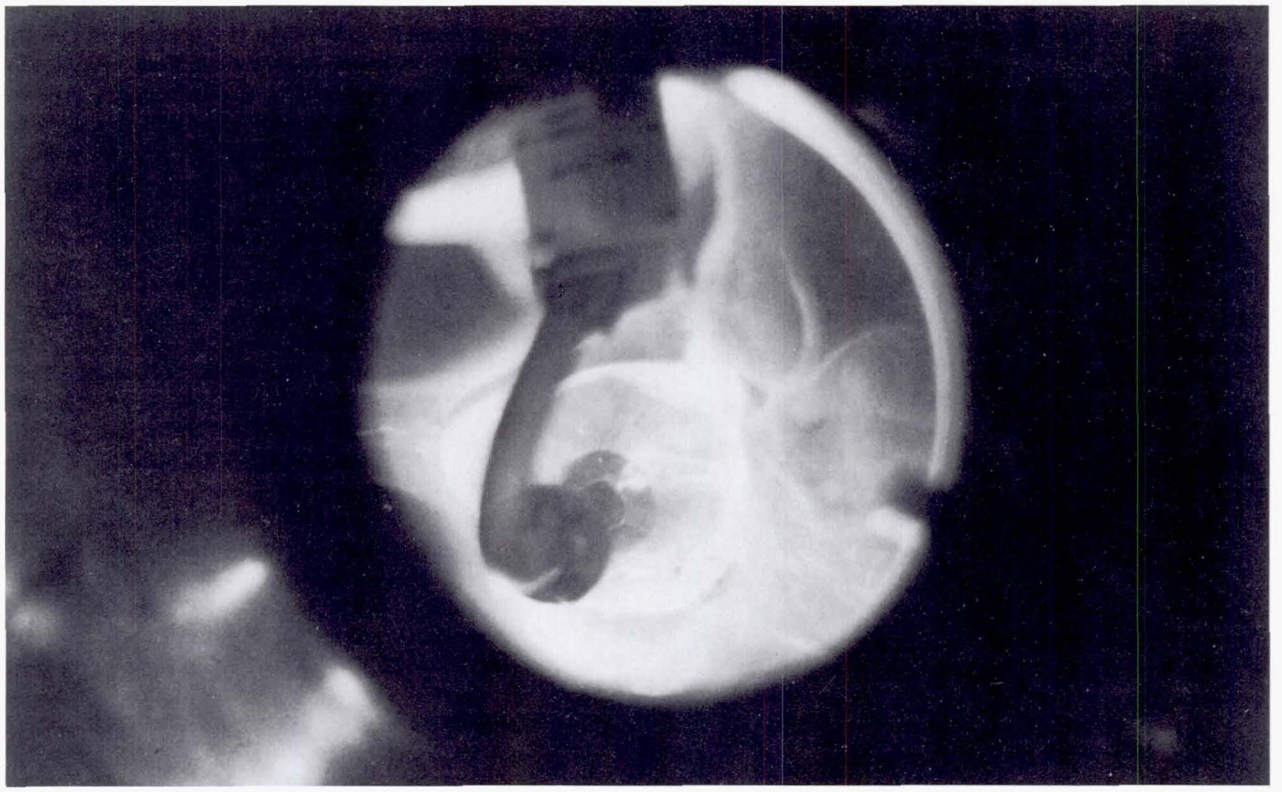

Figure 6.2. The burning of polyurethane in space. This photograph of burning polyurethane foam was taken through the Materials Processing Facility viewport by Commander Carr. Note the spherical shape of the flame. The material did not self-extinguish because oxygen was trapped in the cells of the foam.

Figure 6.3. *Zero-gravity smoke patterns. Smoke patterns are clearly discernible in this photograph taken by Commander Carr immediately after the flame shown in figure 6.2 was extinguished by fuel exhaustion. Notice the same pattern as that exhibited by the flame corona. Carr reported that the pattern persisted for a long period of time. Patterns such as this can be of value in studying Brownian movement of solids in gases under conditions of weightlessness.*

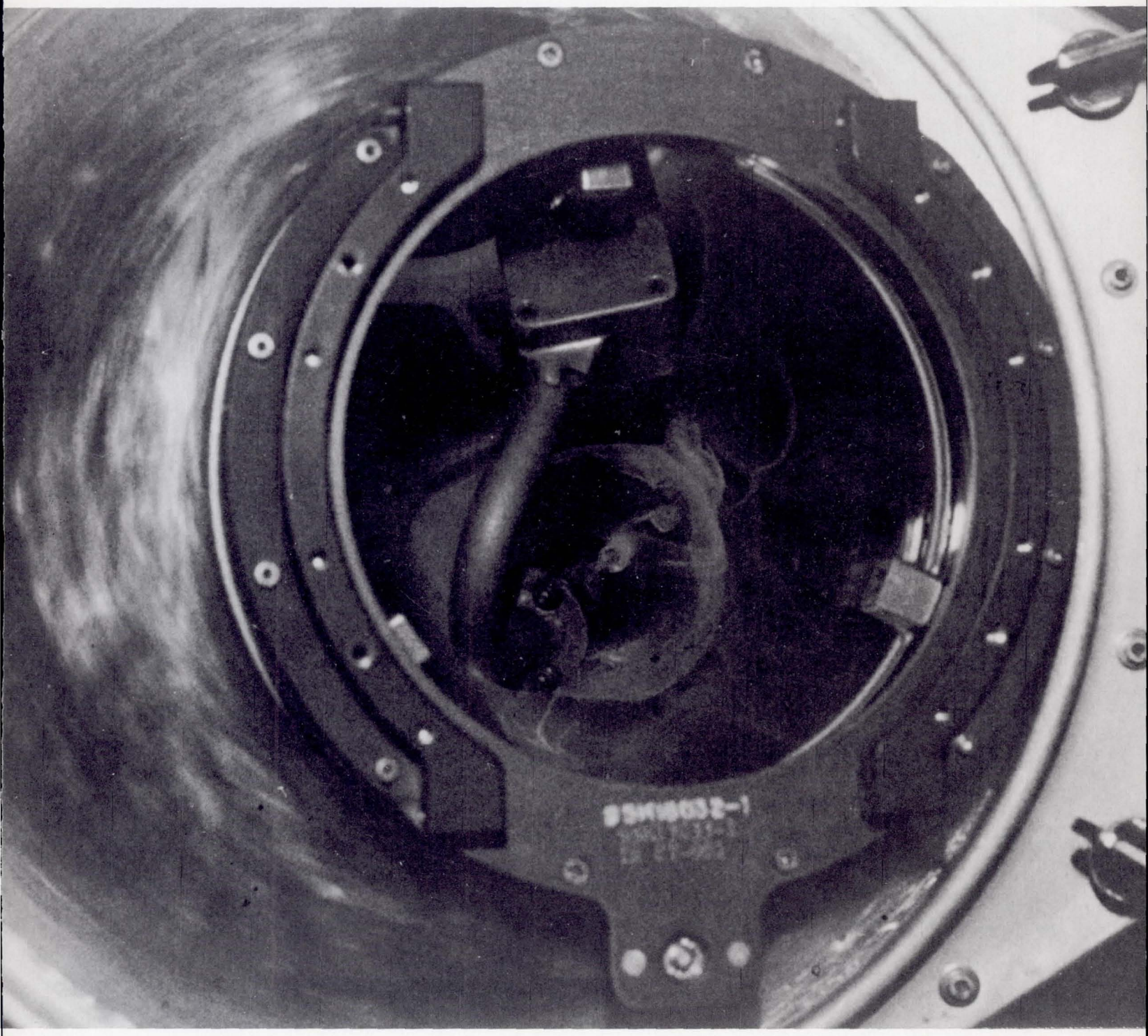

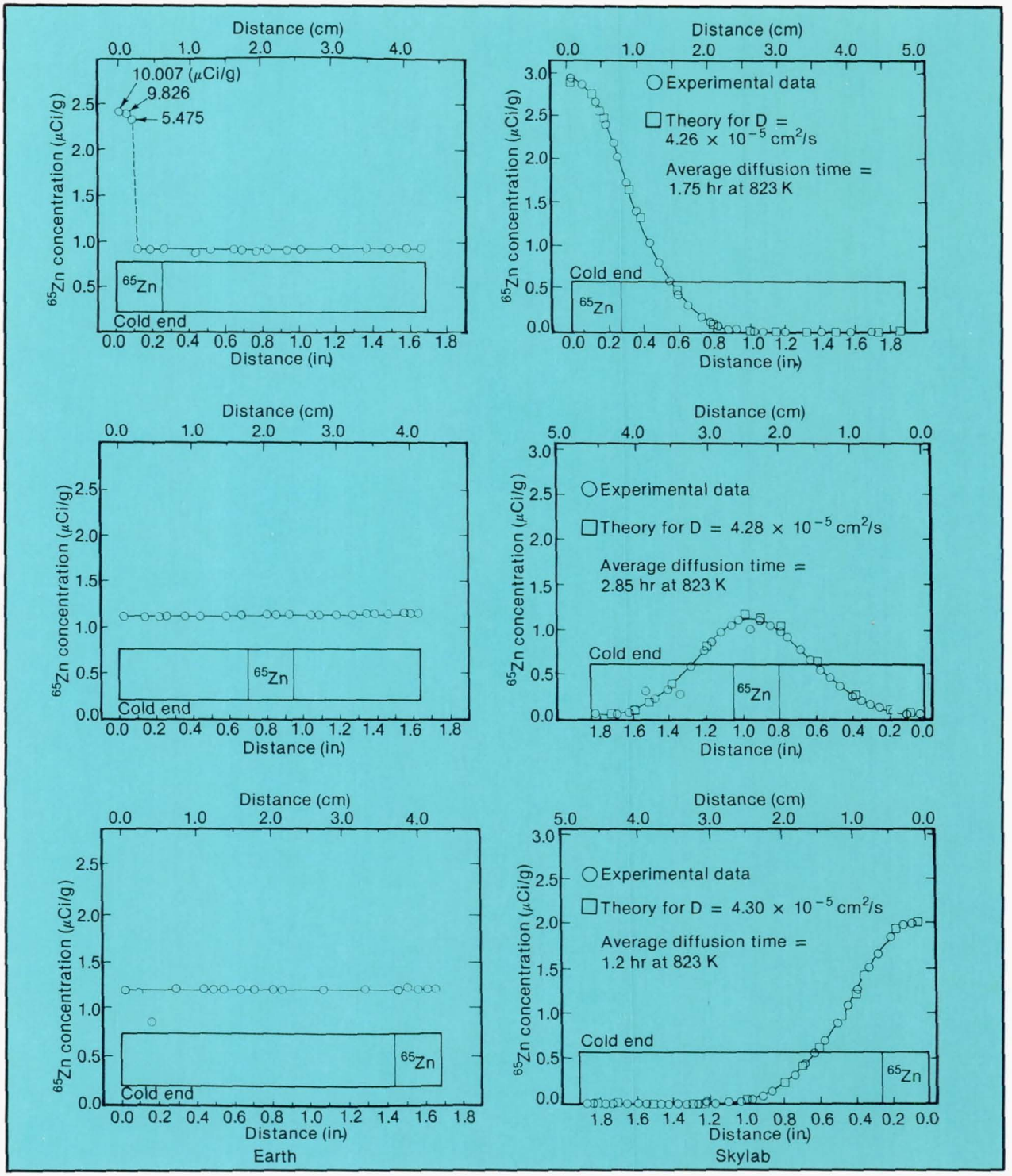

Figure 6.4. Results of Skylab's liquid zinc diffusion experiment. All samples were processed identically. The curves show the distribution of the radioactive zinc atoms after melting and resolidification. All Earth samples showed uniform distribution of ^{65}Zn caused by convection and diffusion in the melted metal (the upper left sample shows nonuniform distribution caused by incomplete melting of the sample). The Skylab samples indicate a ^{65}Zn distribution attributed to pure diffusion in excellent agreement with theoretical curves, allowing the determination of an average coefficient of diffusion of 4.28 x 10^{-5} cm^2/s.

Several methods of extinguishing fires were investigated. Simply evacuating the chamber is quite effective. However, the flow produced by such a process feeds fresh oxygen into the flame and causes it to burn more intensely until a sufficiently low pressure is reached such that combustion can no longer be sustained. Water is effective in extinguishing flames in low gravity provided its application is controlled and the quantity is adequate. Again, the disturbance caused by the application may produce a larger fire.

Experiment 558, Radioactive Tracer Diffusion

The purpose of this experiment, developed by A. O. Ukanawa of Howard University, was to measure the degree of mixing of a single-component molten metal in the spacecraft environment to see what effects, if any, could be attributed to residual accelerations. This represents the simplest possible system. There are no segregation effects due to compositional variations. The only mixing effects other than pure diffusion are thermal convection and flows associated with volume change. The first is gravity dependent; the latter is gravity independent.

This was accomplished by measuring the self-diffusion of zinc. A small pellet of radioactive ^{65}Zn was joined to a sample of ordinary zinc and soaked for 1 hour in a thermal gradient of 45° C/cm with a midpoint temperature of 550° C. The diffusion of the Zn tracer into the ordinary zinc was measured by standard radiographic techniques. The results are shown in figure 6.4. The curves are almost classic textbook examples of the solution of the one-dimensional, time-dependent diffusion equation (Fick's law).

There was evidence of a small flow of the original radioactive pellet that was normal to the direction of primary diffusion. This may have resulted from the shrinkage during solidification. Convective flows from the residual accelerations of the spacecraft appeared to be negligible. The self-diffusion coefficient for zinc required to fit the experimental data is 4.28×10^{-5} cm^2/s, which is slightly lower than the best accepted value measured by conventional techniques using capillary tubes.

The corresponding ground control sample was almost totally mixed after soaking for the same period as the flight sample. This indicates that gravity-driven convection produces about 50 times more transport than does pure diffusion.

Experiment TV101, Liquid Floating Zone

This experiment was designed and developed by John Carruthers of Bell Laboratories after Skylab was launched. With the help of Astronaut Gibson, sufficient equipment was found on board to perform a remarkably sophisticated study of the stability of liquid floating zones. The apparatus is shown in figure 6.5. It consists primarily of a pair of socket wrench extensions supported by four camera mounts to form a sort of lathe. Thin aluminum discs were fixed to the ends of the socket wrench extensions with double-coated masking tape to form the end caps for the floating zone. Water was used as the test liquid, and various amounts of soap and other additives were used to vary the surface tension and viscosity. The aluminum discs were coated with grey tape treated with acetone to reduce the contact angle of the water. The outer edges of the disc were coated with Krytox oil to prevent the water from wetting the entire disc. Rotation was provided by means of a twine wrapped around the wrench extensions. This is one of the most outstanding examples of resourcefulness in developing an experiment from scratch during a manned spaceflight.

As discussed in chapter 1, the floating zone technique is a method of processing materials that are extremely corrosive in the melt; it is used extensively to prepare high-quality silicon. There are some important advantages to performing floating zone crystal growth in a low-gravity environment. The absence of hydrostatic pressure removes some of the constraints on the size of floating zones that can be formed. Also, the process can be extended to materials that have insufficient surface tension to support a reasonable zone in 1 g. In addition, the absence of hydrostatic head may make possible extensive geometrical modifications of the zone to provide steeper gradients and more nearly planar interfaces between the melt and the growing crystal.

Liquid floating zones were first studied by Plateau in 1859 using neutrally buoyant immiscible liquids such as oil and a mixture of alcohol and water adjusted to have the same density as the oil. In a remarkable series of experiments Plateau found that the maximum stable length for a stationary zone was approximately 3 times the diameter of the zone.* Lord Rayleigh showed that the theoretical limit for stable length was equal to the circumference or π times the diameter. Since it is customary to rotate the floating zones to provide thermal symmetry in the system,

*Considering that Plateau was blind, these experiments are even more remarkable.

Carruthers had studied various rotational instabilities in such systems using the neutral buoyancy technique of Plateau (fig. 6.6). There is an inherent limitation in the use of such a system to simulate an actual liquid floating zone in zero gravity because of the existence of an outer layer of fluid surrounding the zone. This liquid influences the rotational and vibrational instability modes of the zone in ways that are difficult to predict.

For example, the ultimate rotation rate in the Plateau tank was limited by an axisymmetric instability in which the floating zone assumes an hourglass shape and pinches in at the center. However, the water zone in Skylab exhibited a totally different instability that apparently was not permitted in the Plateau tank. The zone deformed into a C shape and swung much like a jump rope (fig. 6.7). When a soap solution was added to increase the viscosity and lower the surface tension, the expected hourglass shape was observed (fig. 6.8).

It was also found that nonrotating zones could be stretched approximately 5 percent beyond the theoretical limit for stability predicted by Rayleigh. Beyond the stable length the zone is no longer cylindrical but assumes the shape of an unduloid (fig. 6.9), which apparently increases the stability.

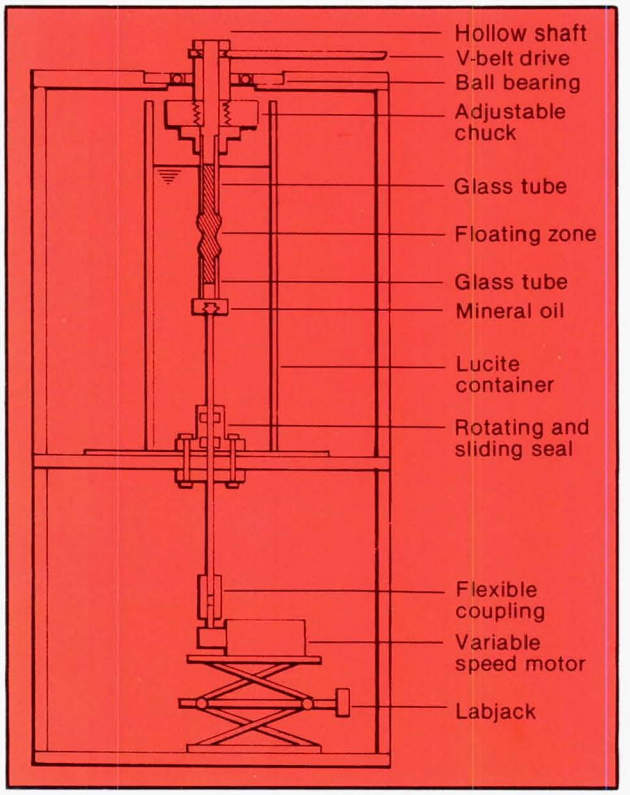

Figure 6.6. Plateau tank used to investigate the low-gravity behavior of liquid floating zones on the ground. The floating zone is a mixture of alcohol and water adjusted to have the same density as the mineral oil that is used to support the floating zone.

Figure 6.5. Schematic of the Skylab floating zone experiment assembled from available parts. Rotation was provided by slowly pulling the pinch bar. The tape marks on the socket wrench extensions provided reference marks to determine rotation rates from the TV images.

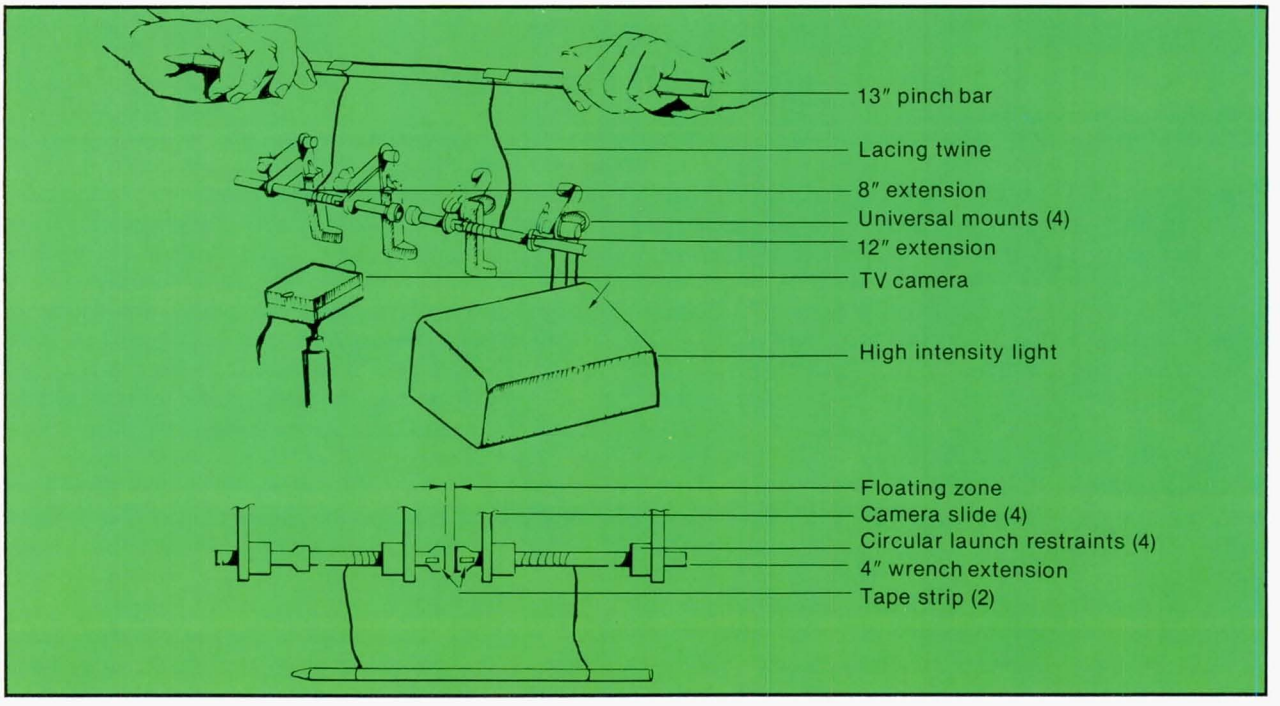

Figure 6.7. *Asymmetric instability discovered in Skylab liquid floating zone experiment. The rotation of water zones in the experiment produced a mode of instability never before observed. The water assumed a jump-rope shape much like the letter C being rotated about its ends. All Skylab tests with water assumed this mode of instability.*

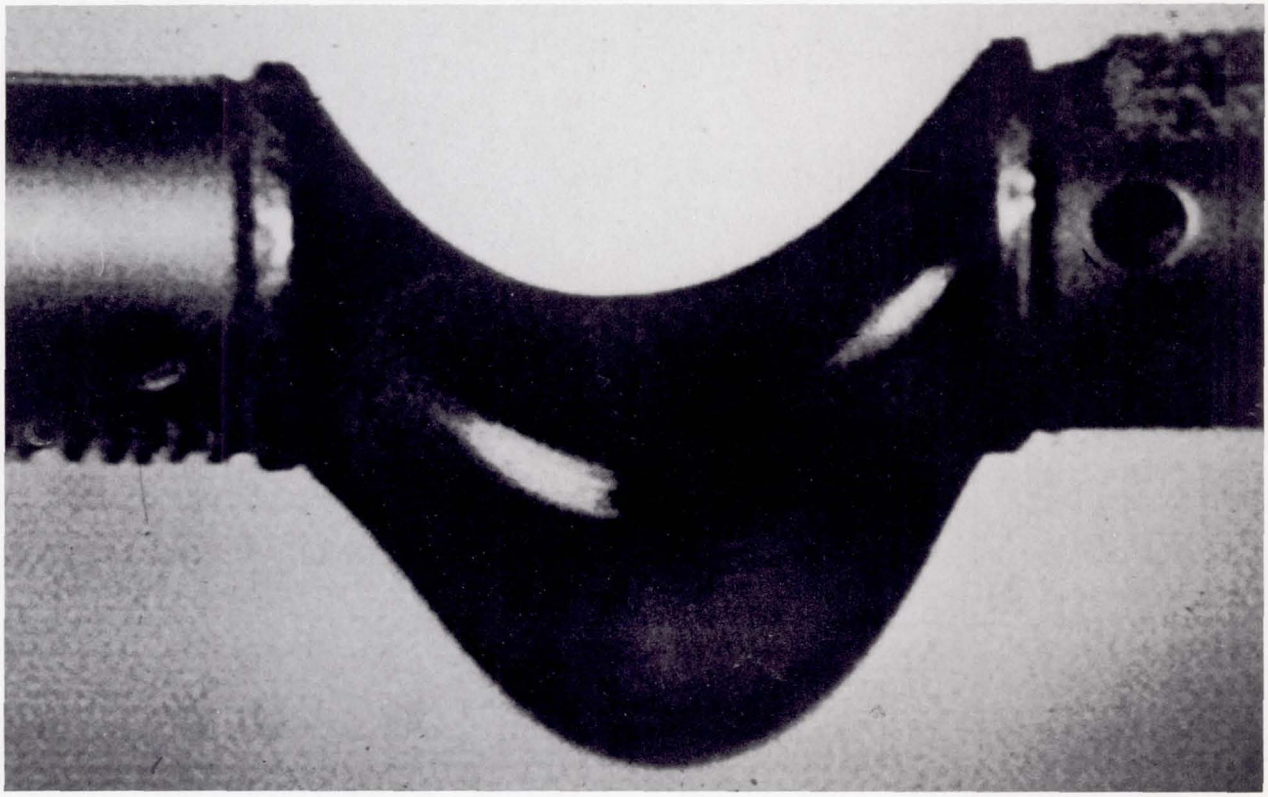

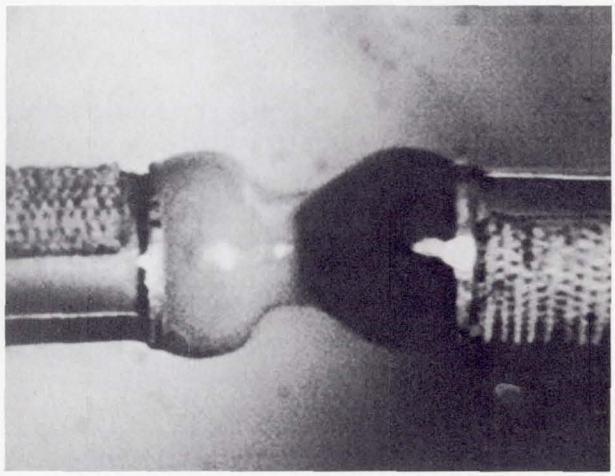

Figure 6.8. *The hourglass shape of rotating liquid zones. The expected axisymmetric mode of instability was observed in the liquid floating zone experiment when the rotating liquid—water—was replaced by a soap solution and air foam, thereby increasing the effective viscosity. This is the form of instability often observed in terrestrial Plateau simulations of floating zones.*

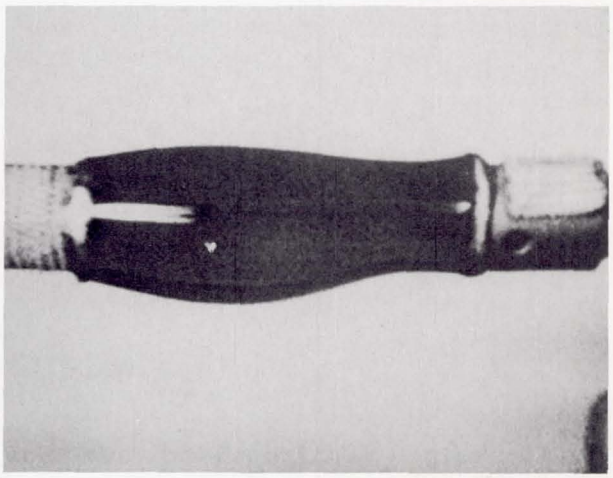

Figure 6.9. *Skylab's longest stable floating zone. Theoretically, the maximum length of a nonrotating liquid zone in zero gravity is equal to the circumference of the zone. For the zone tested, with a diameter of 22.2 mm, the maximum theoretical length is 69.8 mm. The maximum stable length observed during the Skylab liquid floating zone experiment was 73.7 mm, which was in excess of the theoretical limit. However, it can be seen that the shape is not one of a right circular cylinder, as predicted, but is distorted into a wave form.*

Experiment TV102, Immiscible Liquids

This experiment was developed by Lewis Lacy of the Marshall Space Flight Center and Guenther Otto of the University of Alabama, Huntsville. The object was to determine the stability of immiscible systems in low gravity. As discussed previously, immiscibility results when two liquids have limited mutual solubility. On an atomic scale this means that the attractive forces between like atoms (or ions) are sufficiently greater than the equivalent interaction between unlike atoms to overcome the tendency to become randomized. If such a mixture is disrupted by vigorous shaking, for example, inclusions of the minority fluid will spheroidize and begin to grow by coalescence. In 1 g, the droplets, after they have grown to a few micrometers, will rapidly settle out of solution because of their density differences. This usually happens so rapidly that unless means are taken to stabilize the emulsion (such as the use of a surfactant), it is difficult to study the growth and agglomeration processes. These processes are important in the formation of immiscible metal alloys, as discussed in chapter 5, as well as in many industrial chemical processes.

At first glance, it would appear that such a mixture would be quite stable in low gravity. The primary force causing agglomeration has been reduced by several orders of magnitude. However, it must be recognized that such a mixture is inherently unstable or, at best, metastable because of the large amount of interfacial energy associated with the greatly increased surface area provided by a fine emulsion. Clearly, the system would have a much lower energy if configured in two concentric spheres with the fluid having the lowest surface energy on the outside. The question is, how does the system go from the emulsified state to the stable configuration? How long does it take? What is the activation energy required?

The experiment apparatus consisted of three tubes containing mixtures of 25 percent, 50 percent, and 75 percent, respectively, Krytox oil and water (fig. 6.10). The black lines behind the vials were provided to aid in determining when the mixture had clarified. A brass nut was included in each vial to act as a shaker.

When the experiment was performed on the ground, a maximum of only 10 seconds was required to separate all the mixtures. The 75 percent oil mixture was the slowest because the viscosity of the oil slows the motion of the suspended water droplets. The mixtures remained

Figure 6.10A. *Krytox oil and water emulsion prepared on Earth. The dispersions obtained were highly unstable. The concentration of oil and water in the three vials was chosen such that in vial 1 water is the matrix, in vial 2 oil is the matrix, and in vial 3, with a volume ratio of 50 percent, water is again the matrix. At 0.7 seconds after the end of the mixing action, the dispersed oil had completely cleared from the water matrix in vials 1 and 3 because of the low viscosity of the water. Gravity-induced coalescence of the dispersed oil droplets had already occurred. In contrast, vial 2 did not yet show an appreciable amount of density segregation because of the relatively high viscosity of the oil matrix. After 3 seconds, the degree of separation by coalescence had progressed, whereas after 10 seconds, a complete separation of the two liquids was observed.*

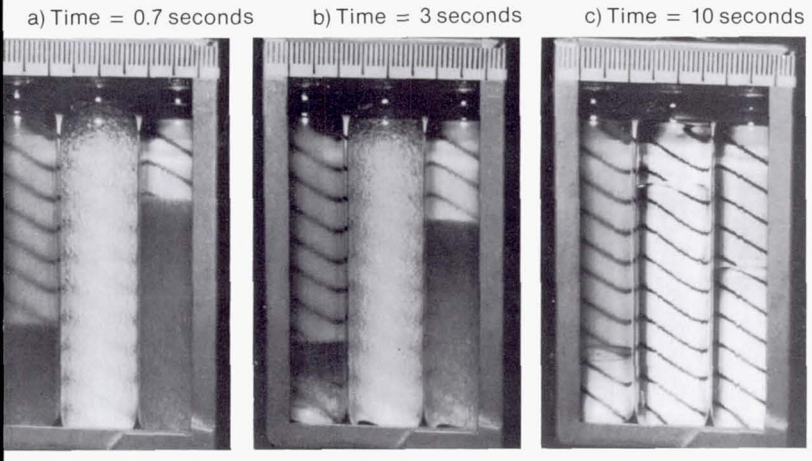

Figure 6.10B. *Emulsions after 4 minutes. The quality of the original color transparencies and video data is much better than can be reproduced here. The relative stability of the low-gravity and 1-gravity emulsions was determined by measuring the volume fraction of separation of the emulsions using the parallel background lines. As gravity-induced segregation separated the emulsions into clear oil and water, the background lines became visible in the pictures and could be counted.*

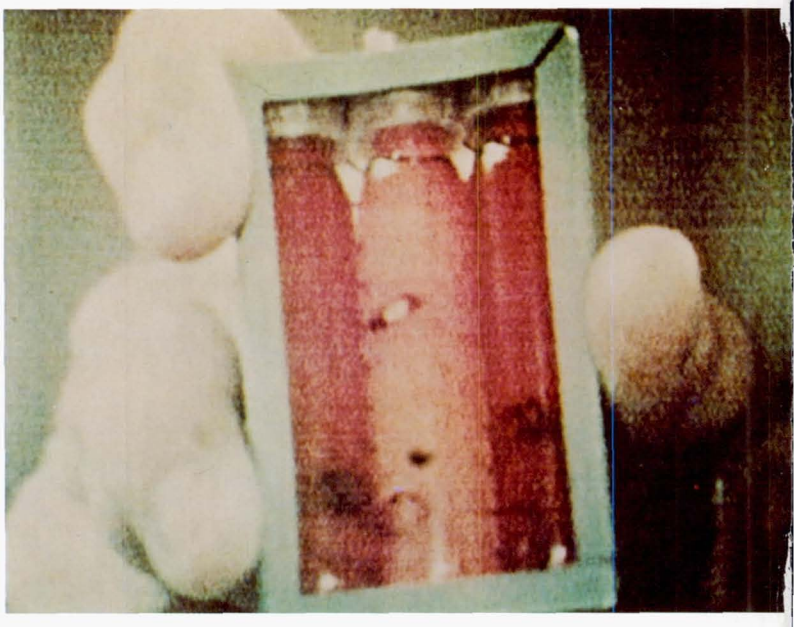

remarkably stable in space. After 10 hours (36 000 seconds) in the Skylab environment, no change could be detected (fig. 6.11). This is a little surprising since the gravity levels were estimated to be on the order of 10^{-3} to 10^{-4} g. Unfortunately, there were no accelerometer data available during the mission to correlate with the experiment. Apparently the g-jitter was not sufficient to cause agglomeration, and the fact that the gravity forces were random prevented the low-level accelerations from causing significant sedimentation or creaming. This is an important piece of information for planning future space experiments involving emulsions.

It should be pointed out that this experiment demonstrated the stability of an isothermal system. Additional destabilizing effects may occur in the presence of thermal gradients or from volume changes associated with solidification.

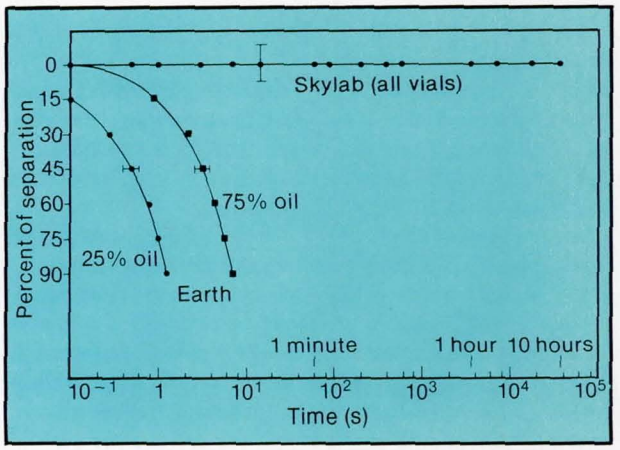

Figure 6.11. The volume fraction of separation of two oil-water emulsions in low gravity and 1 g as a function of time. The 25-percent oil mixture is more separated after 0.1 second on Earth than the same mixture is after 10 hours on Skylab.

Experiment TV103, Liquid Films

A simple demonstration of the behavior of liquid films in near weightlessness was suggested by Wesley Darbro of Marshall Space Flight Center. Simple two- and three-dimensional shapes were fashioned out of wire and used to support liquid films. In low gravity the films are much more stable because the liquid does not have the tendency to sag. It is possible to make films with plain water without a surfactant such as soap to lower the surface energy. Figure 6.12 shows some of the films obtained. Of particular interest is the minimum energy surface of the cubical structure.

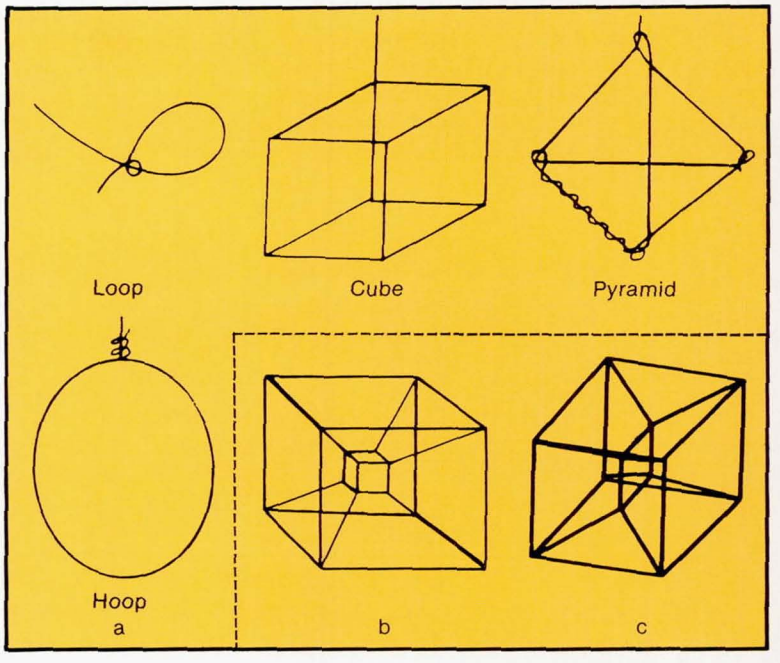

Figure 6.12. Behavior of liquid films in low gravity. A variety of shapes (a) were fashioned from scrap wire and used to investigate the behavior of liquid film in the absence of gravity. When the cubical frame was inserted in a soapy solution and withdrawn, a cube of water was extracted with it. As water was removed by gently shaking the frame, the remaining water formed a cube supported by 12 films (b). As still more water was shaken out, the cube became smaller until it flattened into a two-dimensional film resulting in the familiar shape seen in soap films in a cubical structure on the ground (c).

Experiment TV105, Rochelle Salt Growth

Crystals with water-soluble components can be grown from aqueous solution. The most common example of this technique is the growth of rock candy sugar crystals. However, many important technological crystals are also grown this way. I. Miyagawa of the University of Alabama suggested a simple carry-on experiment to determine how this process would work in low gravity.

On Earth, the solute is dissolved in an aqueous solution to an elevated temperature until the solution becomes saturated. A seed crystal is immersed in the solution, and

the system is cooled very slowly, usually by immersing it in a controlled temperature bath. The object is to keep the solution slightly supersaturated at the seed. Too much saturation results in many smaller crystals forming. Too little saturation results in the seed dissolving.

As the solute is incorporated into the growing crystal, the depleted solvent is usually lighter and rises as a convective plume, as seen in figure 1.6. This concentration-driven convection is important in removing the depleted solution from the growth interface and bringing in fresh nutrients. It is customary to stir the solution gently to help this process as well as to maintain temperature uniformity. Recall that in cooling the heat is being lost from the walls, and the fluid there will tend to be more supersaturated, which will promote the growth of many small crystallites unless the solution is gently stirred.

The situation can be expected to be quite different in low gravity. With no stirring, only diffusion acts to bring nutrients to the growing crystal. This is a limiting process, and the growth rates will be much slower than with convective stirring. This may be expected to alter the growth kinetics, which may change the growth habit or the shape of the crystal. Without mixing, the solution can be expected to be least saturated in the growth region of the crystal, hardly the optimum situation for growth. Small crystals will form elsewhere in the solution; however, equilibrium favors the growth of larger crystals at the expense of smaller crystals to minimize the total surface energy. This process is known as Ostwald ripening. As can be seen, solution growth in low gravity is not a simple process. The primary motive for the experiment was to gain some insight into the interplay of these effects.

The experiment was performed in a 4-inch-diameter food can with a transparent lid. Rochelle salt powder and a larger seed crystal were dissolved in the can while it was being heated on the food heating tray. After the seed was three-fourths melted, the heat was removed and the can was wrapped in towels to provide a slow cool-down.

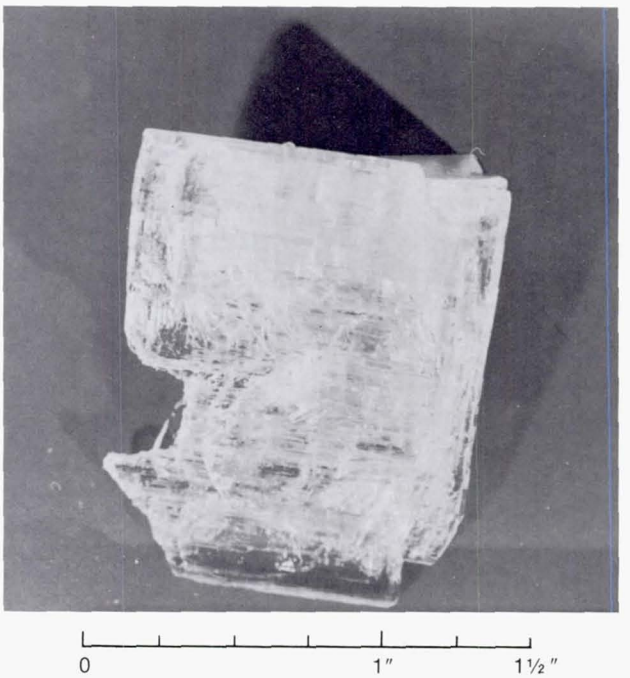

Figure 6.13. *Rochelle salt crystal grown on Skylab. The most unique features are the small diameter tubes that run along the crystal c-axis. Almost all the defects in the crystals returned are small diameter tubes elongated in this way. Such extremely small diameter-to-length ratios are rarely found for cavities in Earth-grown crystals.*

Many small crystals formed, giving the liquid a "slushy" appearance. The nucleated crystals were thin platelets, described as "mica-like." Compare these (fig. 6.13) with conventionally grown Rochelle salt. The seed had regrown into the form of a plate approximately 40 mm wide by 6 mm thick. An unusual feature is the presence of cavities, 0.1 mm diameter and up to 1 cm in length, that seem to run in the direction of the optical axis of the crystal. The cause of these cavities is not understood.

Experiment TV106, Deposition of Silver Crystals

A different type of crystal growth process was suggested by Philomena Grodzka of the Lockheed Missiles and Space Company. This experiment used a chemical reaction between $AgNO_3$ and a Cu wire in which the Cu ions combine with the NO_3, freeing the Ag, which deposits on the wire. The heat of reaction and the change in density can drive convective flows on the ground which influence the deposition of the Ag. Normally the depositing silver has the appearance of tree-like dendrites, as seen in figure 6.14. In low gravity, the reduction of such flows apparently promoted the growth of much longer dendrites, also shown in figure 6.14. In addition, the microstructure seems quite different; the space-grown material appears to be powdery, whereas the Earth-grown crystals appear to be smooth. The reason for this difference is not clear.

Figure 6.14. Silver crystals grown in Skylab compared with ones grown on Earth. The crystals were grown by immersing a notched copper wire in a silver nitrate solution. Silver replaced the copper at the notches. The space-grown crystals had been in the form of long filmy dendrites, which were so delicate that they broke off during handling and fell to the bottom of the vial.

Experiment TV107, Fluid Mechanics

A number of simple fluid experiments with liquid drops were videotaped by the Skylab IV crew. These experiments were suggested by O. Vaughan and Barbara Facemire of the Marshall Space Flight Center, Sid Bourgeois of Lockheed, and R. T. Frost of G. E. Valley Forge. The purpose was to provide graphic illustration of the unusual behavior of free droplets that can only be approximated in a Plateau-type experiment. It was also demonstrated that viscosity and surface tension could be measured nonintrusively by observing the frequency and damping of liquid droplets.

Perhaps the most dramatic of the demonstrations was the collision of two droplets, shown in the sequence of photographs in figure 6.15. Apart from the interesting shapes, it is quite remarkable to observe the lack of mixing taking place between the two fluids, despite the rather vigorous motion undergone by the undulating droplet after collision.

Figure 6.15. Impaction and coalescence of water drops. The drops had a volume of 30 cm^3, and they impacted at 3.4 cm/s. The red drop was colored with strawberry drink and the purple with grape drink. Despite the rather violent deformations in the drops, little mixing was observed.

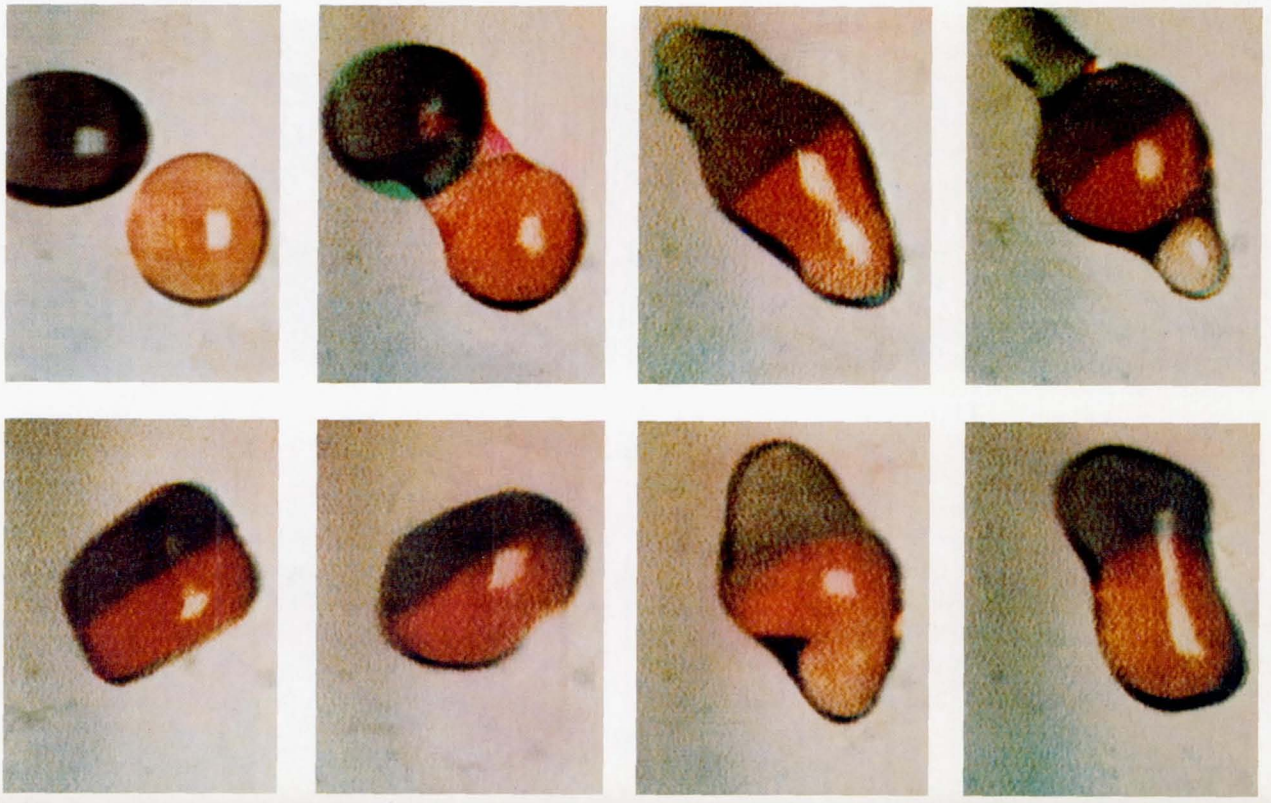

Experiment TV117, Charged Particle Mobility

As discussed in chapter 3, the continuous flow electrophoresis experiment originally planned for Skylab ran into technical difficulties that prevented its being included in the flight manifest. Instead, a simple demonstration unit was quickly developed by Milan Bier of the Veterans Administration Hospital, Tucson, Arizona, in conjunction with Robert Snyder of the Marshall Space Flight Center. The unit consisted of two static columns with manually operated gates to release the sample into the separation column (fig. 6.16). One column contained human red blood cells, which is somewhat of a standard to test the degree of sharpness of the resolution of the instrument. The other tube contained two proteins, ferritin and hemoglobin, to be separated.

The primary difference between Bier's device and the electrophoresis demonstrations flown on Apollo 14 and 16 was that Bier used a technique known as isotachophoresis. This technique differs from ordinary electrophoresis in that the sample is inserted between two buffers. The leading buffer's anions have greater electrophoretic mobility than the sample, and the trailing buffer's anions have less mobility. As voltage is applied, the various components tend to form sharp, distinct bands according to the mobility of the anions. These bands progress across the column with equal velocity, hence the name isotachophoresis. The primary advantage is that the interface is self-regulating; that is, any molecule that diffuses across the interface is automatically returned to the region corresponding to its mobility. Since the boundaries tend to be self-sharpening, diffusive mixing is inhibited and the resolution can be extremely high if convective mixing can somehow be suppressed.

The goal of the Skylab isotachophoresis experiment was to determine if the use of low gravity could alleviate the convective mixing and sedimentation problems inherent in the 1-g process to achieve protein separation comparable to gel techniques and to see if larger particles such as cells could be separated by this process.

The protein separation attempt failed. Apparently slight leaks developed during the launch and intervening activities, allowing a small amount of air to enter the system. An examination of the anode revealed that no current flowed, probably because the electrode was isolated by a gas bubble. Such a bubble would have floated away in the laboratory, which points out one of the difficulties in designing space experiments.

The tube with the red blood cells produced better results. The interface was shaped like a blunt parabola, possibly because of the competing effects of electro-osmosis and the self-sharpening feature of the isotachophoresis.

Figure 6.16. *Skylab charged particle mobility apparatus. The material in column 1 has progressed three-quarters of the distance in the tube. The material in column 2 did not move because an air bubble inadvertently leaked into the column and isolated the electrode.*

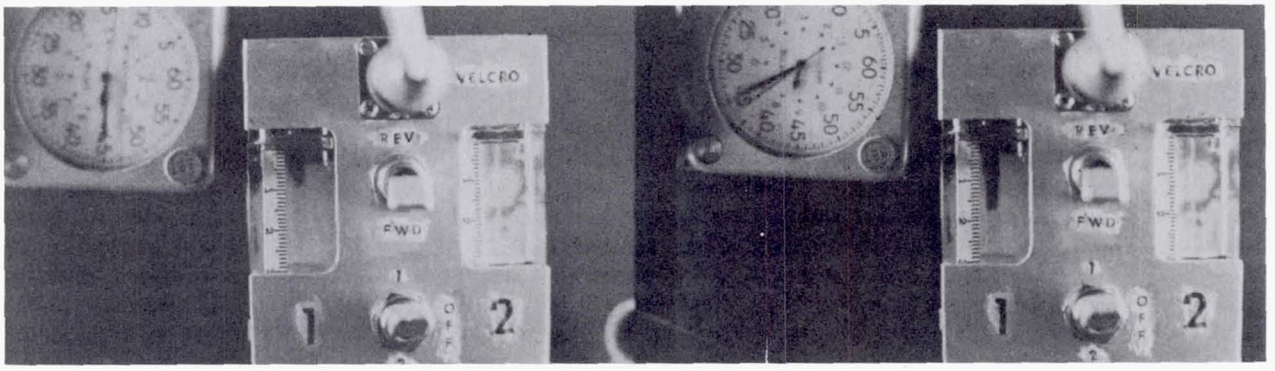

Diffusion in Liquids Demonstration

A very simple demonstration to dramatize the diffusive mixing of liquids in zero gravity was suggested by Barbara Facemire of the Marshall Space Flight Center. A plastic tube 12 cm long and 2 cm in diameter was filled with water from a syringe. A few drops of instant tea (about 7 times normal concentration) were carefully placed at one surface of the tube, which was periodically photographed over a period of 3 days. The tea in the center of the tube diffused in a distance of about 2 cm in 45 hours, illustrating how slow diffusive mixing tends to be. One unexpected effect was that the tea did not diffuse as rapidly along the wall, possibly because of some electrostatic repulsion between the wall and the molecules of tea.

Ice Melting Demonstration

Another simple dramatization of fluid behavior in low gravity was suggested by L. L. Lacy of the Marshall Space Flight Center and G. Otto of the University of Alabama. A cylinder of ice was frozen on a wand tipped with cotton in a pill dispenser bottle (fig. 6.17). The ice was removed from the bottle, and periodic photographs were made while it melted. With no force to make the water drip off the ice, all of the melt adhered to the ice, first forming an elliptical shape and later a spherical shape. Because of the insulating effect of the water and the lack of natural convective cooling, it took approximately 1 hour longer for the ice to melt on Skylab than in a similar experiment performed on the ground.

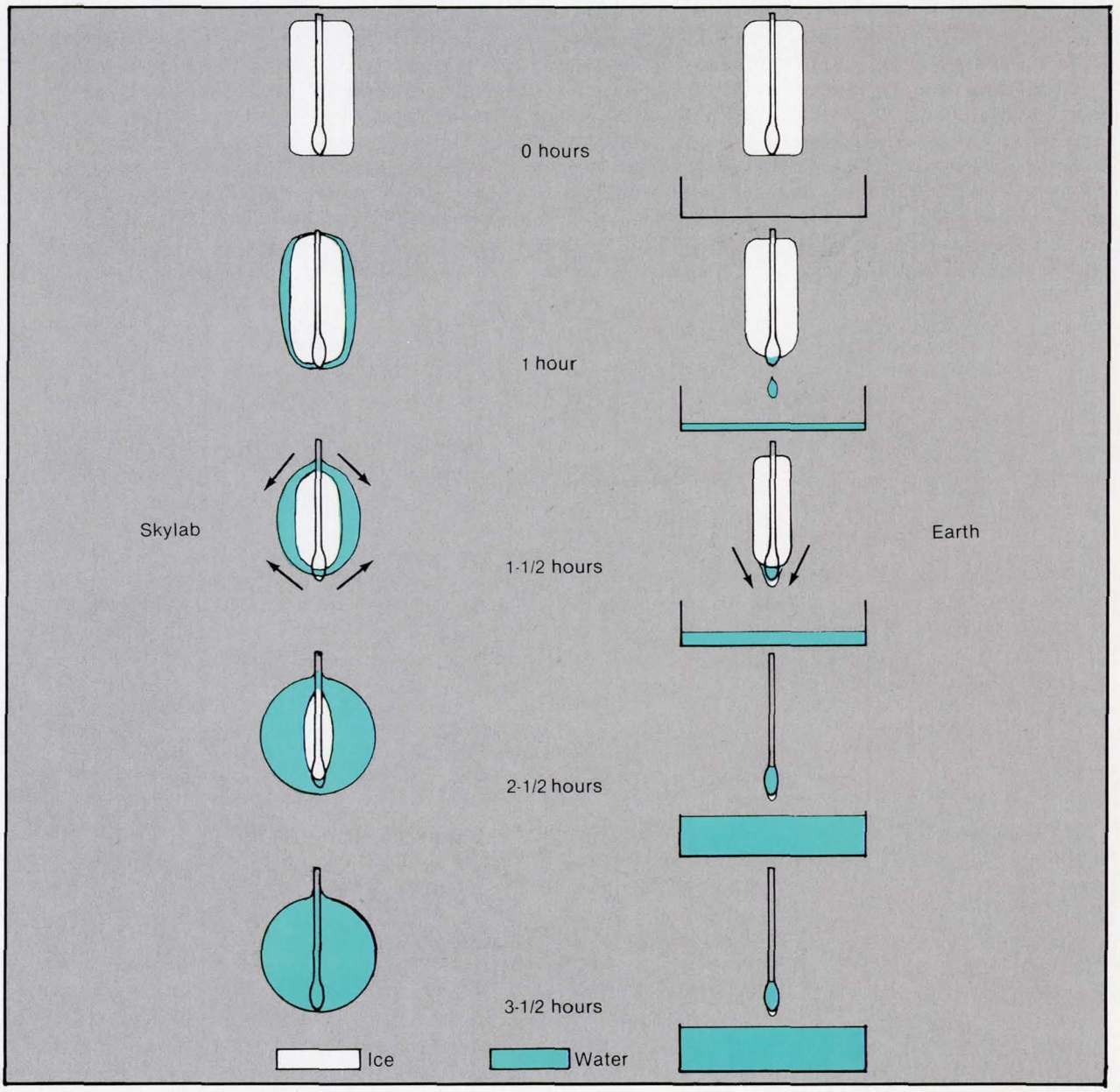

Figure 6.17. *Sketch of the observed phenomenons of ice melting on Skylab. The lack of gravity permitted the water to remain around the ice. Transfer on the ground results in more melting than in low gravity.*

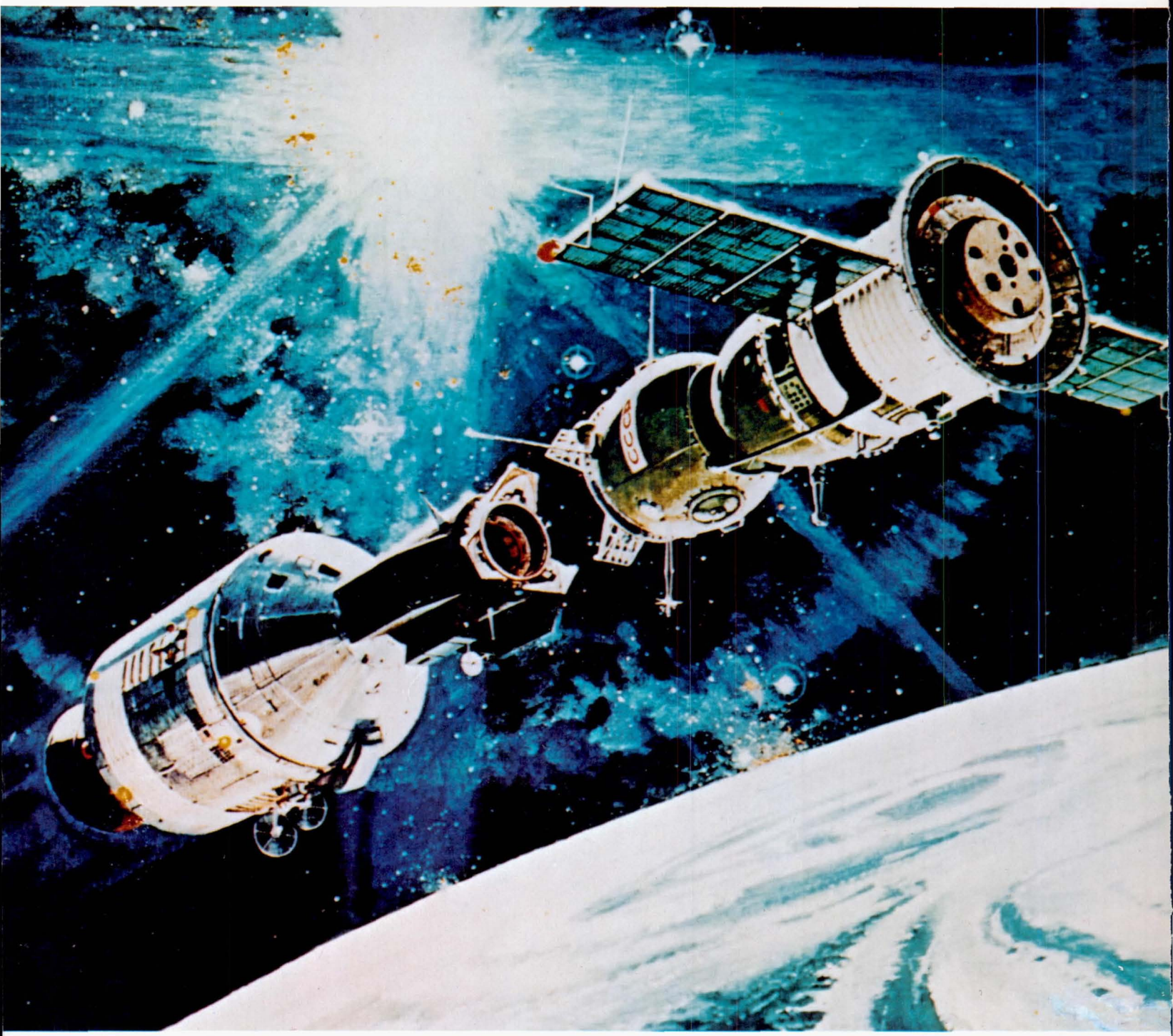

Figure 7.1. Apollo-Soyuz vehicle.

Chapter 7. POST-SKYLAB ACTIVITIES

APOLLO-SOYUZ TEST PROGRAM

Shortly after the Skylab mission was completed, a new manned flight opportunity arose: the joint U.S.-Soviet Apollo-Soyuz Test Project (ASTP). This 9-day mission took place in July 1975 and consisted of three American astronauts in a Saturn 1B-launched Apollo Command and Service Module that rendezvoused with a Soviet Soyuz spacecraft carrying two Russian cosmonauts (fig. 7.1). The time to develop experiments was short and the time and resources available for experiments during the mission were more restricted than on Skylab. Nevertheless, a number of materials science experiments were carried out. This opportunity allowed several investigators to confirm Skylab results and make additional tests of some of the phenomena observed previously. In addition, several experiments were attempted for the first time. A modification of the Skylab furnace was developed that had a maximum temperature of 1200° C, a programmed cool-down to give more uniform growth rates, and a helium quench system to shorten the time required to reach allowable touch temperature. The furnace is shown in figure 7.2. However, like the Skylab furnace, it had only one heated zone and therefore subjected the sample to a continuously changing gradient during cool-down.

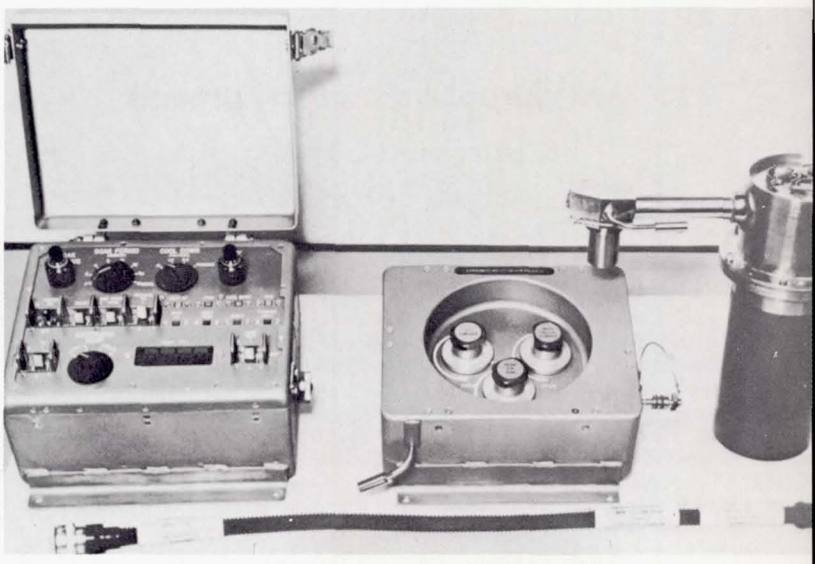

Figure 7.2. *Multipurpose Electric Furnace used in the Apollo-Soyuz Test Project.*

Experiment MA060, Interface Marking in Crystals

H. C. Gatos and A. F. Witt of the Massachusetts Institute of Technology conducted this experiment. It was similar to their Skylab experiment except that Ga-doped Ge was used instead of InSb. A new capability was introduced in the form of a current pulsing device that forced a short pulse of current through the sample every 4 seconds. The Peltier cooling at the solid-liquid interface produced an increase in growth rate over a microscopic scale. It was shown in chapter 4 that the incorporation of dopants is related to growth rate. Therefore, these pulses introduced microscopic striations

C-2

that could be observed by sectioning the crystal and using a differential etching process. The striations provide a convenient method of recording the position and shape of the interface as a function of time. This allows a direct measure of the growth rate of the crystal. With such data, details of the transient growth region before steady state growth is attained may be elucidated. Also, accurate values of the segregation coefficient K_0 (discussed in chapter 4) can be obtained.

In contrast to the Skylab experiment, uniform dopant distribution was not achieved after the initial growth transient in the ASTP experiment (fig. 7.3). Furthermore, it was found that the distribution of dopants varied depending on the distance from the axis of the crystal. It was determined through analysis of the interfacial markings that the ASTP furnace had an asymmetrical heat flow that did not provide flat solidification interfaces, probably because of thermal interactions between the three heating modules in the furnace. These asymmetries caused unequal growth rates, resulting in radial segregation. A similar situation probably occurred in the Skylab experiment but was not as pronounced because of the difference in segregation coefficients of the materials used and because the higher resolution of the measurements on the ASTP samples made small differences easier to detect.

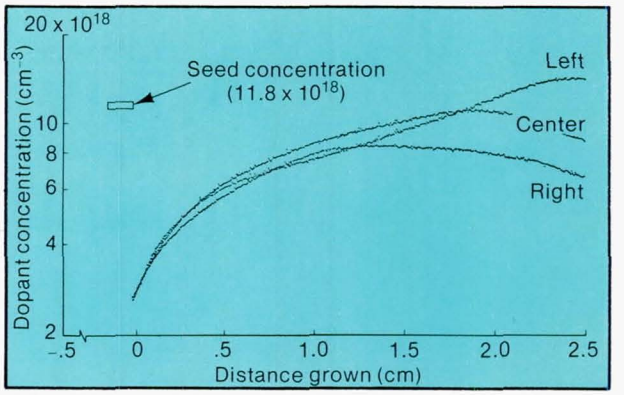

Figure 7.3. Longitudinal composition profiles of Ga-doped Ge crystals regrown in space. The three curves give the data obtained by scans performed on the left, center, and right of the investigated axial plane.

It was again found that the flight samples did not wet the quartz ampoule, but were supported by thin ridges just as the Skylab InSb samples. This was unexpected, since both of these materials wet the quartz in 1-g experiments.

Experiment MA085, Crystal Growth from the Vapor Phase

H. Wiedemeier repeated his Skylab vapor growth experiment using more complex systems: $GeSe_{0.99}Te_{0.01}$ with GeI_4 as the transport agent $GeS_{0.98}Se_{0.2}$ with $GeCl_4$ as the transport agent, and GeS with $GeCl_4$ and Ar. The Ar was added to vary the partial pressure of the transport agent independently of the total system pressure in an attempt to gain further insight into the anomalous transport rates observed in the Skylab experiment. The results were similar to those of the Skylab experiment. The transport rates in the flight samples were substantially larger than the values obtained by extrapolating the ground-based experiments at low pressures, where diffusion dominates, to the pressures used in the flight experiment (fig. 7.4). Again, the improvement in crystalline perfection and growth habit is sug-

Figure 7.4. Anomalous growth rates observed in the vapor growth experiment. The observed growth rate at low pressures at which the transport is dominated by diffusion in a 1-g field is extrapolated to higher pressures at which convective flow would begin to increase the transport rate. The solid squares represent the flight results. In the $GeSe_{0.99}Te_{0.01}$ system (left) the flight result is a factor of 2 lower than the observed convective transport in the ground control experiment and a factor of 3 higher than the expected value obtained by extrapolating one diffusion branch. In the $GeS_{0.98}Se_{0.02}$ system (right) the flight data were exactly the same as the convection-dominated ground-based results.

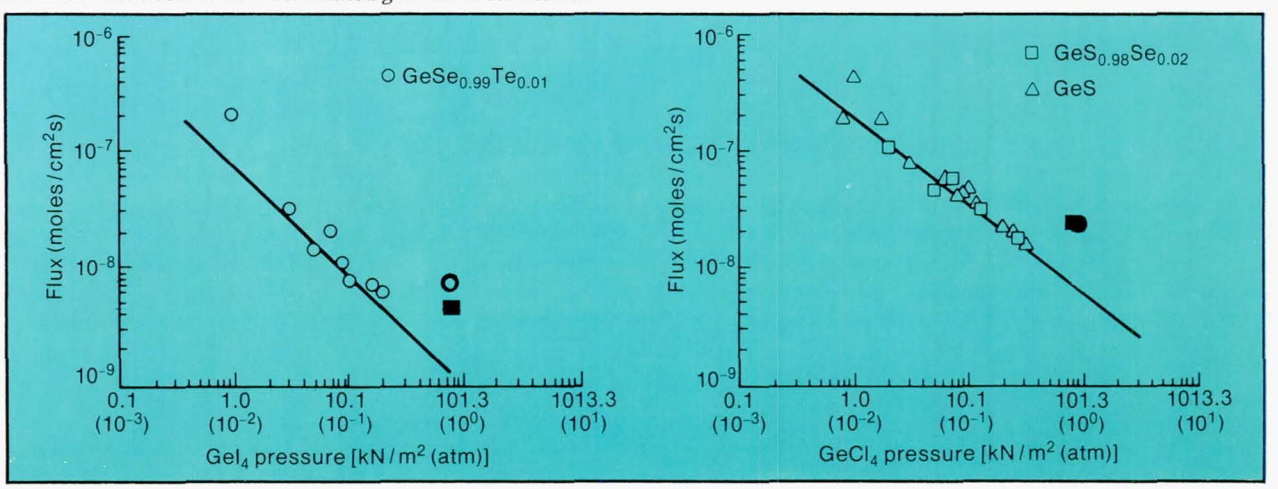

gestive of the quiescent conditions associated with diffusion-controlled transport.

Wiedemeier has suggested a thermochemically driven convective flow to explain the unusually high growth rates in the flight results. Apparently, chemical reactions take place in the transport gas throughout the tube. The heat of reaction causes localized pressure increases that drive the flow. As mentioned in chapter 4, an alternative possibility is the presence of a gravity-driven effect, such as Clusius-Dickel separation, that inhibits transport at low pressures.

In either case these unexpected results are of fundamental interest to the understanding of crystal growth by chemical vapor transport.

Experiment MA131, Halide Eutectic Growth

A. S. Yue repeated his Skylab experiment in which continuous fibers of alkali halide crystals were grown in a sodium-chloride matrix. In the ASTP experiment, however, he substituted lithium fluoride for sodium fluoride. Figure 7.5 shows the LiF fibers in the NaCl matrix. As before, the flight samples had better optical properties (transmission) than those on Earth, which is evidence that they are more continuous. Again, it should be noted that simple binary eutectic growth is diffusion controlled even in the Earth's gravitational field if reasonable precautions are taken to choose a convectively stable geometry and to maintain good control of temperature and growth velocity. This is because the diffusive processes are thought to take place in a layer that is much thinner than the boundary layer for convective flow under 1-g conditions.

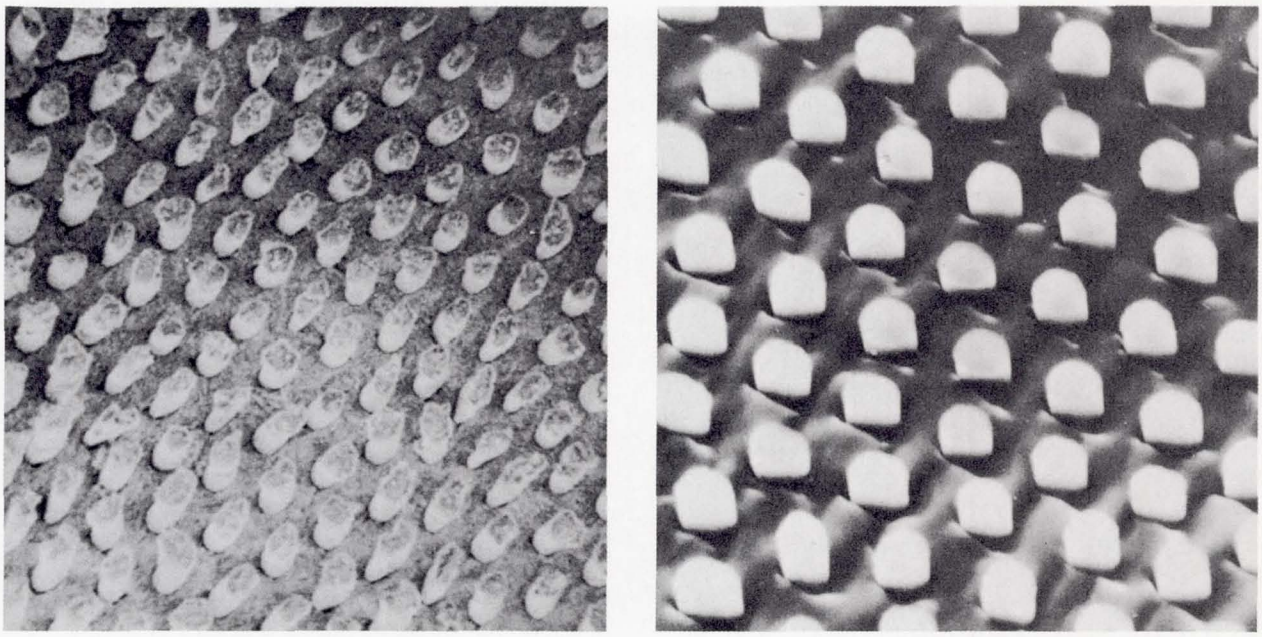

Earth-grown LiF fibers (1058x)

Space-grown LiF fibers (1900x)

Figure 7.5. Scanning electron microscope studies of lithium fluoride (LiF) fibers grown in a sodium chloride matrix.

Experiment MA070, Zero Gravity Processing of Magnets

This experiment, developed by D. J. Larson of the Grumman Aerospace Corporation, involves the directional solidification of another eutectic system, Bi/MnBi. In this system, MnBi rods grow in the matrix of Bi. Since MnBi is a magnetic material, one of the objectives was to see if directional solidification in low gravity produced any change in the microstructure that might alter the magnetic properties.

A surprising result was obtained. Not only were the MnBi rods in the flight sample finer and more regularly spaced, but their low-temperature coercive strength

(magnetic field required to demagnetize) was among the highest that had ever been measured. In fact, the strongest magnets at the Francis Bilter National Magnet Laboratory were required to perform the demagnetization tests.

Some previous work on the MnBi system had suggested the existence of a low-temperature, high-coercive phase. The unusual results from the ASTP experiment prompted additional research of this system. This work confirmed the existence of this high-coercive phase and discovered a previously unknown ordering effect that exhibits even higher coercivity at the extremely high demagnetizing fields.

It is still not completely clear why the flight sample had a different microstructure and higher coercivity than the ground control sample that was processed in a similar manner, but an interesting picture is beginning to emerge. The MnBi / Bi is a faceted / nonfaceted eutectic system whose growth may be more influenced by gravity than is that of eutectic systems discussed previously. However, additional research revealed an error in the published phase diagram for the MnBi / Bi system. The flight samples contained 97.8 atomic percent Bi and 2.2 atomic percent Mn, which was thought to be the eutectic composition. When this was checked, it was found that the eutectic composition was actually 2.6 atomic percent Bi and 97.4 atomic percent Mn. Thus the samples had an "off-eutectic" composition.

The solidification of an off-eutectic is very much influenced by gravity. Instead of simultaneously solidifying the two solid phases, as would be the case with a eutectic composition, an off-eutectic composition will initially solidify into one solid and reject a liquid phase rich in the other component. In a low-gravity environment, a diffusion layer will rapidly build up until the eutectic composition is reached at the growth interface. Once this occurs, both the α and β phases will solidify, but the relative amount of the two phases will be controlled by the composition of the melt entering the diffusion layer. Since the composition used in the ASTP flight experiment contained more Bi than required for the eutectic mixture, the result would be finer MnBi rods than would be obtained from the eutectic composition. The enhanced magnetic performance is undoubtedly related to the microstructure. Possibly the finer rod diameter may approach the optimum size for elongated single domains which allows the theoretical coercive strength to be approached.

The ground control sample, on the other hand, would undergo some convective mixing because of radial gradients. This will vary the composition of the mixture entering the diffusion layer, resulting in a rod diameter that varies with distance until it approaches the normal eutectic value.

Another factor that enhanced the magnetic performance of the samples grown in the ASTP furnace is that the gradient freeze method subjects the solidified material to a much longer high-temperature soak than does the conventional Stockbarger technique. This heat treatment has been found to promote the formation of the normal magnetic phase which exhibits high coercivity at ambient temperatures.

In retrospect, the dramatic increase in magnetic performance of the space-processed samples may be regarded as a lucky accident. However, the research prompted by this surprising result has added significantly to our understanding of this system. Even higher coercive strengths have been obtained in carefully controlled experiments on the ground using this knowledge. Furthermore, the ability to control solidification of off-eutectic compositions adds a new dimension to processing such systems. By using different growth rates it may be possible to choose off-eutectic compositions that can provide a near optimum diameter of the MnBi rods while producing many more such rods. Since all the magnetic contributions come from the MnBi and Mn is only 0.71 percent by weight of the eutectic composition, it would be highly desirable to increase the percentage of the magnetic composition for any practical application of this system.

Experiment MA044, Monotectic and Syntectic Alloys

This experiment, developed by L. L. Lacy of the Marshall Space Flight Center and C. Y. Ang of the Aerospace Corporation, attempted to utilize the low-gravity environment to prevent density separation during solidification of two alloys, Pb-Zn and Al-Sb.

The Pb-Zn is an immiscible system similar to those studied by Reger on Skylab (see chapter 5). The material was soaked for 2 hours at 40 K above its published consolute temperature to homogenize it and was then solidified in low gravity. Almost complete separation was observed between the Pb and Zn, although there are some dispersed Pb particles in the Zn and some Zn particles in the Pb (fig. 7.6). It is not clear whether this separation resulted from incomplete mixing or whether there are nongravity-dependent flows that tend to cause unmixing in the two-phase region. There is evidence based on the profile of Pb dissolved in the Zn and vice versa that the diffusion coefficient may have been much lower than expected because the system was close to the consolute temperature and proper mixing was never achieved. Later ground-based experiments were conducted to check the published value of the consolute temperature, which was found to be 20 K too low. This confirmed that the sample had been soaked above the consolute temperature, although the soak times were

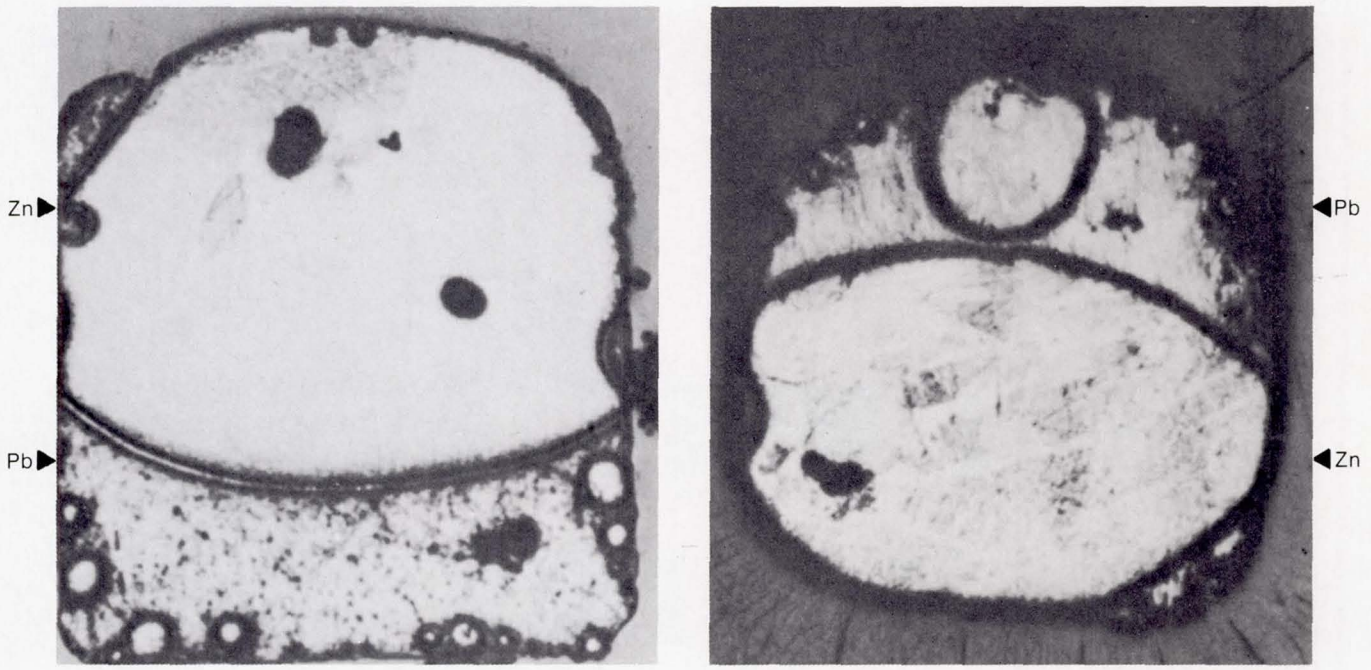

Figure 7.6. Photomacrographs of Pb-Zn flight and GBT ingots. The Pb-rich and Zn-rich portions of the GBT ingots are reversed because of sedimentation.

marginal to achieve mixing. Therefore, it could not be determined whether nongravitational flows or other effects produced massive separation of the phases during solidification or whether the sample was simply not homogenized.

It was suspected by some investigators that the Al-Sb system may have a small miscibility gap near the melting point. This suspicion arose because there was some uncertainty in the melting point and because it was difficult to prepare homogeneous Al-Sb from the melt. A system that forms a compound by a reaction from two immiscible liquid phases is termed a syntectic. Hence the original motivation for the experiment was similar to that for the other experiments with immiscible systems, that is, the prevention of phase separation between the two liquids of different densities before the compound was formed by the syntectic reaction.

The samples were prepared, paying close attention to maintaining chemical stoichiometry, that is, exactly 50 atomic percent Al, 50 atomic percent Sb. The samples were soaked at 50° C above the melting point (1080° C) for 1 hour and cooled isothermally. The comparison between the space-processed samples, the ground control samples, and prototype samples (best available commercial material) is shown in figure 7.7. It may be seen that the Earth-processed samples contain regions that are Al-rich or Sb-rich, in addition to the stoichiometric compound AlSb. The space-processed sample is virtually all AlSb.

More recent refinements of the melting point data for AlSb place it at 1080° C, which means that the system is not syntectic but instead melts congruently, as may be seen from the phase diagram in figure 7.8. One wonders how an improvement in homogeneity could result from processing in low gravity. In principle it should be possible to start with a 50-50 atomic percent melt and solidify along the compound line.

One possible explanation is that the local deviations from stoichiometry exist in the melt, either because of inadequate mixing or because of statistical fluctuations. Such a local departure from stoichiometry will reject either Al-rich or Sb-rich molten liquids as they solidify. Diffusion will tend to equilibrate such regions, but because of density differences of the constituents, buoyancy effects will cause the Al-rich regions to rise and the Sb-rich regions to settle. This separation prevents complete homogenization of the solid and should result in more Al-rich regions at the top of the sample and Sb-rich regions at the bottom. Indeed this is the case, as may be seen in figure 7.9. In low gravity, of course, this buoyancy-driven separation does not occur, and fluctuations in the melt are homogenized by diffusion.

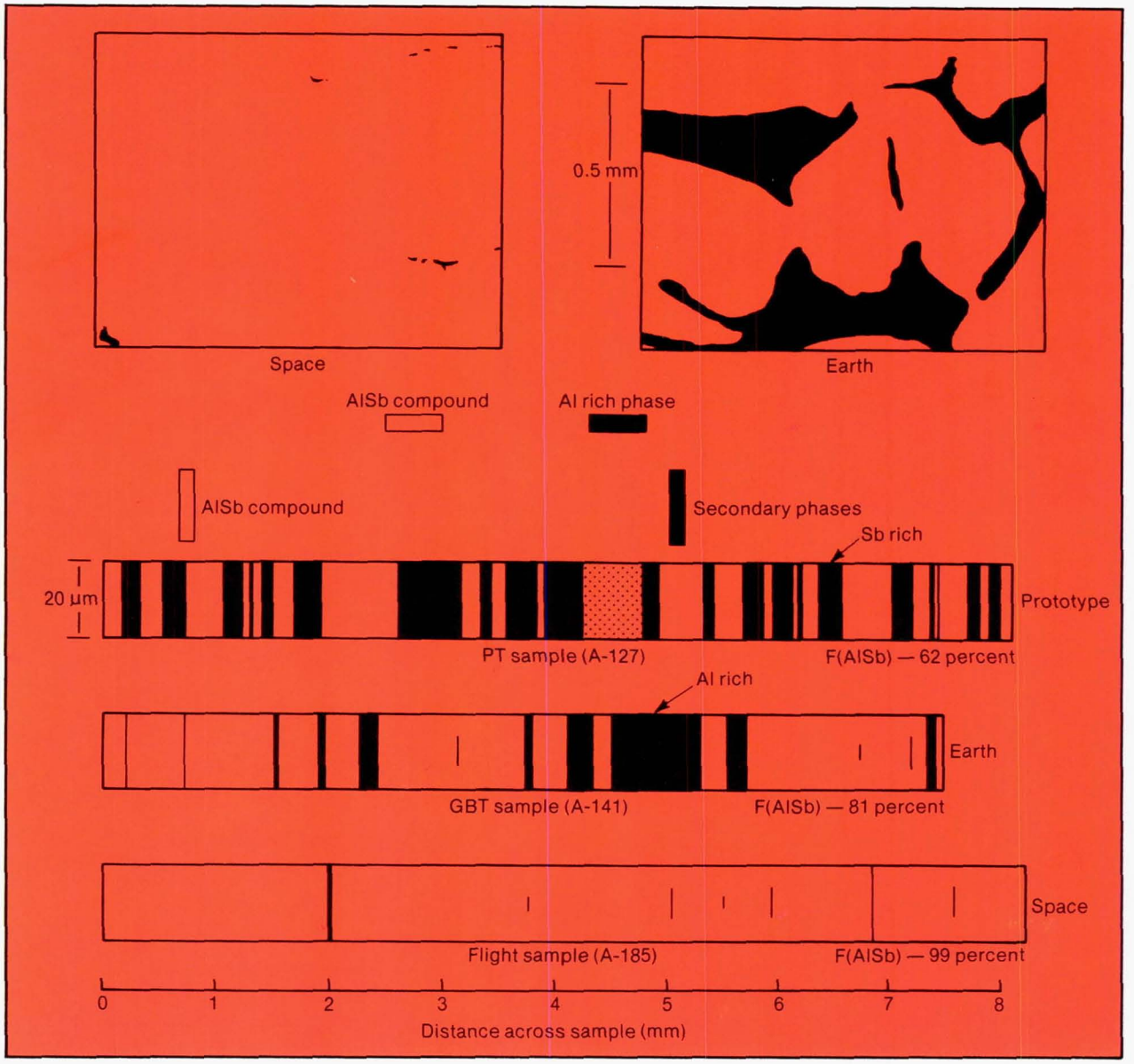

Figure 7.7. Distribution of AlSb compound throughout the samples. The top shows a typical cross section of space sample (left) compared with an Earth control sample (right) processed under identical conditions except for the gravity. The bottom shows comparisons between 20- µm scans taken across a prototype sample (top) that represents commercially available AlSb, the ground-based test sample (middle), and the flight sample (bottom). It is apparent that low-gravity processing results in the formation of considerably more of the desired AlSb compound and much less of the secondary phases than either the Earth control sample or the prototype sample.

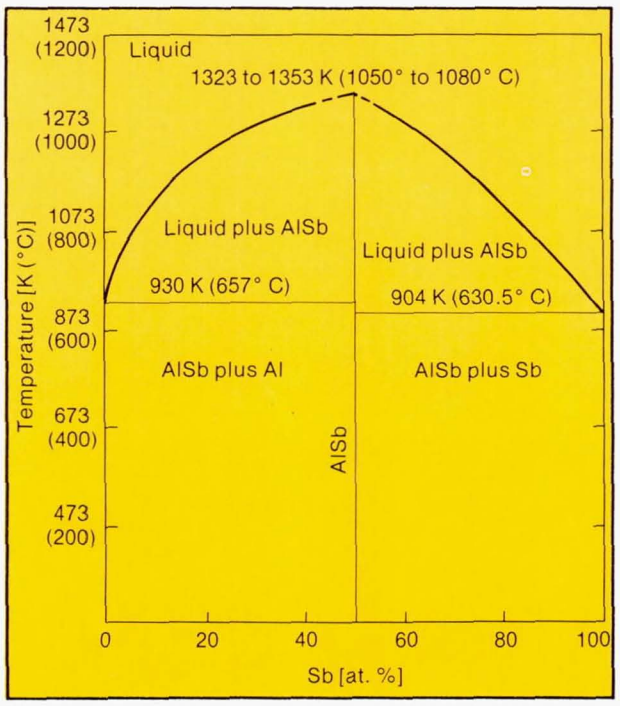

Figure 7.8. Phase diagram for AlSb.

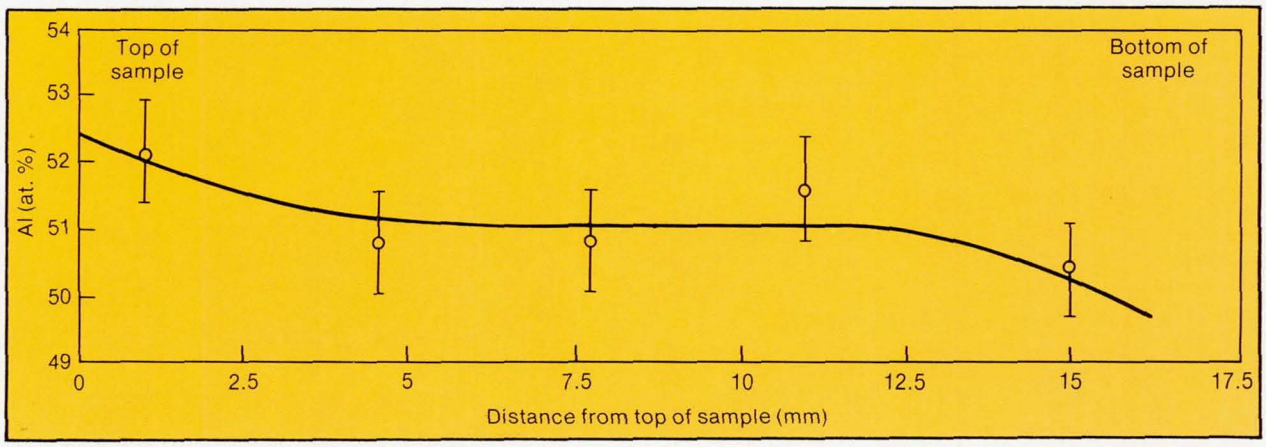

Figure 7.9. Aluminum content in the ground control AlSb sample based on atomic absorption spectroscopy.

Experiment MA041, Surface Tension Induced Convection

This experiment, like the experiment described in chapter 5, was devoted to understanding nongravitational fluid flow. R. E. Reed of the Oak Ridge National Laboratories led a team of investigators to evaluate the effects of surface tension driven flow (Marangoni convection) resulting from composition gradients, as opposed to the surface tension driven flow resulting from thermal gradients investigated by Bannister on Apollo 14 and 16 (see chapter 3).

The sample consisted of a Pb-Au alloy pressure bonded to a Pb sample. The samples were melted and solidified in the isothermal region of the ASTP furnace. A total of six samples were used, three in the hot zone (923 K) and three in an intermediate zone (723 K), to investigate diffusion at two different temperatures. Of the three samples in each zone, two were in graphite crucibles that the Pb did not wet and the other was in a steel crucible that the Pb did wet. The two graphite crucibles were oriented in opposite directions to determine if there were any effects from the small gradient present during solidification.

The ground control samples are shown in figure 7.10. The distribution of Au is shown by neutron activation that converts 197 Au to 198 Au which undergoes beta decay. A

Basic color scheme relating pseudocolors to Au concentrations.

Pseudocolor	*Au concentration (at. p/m)*	*Percentage of original Au concentration*
Black	0 to 5	0 to 1.0
Yellow	6 to 10	1.2 to 2.0
Blue-green	11 to 20	2.2 to 4.0
Red	21 to 40	4.2 to 8.0
Green	41 to 80	8.2 to 16.0
Purple	81 to 120	16.2 to 24.0
Dark blue	121 to 160	24.2 to 32.0
Orange	161 to 254	32.2 to 50.8

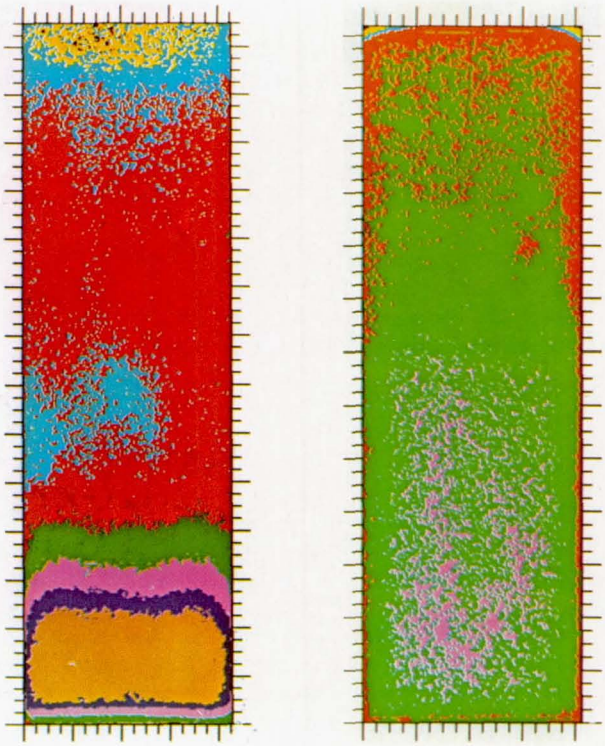

Figure 7.10. *Distribution of Au in Pb samples after thermal soak at 723 K on the ground. The sample on the left had the heavier Au on the top whereas the sample on the right had the Au on the bottom. It can be seen that the unstable (top heavy) configuration results in almost complete mixing, whereas mixing is somewhat suppressed in the stable (bottom heavy) configuration. However, it is important to note that some convective mixing does occur even in the stable configuration.*

photographic film placed over a cross section of the sample is exposed by the electrons from the 198 Au, and the density of the exposure is a measure of the concentration of the Au. This is dramatically illustrated by the pseudocolor photograph.

The effect of a convectively stable system compared to an unstable configuration can be readily seen by comparing the sample in which the heavier Au was on bottom with the sample in which it was on top. However, even in the configuration in which the system was in a completely stable configuration (both thermally and concentration) there was considerable mixing in contrast to the flight samples shown in figure 7.11.

Inspection of the flight results shows a significant difference in the diffusion of the Au in the samples that were held at different temperatures, as would be expected. There were slight differences in the samples, depending on the direction of solidification. This is probably caused by segregation effects at the interface. The curved concentration contours were interpreted by the investigators as evidence of surface tension driven flow due to the difference in surface tension between the Pb-Au and Pb for a free surface. These unbalanced forces can give rise to flows for free surfaces, but such flows are not expected for liquids contacting a solid surface. Apparently, in the absence of hydrostatic pressure, the nonwetting fluid does not remain in contact with the ampoule walls, and solutal concentration gradients produce flows at free surfaces.

The samples placed in the steel containers that were supposed to be wetted by the melt did not wet in low gravity. The distribution of Au in these samples was almost identical to that in the samples contained in graphite.

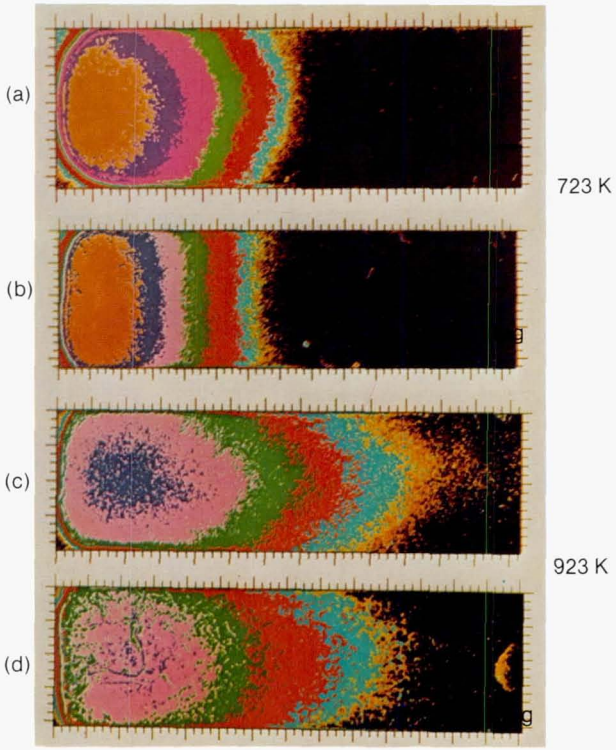

Figure 7.11. Distribution of Au in flight specimens. The top pair (a and b) were soaked at 723 K, and the bottom pair (c and d) were soaked 923 K. As would be expected, this produced considerably more diffusion. In all cases the Au-rich alloy was at the left-hand side of the sample. In (a) and (c) the direction of melting was from the left to right, whereas in (b) and (d) melting proceeded from right to left. This seems to have had a slight effect on the amount of diffusion and on the curvature of the diffusion regions.

Experiment MA028, Crystal Growth

This experiment, proposed by M.D. Lind of the Rockwell Science Center, was another attempt at growing crystals from aqueous solution in a low gravity environment. It was similar to the demonstration experiment described in chapter 6, except that the crystal is grown from the precipitation of a more or less insoluble product of a chemical process in which two or more reactants are allowed to interdiffuse in a region of pure solvent. This would normally be accomplished on Earth by separating the two reactants with a gel, preventing convective mixing while allowing diffusive flows (fig. 7.12). The gel, however, introduces certain disadvantages such as excessive nucleation that results in small crystal sizes, contamination of the crystal by gel constituents, and perturbation of the natural growth habit.

Lind's experiment can best be described as a gel-less gel growth in which the low gravity environment is used to suppress the uncontrolled convective mixing. The apparatus

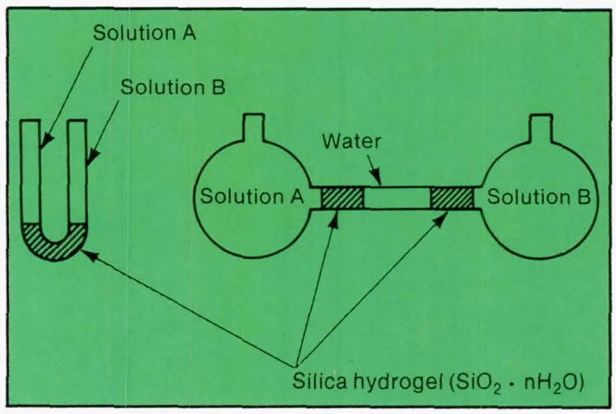

Figure 7.12. Typical experimental arrangements for gel methods of crystal growth.

is shown in figure 7.13. The materials chosen were calcium tartrate, calcium carbonate, and lead sulfide. These can be grown reasonably well without precise temperature control, which was not available during the flight.

The calcium tartrate crystals were the largest and highest quality, as was confirmed by microscopic and x-ray topographic analysis. Both prismatic and platelet habits were observed, with the platelet variety being more numerous. This is contrary to the situation in gel growth, where the prismatic habit dominates. The calcium carbonate formed clear rhombohedral crystals that were very similar to those grown on Earth. The lead sulfide crystals were extremely small and were accompanied by a fine precipitate, indicating that insufficient time was available for the reaction to go to completion. In all cases, the crystals were quite small and numerous, indicating excessive nucleation. Better control of nucleation and more time is required to grow large crystals by this technique.

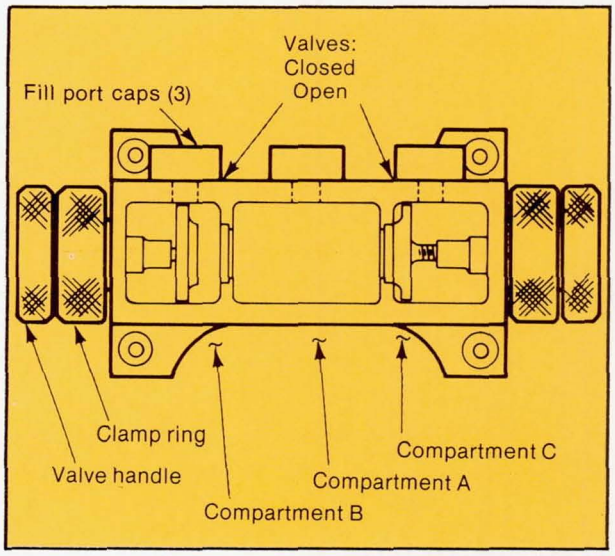

Figure 7.13. Schematic of the reactor used to grow crystals in space.

Experiment MA011, Electrophoresis Technology

The object of this experiment was to determine the feasibility of static free-fluid electrophoresis in low gravity. Considerable effort was devoted to overcoming some of the difficulties encountered in earlier demonstrations, such as sample band distortions caused by electro-osmosis, by developing a special zero zeta potential coating.

The investigation team, led by R. E. Allen of the Marshall Space Flight Center, attempted to separate various cells, including three types of red blood cells (rabbit, horse, and human), human lymphocytes, and kidney cells. The cells were frozen prior to flight, transported to orbit, thawed and separated, refrozen, and returned. Approximately 25 percent viability was maintained throughout this treatment with no evidence of contamination.

The apparatus is shown in figure 7.14. The astronaut selects a sample column and inserts it into the holder that connects the electrode rinse tubes. The electrodes are isolated from the buffer by a membrane, and fluid is circulated to sweep away bubbles that form when electricity is turned on. After electrophoresis is completed, the column is frozen by a three-stage thermoelectric cooler to prevent disturbance of the sample bands. The column is then removed and inserted into a cryogenic dewar for storage.

The columns containing the horse, human, and rabbit red blood cells produced close to the expected separation based on laboratory mobility measurements. The band containing the horse cells was sharp and well defined, but slightly more compressed than expected. The rabbit cells seem to have somewhat greater mobility in space than on the ground and overlapped with the human cells more than expected. In all cases the bands were planar, indicating that the specially developed zeta potential coating effectively

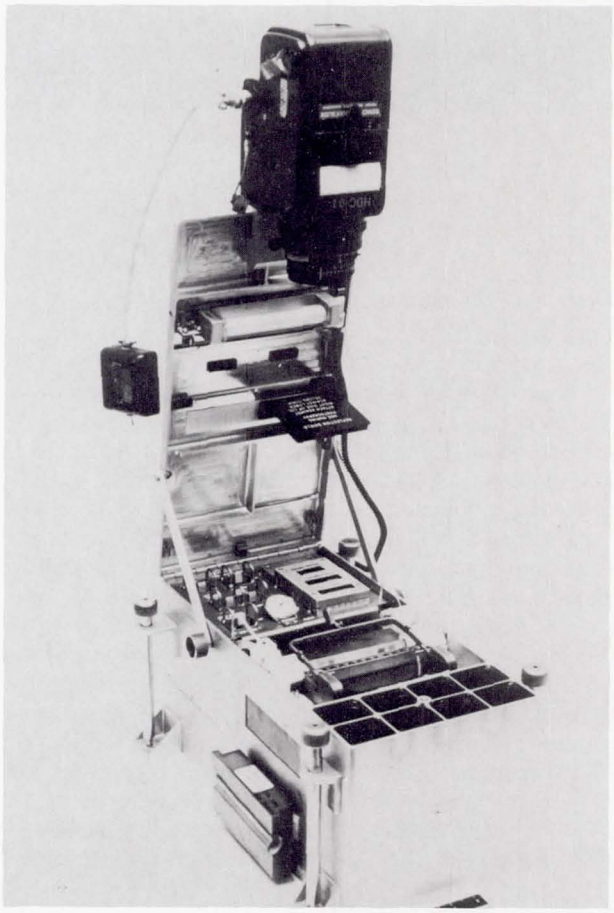

Figure 7.14. Column electrophoresis apparatus.

controlled electro-osmosis that had severely distorted the sample bands in previous attempts (see chapters 3 and 6).

The columns containing the human lymphocytes malfunctioned. Postflight analysis revealed that the electrode rinse lines had become clogged by the sealant material when they were connected. This produced bubbles in the electrode chamber that blocked the current flow after a short time.

The most intriguing results were obtained with the kidney cells. It is known that a number of extremely useful proteins are secreted by cells in the kidney. The enzyme urokinase is one of these products that was of special interest to one of the investigators, Grant Barlow of Abbott Laboratories. Urokinase is one of the few substances that can dissolve blood clots once they have formed, and it would have a significant value as a pharmaceutical product if it were readily available. It is present in trace quantities in human urine and can be produced in limited quantities and at great expense from this source. Barlow was working to develop an alternative source by culturing the kidney cells that produce the enzyme and harvesting the product. Unfortunately, only about 5 percent of the kidney cells produce urokinase; thus this is not a particularly efficient process. Barlow reasoned that if he could separate out those cells which produce urokinase producers from those which do not, such a process might become viable.

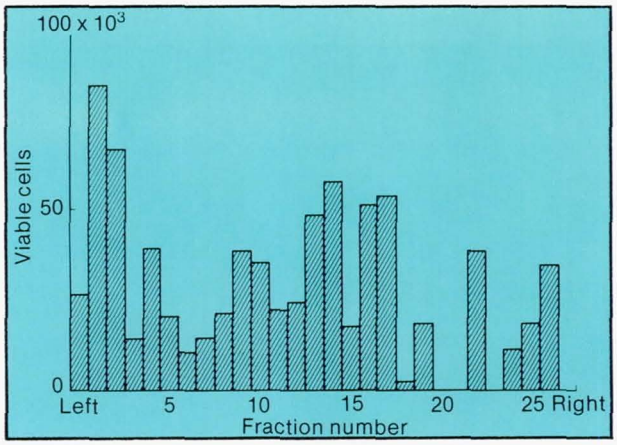

Figure 7.15. Histogram of viable kidney cells.

A column containing live human fetal kidney cells was electrophoresed and returned frozen. The frozen cylinder was carefully sliced into thin discs, and the cells in each disc were placed in a culture medium to test for viability and urokinase production. There is no obvious interpretation for the observed distribution of viable cells shown in figure 7.15; however, enhanced urokinase activity was found in fraction number 15, hinting that kidney cells may be electrophoretically separable according to function. In addition, two other fractions, 14 and 17, respectively, showed enhanced production of erythropoietin, a valuable drug for treatment of anemia, and of human granulocyte conditioning factor (HGCF).

Experiment MA014, Electrophoresis

A continuous flow electrophoresis experiment was developed by Kurt Hannig of the Max Planck Institut für Biochemie, Munich. In a continuous flow system, the material is electrophoresed transversely to the direction of flow, as shown in figure 2.20. This overcomes some of the problems of cell sedimentation and convective mixing that prevent free-flow static electrophoresis from being conducted on the ground. To operate such systems on the ground, it is necessary to have a very small spacing between the front and rear walls in order to remove the heat generated by the current flowing through the buffer and to prevent convective instabilities resulting from thermal gradients. This limits the throughput of the device by requiring a very small sample stream and introduces distortions from wall effects that degrade the resolution of the device. By operating such a device in space, it should be possible to greatly improve both the resolution and the throughput of continuous flow electrophoresis. Another major advantage of the continuous flow technique is the collection system, which eliminates the requirement for the cells to be frozen in place after they are separated.

In the Hannig flight experiment, collection of the separated cells was not attempted. Instead, an ultraviolet photodiode array monitoring system was used to evaluate the separation. This technique gives higher resolution than collection and is quite useful for determining the number and sharpness of fractions and how they vary with time (fig. 7.16). Samples included rat bone marrow cells, mixtures of human and rabbit erythroytes (red blood cells), rat spleen cells, and mixtures of rat and human lymphocytes.

The flow systems apparently functioned as planned; however, an unexpected increase in brightness of the halogen lamp that provided the illumination for the ultraviolet detector caused the detector elements to saturate. Thus they were only able to detect when more than one cell passed through their feld of view. This greatly limited the amount of useful data, but the events detected appeared to be consistent with the expected operation of the system.

The reason for the anomalous brightness of the lamp is not completely understood. In ground tests the lamp functioned normally. It can only be surmised that the lack of convective flow in the low-gravity environment influenced the operation of the lamp and caused it to put out more light. This effect obviously should be considered in future flight experiments.

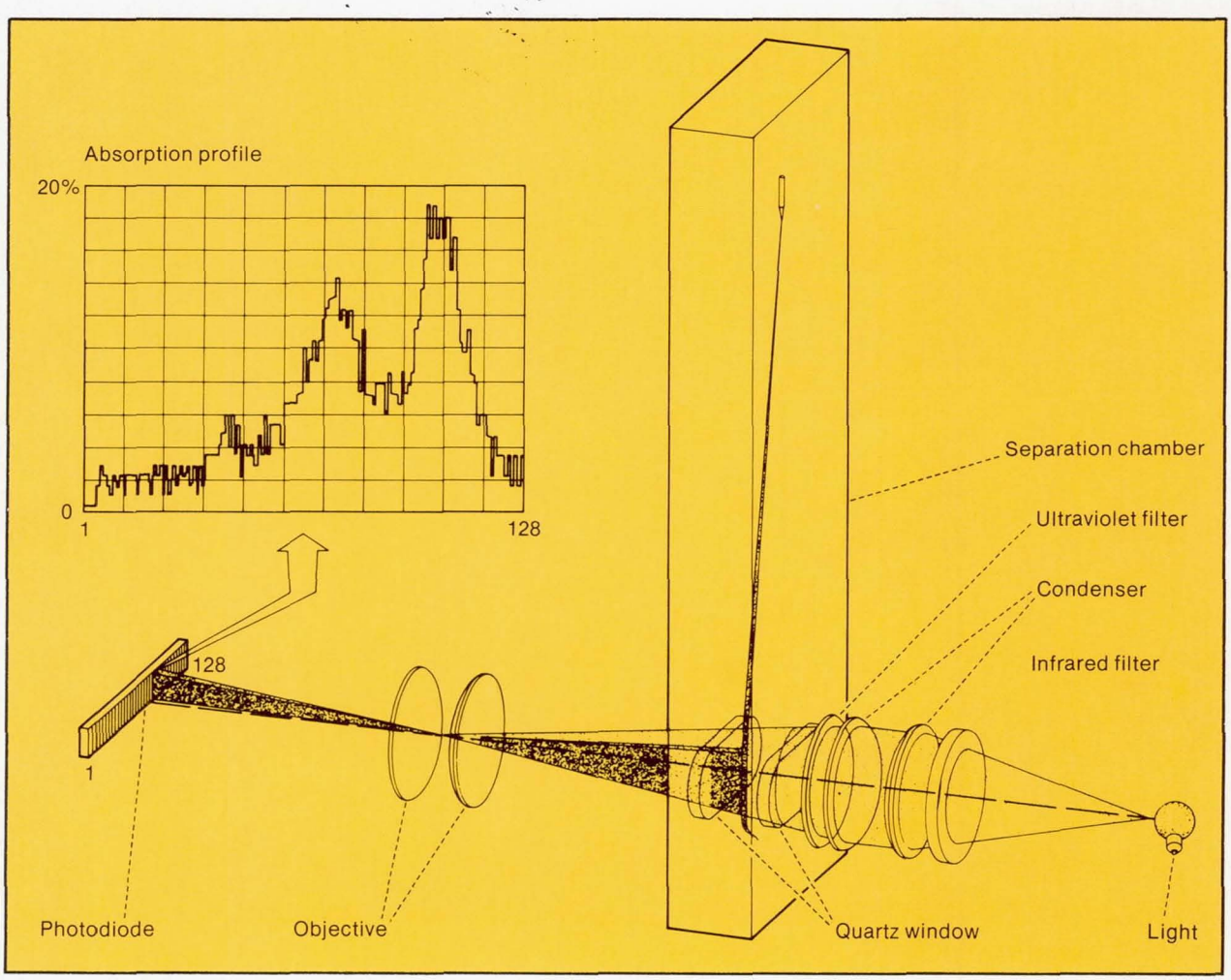

Figure 7.16. The principle of sample absorption measurement.

SPACE PROCESSING APPLICATIONS ROCKET (SPAR) PROGRAM

As discussed in chapter 3, sounding rockets can provide short-duration periods of low gravity suitable for a number of experiments and for testing equipment concepts. Since there was to be a period of many years between the ASTP flight and the next manned space flight opportunity with the Space Shuttle, the Space Processing Applications Rocket (SPAR) program was initiated to provide some continuity in flight experimentation.

The SPAR rocket is a Black Brant vehicle equipped with a stabilized attitude control system to prevent rotation-induced accelerations and a recovery system. An optional Nike booster can be used to increase the low-gravity time or for heavier payloads. Nominal low-gravity times of 5 minutes are obtained with this system for payload weights of 300 kg. Figure 7.17 shows a typical SPAR payload.

Developing an experiment for a SPAR flight is in many ways more difficult than developing one for a manned flight. Everything must be automated and must fit into a cannister only 17 inches in diameter. The launch environment is harsh in terms of acceleration and vibration. The rocket is spun at launch to stabilize it, and despun after burn-out, creating high angular accelerations that produce vorticity in fluids that must be allowed to damp out before low-gravity experimentation can commence.

The short times available are not conducive to crystal growth, biological separation, or other experiments that require carefully controlled conditions over a long time. Certain fluid and solidification experiments, however, can be conducted reasonably well in such a facility. The following paragraphs describe some of the more significant results obtained from SPAR.

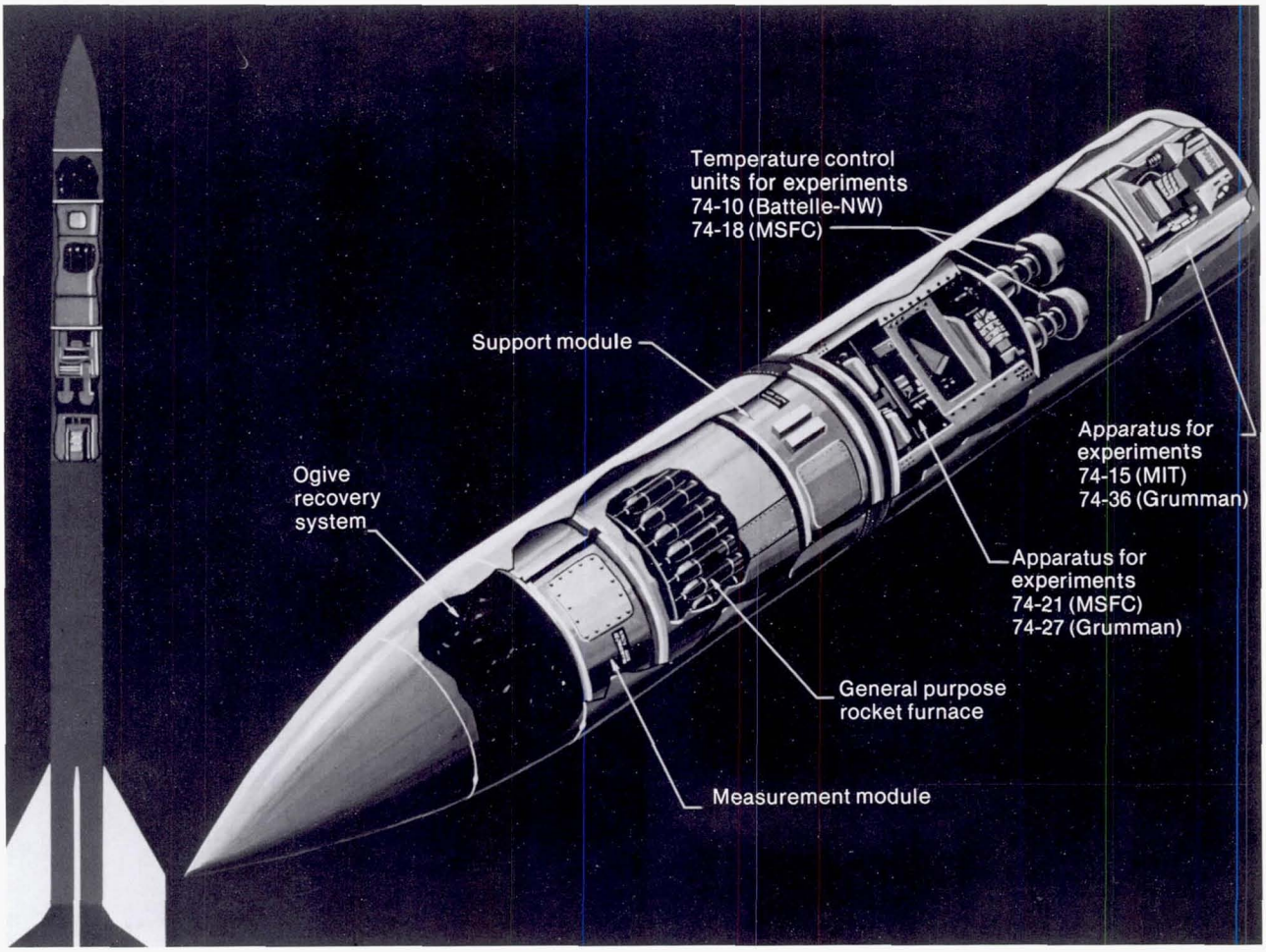

Figure 7.17. Typical SPAR payload.

Liquid Mixing Experiments

One of the first experiments conducted in the SPAR program was designed by C. F. Schafer of the Marshall Space Flight Center to characterize the low-gravity environment and its effect on fluid mixing. Metal samples were constructed in the form of cylinders, with half of each sample being composed of pure indium and the other half being an In (80 weight percent) and Pb (20 weight percent) alloy (the samples were axially symmetric). These were enclosed in aluminum cartridges and placed in heater assemblies so that each sample was either parallel or perpendicular to a radius from the rocket payload axis. This ensured that the density gradient in the samples was either parallel or perpendicular to the effective residual accelerations, assuming that they would arise mainly because of the residual rotation (spin) of the payload. The samples were melted after entry into the low-gravity portion of the payload trajectory and resolidified before leaving low gravity.

Samples oriented such that the denser material was inward (closer to the payload longitudinal axis) experienced flow over nearly the length of the sample. This flow was predictable, using analysis that provided a Rayleigh number as a flow predictor, when the residual acceleration levels were taken to be on the order of 10^{-6} g. Samples with density gradients perpendicular to the radius vector (from the payload longitudinal axis) experienced only a slight deformation of the interface. This region was within the predicted diffusion distance of approximately 1 mm from the original interface. Estimates of flow based on a related model system yield an upper bound on residual accelerations of approximately 10^{-5} g. These levels are consistent with those measured by the flight accelerometers and are apparently the result of a very slow residual rotation about the longitudinal axis.

STUDIES OF SOLIDIFICATION PROCESSES

A series of experiments were carried out independently by Mary Helen Johnston of the Marshall Space Flight Center, and John Papazian of the Grumman Aerospace Corporation to investigate solidification processes in castings and in welds. Of particular interest is the mechanism by which the equiaxed zone is formed in the center of the casting or weld. As heat is extracted from the outside surfaces, the material undercools until nucleation occurs, usually at points on the container wall. Dendrites grow rapidly from these nucleation sites, and many new nucleation sites are produced as some of the dendritic arms are broken off and transported by the flow. Large columnar grains grow from the walls until sufficient nucleation sites find their way to the central region, where they initiate a random, equiaxed grain structure. One of the questions is whether gravity-driven convection is primarily responsible for the breaking off and transport of the dendritic arms, or whether such breakage results from nongravitational effect such as interdendritic flows associated with the solidification process.

A transparent model material, $NH_4OH + H_2O$ is often used to study such phenomena. It has an enthalpy of solidification similar to that of many metal systems and forms easily seen dendritic structures. In the space experiments only a few nucleation sites were observed, and the entire solidification took place from those relatively few sites. There was no evidence of dendritic breakage and multiplication of nucleation sites in either Johnston's or Papazian's experiment. Growth was completely columnar, with no transition to an equiaxed zone.

One of the motivations of Papazian's experiment was to try to understand why the welds done in Skylab had a larger equiaxed zone than had those done on Earth. Clearly, dendrite multiplication is not the explanation, since this was not observed in low gravity.

In a different kind of solidification experiment, R. B. Pond of Marvalaud, Inc., attempted to solidify a complete eutectic structure in 88 percent Pb-11.2 percent Sb. Such a eutectic is of interest because it should be superplastic, allowing it to undergo tensile strains of 100 percent before rupturing.

One of the problems encountered in solidifying such a material is that if nucleation of either of the primary phases occurs, the density difference of the two phases results in segregation. It was thought that such segregation could be eliminated in low gravity.

Both ground control samples and flight samples contained primary Sb and primary Pb crystallization products, indicating a shift in the eutectic point due to supercooling. There was no discernible differences between the mechanical properties of the samples and those processed on the ground.

Immiscible Alloy Solidification

Several more attempts were made by H. Ahlborn of the University of Hamburg, and K. Lohberg of the Technical University of Berlin, and separately by S. H. Gelles of S. H. Gelles Associates to produce a fine dispersion in various compositions of the immiscible system Al-In. Again, the results were similar to those found by Lacy and Ang in their ASTP experiment; almost complete separation of the two phases resulted. Subsequent ground-based experiments in which the samples were X-rayed while they were being soaked above their consolute temperature revealed that the material did take longer than anticipated to homogenize. Since immiscible materials held above their consolute temperatures act as true solutions, they do not tend to separate in a gravitational field. Therefore they may be melted and homogenized on the ground before launch and solidified in low gravity. On a more recent flight Gelles soaked his sample for 16 hours above its consolute temperature prior to launch to remove any question about its homogeneity before solidification. It too separated almost completely, indicating that there are indeed some nongravitational flows or other effects causing massive separation in the solidification process. This is unexpected and very puzzling, particularly in light of the fact that GaBi dispersions were prepared in the drop tower (chapter 3), and it was demonstrated that oil and water mixtures were completely stable for long periods of time in Skylab under static conditions (chapter 6).

Preparation of Composite Materials

Several attempts were made to prepare unique composite materials during the short low-gravity time available during a SPAR flight. L. Raymond and C. Y. Ang of the Aerospace Corporation developed an experiment to produce dispersion-hardened Mg by compacting 5 μm thoria (ThO_2) particles with Mg particles, and then melting and resolidify-

ing the sample in low gravity. Considerable sedimentation was observed in the ground control samples. The first flight sample had a more uniform distribution of dispersed particles, but it also had regions in which the dispersion particles were sparse.

The experiment was repeated on a later SPAR flight using a mixture of Mg, Th, and MgO. The ThO_2 was formed by the gettering reaction $Th + 2\,MgO \rightarrow 2\,Mg + ThO_2$. More care was taken to remove any trapped gas in the starting materials, which could cause nonuniformities in the distributions. This produced a much more uniform distribution of thoria particles in the Mg matrix. The average hardness was considerably greater in the flight sample than in the ground control sample.

W. Heye and M. Klemm solidified a composite of Pb, Ag, and BaO particles in an attempt to produce a ductile superconducting material. The idea was to covert Pb, a type I (magnetically soft) superconductor to a type II (magnetically hard) superconductor by adding 10 percent Ag in a fine dispersion to act as flux pinning sites. The BaO particles were to dispersion harden the Pb so that the Pb and Ag would deform at nearly the same rate when drawn. It was hoped that the solidification in low gravity would prevent density segregation of the components.

Fairly uniform dispersions were obtained in the flight samples. Code formation of the Pb and Ag was achieved, and the material did exhibit type II superconductor behavior.

A unique attempt at production of a closed-cell aluminum foam was devised by J. W. Patten of Battelle-Northwest Laboratories. The material was prepared by sputter depositing Al in the presence of an inert gas such as Ar. Considerable quantities of Ar are trapped in the metal by this process. It was thought that during melting the trapped gas atoms would migrate to nucleation sites and form relatively uniform voids or a closed-cell foam.

Some evidence for bubble nucleation and growth was observed; however, there was a wide variation in cell size. Also, the formation of oxide layers on the surface of the sample produced irregular mechanical restraint of the expanding foam, which severely distorted the samples and limited the amount of information that could be derived from postflight analysis.

Behavior of Bubbles and Dispersed Particles During Solidification

One of the most fundamental questions that must be addressed in designing experiments to take advantage of the lack of sedimentation to prepare unique composite materials concerns the behavior of bubbles and dispersed particles during solidification. There is a force due to long-range molecular interactions between the solidification front and a second-phase particle that tends to push the particle ahead of the front. This force, called the disjoining pressure, is opposed by the drag force, which tends to resist the motion. At sufficiently high solidification rates, the drag force will overcome the disjoining pressure and the second-phase particle will become incorporated. An approximate theory has been developed to estimate the critical velocities. This can be tested to some degree on the ground by allowing the solidification to proceed horizontally between two microscope slides. The particles, in the form of microscopic size spheres, are allowed to roll on the bottom slide. This introduces an unknown error, namely, the rolling friction. A low gravity test of this theory was carried out in a SPAR experiment developed by Don Uhlmann of the Massachusetts Institute of Technology. The results are still being analyzed.

Several attempts to study the motion of bubbles in thermal gradients and in the vicinity of solidification fronts have been made by John Papazian of the Grumman Aerospace Corporation. Since the surface tension varies with temperature for most materials, a bubble in a thermal gradient will feel an unbalanced force that generally tends to move it in the direction of the thermal gradient. This may be a useful mechanism for bubble removal in space processes such as glass formation, where buoyancy does not act to fine the glass. Papazian used CBr_4 as model material that was melted and saturated with gases such as N_2 and Ar prior to launch. The samples were directionally solidified and photographed during flight. Bubbles apparently nucleated throughout the melt during launch and did not appear to move during the flight. The solidification was dendritic, and bubbles became trapped among the dendrites, which made it difficult to conclude anything about their interactions with a planar solidification front. The lack of motion of the bubbles in the thermal gradient is also puzzling. Several explanations are possible: the bubbles may have been trapped on the walls; surface active impurities may be present in the melt which may distribute themselves on the bubble surface in such a way as to eliminate the unbalanced force; or the thermal gradient may have been reduced by the convective mixing during launch. Unfortunately, there is still a large uncertainty surrounding this important area.

Tests of Containerless Processing Techniques

Several types of containerless processing apparatus have been flown in SPAR to develop a better understanding of the operation of these devices.

The three-axis acoustic levitator, developed by Taylor Wang of the Jet Propulsion Laboratory, successfully deployed a 2.5 cm diameter sphere of water and captured it in the acoustic field. An electronic malfunction caused a premature loss of sound field before the remaining tasks of oscillating and rotating the sphere of water were accomplished. However, the drift rate and direction of the sphere provided confirmation of the g levels.

The electromagnetic levitator, developed by R. T. Frost of General Electric, successfully melted and solidified a sphere of beryllium containing a dispersed phase of beryllia. The experiment, developed by G. Wouch of General Electric and N. Pinto of Kawecki Berylco Industries, investigated the utilization of a dispersed oxide, BeO, as a grain refining agent to improve the microstructure of cast beryllium. The containerless process prevented any wall-induced nucleation, thus ensuring that the dispersed phase would act as the nucleating agent.

The sample was successfully positioned by the electromagnetic field during the flight. Melting and solidification were accomplished without any physical contact with the coils. A fairly uniform dispersion of the BeO was obtained in the flight sample. However, the BeO dispersoid did not produce the anticipated fine grain structure.

The high-temperature, single-axis acoustic levitator furnace, developed by Roy Whymark of Intersonics, Inc., has demonstrated sample capture at high temperature in a KC-135 flight. It will be used to process a gallia calcia glass sample in a later SPAR flight. This is one of many potential glass-forming systems that are distributed by container-induced nucleation.

The foregoing represent systems of the type that will provide much of the containerless processing capability that will be developed for the more sophisticated experiments planned for the Spacelab era. The primary value of these early SPAR experiments is to gain experience in the design and operations of such devices.

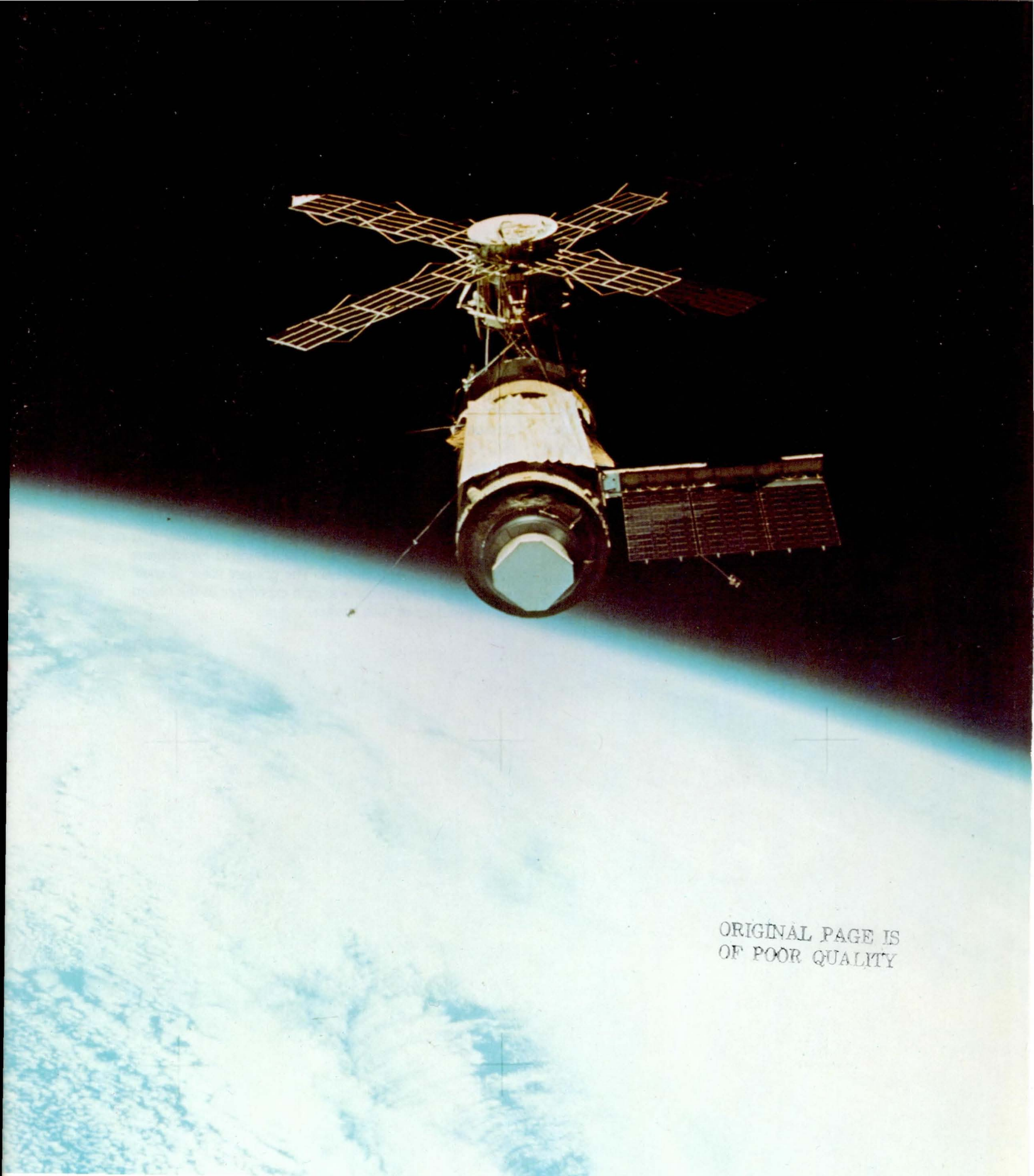

Skylab.

Chapter 8. FUTURE PROGRAMS

The first generation of materials processing in space is described in chapters 1–7. A number of the experiments were exploratory in nature to determine what, if any, effect the low gravity in an orbiting spacecraft might have on processes that are normally carried out on Earth. In many cases the expected results were confirmed, but there were also a number of surprises, some of which may have significant scientific value.

SUMMARY OF THE PRESENT STATE OF KNOWLEDGE

Significant findings in the area of crystal growth:

1. Control of macrosegregation in melt growth has been demonstrated. It was shown that a steady state diffusion layer can be established over a short growth distance, resulting in a macroscopically uniform dopant distribution over most of the length of the boule. The distribution of dopants in the steady state growth Skylab experiment resembles the classic textbook description of diffusion-controlled growth.

2. Elimination of microsegregation due to growth rate fluctuations has been demonstrated. This indicates that it may be feasible to grow some of the higher composition alloy semiconductors such as HgCdTe and PbSnTe from the melt without interfacial breakdown resulting from uncontrolled growth rate fluctuations and under conditions such that defects resulting from the growth process may be eliminated.

3. Seeded containerless growth has been demonstrated. Extremely flat surface facets were formed, indicating that the crystalline ordering forces dominated over surface tension forces. Elimination of the container also resulted in a substantial reduction of strain-induced defects.

4. Crystals grown by chemical vapor transport in low gravity showed improved growth habit, surface morphology, and lower defect density than those grown on Earth. These differences imply a more uniform growth environment in the absence of gravity-driven convection.

5. Observed growth rates by chemical vapor transport in low gravity were substantially higher than expected on the basis of extrapolation of laboratory data from the low-pressure regime in which convective effects were thought to be insignificant. This indicates a fundamental lack of understanding of the transport mechanisms and their dependence on gravity-driven flows.

6. The ability to produce and maintain extended floating zones was demonstrated. Predicted rotational liquid surface instabilities were confirmed experimentally, and an unexpected nonaxisymmetric instability mode was discovered.

7. There was no evidence of surface tension-driven flows in some of the high-temperature melts that apparently had free surfaces.

Significant findings in the field of metallurgy:

1. Welding and brazing can be performed in space. Voids due to trapped gases were effectively prevented. The observed microstructure of weldments in low gravity was different from that observed in 1 g and in fact was contrary to what was expected. The reason for this is not understood.

2. A number of experiments were designed to produce composites with uniformly dispersed second phases. It was shown that buoyancy effects were effectively eliminated but that close attention must be paid to sample preparation, elimination of gases, and control of solidification rates in order to achieve uniform distributions.

3. The dominant role of gravity-driven convection in the process of dendrite multiplication was confirmed experimentally.

4. Unexpected agglomeration of some immiscible metallic systems occurred during solidification. This indicates that there are strong driving forces for droplet growth or coalescence in the Al-In system, for example, which act in the absence of appreciable buoyancy and are much too fast to be a diffusion effect. One hypothesis is that this massive agglomeration is a constitutional effect.

5. Attempts to understand some of the results obtained in the flight experiments have prompted the re-examination of published phase diagrams of several systems. Several refinements were established; for example, the previously accepted value for the consolute temperature of Pb-Zn was low by 20 K and the eutectic composition of Mu-Bi was found to be 2.6 atomic percent Mn and 97.4 atomic percent Bi.

6. The ability to melt and solidify samples without physical contact has been demonstrated in space. Recent results using drop tubes and electromagnetic levitators have shown that extreme undercooling can be achieved in the absence of wall contact.

7. The low-temperature, high coercive strength magnetic phase of MnBi has been studied in detail, and a new ordering effect at high magnetic intensities has been discovered. The enhanced magnetic performance of the MnBi samples processed in space is now thought to be the result of finer rod dimensions of the MnBi phase obtained by directionally solidifying an off-eutectic composition that remained uniform in the absence of convective stirring.

In the area of fluid phenomena there appears to be considerable confusing and conflicting data, indicating that there is still much to be learned about the behavior of fluid in a low-gravity environment. The present understanding of these phenomena is summarized as follows:

1. Although a few of the experiments were apparently disturbed by vehicular accelerations, crew activity, or inadvertant crew contact, most of the experiments did not seem to be adversely influenced by the residual g levels of Skylab and ASTP. There was no evidence of major bulk flows from the random acceleration environment associated with the manned missions, in which the accelerations tend to average to zero. Only in the case of slow, sustained rotation and highly unstable liquid configurations, such as encountered in SPAR, do such low-level accelerations produce significant flows.

2. Anomalous wall contact behavior was observed in a number of solidification experiments in which the solid pulled away from the wall even though the liquid presumably wet the container. In one case the type of dopant atoms present in trace quantities seemed to influence this behavior. Whether such effects result from different wetting behavior in the absence of hydrostatic pressure, from the presence of trapped gases, or from volume change phenomena during solidification is not clear.

3. There is still much to be learned about the importance and control of surface tension driven flows in low gravity. The Heat Flow and Convection Experience flown on Apollo demonstrated unstable surface tension driven flow in an oil film with a free surface with a destabilizing perpendicular thermal gradient. Surface tension driven flows resulting from concentration gradients were apparently responsible for the observed mixing in an experiment on ASTP. Such flows apparently can occur in contained systems provided the liquid does not wet the container walls. On the other hand, there was no evidence of surface tension driven flows in the crystal growth experiments in which the solid pulled away from the wall.

4. Some anomalous effects were noted in the diffusion experiment and in the simple Skylab demonstration experiment using a mixture of tea and water. Although the expected diffusion profile was obtained near the center of the sample, this profile was distorted near the walls as though the diffusive transport was retarded.

5. Long-term stability of a fine dispersion of oil and water was demonstrated. This indicates that low-level residual accelerations or other effects do not cause significant agglomeration in an isothermal environment. The importance of droplet migration because of differential surface tension effects in a thermal gradient is still an open issue.

6. Free-column electrophoresis was successfully demonstrated. Methods for controlling nongravitational flows due to electro-osmosis were developed.

In many cases, these first experiments were constrained by available resources: development time, flight facilities, power, on-orbit processing time, processing environment, and so on. Ambiguities still exist because many of the results were unanticipated and could not be investigated in sufficient detail with the available experiment designs and instrumentation. However, these experiments have provided an extremely valuable first step in the learning process and form an essential background for the next generation of space experiments.

MATERIALS PROCESSING IN THE SPACE TRANSPORTATION SYSTEM FACILITIES

The next major opportunity to conduct materials processing experiments in space will come with the operation of the Space Transportation System (STS) which consists of the Space Shuttle and the Skylab experiment carrier (fig. 8.1). Although power is still a limiting factor, particularly in the manned Spacelab module which can only provide a total of 2 kW to experiments, up to 4.7 kW can be made available on Shuttle missions such as satellite or planetary probe deployment missions. Experiments requiring high power and heat rejection will be carried on a pallet and operated remotely by the crew after the satellite or probe is deployed (figs. 8.2 and 8.3). In this manner the entire resources of the Shuttle can be made available to the experiments. Eventually, the 25 kW power module will be able to provide adequate power for most of the presently envisioned materials processing experiments.

Experiments that do not require the high power and sophistication of the new hardware being developed for the STS missions can be carried out in existing SPAR sounding rocket hardware. A convenient self-contained carrier is being developed that can accept up to four SPAR experiment packages and provide power, heat rejection,

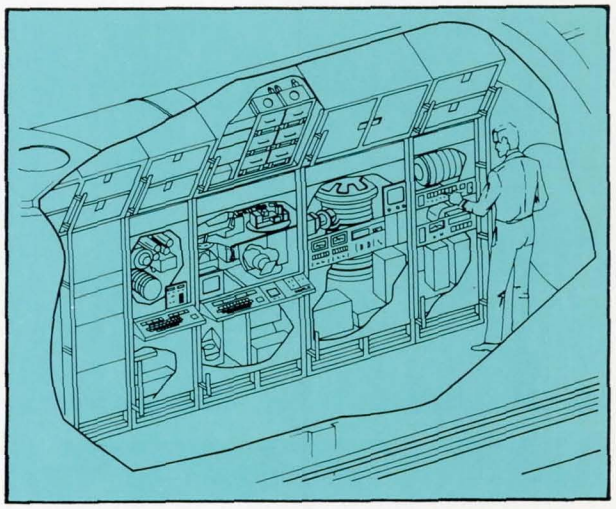

Figure 8.2. *Artist's concept of the materials processing experiments to be carried out by the Space Transportation System. Experiments that require manned operation and have modest power requirements will be carried out in the Spacelab Module.*

Figure 8.1. *Space Transportation System consisting of the Space Shuttle Orbiter containing the Spacelab Module and Pallet in the cargo bay.*

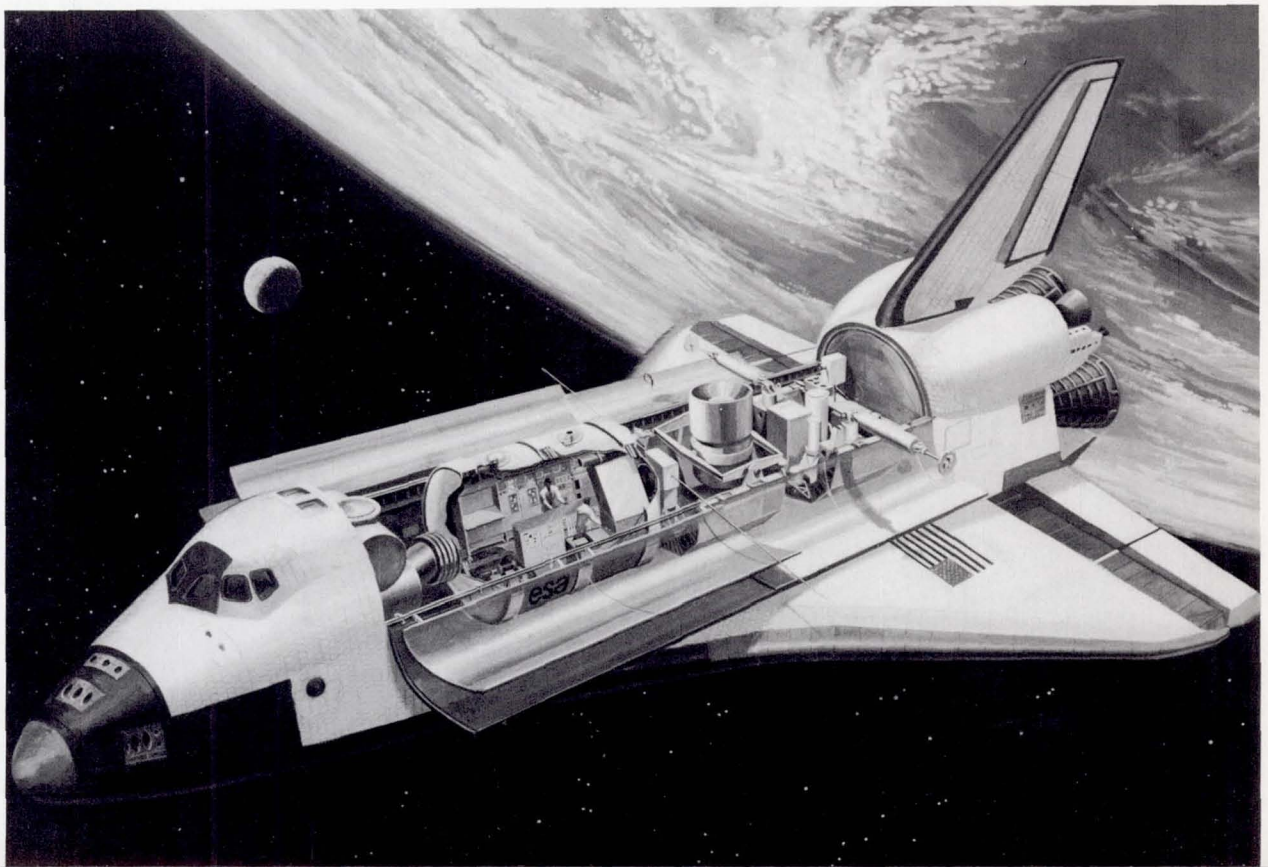

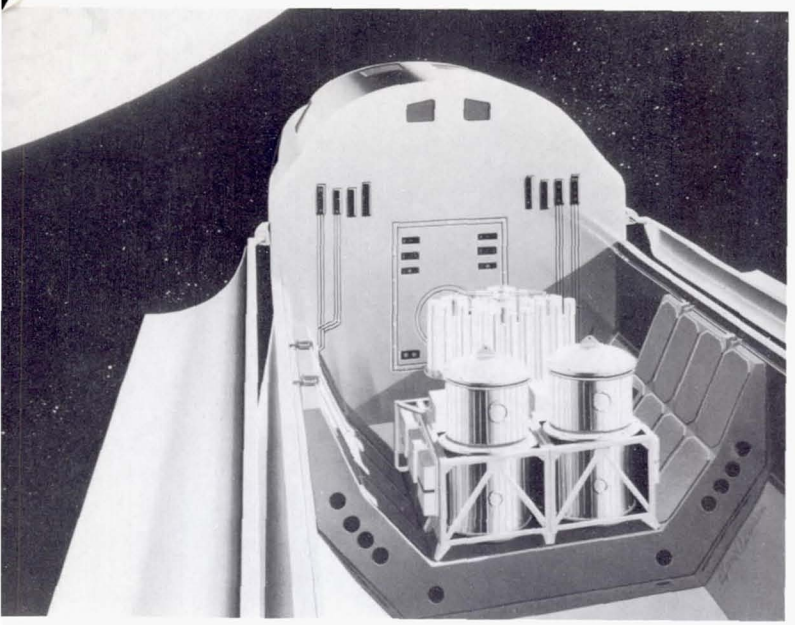

Figure 8.3. Experiments requiring high temperatures and high power levels will be carried out in the automated Solidification Experiments System on the Pallet shown here. Samples to be processed are contained in the cartridges mounted on the turret. These can be automatically inserted in the furnace module for processing.

automatic sequencing and control, and data acquisition and recording. This carrier, termed the Materials Experiment Assembly (MEA), is shown in figure 8.4. Since it is self-contained, the integration requirements are minimized. It is hoped that such a package can be flown many times at low cost on a space-available basis once the Shuttle is operational.

Ultimately, to avoid the high transportation cost of taking processing facilities into orbit for each mission, a permanent facility will be left in space. This will also accommodate experiments that require longer times than can be provided by Shuttle missions. The Shuttle will periodically retrieve processed samples and supply fresh samples for processing. A concept is shown in figure 8.5. Such a facility together with Spacelab module facilities will comprise a national low-gravity research laboratory. The cost of processing material in such a facility should be low enough to encourage commercial corporations to conduct experiments or produce products for their own private use.

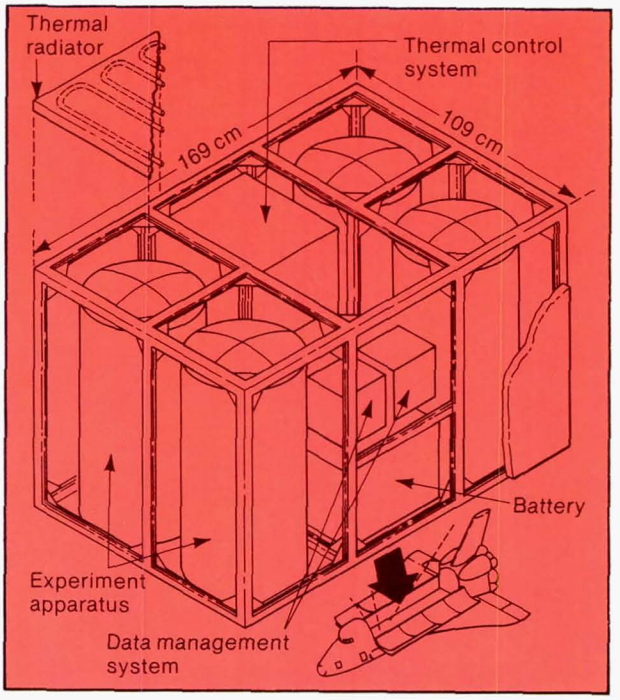

Figure 8.4. Materials Experiment Assembly. This self-contained structure serves as a carrier for up to four SPAR experiment packages and provides power, sequencing, control, data acquisition, and heat rejection. It allows relatively simple experiments to be carried out during Shuttle flights on a space-available basis at relatively low cost.

Figure 8.5. Materials Experiment Carrier. A larger, more sophisticated materials processing system that is left in orbit is shown here attached to the 25 kW Power Module. Samples are delivered and retrieved by the Space Shuttle.

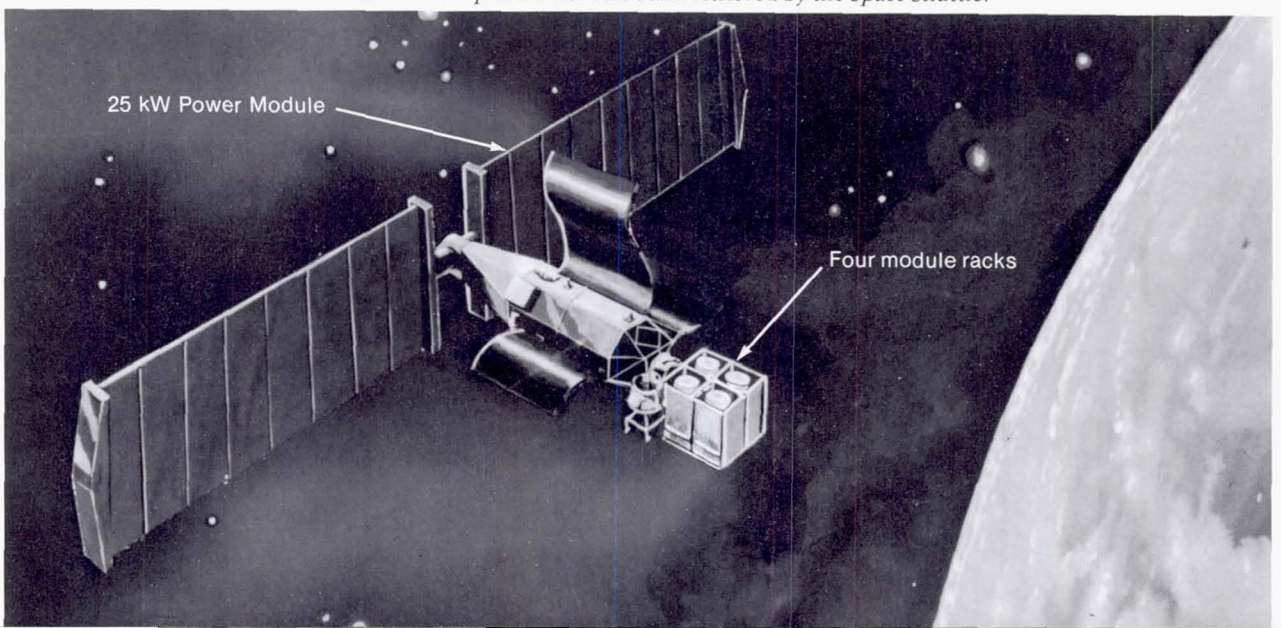

PROSPECTS FOR SPACE COMMERCIALIZATION

A goal of the Materials Processing in Space Program is to develop a viable commercial interest in using space to (1) perform research to improve industrial technology or to develop new products, (2) prepare research quantities of material to serve as a paradigms with which to compare current Earth-based technologies, (3) manufacture limited quantities of a unique product to test market or to fulfill a limited but compelling need, and (4) produce materials of sufficient quantity and value to stand on their own economically.

There are a number of steps that must take place before this can happen. Since the present cost of space experimentation is high, the commercial benefits are not yet clear, and the potential payoff time is long, it is probably not realistic to expect major commitments from industry until a more adequate background of experimental results is available. Also, the details of how NASA and industry might work together are in the process of being clarified with regard to patent protection rights, proprietary rights, liabilities, leasing policy, pricing, exclusivity, and recoupment.

An important first step will be the establishment of joint endeavors with industrial users to assist them in exploratory studies. Arrangements are also being worked out to lease NASA facilities. Increasing commitment on the part of the user will be required as the project matures. There is active interest on the part of several users, and negotiations are currently in progress.

It is difficult to predict at this time what products might ultimately be produced in space. It should be remembered that although the costs of transportation of materials and processing facilities to and from orbit will be dramatically reduced when the Space Shuttle becomes operational, space operations will always be expensive and transportation costs will contribute disproportionately to prices when compared with the products of ground-based manufacturing processes. Shuttle payload costs to the user are currently estimated to fall within the range $250 to $1000 per kilogram. Since space processing, to be profitable, must add value to a product in excess of this plus operational costs not yet defined, the identification of candidate processes or products is not a simple task. It is almost mandatory that such a product have unique attributes unobtainable through the application of any ground-based technology; otherwise it will virtually always be less expensive to produce the item on the ground. Furthermore, these attributes must be sufficiently useful and unique to justify their added cost, and the demand for the product must be large enough to offset the required investment and operating costs. Given the rapid evolution of technology, it is possible that some of the application currently envisioned for space processing will be surpassed as a result of Earth-bound ingenuity before the opportunities to work in space become available. On the other hand, the general trend of technology is toward more demanding requirements in materials and processes. Thus there is reason to believe that the technology of the 1980s will place even more urgency on the development of space processing than does current technology.

The economic viability of manufacturing or processing materials in space can only be assessed when a suitable base of knowledge has been established. Such knowledge can also be expected to contribute significantly to a number of scientific disciplines and technologies. For example, by developing ultrapure materials for the measurement of basic properties, a researcher can obtain a better understanding of how such properties relate to the atomic structure of the material and to what extent the material must be purified or alloyed to obtain the desired properties. Also an understanding of exactly how convection or container contamination affects a process is often extremely useful in developing control techniques to minimize these effects. Such knowledge gained from process research in space may lead to improvements in a number of ground-based processes. Additionally, the interdisciplinary interest attached by the prospect of participating in such materials processing research activity will result in innovative advances in the biological as well as the materials sciences.

The second benefit that will undoubtedly be realized from the space processing effort is the production of novel materials, that is, various crystals of larger size and higher perfection, unique composites and alloys, exotic glasses and ceramics, and so on. Some of these may only be curiosities with no outstanding properties that would give them special advantage over Earth-produced materials. The principal value of such materials is their contribution to our understanding of processes and their use as a model of more interesting systems. For example, it may be cost effective for an industry to make a limited number of exemplary materials in space that represent the ultimate of what can be achieved by a particular process. These could serve as models to determine how much expenditure is justified to improve a process. Other products, such as certain types of detector materials, may have highly useful applications but a limited market. Small-scale production might be justified, but the limited quantities required may not be attractive for industrialization. Even so, such materials could have a profound impact on our research or military capability, eventually leading to a commercial application that would provide a basis for space industrialization. Certainly there are a

number of high technology materials, particularly in the electronics and pharmaceutical industries, that have sufficiently high intrinsic value that the high cost of space manufacturing would not be a deterrent provided that superior products were produced by space processing.

It must be recognized that even if a material is identified that is sufficiently unique, useful, and valuable to be manufactured or processed in space, the high inherent cost of space processing will be a strong incentive for industry to find the means of duplicating the process on the ground to find a cheaper substitute for the material. Such activities are expected to be an important competitive factor in enhancing materials technology.

ACKNOWLEDGMENT

We wish to express our gratitude to our respective staffs and other personnel at the Marshall Space Flight Center who contributed to this document. In particular, we wish to thank Mathias Siebel for his contributions to chapter 3 and Mirt Davidson for his inputs to chapter 4. Also we wish to express our gratitude to John Carruthers and James Bredt for their helpful comments and suggestions in editing the text.

R.J.N.
H.W.H.

INDEX

Abbe number 23
acoustic levitation 9-10, 18, 44, 103
Ahlborn, H. 101
aircraft, research 35
Allen, R. E. 97
alloy semiconductors 16
alloys
  monotectic and syntectic 92-94
Ang, C. Y. 92, 101
Apollo experiments 36-39
Apollo 14 36-39, 86
Apollo 16 38-39, 68, 86
Apollo 17 36
Apollo-Soyuz test program 88-89
atmosphere 4, 5

Barlow, Grant 98
Bernard cells 36, 38
Bier, Milan 86
biological materials 28-32
bismuth 33-34
blood 26, 97
Bourgeois, Sid 85
brazing 33, 42, 45, 67, 105
Brownian motion 8, 22, 27, 77
buoyancy 5, 7-8, 20, 23, 26

Carr 76-77
Carruthers, John 79-80
ceramics 22-24
charged particles 86
chemical processes 25-28
Clusius-Dickel separation 91
composite casting 36-37
containerless processing 9-12, 18, 23
  on Skylab 43
  tests 103
convection 5-8, 12, 16, 19, 25, 29, 36, 38, 76, 106
  Marangoni 8, 40, 55, 75, 95-96
counter-current distribution 29
crystal growth 6, 15-17, 50-62, 89-91, 96-97, 105
  Bridgeman technique 52
  by vapor transport 59-62
  Czochralski method 11, 55, 58
  defects 51
  electroepitaxy 17
  floating zone method 8, 9, 12, 79-83
  from vapor 16, 52, 90-91
  gel method 96
  halide eutectic 91
  interface marking 89-90
  silver 84-85
  Stockbarger technique 52, 92
crystallography 25-26

Darbro, Wesley 83
dendrites 19, 25-26, 61, 84-85, 101
diffusion 17, 25, 53, 62, 75, 78-79, 84, 86, 90-93
dopants 15-16, 50, 53-55, 58, 89
drop tower 34
  experiments 33-35, 43
durene 27

Einstein's principle of equivalence 1, 2
electromagnetic levitation 9, 10, 12, 103
electrophoresis 25, 29-30, 32, 37-38, 86, 97-99
electrotransport 13, 17
eutectics 19, 70, 91-92

Facemire, Barbara 85-86
Fick's law 79
flammability 75-77
floc formation 26
fluid mechanics 85

fluids 25-28, 75-89, 106
Francis Bilter National Magnet Laboratory 92
Frost, R. T. 85, 103
furnace, composite casting 36-37, 39
fusion, inertially confined 23-24

g-jitter 3, 83
gallium 33, 34
gallium arsenide 17
Gatos, H. C. 54-55, 89
Gelles, S. H. 101
Gibson 79
glass 21, 22-24
gradients
  density 5, 29, 100
  pH 29, 31
  temperature 5, 29, 59-60
  thermal 5-8, 12, 16-19, 25, 41, 57, 59, 71, 83, 102
Grashof number 6-7
gravity
  Earth 1-3, 7-9, 19-20
  low 1-4, 8-10, 15, 19-20, 23-28, 32-35, 62, 64-65, 69, 75, 82-83, 87, 93, 96, 100, 102
  zero 1, 33, 35, 54, 75-77, 81, 91
Grodzka, Philomena 84

Haines 28
halides 72
  eutectic crystal growth 91
Hannig, Kurt 98
Hasemeyer, Earl 71
Heye, W. 102
hydrostatic pressure 8-11, 16, 19, 28, 79, 93
hysteresis 8, 28

ice 87
indium antimonide 41, 54-57
isoelectric focusing 29, 31
isotachophoresis 86

Jet Propulsion Laboratory 23, 104
Johnson Space Center 47, 75
Johnston, Mary Helen 101

Kawada, T. 70
Keplerian trajectory 7, 35
Kimzey, J. H. 75
Klemm, M. 102
Krytox 36-38, 82-83

Lacy, L. L. 68, 82-83, 87, 92
Larson, D. J. 91
laser 23, 24
latex 27, 28

Lind, M. D. 96
liquid films 83
liquid floating zone 8, 79-83
liquid membranes 26
liquid phase partitioning 29-30, 32
liquids, immiscible 26, 83
Lohberg, K. 101
Lord Rayleigh 79-80
lymphocytes 28, 97-98

macrosegregation 6, 18
magnetohydrodynamic power systems 18
magnets 91-92
Marshall Space Flight Center 20, 33-34, 64, 67, 71, 82-83, 86-87, 92, 97, 100-101
Materials Experiment Assembly 108
Materials Experiment Carrier 108
Materials Processing Facility 44-47, 64, 75
McKannan, E. C. 64
melt growth 53-59
mercuric iodide 16, 17
metals 18-22
metal alloys 18-22
  solidification 19-20
metallurgy 18, 20, 63, 68, 105
microsegregation 6, 18, 58
Miyagawa, I. 83

neutron transmutation 15
Newton's law of gravitation 1
  laws of motion 25
niobium 21
nucleation 18, 23, 52, 73-74, 97, 101, 103

oscillation 16, 18, 23, 59
Ostwald ripening 8, 26, 84
Otto, Guenther 68, 82, 87
oxide skin 19, 20

Papazian, John 101-102
Patten, J. W. 102
Peltier cooling 17, 89
Pinto, N. 103
Plateau, J. 9, 79-81, 85
Plateau tank 80, 83
polymerization 8, 27
polyurethane 75-76
polyvinyl latex 27
Pond, R. B. 101
Poorman, R. M. 64
precipitation 26

Raymond, L. 101
Reed, R. E. 95
Reger, J. L. 68, 92

Schafer, C. F. 100
Schlieren photograph 6, 7
sedimentation 4, 8, 22, 27-28, 32, 93, 102
semiconductors
  electronic properties of 49-50
  in crystal growth 15-16, 51-53
  in melt growth 16, 53-54
separation techniques 26, 28-29, 32
silicate glass 22
silicon 11, 15, 50
skull melting 12
Skylab 3, 33
  brazing apparatus 42
    experiments 63, 67
  charged particle mobility experiments 86
  contained materials processing 40-42
  containerless processing apparatus 43
  crystal growth 51-62, 89-90
  diffusion experiments 78, 79
  diffusion in liquids demonstration 86
  experimental facilities 40-47
  flammability experiment 75-77
  fluid mechanics experiment 85
  ice melting demonstration 87
  immiscible liquids experiment 82
  liquid film experiment 83
  liquid floating zone experiment 79-82
  Materials Processing Facility 44-47
  melt growth experiments 53-59
  Multiple Docking Adapter 44
  multipurpose electric furnace 40-41, 44, 45, 47, 60, 68, 72, 89
  Rochelle salt growth experiment 83-84
  silver crystal experiment 84-85
  sphere-forming experiment 43, 45
  steady state growth 54-56, 58-59
  vapor growth experiment 90
  vapor transport 59-62
  welding experiment 63-66
slagging 18
smoke patterns 75, 77
Snyder, Robert 86
solidification 6-7, 17-22, 27, 33-34, 43, 54-55, 58, 63-71, 73-74, 91-95, 99, 101-103
  of immiscible alloys 13
  of indium antimonide 56
  of metal alloys 19-21
sounding rocket experiment 99
Soyuz 89
Space Processing Applications Rocket program 99-103
Space Shuttle 99, 107-109
Space Transportation System 107-108
space vacuum facility 4, 5
Spacelab 103, 107-108
sphere-forming experiment 43
splat cooling 20, 23
stoichiometry 93
superconductors 20-22
supercooling 56, 59
superionic conduction 22
surface tension 8, 10, 12, 18, 23, 36, 58, 63-64, 67, 71, 79-80, 85, 93, 102

triglycene sulfate 17

Uhlmann, Don 102
Ukanawa, A. O. 79
ultrahigh vacuum processing 12-13, 18
undercooling 20, 23, 25, 73-74, 101

vacuum distillation 12
vacuum melting 12
vapor transport 59-62
Vaughan, O. 85
Voltmer, F. W. 58

wall effects 11
Walter, H. U. 56
Wang, Taylor 23, 104
Weidemeier, Herbert 59, 90-91
weightlessness 1, 2, 27, 77, 83
Whymark, Roy 103
Wilcox, W. R. 58
Williams, J. R. 67
Witt, A. F. 54, 55, 89
Wouch, G. 103

Yates 68
Yue, J. T. 58, 72, 91

zone leveling 54
zone refining 13

NASA

National Aeronautics
and Space Administration